

Sialyltransferases: Expression and Application for
Chemo-enzymatic Syntheses

Inauguraldissertation

zur

Erlangung der Würde eines Doktors der Philosophie

Vorgelegt der

Philosophisch-Naturwissenschaftlichen Fakultät

Der Universität Basel

von

Tamara Visekruna

aus Kroatien

Basel, 2005

Genehmigt von der Philosophisch-Naturwissenschaftlichen Fakultät

auf Antrag von

Prof. Dr. Beat Ernst, Prof. Dr. Monica M. Palcic

Basel, den Juli, 5 2005

Prof. Dr. Hans-Jakob Wirz

Acknowledgment

First of all I would like to thank Prof. Dr. Beat Ernst for giving me an opportunity to be a part of an extraordinary international group at Institute of Molecular Pharmacy, University of Basel, and for giving me a possibility to work on my thesis within a multidisciplinary Myelin Associated Glycoprotein (MAG) project. His constant optimism and professional devotion, as well as his permanent and helpful suggestions enable successful finish of my Thesis.

Furthermore, I am really glad to have Prof. Dr. Monica M. Palcic as a coreferee and I would like to thank her, despite of distance, for being a part of mine examination board.

During my PhD I was honored to work with Prof. Dr. Harald S. Conradt and Dr. Eckardt Grabenhorst at Department of Protein Glycosylation at German Research Center for Biotechnology (GBF). Since I obtained the basics of protein glycosylation in their research group, I would like to thank them for all constructive suggestions and professional guidance.

Working on MAG project I was able to communicate and exchange the knowledge from different scientific areas with appreciated scientist, my colleagues and friends. In this environment it was very productive and I prospered in scientific term. Therefore, I would like to thank Dr. Oliver Schwardt for cooperation and interpretation of all chemistry data, Dr. Ganpan Gao and Sachin Shelke for permanent drawing of my chemical structures, Daniel Strasser for a MAG support and Michele Porro for *in silico* help.

It will not be fair to exclude my diploma students, Daniela Friedli and Gabriela Zenhäusern, who did an excellent work and certainly contributed to the conclusion of my work.

My extraordinary thank goes to Dr. Zorica Dragic, my friend, my colleague, my flat-made, who showed me a way to solve the problems where there was no solution. Also, for small talks in “little hours” she was always open-minded and ready for any discussion in front of the kitchen table. Let me say, the years that I spent with Zoki were simply unforgettable.

Girls, Zoki, Claudia, Ganpan, Tina, Salome, Karin, and Daniela, I will always remember

and treasure our “Mittagessen” hours full of dynamic conversation.

Moreover, I would like to show my gratitude to all who participated in my work and made my stay in Institute amusing and interesting.

Last but not least, I appreciated all wonderful moments that I spent with “Basel community” and whole lively trips across Switzerland and Europe. During all moments there was a person who deserved special thanks and who was there when I needed somebody to rely on. Either way in good or bad, Filip was there always ready to listen and help.

Finally, I would like to dedicate my work to my mama Jasna, my tata Vito and my brother Gogi. U svakom trenutku su bili puni razumjevanja i velika potpora tijekom čitavog mog školovanja pa i sada na kraju moje doktorske dizertacije. Gotovo je nemoguće zamisliti da bih bez njihove podrške uopće mogla privesti kraju stvaranje ovoga rada.

Abstract

Glycosylation is a complex yet common form of post-translational protein/lipid modification in the eukaryotic cells. It is processed by glycosyltransferases (GTs), a large group of enzyme, that are involved in the biosynthesis of glycoprotein and glycolipid sugar chains. Moreover, carbohydrates represent major components of the outer surface of mammalian cells and there is now abundant evidence that terminal glycosylation sequences are involved in adhesion, immune response, and neuronal outgrowth events. Sialylated oligosaccharide sequences have long been predicted to be information – containing molecules and critical determinants, e.g. in cell-cell recognition processes, cell-matrix interactions and maintenance of serum glycoproteins in the circulation. Enzymes responsible for the terminal sialylation are sialyltransferases (STs), a subset of the GT family that use CMP-NeuNAc as the activated sugar donor to catalyze the transfer of sialic acid residues to terminal non-reducing positions of oligosaccharide chains of glycoproteins and glycolipids.

The Myelin-Associated Glycoprotein (MAG), expressed in myelin of the central and peripheral nervous system, has been identified as one of the neurite outgrowth-inhibitory proteins, together with Nogo-A and the oligodendrocyte myelin glycoprotein (OMgp). Among all MAG physiological ligands, i.e. brain gangliosides, the GQ1b α is the most potent natural ligand identified so far. Moreover, only the sialic acid containing part of the whole GQ1b α molecule was shown to be important for MAG binding. Therefore, we decided to use a chemo-enzymatic approach for syntheses of the GQ1b α mimetics. For that purpose we expressed recombinant eukaryotic rST3Gal III (EC 2.4.99.6) and hST6Gal I (EC 2.4.99.1), and recombinant prokaryotic *Campylobacter jejuni* α -2,3/2,8 bifunctional sialyltransferase (Cst-II) using different expression systems. The enzymes were purified and biochemical characterized towards several natural and non-natural acceptor substrates, and used for the preparative chemo-enzymatic synthesis of different carbohydrate structures, e.g. [NeuNAc α (2,8)]NeuNAc α (2,3)Gal β (1,3)GlcNAc- β -OLEm; NeuNAc α (2,3)Gal β (1,4)GlcNAc- β -OLEm; NeuNAc α (2,3)Gal β (1,4)Glc- β -OLEm;).

TABLE OF CONTENT

| | | |
|----------|---|----------|
| 1 | Introduction | 1 |
| 1.1 | The carbohydrates | 1 |
| 1.2 | The eukaryotic glycosyltransferases | 2 |
| 1.2.1 | Sequential glycosyltransferase action..... | 4 |
| 1.2.2 | Recombinant DNA technology of the glycosyltransferase gene | 5 |
| 1.2.3 | Primary sequence and secondary structure similarity of glycosyltransferases | 5 |
| 1.2.4 | Topogenesis and intracellular transport of glycosyltransferases..... | 7 |
| 1.2.5 | Regulation of glycosyltransferase gene expression | 8 |
| 1.2.6 | Glycosyltransferases as glycoproteins..... | 8 |
| 1.2.7 | The catalytic domain: structure and mechanism..... | 8 |
| 1.2.8 | Sialyltransferases..... | 11 |
| 1.2.8.1 | Donor and acceptor substrate of the sialyltransferase | 13 |
| 1.2.8.2 | Cloning of mammalian sialyltransferases..... | 16 |
| 1.2.8.3 | Regulation of the sialyltransferase gene expression and functionality | 16 |
| 1.2.8.4 | Sialyltransferase classification and nomenclature..... | 17 |
| 1.2.8.5 | Sialyltransferase family | 17 |
| 1.3 | Prokaryotic glycosylation | 21 |
| 1.3.1 | Possible role of protein glycosylation in pathogenic bacteria | 22 |
| 1.3.2 | Bacterial glycosyltransferases | 22 |
| 1.3.3 | <i>Campylobacter jejuni</i> | 23 |
| 1.3.3.1 | Lipo(oligo)polysaccharides (LOS/LPS) | 25 |
| 1.3.3.2 | Bifunctional α -2,3/2,8 sialyltransferase (Cst-II) | 27 |
| 1.4 | Enzymes for chemical synthesis | 29 |
| 1.5 | Myelin-associated inhibitors of axonal regeneration in the adult | |

| | |
|--|-----------|
| mammalian CNS | 31 |
| 1.5.1 Myelin and myelin-associated inhibitors..... | 31 |
| 1.5.1.1 Myelin-associated glycoprotein | 32 |
| 1.5.1.2 Nogo | 34 |
| 1.5.1.3 Oligodendrocyte myelin glycoprotein | 35 |
| 1.5.2 Receptors for myelin-associated inhibitors of axonal regeneration..... | 36 |
| 1.5.3 Gangliosides as a MAG functional ligands..... | 38 |
| 2 The Aim | 40 |
| 3 Materials and Methods | 41 |
| 3.1 <i>r</i> ST3Gal III expression in baculovirus-infected cells, purification and characterization | 41 |
| 3.1.1 Insect cell culture and virus methods | 41 |
| 3.1.1.1 Insect cell culture | 41 |
| 3.1.1.2 Long-term insect cell storage [231] | 42 |
| 3.1.1.3 Amplification of virus stocks [231] | 43 |
| 3.1.1.4 Determining virus titer by end-point dilution | 44 |
| 3.1.1.5 Virus storage [231]..... | 45 |
| 3.1.2 <i>r</i> ST3Gal III expression in baculovirus infected insect cells | 45 |
| 3.1.3 Analysis of the expressed <i>r</i> ST3Gal III..... | 46 |
| 3.1.3.1 Sodium dodecyl sulfate – polyacrylamide gel electrophoresis (SDS-PAGE) | 46 |
| 3.1.3.2 SDS-PAGE staining [233] | 48 |
| 3.1.3.3 Western blot analysis [234]..... | 49 |
| 3.1.3.4 Immunodetection | 50 |
| 3.1.4 Purification of the <i>r</i> ST3Gal III protein [236]..... | 51 |
| 3.1.4.1 Bradford protein assay [237,238]..... | 51 |

| | | |
|---------|--|----|
| 3.1.5 | <i>r</i> ST3Gal III enzyme activity assay [239]..... | 52 |
| 3.1.5.1 | Stability of <i>r</i> ST3Gal III during the long-period incubation | 53 |
| 3.1.6 | Long-term enzyme storage | 53 |
| 3.1.7 | Determination of the enzyme kinetic parameters [241] | 54 |
| 3.1.8 | Preparative synthesis [242,243]..... | 55 |
| 3.1.8.1 | A synthesis of NeuNAc α (2,3)Gal β (1,4)GlcNAc- β -OLem (7) product | 55 |
| 3.1.8.2 | A synthesis of NeuNAc α (2,3)Gal β (1,3)GlcNAc- β -OLem (8) product | 55 |
| 3.1.8.3 | A synthesis of NeuNAc α (2,3)Gal β (1,3)GalNAc- β -OSE (9) product | 56 |
| 3.1.8.4 | A synthesis of NeuNAc α (2,3)Gal β (1,3)GalNHTCA- β -OSE (10) product | 56 |
| 3.1.8.5 | A synthesis of NeuNAc α (2,3)Gal β (1,3)Gal- β -OSE (11) product | 56 |
| 3.1.8.6 | A synthesis of NeuNAc α (2,3)Gal β (1,3)[NeuNAc α (2,6)]Gal- β -OSE (12) product | 56 |
| 3.2 | <i>h</i> ST6Gal I expression in BHK-21 cells, purification and characterization | 58 |
| 3.2.1 | BT- <i>h</i> ST6Gal I cloning and expression | 58 |
| 3.2.1.1 | Cell culture..... | 58 |
| 3.2.1.2 | Long-term storage..... | 59 |
| 3.2.1.3 | Determination of cell number and viability [249] | 59 |
| 3.2.1.4 | Stable transfection and selection [248] | 59 |
| 3.2.1.5 | The cell clone selection [251]..... | 60 |
| 3.2.1.6 | Optimization of the protein expression..... | 61 |
| 3.2.2 | Analysis of the expressed BT- <i>h</i> ST6Gal I | 61 |
| 3.2.2.1 | SDS-PAGE [239] | 61 |
| 3.2.2.2 | Western blot analysis [239]..... | 62 |
| 3.2.2.3 | Overlay assay | 62 |
| 3.2.3 | BT- <i>h</i> ST6Gal I production [239] | 63 |
| 3.2.4 | Purification of recombinant BT- <i>h</i> ST6Gal I..... | 64 |

| | | |
|---------|--|----|
| 3.2.4.1 | Protein dialysis..... | 65 |
| 3.2.4.2 | Enzyme concentration [239] | 65 |
| 3.2.4.3 | Enzyme storage and stability | 65 |
| 3.2.5 | <i>h</i> ST6Gal I enzyme activity assay [239]..... | 65 |
| 3.2.5.1 | <i>h</i> ST6Gal I turnover..... | 66 |
| 3.2.5.2 | Cell lysis [239]..... | 67 |
| 3.2.6 | Preparative (<i>in vitro</i>) sialylation of glycoconjugates [239] | 67 |
| 3.2.6.1 | Purification of glycoconjugates | 68 |
| 3.2.7 | Mild hydrolysis of NeuNAc | 68 |
| 3.2.8 | Neuraminidase (sialidase) specific cleavage | 69 |
| 3.2.9 | High pH anion-exchange chromatography – pulse amperometric detection of oligosaccharides (HPAEC-PAD) [248]..... | 69 |
| 3.2.10 | Mass spectrometry and methylation analysis of <i>N</i> -glycans..... | 70 |
| 3.3 | α -2,3/2,8 bifunctional sialyltransferase (α -2,3/2,8 ST) expression in <i>E. coli</i> cells..... | 71 |
| 3.3.1 | Bacterial cell growth and culture | 71 |
| 3.3.1.1 | Bacterial strains [252,253] | 71 |
| 3.3.1.2 | Growth media [250]..... | 72 |
| 3.3.2 | Cell competence | 73 |
| 3.3.3 | Cell transformation..... | 75 |
| 3.3.3.1 | Transformation efficiency test (colony forming units)..... | 76 |
| 3.3.4 | Long-term storage of <i>E. coli</i> strains | 77 |
| 3.3.5 | Cloning, expression and purification of α -2,3/2,8 bifunctional sialyltransferase in pEZZ18 vector | 77 |
| 3.3.5.1 | PCR amplification and restriction enzyme digestion of <i>cst-II</i> gene [256,257]..... | 77 |
| 3.3.5.2 | Agarose gel analysis [258]..... | 79 |
| 3.3.5.3 | pEZZ18 vector preparation [259] | 80 |

| | | |
|----------|--|----|
| 3.3.5.4 | DNA quantification [258] | 81 |
| 3.3.5.5 | Ligation | 82 |
| 3.3.5.6 | Analysis of pEZZ18 recombinants | 82 |
| 3.3.5.7 | α -2,3/2,8 bifunctional sialyltransferase expression and determination [259] | 83 |
| 3.3.5.8 | α -2,3/2,8 bifunctional sialyltransferase purification [259] | 84 |
| 3.3.6 | Cloning, expression and purification of α -2,3/2,8 bifunctional sialyltransferase in pET vector expression system | 85 |
| 3.3.6.1 | PCR amplification of <i>cst-II</i> gene [252,257] | 85 |
| 3.3.6.2 | Restriction enzyme digestion of the plasmid DNA and the gene of interest | 87 |
| 3.3.6.3 | Ligation | 87 |
| 3.3.6.4 | Analysis of pET recombinants | 88 |
| 3.3.6.5 | α -2,3/2,8 bifunctional sialyltransferase expression and determination | 88 |
| 3.3.6.6 | Determination of the target protein solubility [260] | 89 |
| 3.3.6.7 | Optimization of the cell growth and enzyme production | 89 |
| 3.3.6.8 | Time course analysis [258,260] | 90 |
| 3.3.6.9 | IPTG induction optimization [252] | 91 |
| 3.3.6.10 | α -2,3/2,8 bifunctional sialyltransferase production | 91 |
| 3.3.6.11 | α -2,3/2,8 bifunctional sialyltransferase purification | 91 |
| 3.3.7 | α -2,3/2,8 ST enzyme characterization | 92 |
| 3.3.7.1 | Enzyme activity assay optimization | 93 |
| 3.3.7.2 | Enzyme activity assay | 94 |
| 3.3.7.3 | Catalytic activity | 94 |
| 3.3.7.4 | Temperature dependent activity | 94 |
| 3.3.7.5 | pH optimization | 95 |
| 3.3.7.6 | Metal ions optimization | 95 |
| 3.3.7.7 | Cofactor dependent enzyme activity | 95 |

| | | |
|----------|--|-----------|
| 3.3.7.8 | Dimethyl sulfoxid dependent enzyme activity | 95 |
| 3.3.7.9 | Determination of the enzyme kinetic parameters [241] | 95 |
| 3.3.8 | Preparative synthesis..... | 96 |
| 4 | Results and discussions | 97 |
| 4.1 | <i>r</i> ST3Gal III expression in baculovirus-infected cells, purification and characterization | 98 |
| 4.1.1 | <i>r</i> ST3Gal III expression and purification | 99 |
| 4.1.1.1 | Amplification of the virus stocks and determination of the virus titer | 99 |
| 4.1.1.2 | Purification of the <i>r</i> ST3Gal III | 99 |
| 4.1.2 | Characterization of the <i>r</i> ST3Gal III enzyme | 103 |
| 4.1.2.1 | <i>r</i> ST3Gal III catalytic activity | 103 |
| 4.1.2.2 | Determination of the enzyme kinetic parameters | 104 |
| 4.1.2.3 | Stability of an enzyme during long-period incubation..... | 107 |
| 4.1.2.4 | Long-term storage of the <i>r</i> ST3Gal III enzyme..... | 108 |
| 4.1.2.5 | Preparative chemo-enzymatic synthesis using <i>r</i> ST3Gal III..... | 109 |
| 4.2 | <i>h</i> ST6Gal I expression in BHK-21 cells, purification and characterization | 111 |
| 4.2.1 | BT- <i>h</i> ST6Gal I cloning and expression | 111 |
| 4.2.1.1 | Overlay assay and Western blotting | 112 |
| 4.2.1.2 | Enzyme activity of BT- <i>h</i> ST6Gal I expressed by BHK-21 isolated cell clones | 114 |
| 4.2.2 | Purification of recombinant BT- <i>h</i> ST6Gal I enzyme | 115 |
| 4.2.3 | Characterization of the BT- <i>h</i> ST6Gal I enzyme | 118 |
| 4.2.3.1 | BT- <i>h</i> ST6Gal I catalytic activity | 118 |
| 4.2.3.2 | Neuraminidase specific cleavage..... | 120 |
| 4.2.3.3 | Preparative <i>in vitro</i> sialylation of glycoconjugates..... | 122 |
| 4.3 | α -2,3/2,8 bifunctional sialyltransferase (α -2,3/2,8 ST) expression in <i>E.</i> | |

| | |
|---|-----|
| <i>coli</i> cells..... | 127 |
| 4.3.1 α -2,3/2,8 ST cloning and expression in pEZZ18 vector | 127 |
| 4.3.1.1 PCR <i>cst-II</i> gene amplification..... | 127 |
| 4.3.1.2 Analysis of pEZZ18 recombinants | 129 |
| 4.3.1.3 α -2,3/2,8 ST enzyme expression | 130 |
| 4.3.1.4 α -2,3/2,8 ST enzyme activity towards non-sialylated acceptors..... | 131 |
| 4.3.1.5 α -2,3/2,8 ST catalytic activity | 133 |
| 4.3.2 α -2,3/2,8 ST cloning and expression in pET vector systems | 134 |
| 4.3.2.1 PCR <i>cst-II</i> gene amplification..... | 134 |
| 4.3.2.2 Analysis of pET recombinants | 135 |
| 4.3.2.3 Determination of the target protein solubility..... | 136 |
| 4.3.3 α -2,3/2,8 ST analysis and purification..... | 138 |
| 4.3.3.1 Enzyme expression and activity optimization..... | 138 |
| 4.3.3.2 Time course analysis of the soluble protein form..... | 139 |
| 4.3.3.3 The enzyme activity related to the culture grown at different temperatures | 140 |
| 4.3.3.4 Purification of the recombinant α -2,3/2,8 ST enzyme | 141 |
| 4.3.4 α -2,3/2,8 ST enzyme characterization | 147 |
| 4.3.4.1 α -2,3/2,8 ST catalytic activity | 147 |
| 4.3.4.2 Temperature dependent enzyme activity | 148 |
| 4.3.4.3 pH dependent enzyme activity | 149 |
| 4.3.4.4 Metal ion-dependent enzyme activity..... | 150 |
| 4.3.4.5 Cofactor dependent enzyme activity | 153 |
| 4.3.4.6 Influence of the dimethyl sulfoxid on the enzyme activity..... | 154 |
| 4.3.4.7 Determination of the enzyme kinetic parameters..... | 155 |
| 4.3.4.8 α -2,3/2,8 enzyme activity of the mutated and truncated enzyme..... | 162 |
| 4.3.4.9 Preparative chemo-enzymatic synthesis using α -2,3/2,8 ST | 163 |

| | | |
|----------|-------------------------------------|------------|
| 5 | Conclusions and Outlook..... | 166 |
| 6 | Abbreviations | 169 |
| 7 | References | 173 |
| 8 | <i>Curriculum vitae</i>..... | 185 |

1 Introduction

1.1 The carbohydrates

Carbohydrates represent major components of the outer surface of mammalian cells. There is now abundant evidence that terminal glycosylation sequences are differentially expressed in cells and are subject to change during development, differentiation and oncologic transformation [1-10].

Many different theories have been advanced concerning the biological role of the oligosaccharide units of individual classes of glycoconjugates. The ability to accurately sequence the oligosaccharide units of glycoconjugates has revealed a remarkable complexity and diversity. However a single common theory has not emerged to explain this diversity [11].

The importance and biological role of the oligosaccharides was presented in number of monographs and review articles. These include a purely structural role in respect to conformation and stability of proteins, the provision of target structures for microorganisms, toxins and antibodies, the masking of such target structures, the control of the half life of proteins and cells, the modulation of protein functions, and the provision of ligands for specific binding events mediating protein targeting, cell-matrix interactions or cell-cell interactions [11]. The covalent addition of sugars to proteins is one of the major biosynthetic functions of the ER. The oligosaccharide could be transferred to the side-chain amide group of asparagine in tripeptide consensus sequence Asn-Xaa-Ser/Thr, *i.e.* N-linked or asparagine-linked glycosylation or to the side-chain OH group of serine/threonine, *i.e.* O-linked glycosylation.

Recently, the correlation of glycosyltransferases (GTs), more precisely, sialyltransferase expression with cancer formation was presented [5]. Thus, the up-regulation of a sialyltransferase in a cancer cell might indicate that a specific signaling pathway has been activated. An example is provided by the up-regulation of ST6Gal I by *ras* oncogene overexpression [12]. Distinct carbohydrate structures and antigens can be formed by coordinated expression of several GTs. For instance, carbohydrate structures containing

GalNAc or Gal β (1,3)GalNAc disaccharide O-glycosidically linked to serine or threonine, as well as their sialylatable forms (*Table 1.1*) are collectively referred to as Thomsen-Friedenreich-related antigens (TF antigens). The biosynthesis of these and other simple O-linked structures depend on the expression of different GTs and has often been correlated with cancer prognosis [5].

Table 1.1 The names and structures of some common oligosaccharide structures used from distinct glycosyltransferases.

| Name | Functional structure |
|---------------------------|--|
| Type I | Gal β (1,3)GlcNAc-R |
| Type II | Gal β (1,4)GlcNAc-R |
| Type III | Gal β (1,3)GalNAc-R |
| Sialyl-Tn antigen | NeuNAc α (2,6)GalNAc-O-Ser/Thr |
| Sialyl-T antigen | NeuNAc α (2,3)Gal β (1,3)GalNAc-O-Ser/Thr |
| Sialyl-Lewis ^a | NeuNAc α (2,3)Gal β (1,3)[Fuc α (1,4)]GlcNAc |
| Sialyl-Lewis ^x | NeuNAc α (2,3)Gal β (1,4)[Fuc α (1,3)]GlcNAc |

1.2 The eukaryotic glycosyltransferases

Glycosylation is a complex yet common form of post-translational protein/lipid modification in cells. Glycosyltransferases (GTs) constitute a large group of enzyme that are involved in the biosynthesis of glycoprotein and glycolipid sugar chains [13,14]. The GTs catalyze transglycosylation reactions where the monosaccharide component of a high-energy nucleotide sugar donor (*e.g.*, GDP-Fuc or CMP-NeuNAc) is transferred to an acceptor (*Figure 1.1*). The acceptor molecules for most GTs are usually oligosaccharides themselves (*Table 1.1*).

It has been estimated that more than 100 distinct glycosidic linkages are present in the glycoconjugate repertoire of vertebrate species. Furthermore, it appears that there are at least several hundred different GT loci in the genome of vertebrates [13,15]. Most of eukaryotic GTs are found within the endoplasmic reticulum and Golgi apparatus [16]. The GTs are a very large family of enzymes of ancient evolutionary origin [17,18]. These enzymes are typically grouped into families based on the type of sugars they transfer (*i.e.*

Figure 1.1 (a) Schematic illustration of the reaction catalyzed by human α -1,3-fucosyltransferase V. The enzyme can utilize both uncharged structures such as *N*-acetylglucosamine (LacNAc) or charged structures such as sialyl-LacNAc [20]. **(b)** Glycosyltransferases utilize a glycosyl donor and an acceptor substrate. Glycosyl donors include nucleotide sugars and dolichol-phosphate-linked mono- and oligosaccharides. Acceptors are most commonly oligosaccharides or rarely monosaccharides. Proteins and ceramides are also acceptors for the glycosyltransferases that initiate glycoprotein and glycolipid synthesis.

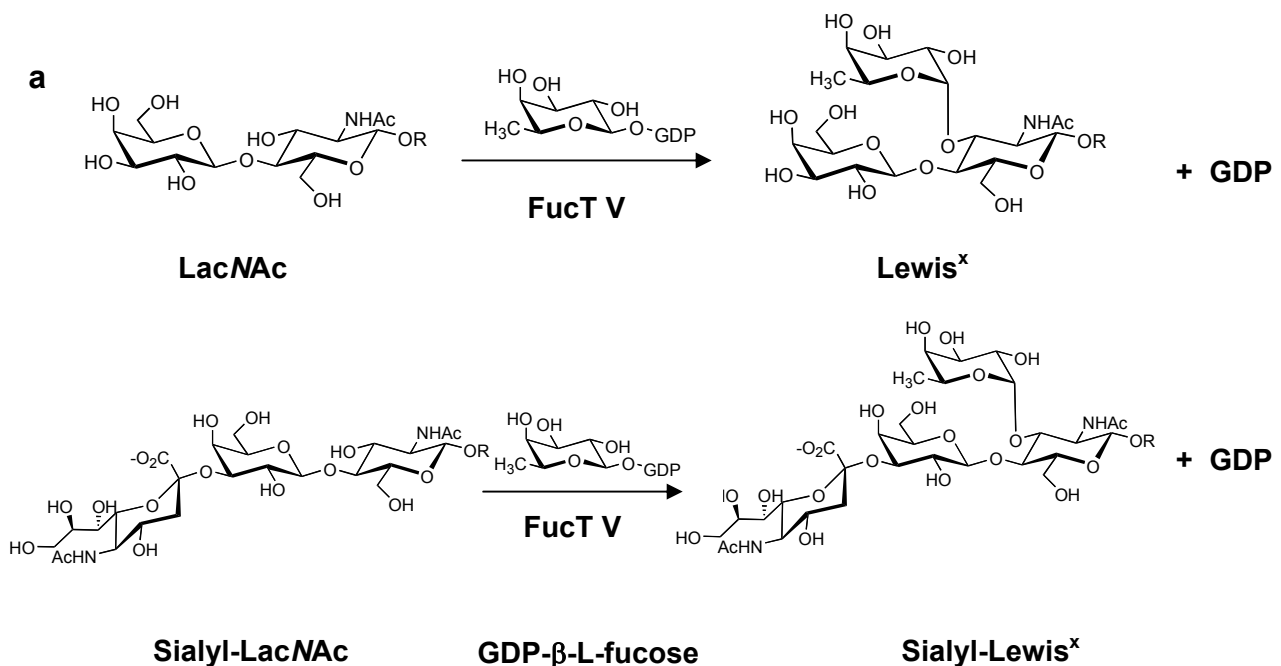
Glycoprotein synthesis can require an initiating attachment of a single monosaccharide to a threonine or serine residue (*O*-glycosylation) and asparagine residue (*N*-glycosylation) [21]. In this instance, a protein serves as the acceptor substrate. Finally, glycolipid biosynthesis begins with a galactosyltransferase or glucosyltransferase that utilizes a ceramide as an acceptor molecule. There are, of course, other GTs in Nature that are not involved in glycan biosynthesis, such as those involved in forming small sugar glycosides (*e.g.*, in the detoxification of drugs by glucuronidation).

1.2.1 Sequential glycosyltransferase action

Glycosyltransferases act sequentially, such that the oligosaccharide product of one enzyme yields a product that serves as the acceptor substrate for the following action of other GTs, a characteristic known as “cooperative sequential specificity” [17,22]. The final result is a linear and/or branched polymer composed of monosaccharides linked to one another specifically [22]. This precision is a result of the very narrow acceptor substrate specificity exhibited by most GTs. A central dogma of glycobiology, concerning virtually all known vertebrate GTs, is that each glycosidic linkage is the product of a single enzyme. This is known as “one (glycosidic)-linkage, one enzyme” principle [17].

The “one (glycosidic)-linkage, one enzyme dogma” has several exceptions, *i.e.* it is becoming clear that a specific glycosidic linkage may actually be the product of one of several structurally and genetically related enzymes, that a few GTs (*e.g.*, Cst-II) can synthesize two different glycosidic linkages, and that the acceptor specificity of an enzyme can be modified by another protein (*e.g.*, α -lactalbumin) [23,24].

galactosyltransferases, sialyltransferases etc.). The GT families that received the most attention are those that add terminal sugars to glycoconjugates and that therefore play major roles in recognition and signaling events, *i.e.* sialyltransferases and fucosyltransferases. Also of importance are the polypeptide: *N*-acetylgalactosaminyltransferases that initiate mucin-type *O*-glycosylation. Despite the fact that many GTs recognize identical donor and acceptor substrates, few regions of enzyme homology have been found among the different classes of eukaryotic glycosyltransferases. Therefore, the enzymes that are structurally related most often catalyze the same or similar reaction [19].



b

| Glycosyl donors | Glycosyl acceptors |
|------------------------------------|---------------------------|
| CMP-Sialic acid (CMP-NeuNAc) | Oligosaccharides |
| GDP-Fucose | Monosaccharides |
| GDP-Mannose | Proteins |
| UDP-Galactose | Lipids (Ceramides) |
| UDP- <i>N</i> -Acetylgalactosamine | |
| UDP- <i>N</i> -Acetylglucosamine | |
| UDP-Glucose | |
| UDP-Glucuronic acid | |
| UDP-Xylose | |
| Dolichol-P-Glucose | |
| Dolichol-P-Mannose | |

In a few cases, the underlying protein is known to specifically dictate the action of a particular GT (e.g., glycoprotein glucosyltransferase).

1.2.2 Recombinant DNA technology of the glycosyltransferase gene

The problem in molecular cloning of GTs can be explained by the fact that these enzymes are often extraordinarily difficult to purify in quantities sufficient to obtain protein sequence information or to generate specific antisera [16,17]. Subsequently, it has become possible to clone new GT loci using low-stringency cross-hybridization approaches, and methods involving PCR with primers derived from conserved sequences among members of a GT gene family [15,17,18,25-27]. Recently, expressed sequence tag (EST) databases have served as a rich source for finding new GTs.

1.2.3 Primary sequence and secondary structure similarity of glycosyltransferases

Cloned GTs clearly show similarity in the nucleotide sequence within members of some enzyme families [27]. However, there is relatively limited homology between members of different families [13,28]. These observations imply that the different GT families are evolutionarily very ancient and that there have been strong selection pressures maintaining sequence similarities within families [17,18]. Sensitive hydrophobic cluster analysis (HCA) of sequence similarities within families has yielded a few shared amino acid sequence motifs [29-31]. The first of these recognized were the "sialyl motifs" that are shared among different sialyltransferases [27].

Despite the lack of sequence homology between different families of GT, almost all of the Golgi enzymes do share some secondary features [17]. Early studies of the cell biology and biochemistry of vertebrate GTs indicated that some GT could be found as soluble forms in secretions and body fluids (e.g., blood, lymph, breast milk, colostrums etc.); others were identified as membrane-bound GTs within cells, whereas some GTs exhibited both properties [17,32].

Golgi GTs share a common secondary structure: a single transmembrane domain flanked by a short amino-terminal domain and a longer carboxy-terminal domain. This structure is characteristic of type II transmembrane proteins consisting of a short amino-terminal

cytoplasmic domain followed by a transmembrane domain (TMD), a proteolytically sensitive “stem” region, and a large globular catalytic domain facing the luminal side of the Golgi apparatus (*Figure 1.2*) [17,18]. The large carboxy-terminal domain corresponds to the catalytic domain of the GT [13,32]. The intraluminal location of this domain allows it to participate in the synthesis of the growing glycans displayed by glycoproteins and glycolipids during their transit through the secretory pathway [33,34].

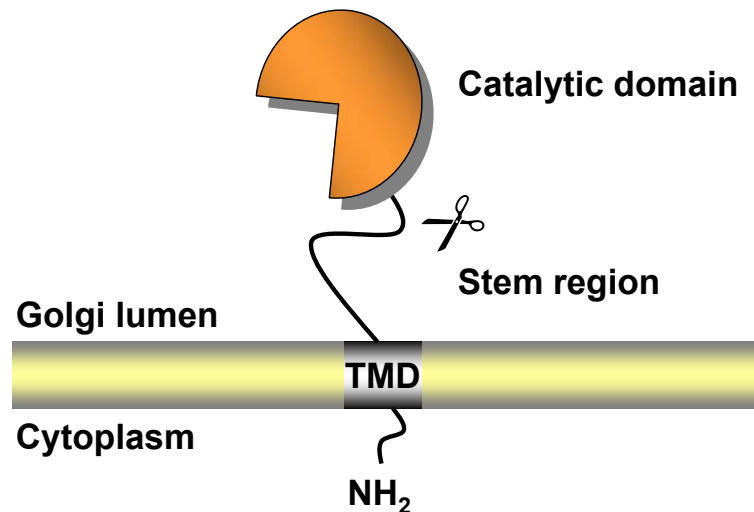


Figure 1.2 Topology of Golgi resident glycosyltransferases. TMD corresponds to the transmembrane domain. Stem region sensitive to proteolytical cleavage generated by cathepsin-like proteases (✂).

Many Golgi enzymes are secreted by cells as soluble or membrane-bound proteins. Soluble forms are derived from membrane-associated forms by virtue of one or more proteolytic cleavage events which occur in the “stem region” [17,32]. These proteolytic cleavage events release a catalytically active fragment of the GT from its transmembrane tether and allow the cell to export this fragment to the extracellular milieu [32]. The nature of the signals within the GT sequence that direct proteolysis is not defined, but it appears that the proteolytic cleavages are relatively specific and are generated by certain cathepsin-like proteases functioning in the *trans* Golgi apparatus [13,32,35,36]. The production of these soluble form of GTs from cell types such as hepatocytes and endothelial cells can also be dramatically up-regulated under certain inflammatory conditions [35]. Since these circulating enzymes do not have access to adequate concentrations of donor sugar nucleotides, which are primarily inside cells, they are functionally incapable of carrying out a transfer reaction.

1.2.4 Topogenesis and intracellular transport of glycosyltransferases

Studies concerning biochemical analysis of the cell indicate that GTs partially segregate into distinct compartments within the secretory ER-Golgi pathway, *i.e.* enzymes acting early in glycan biosynthetic pathways have been localized to *cis*-Golgi network and *cis* and *medial* cisternae of the Golgi, whereas enzymes acting later in the biosynthetic pathway tend to colocalize in the *trans*-Golgi cisternae and the *trans*-Golgi network (TGN) [37-42]. The transport of proteins through the Golgi compartments is mediated by transport vesicles and involves complex budding and fusion events [43-45]. These observations have encouraged extensive exploration of the mechanisms whereby GTs achieve this compartmental segregation [38,46]. Unlike the carboxy-terminal tetrapeptide KDEL associated with the ER-protein retention and retrieval signal, “Golgi retention motif” for distinct GTs are located within the cytoplasmic and transmembrane domains [13,38,46-48]. Most information relevant to retention of GTs within specific Golgi compartments derives from experiments done with α -2,6 sialyltransferase (ST6Gal I), a β -1,4 galactosyltransferase (GalT I), and an *N*-acetylglucosaminyltransferase I (GlcNAcT I). The first two enzymes tends to concentrate in the *trans*-Golgi compartments and the *trans*-Golgi network, whereas GlcNAcT I localizes mostly to the *medial*-Golgi compartment [48,49].

Two types of models were proposed to explain retention of different GTs in specific Golgi subcompartments. The first model, the oligomerization/kin recognition model is based on retention of Golgi proteins through oligomerization and their inability to enter a transport vesicles destined for the next secretory pathway compartment, and the second model, the bilayer thickness model which postulates retention through differences in membrane thickness along the exocytic pathway [48-50].

1.2.5 Regulation of glycosyltransferase gene expression

Apart from the Golgi factors that can regulate GT functions, their actual expression can be controlled at the level of mRNA synthesis or turnover. The level of protein and activity is often directly correlated with the level of mRNA [17]. Studies have indicated that although the expression patterns of some glycosyltransferase mRNAs are highly regulated in a tissue-specific and developmental manner, others have a widespread so-called "housekeeping" type of distribution [17]. Examples of both can be found within any given family of enzymes. For the most part, it appears that differential regulation is due to the action of specific promoter regions in the 5' region of the corresponding genes [51]. In the case of some genes (e.g., ST6Gal I), there is evidence for multiple tissue-specific promoters that are activated under different biological circumstances [52].

1.2.6 Glycosyltransferases as glycoproteins

Many Golgi GTs have consensus *N*-glycosylation sequences, as well as serine and threonine residues that could be modified by glycosylation processes [13,17]. Biochemical analyses indicate that many mammalian GTs are indeed post-translationally modified by glycosylation, especially *N*-glycosylation [38]. Glycosylation is required for proper folding and/or activity, and limited studies indicate that GTs are also subject to "self-glycosylation" and that their activity could be modified and regulated by phosphorylation [53,54].

1.2.7 The catalytic domain: structure and mechanism

For many years, the knowledge of the mechanism of action of GTs was hampered by the lack of 3D-structures particularly of eukaryotic GTs. The first X-ray crystal structure to be solved was the β -glucosyltransferase of phage T4, in 1994 [55]. In the past two years, seven crystal structures of GTs from prokaryotes and eukaryotes have been determined. Furthermore, comparison of crystal structures revealed that GTs are probably comprised of an unexpected small number of protein folds. Although belonging to different GT families showing no primary sequence identity, the various 3D structures reported to date share a similar class of fold, consisting in the three-layer $\alpha/\beta/\alpha$ sandwich that resembles the "Rossmann fold". On a structural basis, these GT structures have been classified into two distinct superfamilies. The so-called GTA (glycosyltransferase A) superfamily is

composed of α/β proteins with a single Rossmann domain [56], a conserved DXD motif and two closely associated domains forming a conical shape with a large active site cleft on one face capable to accommodate both the donor and acceptor substrate [57-59]. The GTB (glycosyltransferase B) superfamily includes α/β proteins (e.g. β -GlcT and β 4-GlcNAcT) comprising two similar Rossmann domain separated by a deep substrate-binding cleft [60,61]. The DXD motif is known to coordinate with two valencies of the cation (see below) involved in binding of the nucleotide sugar through interaction with the diphosphate moiety [62,63]. The metal cofactor is generally considered as a Lewis acid catalyst in the reaction mechanism by stabilization of the leaving nucleoside diphosphate. Mutagenesis studies of the conserved Asp (D) residue in the DXD motif of glycosyltransferases from various species have shown that the removal of the Asp residues, and hence the metal ions, completely eliminates the transferase activity [62-66].

Most glycosyltransferase-dependent transglycosylations involve a 2+ charged cation as cofactor (typically Mg^{2+} or Mn^{2+}), and the enzymes tend to be most active in the pH range of 5.0 to 7.0, which reflects pH values found in various parts of the ER-Golgi-plasmalemma pathway. GTs typically exhibit Michaelis-Menten constants (K_M) for nucleotide sugar substrates in the low micromolar range, when assayed *in vitro*. In general, K_M values for acceptor substrates observed *in vitro* can vary dramatically for different enzymes, ranging from low micromolar values to low millimolar values [18]. However, *in vitro* assays are not likely to faithfully represent circumstances found in the subcellular compartments of the ER-Golgi pathway, *in vivo* function of these enzymes [18]. Moreover, these assays often utilize acceptor analogs composed of only a small portion of the physiological substrate. For these reasons, *in vitro* acceptor K_M data in the literature may not reflect actual affinities for the natural substrates [67]. For most GTs, specific recognition of the acceptor covers only one or a few monosaccharide units or another residue, such as a lipid or an amino acid [14,68,69].

The catalytic sites of most GTs face the lumen of various compartments in the Golgi apparatus, and the low-molecular-weight sugar nucleotide-donors are made in the cytosol [34]. Several factors can regulate the action of each Golgi GT, including the intraluminal concentration of the sugar nucleotide donor resulting from donor transport, the presence of specific sugar nucleotide degrading enzymes, competition by other GTs for the same donors or acceptors, the intraluminal concentration of the acceptors, the intraluminal pH, and the time taken for passage of the acceptor molecule through a given Golgi

compartment. In an intact cell, many or all of these factors may affect the final structures of the glycans synthesized on a given glycoconjugate that is passing through the Golgi apparatus [17,34].

Concerning the mechanism of GTs catalytic reaction, there are two mechanisms proposed for the GTs using sugar nucleotides as a donor substrate. Based on the stereochemistry of the glycosidic bond formed at the C1 position of the sugar donor, two types of GTs can be distinguished: inverting and retaining stereochemistry at the anomeric center (*Figure 1.3*) [31].

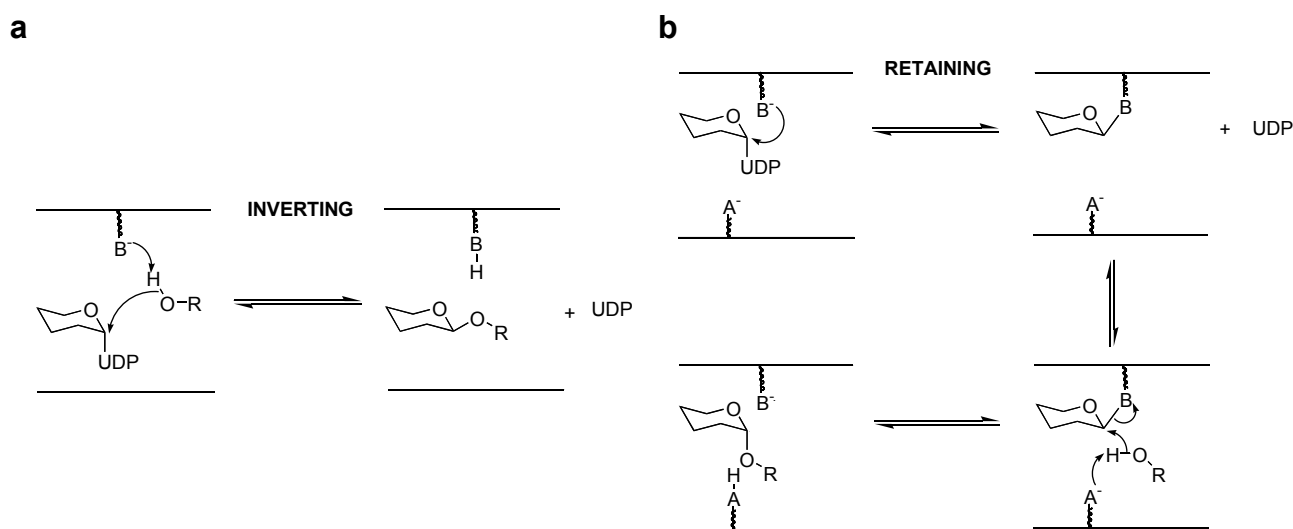


Figure 1.3 The two mechanisms proposed for glycosyl transfer from sugar nucleotides. **(a)** In the inverting mechanism, a single nucleophilic substitution at the anomeric carbon of the donor leads to the formation of a β -linkage from an α -linked donor; ROH represents the acceptor, and B represents the catalytic base. **(b)** The retaining mechanism involves the transient formation of a glycosyl enzyme complex and a subsequent substitution by the acceptor. The two nucleophilic substitutions at the sugar anomeric carbon result in the formation of an α -linkage from an α -linked donor; ROH represents the acceptor, A represents the catalytic base, and B represents the nucleophile [31].

Retaining GTs result in glycosidic bonds with stereochemistry identical to that of the glycosyl donor, whereas inverting enzymes produce glycosidic bonds of the opposite stereochemistry [28,31]. Among the GTs analyzed, catalysis necessarily takes place by an “inversion” mechanism, as the donor substrates used in these reactions are α -linked sugar nucleotides (*e.g.*, UDP-glucose, UDP-*N*-acetylglucosamin *etc.*) from which the sugar is transferred to the acceptor molecule forming a β -linked product. Concerning our work, next

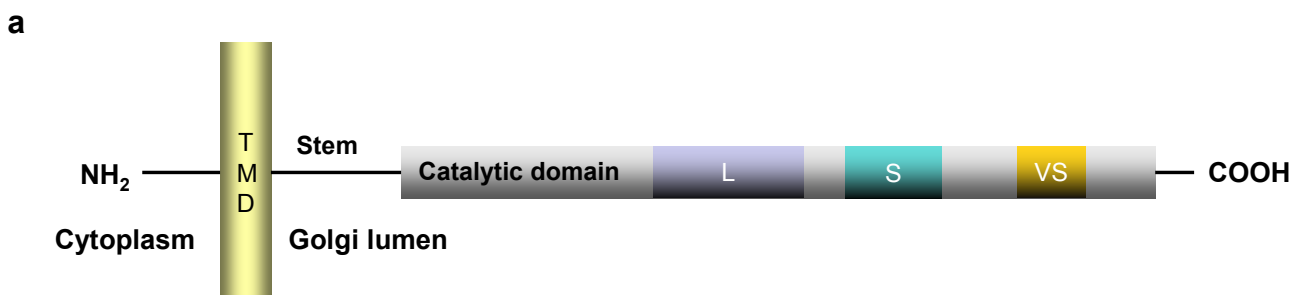
chapter will be related to one of the inverting enzymes, *i.e.* sialyltransferase.

1.2.8 Sialyltransferases

Sialyltransferases (STs) are a family of glycosyltransferase that use CMP-NeuNAc as the activated sugar donor to catalyze the transfer of sialic acid residues to terminal non-reducing positions of oligosaccharide chains of glycoproteins and glycolipids [70,71]. Each of the sialyltransferase genes is differentially expressed in a tissue-, cell type-, and stage-specific manner to regulate the sialylation pattern of cell's glycoconjugates. These enzymes differ in their substrate specificity, tissue distribution and various biochemical parameters. Enzymatic analysis conducted *in vitro* with recombinant enzyme revealed that one linkage can be synthesized by multiple enzymes [23].

The mammalian sialyltransferase family consists of more than 20 Golgi membrane-bound sialyltransferases, 15 of which have been cloned in human [23]. They are Type II transmembrane glycoproteins with a short 3-11 amino acid NH₂-terminal cytoplasmic domain, which is not essential for catalytic activity, a 16-20 amino acid transmembrane (signal anchor) domain, a 30-200 amino acid extended stem region, followed by large 300-350 residue COOH-terminal catalytic domain [13]. These enzymes have been shown to be topologically restricted to trans cisternae and the trans Golgi network of the Golgi apparatus [72], although catalytically active soluble forms can be generated *in vivo* by proteolytic cleavage at the stem region, *e.g.* serum soluble ST6Gal I produced by proteolytic cleavage at the stem domain [32].

Even though eukaryotic sialyltransferases share the same sugar donors and recognize identical acceptor substrates, they do not exhibit similar protein structure except of the three short and conserved consensus sequences present in the catalytic domain (*Figure 1.4 a*) [26,73].



b

| Sialyl motif L | | Residues |
|-----------------------|--|-----------------|
| ST3Gal I | RC AV VGN SGN LKDSS Y GPEIDSHDFV L RMNKAPTGG-FEAD V GSRD | (138-182) |
| ST6Gal I | RC AV VSSAG S LKNSQLGREIDNHDAV L RFNGAPTDN-FQ QD V G TKT | (180-224) |
| ST6GalNAc I | T CA V V GN GGI LND SR VGREIDSHDYV F RLSGAVIKG-YEQ D V G TRT | (292-336) |
| ST8Sia I | K CA V V GN GGI LK MSG CGRQID EAN F VM RCNLPPLSSEYTR D V G SKT | (136-181) |

| Sialyl motif S | | Residues |
|-----------------------|--|-----------------|
| ST3Gal I | P ST GILSII F SIHI C DEV D LYGF | (264-286) |
| ST6Gal I | P SS G M LGIIIM T L C DQ V DIYEF | (318-340) |
| ST6GalNAc I | P TT G A LLLLL T AL Q L C DK V SAYGF | (447-469) |
| ST8Sia I | L ST G L FLV S AAL G L C EE V SIYGF | (272-294) |

| Sialyl motif VS | | Residues |
|------------------------|---|-----------------|
| ST3Gal I | T G V H D G D F E Y NIT | (309-321) |
| ST6Gal I | G A Y H PL L L F E K N M V | (363-374) |
| ST6GalNAc I | Y I N H D F R L E R M V W | (492-503) |
| ST8Sia I | S G Y H A M P E E F L Q L | (304-316) |

Figure 1.4 (a) Schematic structure of sialyltransferase showing the relative positions of sialyl motif L, S and VS. TMD corresponds to the transmembrane domain. **(b)** Amino acid sequences of sialyl motif L, S, and VS in four sialyltransferases. Conserved amino acid residues in the all sialyltransferases are shown in bold red letters.

The L (large, 50 amino acids)-, S (small, 23 amino acids)- and VS (very small, 6 amino acids) sialyl motifs appear to be specific for eukaryotic enzymes, as they are not present in any of the cloned prokaryotic STs that catalyze similar reactions [74-77]. In all of the known ST sequences, the number of invariant residues in L-, S- and VS- sialyl motif is 7, 2 and 2, respectively, with one cysteine residue being conserved in each region (*Figure 1.4 b*). The functional significance of the sialyl motifs has been investigated by site-directed mutagenesis, using ST6Gal I as a model enzyme. The replacement of the most conserved residues by alanine showed that sialyl motif L is mainly involved in donor substrate binding, whereas mutation in the sialyl motif S affected both, donor and acceptor binding [27,78]. The mutation of the two conserved cysteine residues generates inactive enzymes. This supports the hypothesis that these residues are involved in disulfide bond formation, the presence of which is required for the formation of the active conformation [26].

1.2.8.1 Donor and acceptor substrate of the sialyltransferase

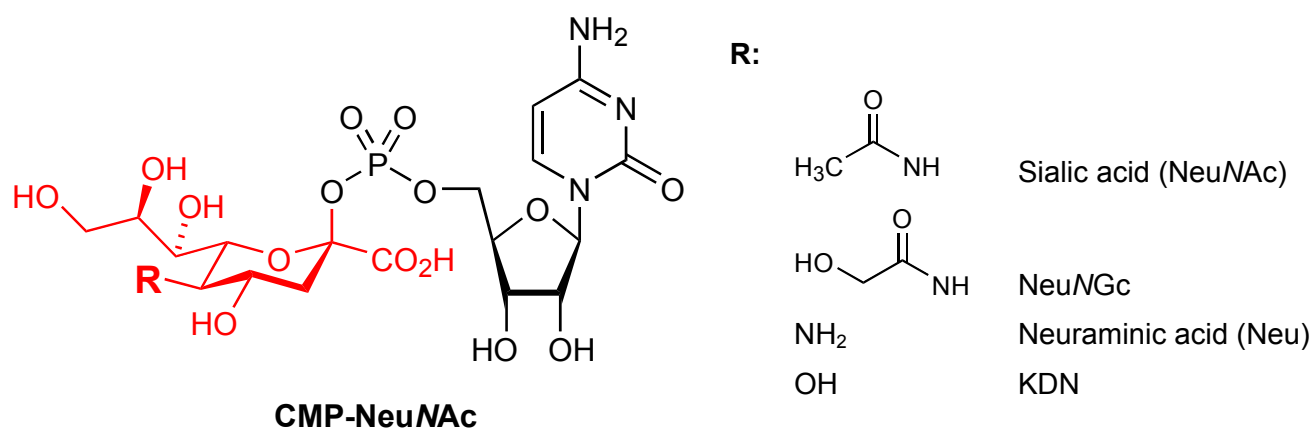


Figure 1.5 Molecular structure of an activated nucleotide-*N*-acetylneuraminic acid (CMP-NeuNAc). Activated sialic acid is shown in red.

Sialic acids (*Figure 1.5*), ubiquitous components of mammalian glycoproteins and glycolipids, are a family of closely related neuraminic acids found at the non-reducing terminal positions of glycoconjugates. Because of their terminal position and their negative charge at physiological pH, sialylated oligosaccharide sequences have long been predicted to be information – containing molecules and critical determinants, *e.g.* in cell-cell recognition processes, cell-matrix interactions and maintenance of serum glycoproteins in the circulation [79,80]. The cell surface sialic acid residues have been known to act as receptors for the influenza virus [81]. They often function in the “anti-recognition” or masking of the carbohydrate groups they terminate [80].

More than 36 derivatives of the sialic acid molecule have been identified [82,83]. The C-5 position commonly bears a *N*-acetyl group (NeuNAc) or a hydroxyl group forming 2-keto-3-deoxy-d-glycero-d-galactonononic acid (KDN). The 5-*N*-acetyl group can also be hydroxylated, giving *N*-glycolylneuraminic acid (NeuNGc) or occasionally de-*N*-acetylated, giving neuraminic acid (Neu) (*Figure 1.5*). These four molecules (NeuNAc, NeuNGc, KDN, and Neu) have the potential for additional substitutions at the hydroxyl groups on the 4-, 7-, 8-, and 9-carbons (*O*-acetyl, *O*-methyl, *O*-sulfate, and *O*-phosphate groups). Sialic acids are glycosidically linked to either the 3- or 6-hydroxyl group of a galactose residue (Gal), or to the 6-hydroxyl group of *N*-acetylglucosamin (GlcNAc) or *N*-acetylgalactosamine (GalNAc) residues. They can form polysialic chains via their 8-hydroxyl group and

terminate with a sialic acid branched via the 8- or 9-hydroxyl group [71].

NeuNAc and KDN are believed to be the metabolic precursors for all other sialic acids. They are derived by the condensation of ManNAc-6-P (for NeuNAc) or Man-6-P (for KDN) with activated forms of pyruvate. Following dephosphorylation, the free sialic acid is activated into the nucleotide donor CMP-NeuNAc (Figure 1.6) [80].

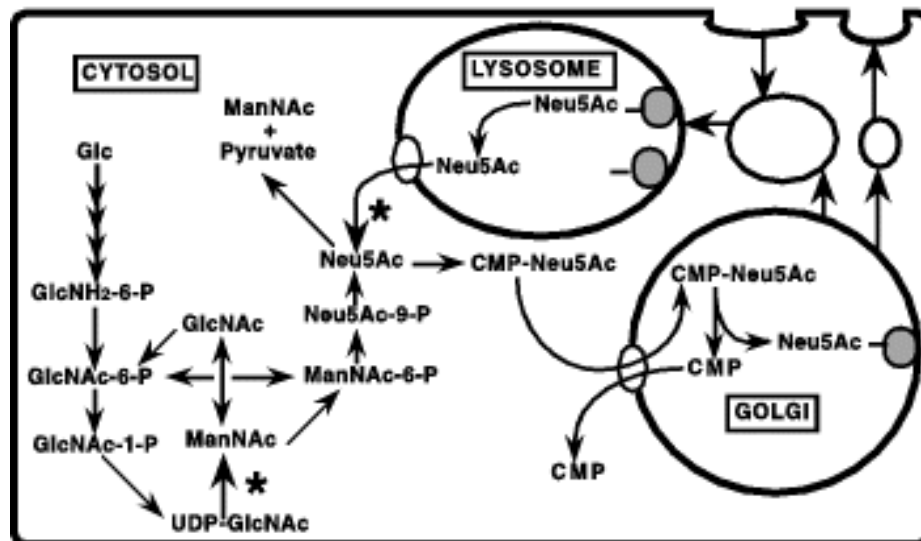


Figure 1.6 Life cycle of sialic acids. The general pathways for biosynthesis, activation, transfer, and recycling of the common sialic acid (NeuNAc). The asterisks indicate the pathways considered to be the major sources of sialic acids for CMP-NeuNAc synthesis.

Polysialic acid (PSA) is a homopolymeric structure made of sialic acid molecules joined by α -2,8 glycosidic bonds, which is found only in a few animal glycoproteins, e.g. the N-CAM molecules, and also in the capsules of neuroinvasive bacteria [84]. The predominant building units of PSA in mammals are NeuNAc and KDN. PSA chains form large, negatively charged and highly hydrated structures, and the expression of these “space filling” carbohydrate chains attenuates cellular interactions and increases motility.

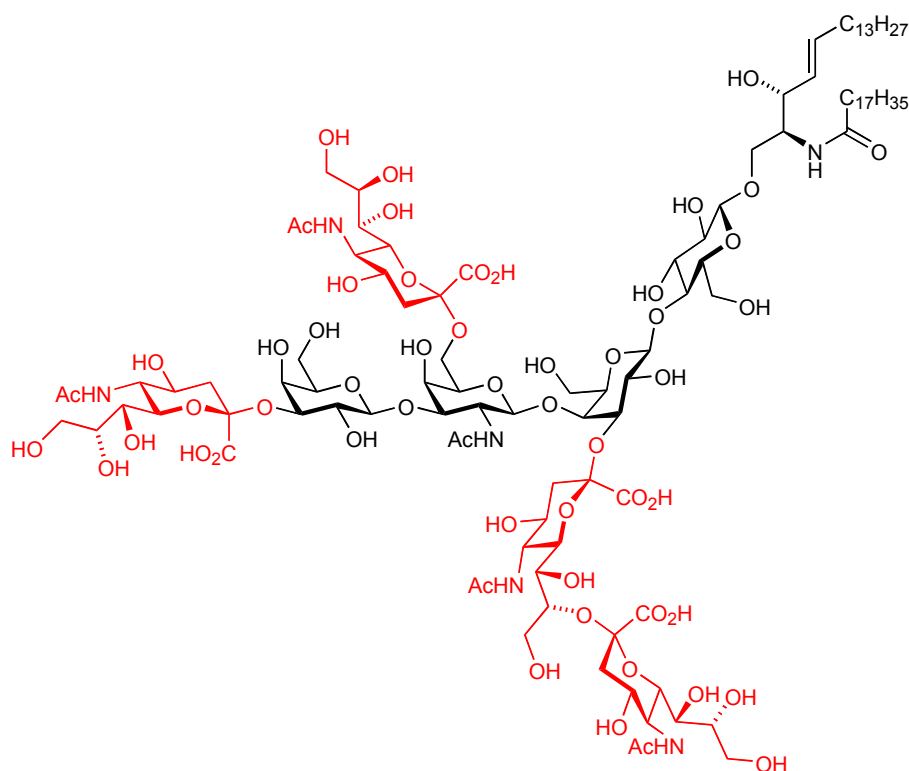


Figure 1.7 Molecular structure of GQ1b α ganglioside. The α -2,3 and α -2,8 sialic acid are red colored.

The minimal motif that defines the glycosphingolipids (glycolipids) is a monosaccharide, e.g. glucose or galactose attached directly to a ceramide unit, e.g. glucosylceramide or galactosylceramide [85]. Ganglioside biosynthesis is achieved by the sequential addition of a carbohydrate unit to an existing glycolipid acceptor and is catalyzed by specific glycosyltransferases acting in parallel pathways. The most complex of the glycosphingolipids, the gangliosides (*Figure 1.7*), contain oligosaccharides with one or more sialic acid residues, which give gangliosides a net negative charge. Those complex molecules are usually synthesized by several sialyltransferases such as ST3Gal V (GM3 synthase), ST6GalNAc V (GD1 α synthase), ST6GalNAc VI (GD1 α , GT1 α , GQ1b α synthase), ST8Sia I (GD3 synthase) and ST8Sia V. Gangliosides are most abundant in the plasma membrane of nerve cells, e.g. in the central nervous system (CNS), where they constitute 5–10% of the total lipid mass. The levels and types of gangliosides change during neural differentiation and development [11,18,86]. Gangliosides are also thought to function in cell-recognition processes, in which membrane-bound carbohydrate-binding proteins (lectins) bind to the sugar groups on both glycolipids (gangliosides) and glycoproteins [87]. More than 40 different gangliosides have been identified and named

according to the system suggested by Svennerholm [88]. The ganglioside GM1 for example, acts as a cell-surface receptor for the bacterial toxin that causes the debilitating diarrhea of cholera. Cholera toxin binds to and enters only those cells that have GM1 on their surface, including intestinal epithelial cells [89]. Furthermore, MAG, a member of the Siglec family of sialic acid binding lectins, binds to sialoglycoconjugates on axons, and particularly to gangliosides GD1a and GT1b, which may mediate some of MAG's inhibitory effects, *i.e.* inhibition of the neurite outgrowth. Obviously, it was important to clone sialyltransferases in order to understand the biosynthetic pathway of sialoglycoconjugates.

1.2.8.2 Cloning of mammalian sialyltransferases

The ST6Gal I from rat is the second GT and the first sialyltransferase to be cloned in 1987 by Weinstein *et al.* [32]. In 1990, Grundmann *et al.* have cloned the first human sialyltransferase (ST6Gal I) [90]. The enzymes were cloned using a traditional approach involving purification of native sialyltransferase and screening of the lambda library. This method was replaced by an RT-PCR method, which took an advantage of conserved sialyl motifs to create degenerate synthetic primers. This allowed the cloning of cDNAs of additional sialyltransferase family members [18]. Because of the fact that unique sialyltransferase genes cloned from the same species typically exhibit <50% homology, the majority of the known sialyltransferase cDNAs were identified by this approach [91].

1.2.8.3 Regulation of the sialyltransferase gene expression and functionality

With only a few exceptions, a single sialic acid structure can be synthesized by more than one sialyltransferase. Strict development and tissue-specific programs govern the expression of the individual sialyltransferase genes [92-95].

The relative expression of sialyltransferases influences the expression of sialylated compound at the cell surface and contributes to the definition of the glycosylation pattern of normal and tumor cells. Sialyltransferase expression appears to be regulated mainly at the level of transcription with a strong correlation between mRNA expression levels and enzyme activity levels. Because sialyltransferases are expressed in most cells and tissues, where their function can be different, evolution of distinct promoters provide additional ways to modulate their expression. Post-translational modifications of sialyltransferase proteins may also modulate enzymatic activity [23].

1.2.8.4 Sialyltransferase classification and nomenclature

Sialyltransferases can be divided into three broad classes according to the glycosidic linkage of sialic acid formed with the acceptor substrate. Under the nomenclature proposed by Tsuji *et al.* [91] these broad classes are designated ST3, ST6 and ST8 to denote the glycosidic bond formed on the 3rd, 6th and 8th carbon on the acceptor sugar, respectively.

1.2.8.5 Sialyltransferase family

α -2,3 sialyltransferase (ST3Gal-) subfamily

All known ST3 enzymes transfer sialic acids to C-3 of galactose residue in acceptor glycans. Six different ST3 enzymes are cloned from different species. Two α -2,3 sialyltransferases (ST3Gal I and ST3Gal II) mediate the transfer of sialic acid residues to a Gal residue of terminal Gal β (1,3)GalNAc oligosaccharide (Type III) found on glycolipids or glycoproteins [96,97]. The **ST3Gal I** *in vivo* predominantly sialylates O-linked chains, while ST3Gal II is a dominant enzyme in ganglioside biosynthesis. Gangliosides containing NeuNAc α (2,3)Gal β (1,3)GalNAc (e.g., GD1a, GT1b) are ligands for MAG (myelin-associated glycoprotein), a member of the Siglec family of sialic acid-binding receptors [98,99]. The **ST3Gal II**, because of its high, pronounced expression in neuronal tissues and preference for glycolipid acceptors is likely the enzyme utilized *in vivo* for the synthesis of MAG ligands. Human Gal β (1,3/4)GlcNAc α -2,3 sialyltransferase (*h*ST3Gal III) cloned by Kitagawa and Paulson [100] preferentially acts on Type I chain and is therefore the candidate for the synthesis of the sialyl-Lewis^a epitope, *in vivo*. The **ST3Gal III** catalyzes the sialylation of Type II chains but with lower catalytic efficiency. The ST3Gal III gene has been shown to be highly expressed in skeletal muscle but not in placenta. The human **ST3Gal IV**, which has been cloned independently from human placenta [96] and from the human Burkitt lymphoma cell line Namalwa [101] uses either glycolipids or glycoproteins containing Gal β (1,4)GlcNAc (Type II) or Gal β (1,3)GalNAc (Type III) sequences. Human ST3Gal IV transcripts are highly expressed in placenta. Recently, human **ST3Gal V** (GM3 synthase) cloned by Ishii *et al.* [102] uses only lactosylceramide (GA3, *i.e.* Gal β (1,4)Glc β -Cer) as acceptor substrate, leading to the synthesis of GM3 (NeuNAc α (2,3)Gal β (1,4)Glc β -Cer), whereas the purified rat liver enzyme exhibited a broader specificity utilizing both galactosylceramide (Gal β -Cer) and asialoganglioside GA2

(GalNAc β (1,4)Gal β (1,4)Glc β -Cer) as well as lactosylceramide (Gal β (1,4)Glc β -Cer) [103,104]. The human ST3Gal V gene was found to be expressed in a tissue-specific manner with predominant expression in brain, skeletal muscle and testis while very low levels of ST3Gal V mRNA were found in the liver. Human **ST3Gal VI** utilizes almost exclusively Gal β (1,4)GlcNAc (Type II) on glycoproteins and glycolipids [105]. Among glycolipid acceptors, ST3Gal VI prefers polylactosamine Type II chains thus generating glycolipids containing NeuNAc α (2,3)Gal β (1,4)GlcNAc structures including sialyl-paragloboside, a precursor of sialyl-Le^x on ceramide. Predominant expression of the ST3Gal VI gene was found in placenta, liver, heart and skeletal muscle.

α -2,6 sialyltransferase (ST6Gal-, ST6GalNAc- and ST6GlcNAc-) subfamily

Biosynthesis of the α -2,6-sialyl linkage to Gal, GalNAc, or GlcNAc is mediated by the α -2,6 STs. **ST6Gal I** mediates the transfer of sialic acid residues with an α -2,6 linkage to the terminal Gal residue of a Type II disaccharide. The disaccharide can be found as a terminal *N*-acetyllactosamine unit of an *N*- or *O*-linked oligosaccharide. The ST6Gal I is unable to use Type I and Type III structures as acceptor substrates (*Table 1.1*, p2).

Three distinct enzymes (**ST6GalNAc I, II, IV**) are known to catalyze the formation of α -2,6 linkages onto GalNAc residues *O*-glycosidically linked to Ser/Thr, and three other STs (**ST6GalNAc III, V, VI**) catalyze the addition of sialic acid residues onto gangliosides [106]. Human **ST6GalNAc I** exhibits a broadest tolerance for the following structures: Tn antigen, T antigen and sialyl-T antigen (*Table 1.1*) [107,108]. The human **ST6GalNAc II** gene is expressed at low levels in heart, skeletal muscle, kidney and liver. The mouse **ST6GalNAc III** and human **ST6GalNAc IV** exhibit the most restricted substrate specificity utilizing only the sialyl-T antigen structure found on either *O*-glycoproteins or ganglioside GM1b, suggesting that they do not discriminate between α - and β -linked GalNAc [93,109]. The mouse **ST6GalNAc V**, expressed only in the brain, seems to be specific for only GM1b [110,111], while mouse **ST6GalNAc VI** [106] is expressed in a wide range of mouse tissues such as colon, liver, heart, spleen and brain. ST6GalNAc VI appears to be specific for glycolipid acceptors and can synthesize all α -series gangliosides. The α -2,6 sialylation of Tn blocks all further modification of the glycan chain. The sialyl-Tn epitope is heavily expressed in embryonic chick brain [108], whereas in adult human tissue it is mostly absent. In humans, expression of sialyl-Tn antigen is limited to adenocarcinomas and

certain malignant tumors [112].

A third class of α -2,6 STs is composed of one or more enzymes that catalyze the transfer of sialic acid to GlcNAc in *N*-glycans. Though the activity has been described in a number of species, the enzyme(s) responsible for this activity have not been yet identified [113,114].

α -2,8 sialyltransferase (ST8Sia-) subfamily

α -2,8 sialyl linkages are present in glycolipids as well as in glycoproteins. In glycoproteins, α -2,8-linked sialic acids exist as long homopolymers (*i.e.*, polysialic acids) in a small set of molecules, *e.g.* in the embryonic form of neural cell adhesion molecule (N-CAM) [115]. Polysialylation alters the homophilic binding properties of N-CAM and has been thought to influence normal changes in cellular adhesion during embryonic brain development [116]. The presence of polysialic acids on N-CAM correlates with expression of polysialyltransferase and promotes neoblastoma cell growth [117]. The human α -2,8 sialyltransferase (**hST8Sia I**) strongly prefers GM3 as a substrate to catalyze the synthesis of GD3 (NeuNAc α (2,8)NeuNAc α (2,3)Gal β (1,4)Glc β 1-O-Cer) [118]. Nakayama *et al.* found that GD3 and GT3 (NeuNAc α (2,8)NeuNAc α (2,8)NeuNAc α (2,3)Gal β (1,4)Glc β 1-O-Cer) structures were synthesized by the same enzyme, ST8Sia I, whereas minimal sialyltransferase activity was found towards glycoproteins [119]. The GD3/GT3 synthase gene is expressed at very low level in fetal brain and fetal lung. The NeuNAc α (2,3)Gal β (1,4)GlcNAc-R α -2,8 sialyltransferase (**ST8Sia II** or **STX**) has been described as the initiating enzyme which transfers the first sialic acid residue to the 8-hydroxyl of NeuNAc residues, which are linked to the terminal position of *N*-linked glycans. Such glycans are the predominant form found attached to the N-CAM molecules [96,120]. This enzyme did not show any activity towards glycolipids including GM3 structure. The hST8Sia II gene is expressed in fetal brain and kidney but also in adult heart, thymus and brain. A third human α -2,8 sialyltransferase (**ST8Sia III**) was isolated from a brain cDNA library. It shows *in vitro* a high catalytic activity of sialic acid residue transfer to intact fetuin. Murine recombinant enzyme synthesizes oligomeric the α -2,8-sialic acid-linkage on *N*-glycans and to a minor extent on glycolipids, but does not form polysialic acid [119]. Corresponding transcripts of ST8 Sia III were expressed in fetal and adult brain and liver. A fourth α -2,8-sialyltransferase (**ST8Sia IV** or **PST-1**) showed polysialic acid synthase

activity *in vitro* towards N-CAM [121]. The human ST8Sia IV gene has been found to be expressed in fetal brain, kidney and lung, and in adult spleen, thymus, heart, small intestine and leukocyte. Both polysialyltransferases, ST8Sia II and ST8Sia IV were sufficient to add PSA to α -2,3 or α -2,6 monosialylated complex oligosaccharides on N-CAM [122,123]. They differ in their affinity for variable N-CAM isoforms and PSA chains synthesized by ST8Sia IV were found to be longer than those synthesized by ST8Sia II [6]. Kim *et al.* [124] reported the cloning and expression of a fifth type of human α -2,8-sialyltransferase (**ST8Sia V**). As previously shown for the mouse ST8Sia V, the recombinant enzyme exhibited *in vitro* activity towards gangliosides, GM1b, GD1a, GT1b and GD3. Human ST8Sia V is expressed in both human fetal and adult brain, but also in adult heart and skeletal muscle.

The investigation of protein glycosylation in eukaryotes gave a relatively detailed insight into the complex molecular mechanisms of protein glycosylation, and elucidated the coordinate participation of various cell organelles in this process. In the last decades, accumulating evidence for glycosylated bacterial proteins has overthrown the almost dogmatic belief that glycosylation of proteins occurs exclusively in eukaryotes.

1.3 Prokaryotic glycosylation

In prokaryotes (*archaea* and (*eu*)*bacteria*), the earliest examples of protein glycosylation have been found in *archaea*, which are able to present glycosylated surface layer (S-layer) proteins [125]. Mescher and Strominger [126] characterized the first archaeal S-layer glycoprotein of *Halobacterium halobium (salinarum)* that accounts for 50% of the cell envelope proteins. In 1976, Sleytr and Thorne identified the presence of S-layer glycoprotein in bacteria *Clostridia* [127]. In recent years non-S-layer glycoproteins have been found increasingly in insect and important mammalian bacterial pathogens [128]. Non-S layer glycoproteins can be found either membrane-associated (e.g., plasma membrane glycoproteins, outer membrane proteins), surface-associated (e.g., flagellins, pili), as secreted glycoprotein and exoenzymes (e.g., cellulases, endoglycosidase, phytotoxin), or as a group of non-classified glycoproteins (e.g., platelet aggregation-associated protein, crystal toxin). The glycosylation process in prokaryotes leads to a much greater diversity of glycan compositions, linkage units, and glycosylation sequences on polypeptides than in eukaryotic glycoproteins. The glycosylated amino acids in prokaryotic glycoproteins are not restricted to those known from eukaryotes, *i.e.* asparagine in tripeptide consensus sequence Asn*-Xaa-Ser/Thr (* indicates glycosylated amino acid) for *N*-glycosidic linkages, and threonine, serine, hydroxyproline or hydroxylysine for *O*-glycosidic linkages, but also include tyrosine as a potential glycosylation site [129]. The requirements for *O*-glycosylation are less defined. It may take place in proline-rich domains, but also in several distinct consensus sequences, such as Asp-Ser*, Asp-Thr*-Thr [130] and Val-Tyr* [131]. As prokaryotic cells lack cellular compartments, the biosynthetic pathway of their glycan chains has to follow routes different from those described for eukaryotes. Similar mechanisms such as the utilization of sugar nucleotides for the assembly of the oligosaccharide chain, the occurrence of trimming reactions and the existence of lipid-bound intermediates have been observed during prokaryotic glycoprotein biosynthesis [132]. In contrast, the occurrence of nucleosidediphosphate-linked oligosaccharides is a remarkable difference between pro- and eukaryotic protein glycosylation, the function of which is not completely understood [133].

Thus far the glycosylation machinery has been identified only for a few examples. Some glycoproteins are modified by enzymes of a general glycosylation system, such as in *Campylobacter*, which show similarities to enzymes involved in protein glycosylation in

other species, such as *Neisseria* subspecies [134]. Others have acquired their own glycosylation mechanism, potentially by horizontal gene transfer mechanisms. In addition to general glycosylation system, prokaryotes express specific GTs for the modification of some proteins where glycosylation plays an important role for their maturation and function, e.g. the TibA and the AIDA system in *E. coli* [135-137].

Synthesis of polymeric cell surface carbohydrates takes place at the inner membrane [138] or in the periplasm via lipid-linked intermediates. For capsular antigens, a cell wall spanning synthesis-translocation complex has been suggested [139]. In the case of bacterial protein glycosylation, the organization and localization of components of the general glycosylation system is not known. The presence of protein-specific bacterial GTs (e.g., *E. coli* AAH heptosyltransferase) in the cytoplasm might indicate that protein glycosylation takes place in the cytoplasm [140].

1.3.1 Possible role of protein glycosylation in pathogenic bacteria

In analogy to the various functions of carbohydrate modification in eukaryotic glycoproteins, bacterial glycoproteins can have important roles in maintenance of protein conformation, enhancing stability, protection against proteolytic degradation, surface recognition, cell adhesion or immune evasion [134]. Currently, bacterial glycoproteins can be divided into two groups: one group in which carbohydrate modifications directly affect protein function (e.g., subunit interactions and/or assembly of flagellins and pili (*Campylobacter*, *Neisseria*) and adherence to host cells (*E. coli*). A function of the carbohydrate moiety has been shown in *C. jejuni*, in which the defects in protein glycosylation result in impaired intestinal colonization [141]. In the second group, glycosylation influences the interaction with the host immune system and has an important role in pathogenesis. The carbohydrate moieties rather than amino acid epitopes appear to represent an antigenic determinant [142].

1.3.2 Bacterial glycosyltransferases

Continuing microbial genome analysis and progress in screening and cloning techniques have allowed the cloning of various bacterial glycosyltransferase genes (*Table 1.2*), mainly from pathogenic bacteria. Most of these genes can be expressed as soluble active

proteins in *E. coli*.

Table 1.2 Representation of distinct bacterial glycosyltransferase families [143].

| Family | Enzyme | Source | Reference |
|---------|-------------------------------------|---|-----------|
| GalT | β -1,4 galactosyltransferase | <i>Neisseria gonorrhoeae, N. meningitidis</i> | [144-146] |
| | β -1,4 galactosyltransferase | <i>Helicobacter pylori</i> | [147,148] |
| | β -1,4 galactosyltransferase | <i>Streptococcus pneumoniae</i> | [149] |
| | β -1,4 galactosyltransferase | <i>Streptococcus agalactiae</i> | [150] |
| | β -1,3 galactosyltransferase | <i>Campylobacter jejuni</i> | [151] |
| | β -1,3 galactosyltransferase | <i>Streptococcus agalactiae</i> | [152] |
| | α -1,4 galactosyltransferase | <i>Neisseria gonorrhoeae, N. meningitidis</i> | [144,145] |
| GlcNacT | β -1,3 GlcNAc transferase | <i>Neisseria gonorrhoeae, N. meningitidis</i> | [144,145] |
| | β -1,4 GlcNAc transferase | <i>Campylobacter jejuni</i> | [151] |
| GalNAcT | β -1,3 GalNAc transferase | <i>Neisseria gonorrhoeae, N. meningitidis</i> | [144,145] |
| | β -1,3 GalNAc transferase | <i>Campylobacter jejuni</i> | [151] |
| SiaT | α -2,3 sialyltransferase | <i>Neisseria gonorrhoeae, N. meningitidis</i> | [153] |
| | α -2,3 sialyltransferase | <i>Campylobacter jejuni</i> | [151] |
| | α -2,3 sialyltransferase | <i>Haemophilus influenzae</i> | [154,155] |
| | α -2,3 sialyltransferase | <i>Haemophilus ducrey</i> | [156] |
| | α -2,3 sialyltransferase | <i>Streptococcus agalactiae</i> | [157] |
| | α -2,3/8 sialyltransferase | <i>Campylobacter jejuni</i> | [151] |
| | α -2,6 sialyltransferase | <i>Photobacterium damsela</i> | [77] |
| | α -2,8/9 sialyltransferase | <i>Escherichia coli</i> | [158] |
| FucT | α -1,3 fucosyltransferase | <i>Helicobacter pylori</i> | [159,160] |
| | α -1,2 fucosyltransferase | <i>Helicobacter pylori</i> | [161] |
| | α -1,3/4 fucosyltransferase | <i>Helicobacter pylori</i> | [162] |

The carbohydrate structures similar to the eukaryotic type have been found and characterized in many prokaryotic species. The following chapter will be related to the glycoconjugates expressed by the pathogenic *C. jejuni*.

1.3.3 *Campylobacter jejuni*

Campylobacter jejuni is a microaerophilic, gram-negative, non-spore-forming, flagellate bacterium with a characteristic S-shaped or spiral morphology, similar to the related gastric pathogen *Helicobacter pylori* [163].

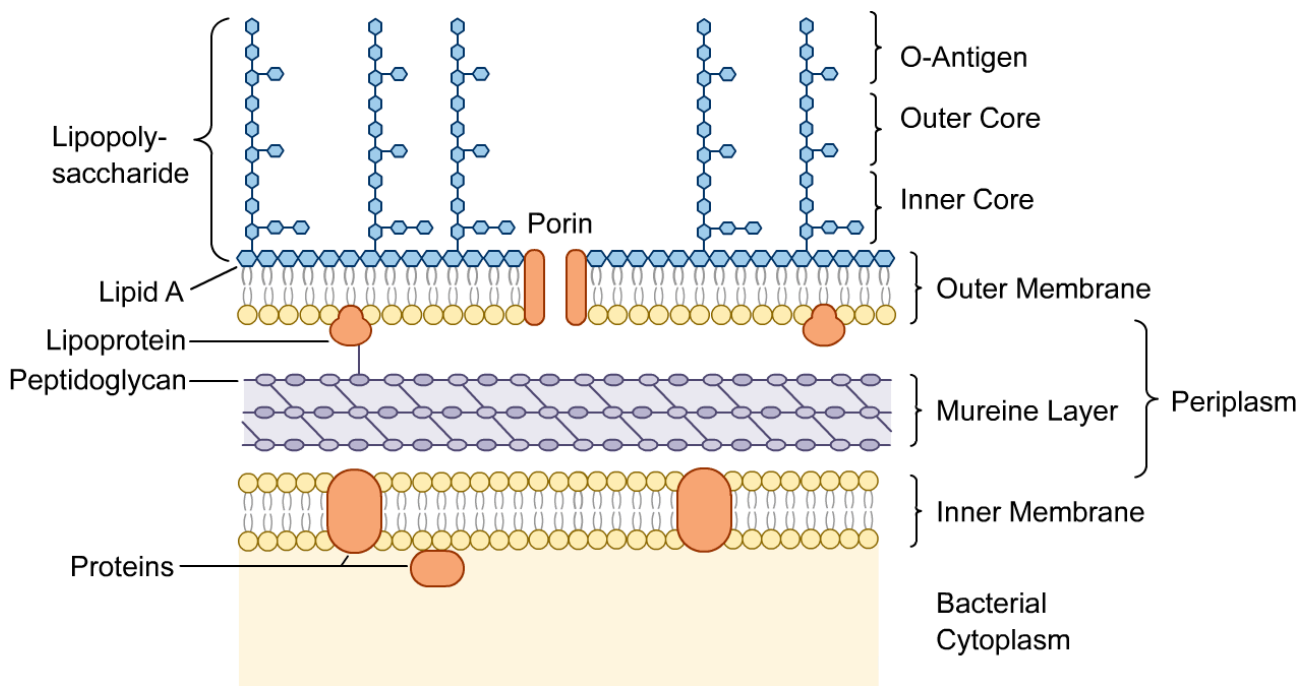


Figure 1.8 Schematic representation of the cell wall of gram-negative bacteria [164].

Since the late 1970s, the mucosal pathogen *C. jejuni* has been recognized as an important cause of acute gastroenteritis in human [165], and has been shown to have variable cell-surface carbohydrates, which are associated with virulence [166,167]. The core oligosaccharide of low molecular weight lipo-oligosaccharides (LOS) expressed on the cell surface of many *C. jejuni* strains (*Figure 1.8*) has been shown to exhibit molecular mimicry of the carbohydrate moieties of distinct gangliosides. The presence of NeuNAc in *C. jejuni* discovered by Moran *et al.* [168] was surprising, as it is not usually found in prokaryotes. Terminal regions of the core oligosaccharide containing α -2,3 NeuNAc linkages to *D*-Gal residue resemble the GM1a, GM2, GM3, GD1a, GD1c, GD3 and GT1a gangliosides purified from the brains of vertebrates [169]. These ganglioside-like structures have all been found in various *C. jejuni* strains. An example of GD1c-like structure is shown in

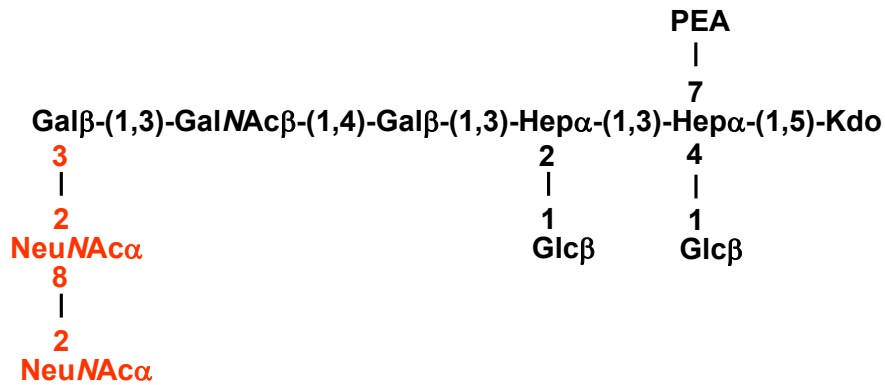


Figure 1.9. The molecular mimicry of host gangliosides by the oligosaccharide portion of the LOS molecule is considered to be a virulence factor of various mucosal pathogens, and play an essential role in neuropathological autoimmune diseases like Miller-Fisher syndrome (MFS) and Guillain-Barré syndrome (GBS). The GBS is a form of neuropathy (neuromuscular paralysis), and is the most common cause of generalized paralysis [170-172]. Using mimicry mechanism, pathogens can evade the immune response and trigger autoimmune mechanisms to *C. jejuni* epitopes, eliciting cross-reactive anti-ganglioside antibodies that target neural cells and tissues bearing gangliosides [142,173].

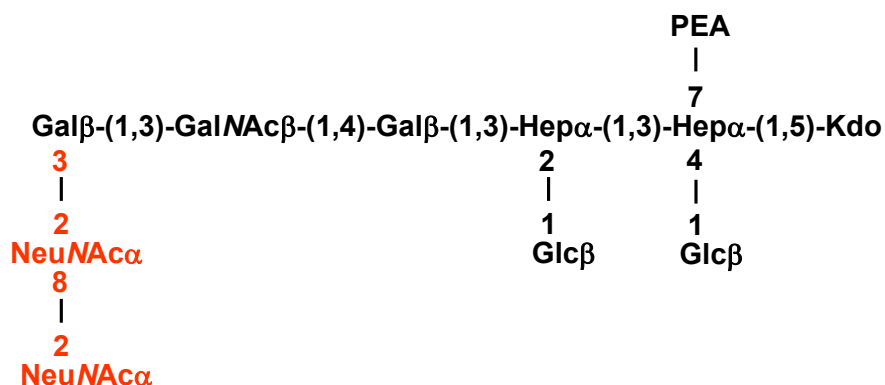


Figure 1.9 Outer core carbohydrate moiety of LOS structure expressed by the ATCC43438 *C. jejuni* strain as a mimic of GD1c ganglioside molecule. Kdo indicates ketodeoxy octulosonic acid, Hep describes heptose and PEA denotes for O-phosphoethanolamine [174].

1.3.3.1 Lipo(oligo)polysaccharides (LOS/LPS)

Lipopolysaccharides are an abundant surface component of the outer membrane of gram-negative bacteria. The LPS molecules consist of three distinct regions (*Figure 1.10*).

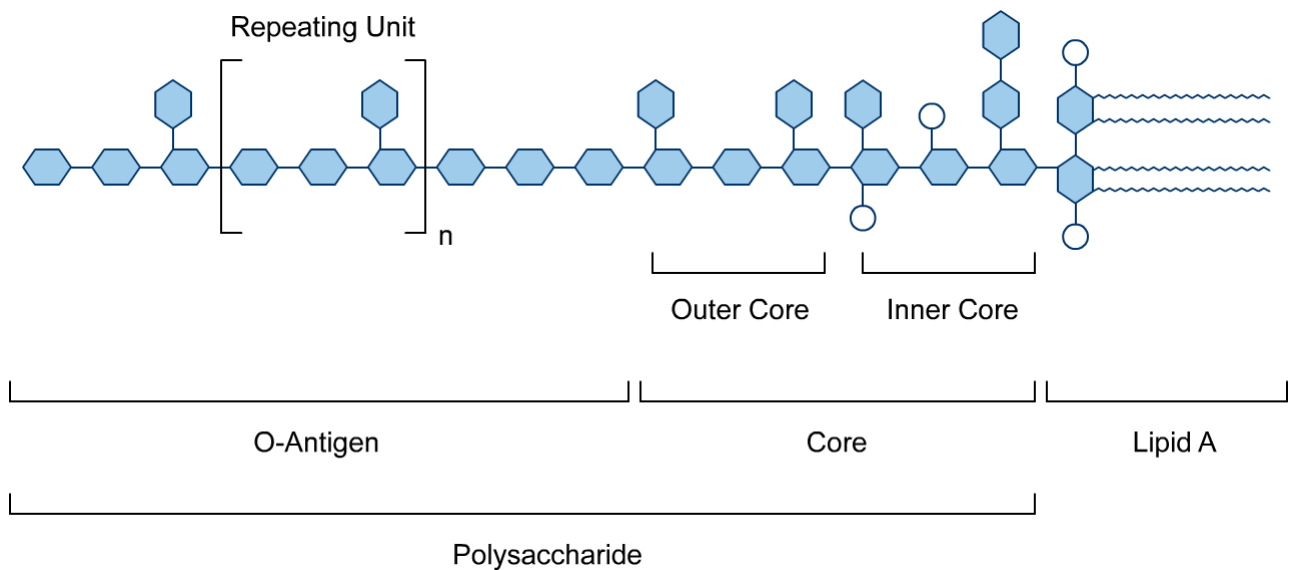


Figure 1.10 Schematic diagram of LOS/LPS molecule structure.

The hydrophobic lipid A moiety, considered as the endotoxic part [175] of LPS molecule, is anchored in the outer membrane. Attached to the lipid A is the core, a branched-chain oligosaccharide linked to a ketodeoxy octulosonic acid (Kdo) molecule, which contains an inner and outer part. Specific to the inner core is the presence of a Kdo and a heptose residue. These structures were not found in the outer core. Extending from the cell surface is the O-antigen, a repeat of 10-30 oligosaccharides composed of 1-5 sugar residues each [176]. The bacterial O-antigen protects the organism against complement and other serum components [177,178]. Comparing to the LPS molecule, the LOS molecule lacks the O-antigen polymer and is considered as a variant of the LPS. The *C. jejuni* strains mainly synthesize LOS molecules, whereas some strains possess polysaccharide repeats (*Figure 1.11*) [179]. Aspinall *et al.* [169,180,181] and Nam Shin *et al.* [174] determined the LOS outer core structures of representative *C. jejuni* reference strains of the Panner serotyping system. The Panner serotyping system is based on heat-stable antigens, and it was suggested that the specificity is due to the capsular polysaccharides rather than to the LOS and/or LPS molecules. Serotyping of *C. jejuni* is based upon differences in the saccharide structure of the bacterial heat-stable antigens, and strains have been designated as either “O”, Panner (e.g. O:10) or heat-stable (HS) serotypes [182]. Because of the fact that strains having the same Panner type could express different LOS outer core structures, *C. jejuni* was named with the specific identification number (e.g., ATCC43438, OH4384) as well as with the Panner type (e.g., O:10, O:19).

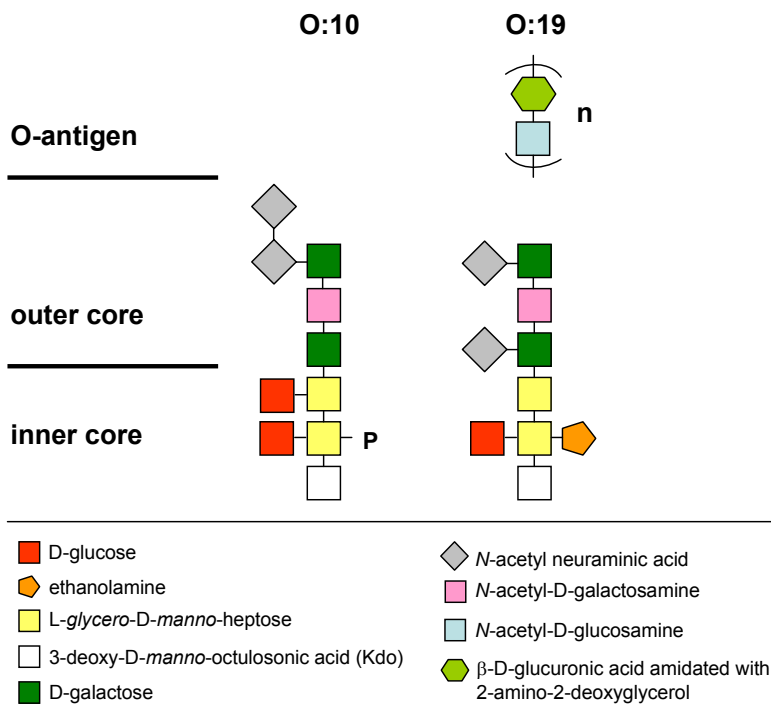


Figure 1.11 Known structures of core molecules and O-antigen-like polysaccharides from O:10 [172] and O:19 [169,181] *Campylobacter jejuni* strains. The “n” indicates that the oligosaccharide is repeated, forming an O-antigen like polysaccharide whereas “P” denotes a phosphate group [175].

The identification of the LOS structures of *C. jejuni* revealed the presence of α -2,3- and α -2,8- sialic acid bond structures.

1.3.3.2 Bifunctional α -2,3/2,8 sialyltransferase (Cst-II)

The *Campylobacter* sialyltransferase II (*cst-II*) gene encoding a bifunctional α -2,3/2,8 ST (Cst-II) is one of the genes responsible for the biosynthesis of the ganglioside mimics in *C. jejuni*. This membrane-associated inverting enzyme in general catalyzes the formation of a α -2,3 sialic acid-linkage to a β -galactose acceptor sugar, and uses this product as an acceptor substrate in a second, α -2,8 sialyltransferase enzymatic reaction (*Figure 1.12*) [151].

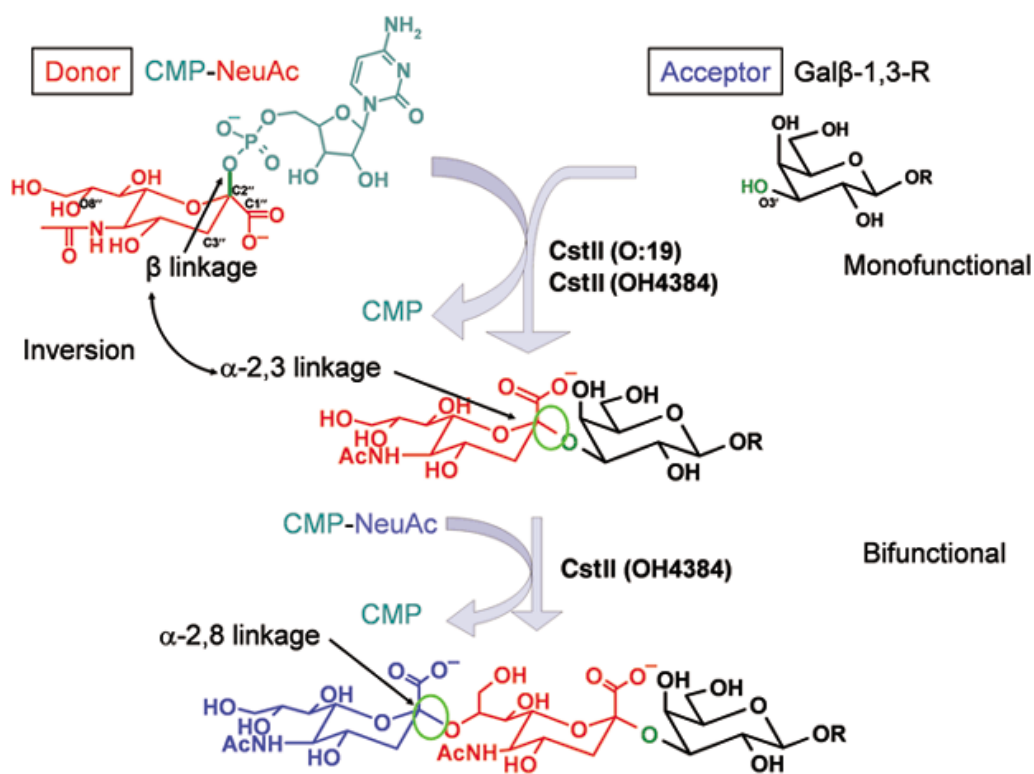


Figure 1.12 Enzymatic reaction catalyzed by α -2,3/2,8 bifunctional sialyltransferase (Cst-II). The bonds created in the monofunctional and bifunctional reactions are highlighted by a green circle [183].

Several versions of *cst-II* genes from different strains of *C. jejuni* have been found. Despite very high sequence identity (97.3%) between these enzymes, some of them showed α -2,3 monofunctional (e.g., Cst-II_{O:19}) and some α -2,3/2,8 bifunctional (Cst-II_{OH4384}, Cst-II_{ATCC43438}) sialyltransferase activity. The Cst-II enzyme expressed in the OH4384 *C. jejuni* strain differs by only eight amino acids from the same enzyme expressed in the ATCC43438 strain of *C. jejuni*.

The GQ1b α molecules, which are highly expressed in CNS, contain sialic acids linked to the galactose residue by α -2,3, α -2,6 and α -2,8 glycosidic bond. Because of the very specific α -2,3/2,8 bifunctional sialyltransferase activity, this enzyme was considered as a powerful tool for the chemo-enzymatic synthesis of the GQ1b α -like molecule.

1.4 Enzymes for chemical synthesis

Recent demonstrations that oligosaccharides play important roles in diverse biological events have resulted in renewed interest in the synthesis of oligosaccharides and their analogs. The availability of such molecules can facilitate the studies on carbohydrate-protein recognition and help to elucidate molecular mechanisms of oligosaccharide-mediated biological process [164,184] that could eventually lead to rationally designed carbohydrate-based therapeutics. The application of oligosaccharides as pharmaceuticals in the fields of the prevention of infections by pathogens, neutralization of toxins, regulation of inflammation, and cancer immunotherapy have been widely recognized [185]. It has been very difficult to synthesize oligosaccharides, and they could be obtained only in limited amount by extraction or chemical synthesis. This is attributed to the inherent chemical difficulties presented by this class of molecules. Each monosaccharide carries at least three hydroxyl groups that must be protected and deprotected during synthesis. Also, glycosylation generates new stereocenter at the anomeric carbon, and there are no general methods for the introduction of all types of glycosidic linkage in a manner that is both stereo-controlled and high yielding. The chemical synthesis of oligosaccharides is therefore very time-consuming.

In Nature, glycosyltransferase enzymes accomplish the construction of diverse and complex oligosaccharide. As mentioned before, these enzymes catalyze the transfer of a monosaccharide from a glycosyl donor to a glycosyl acceptor in a regio- and stereospecific manner. Such a biosynthetic pathway was utilized in the pioneering work by Wong, Haynie and Whitesides on the *in vitro* enzymatic synthesis of *N*-acetyllactosamine with in situ regeneration of uridine 5'-diphosphogalactose (UDP-Gal) [186]. Furthermore, pioneered by Barker [187,188], Whitesides [186] and Augé [189] and their colleagues, enzymatic synthesis of oligosaccharides by glycosyltransferases opened up a new venue avoiding many of the problems encountered in the traditional chemical synthesis. Since then, many synthetic chemists are using enzymes in combination with classical carbohydrate chemistry, *i.e.* chemo-enzymatic approach to produce oligosaccharides on a gram or even kilogram scale [190]. In the chemo-enzymatic synthesis, the most enzymes operate at room temperature, under neutral aqueous conditions, and in the absence of functional-group protection. In organic synthesis, these biocatalysts can be used as the sole catalyst in a reaction, in combination with other enzymes, or with non-biological reagents. The chiral nature of enzymes results in the formation of stereo- and regiochemically defined

reaction products with remarkable rate acceleration (10^5 to 10^8). In addition, many enzymes accept unnatural substrates, and genetic engineering can further alter their stability, broaden their substrate specificity, and increase their specific activity.

1.5 Myelin-associated inhibitors of axonal regeneration in the adult mammalian CNS

In the peripheral nervous system (PNS) regeneration occurs spontaneously after nerve injury, whereas in the central nervous system (CNS) damaged nerves do not regenerate after damage of the brain or spinal cord. Schwab *et al.* [191] were the first to discover a potent growth inhibitory activity in the CNS, and to show that much of this inhibitory activity is associated with myelin. It is now well established that the lack of regeneration in the CNS is due to two main obstacles, namely formation of the glial scar and presence of growth inhibitory molecules within the myelin [192]. The glial scar is formed by astrocytes, which change their morphology to present a physical barrier to growth and also upregulate several extracellular matrix-associated inhibitors of regeneration. However, until the scar fully matures, myelin seems to be the predominant source of growth inhibition.

1.5.1 Myelin and myelin-associated inhibitors

In contrast to the Schwann cells, which are responsible for the single internode formation of the myelin sheath around the axon in the PNS, oligodendrocytes are myelin-producing cells of the CNS capable of elaborating many internodes of myelin simultaneously. The myelin sheath acts as an axon insulator and greatly increases the rate at which an axon can conduct an action potential (*Figure 1.13*).

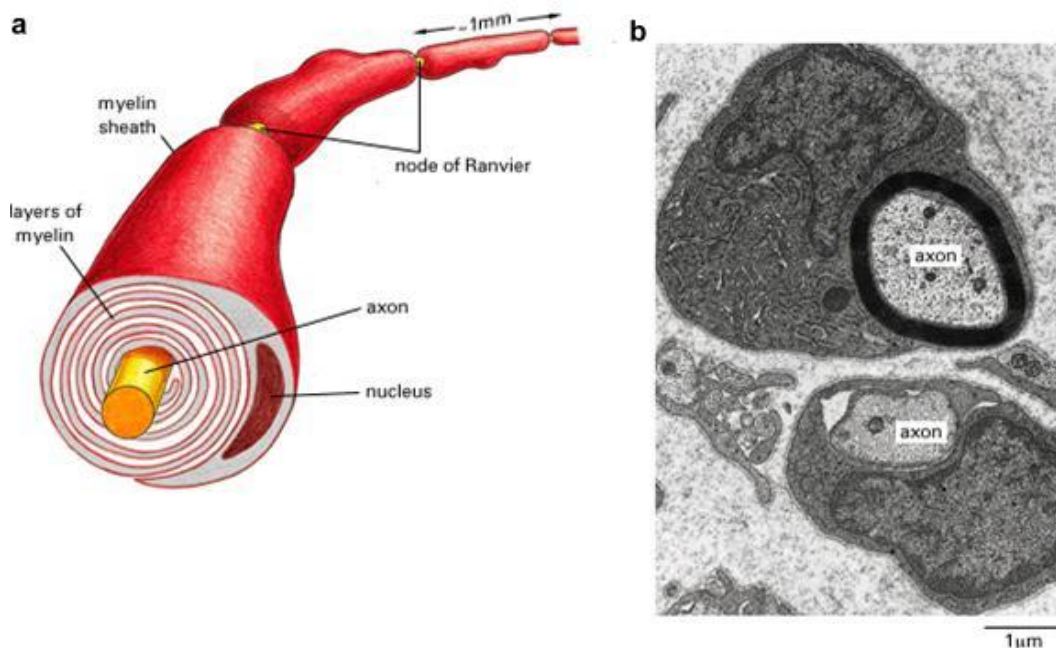


Figure 1.13 (a) Representation of a myelinated axon from a peripheral nerve. Each Schwann cell wraps its plasma membrane concentrically around the axon to form a segment of myelin sheath about 1 mm long. **(b)** Electron micrograph of a section from a nerve in the leg of a young rat. Two Schwann cells can be seen: one (below) is just beginning to myelinate its axon; the other has formed an almost mature myelin sheath [193].

The importance of myelination is dramatically demonstrated by demyelinating diseases in the CNS and PNS such as multiple sclerosis and Guillain Barré syndrome [194]. The sheath is interrupted by regularly spaced nodes of Ranvier allowing propagation of action potential along a myelinated axon by a process called saltatory conduction.

Besides its insulation function, myelin is also recognized as a major inhibitor for axonal regeneration for a variety of neurons both *in vivo* and *in vitro* [195-198]. Even though CNS and PNS myelin differ biochemically and antigenically, Shen's study showed their similar inhibition of axonal regeneration [199]. There are major differences between the oligodendrocyte and Schwann cells behavior after the injury. In contrast to the oligodendrocyte, which shows slow mitotic rate and poor regenerative capacity, the Schwann cell responds vigorously and is engaged in an active phase of mitosis. After the primary demyelination, Schwann cells show the ability to phagocytose damaged myelin [200]. Regeneration takes place only after the myelin debris has been cleared, the Schwann cells have reverted into a non-myelinated phenotype, and the expression of myelin proteins is downregulated [192]. In contrast, oligodendrocytes continue to express myelin and myelin-associated inhibitors without removing myelin debris formed during injury. Therefore, myelin-associated inhibitors such as MAG, Nogo and Omgp, exposed in the damaged myelin sheath in the CNS are the main cause of the inhibition of axonal regeneration [201].

1.5.1.1 Myelin-associated glycoprotein

Myelin-associated glycoprotein (MAG) was initially described in 1973 [202] as a glycoprotein in the CNS and PNS myelin, and was the first myelin protein characterized as a potent inhibitor of axonal outgrowth in culture [203,204]. As a member of the Siglec (sialic acid-binding immunoglobulin like lectin) family [205], MAG (Siglec-4a) contains five extracellular Ig-like domains. The first Ig-domain adopts an unusual conformation by

folding over the second Ig-domain, and cysteine disulfide bridges are formed between the unpaired cysteine residues (*Figure 1.14*). The MAG glycoprotein contains 8-9 potential *N*-glycosylation sites and one-third of its molecular mass of 100 kDa is accounted for carbohydrates [206].

MAG as a transmembrane protein exists in two alternatively spliced isoforms, a large (L) and a small (S) form that differ in their cytoplasmic sequence [207-209]. In the CNS myelin sheath, MAG is located exclusively in the periaxonal oligodendroglial membrane, while in the PNS it is found in the outermost layer of the myelin sheath [210,211].

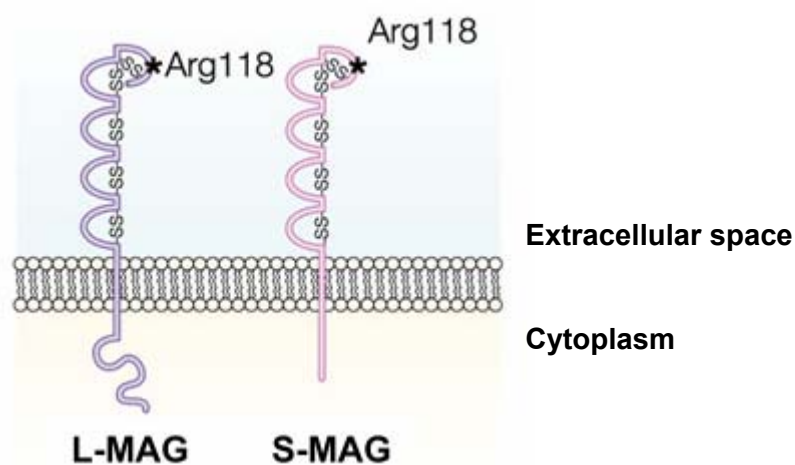


Figure 1.14 Structure of the MAG glycoprotein. The MAG exists in large (L) and small (S) isoforms which differ only in their cytoplasmic sequences. MAG carries five Ig-like domains in its extracellular sequences and the first Ig-domain adopts an unusual conformation by folding over the second Ig-domain. The sialic acid binding site on MAG is Arg118 in the first Ig-domain [192].

Because of its localization close to the axon, it was suggested that MAG has the ability to maintain the normal myelination of axons and preserve axon-myelin integrity [212].

Depending on the age and type of neurons, MAG seems to be bifunctional, and all neurons that have been studied to date switch their response to MAG from promotion to inhibition during development [204,213].

As a member of the Ig-super family and Siglec family, MAG is a sialic acid-binding protein that specifically binds sialo-glycoproteins and sialo-glycolipids (gangliosides), preferably when the sialic acid residue is attached in α -2,3-O-linkage, such as in GT1b [98,99,214]. The sialic acid-binding site on MAG maps to Arg118 in its first Ig-like domain [215]. This

arginine residue is conserved in other members of the Siglec family. When Arg of MAG is mutated, its sialic acid-binding capability is lost. By contrast, when Arg 118-mutated MAG is presented to neurons through expression by recombinant cells, it inhibits neurite outgrowth as effectively as wild-type MAG, indication that the sialic-acid binding site on MAG is distinct from its inhibition site. For soluble MAG, interaction of the inhibition site with the neuron is completely dependent on MAG's inherent sialic acid-binding capacity. In contrast, other proteins (e.g., cell adhesion molecules – CAM) in living cells can compensate for the MAG's sialic acid-binding to the neuron, allowing the inhibition site to interact and elicit the response [215]. This is consistent with the recent findings that the binding of MAG to its receptor, Nogo receptor (Ngr), is sialic acid independent [216,217].

1.5.1.2 Nogo

Although Ramon y Cajal was first suggesting that white matter could block regeneration in the CNS [218], in the late 1980s the work of Schwab and his colleagues confirmed this hypothesis with a molecular insight into the mechanism of Nogo inhibition [219,220]. The IN-1 monoclonal antibody, which was raised against an inhibitory fraction of myelin that did not support neurite extension, allowed axons to grow on myelin in culture [219] and *in vivo* [195]. Three groups independently cloned an antigen of the IN-1 antibody named Nogo for its inhibitory action on axonal growth [221-223].

Nogo belongs to the reticulon family and exists in three isoforms A, B and C (*Figure 1.15*) in the CNS but not in the PNS [222]. The Nogo-A isoform is the only one that is expressed in oligodendrocytes. The amino terminus of Nogo-A is unique and possess at least two inhibitory domains: Nogo-66 common to all three isoforms and the amino-Nogo unique to the Nogo-A amino terminus. Although the topology of Nogo-A is still not resolved, the possible topology model place Nogo-66 on an extracellular surface and amino-Nogo on an intracellular surface. Regardless of topology, both of these domains induce growth cone collapse when exposed to the axon after damage of myelin/oligodendrocyte by injury [192].

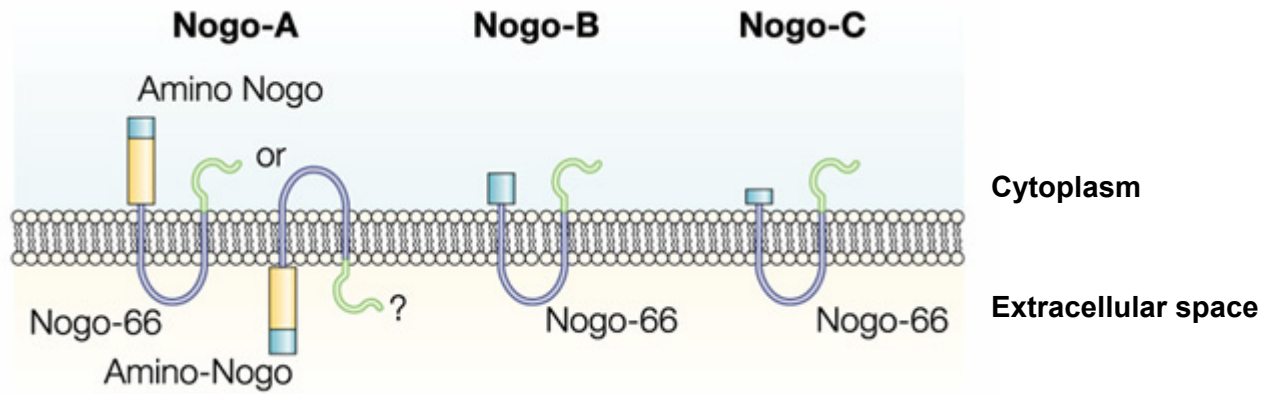


Figure 1.15 Structure of the Nogo molecule. Nogo exist in three isoforms, Nogo-A, Nogo-B and Nogo-C. Sequences that are common to all three isoforms are shown in blue and green. Only Nogo-A is enriched in oligodendrocyte, and it carries two inhibitory domains, one in Nogo-66 that is common to all three isoforms and one in the amino terminus – amino-Nogo – that is unique to Nogo-A. The Nogo-A has been proposed to adopt two topologies depending on whether Nogo-66 or amino-Nogo is extracellular [192].

1.5.1.3 Oligodendrocyte myelin glycoprotein

The oligodendrocyte myelin glycoprotein (OMgp) is a glycosyl phosphatidylinositol (GPI)-linked protein, the third myelin-associated inhibitor of axonal regeneration (*Figure 1.16*) [224]. It is expressed not only by oligodendrocytes, but also at high level in various neurons in the CNS and PNS [225,226]. The OMgp is a minor component of myelin and it is found to be expressed largely in the paranodal loops, close to the nodes of Ranvier. The OMgp contains a leucine-rich repeat (LLR) domain, followed by a C-terminal domain with Ser/Thr repeats. Like MAG and Nogo, OMgp induces growth cone collapse and inhibits neurite outgrowth.

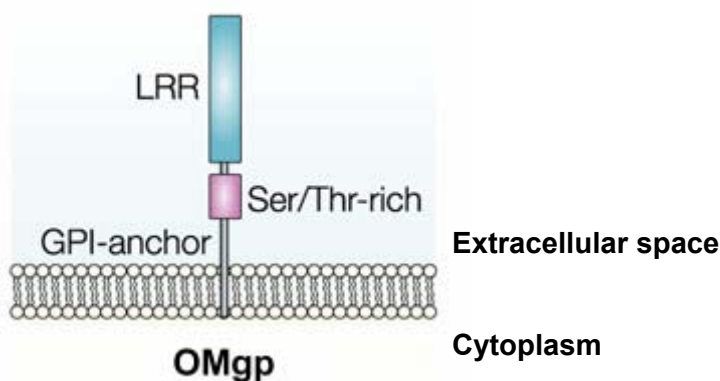


Figure 1.16 Structure of the OMgp molecule. The OMgp is a glycosylphosphatidylinositol (GPI)-linked protein that carries a leucine-rich repeat (LRR) region and a serine/threonine (Ser/Thr) rich region.

1.5.2 Receptors for myelin-associated inhibitors of axonal regeneration

An important step forward after the identification of myelin-associated inhibitors was the identification of the axonal receptor that transduces their inhibitory signal across the axonal membrane. In 2001, by screening an expression library with soluble Nogo-66, Strittmatter and colleagues found the Nogo receptor (NgR), a binding partner of Nogo-66 [227]. The NgR is expressed as a 85 kDa GPI-linked protein on the surface of various neurons [228]. It contains a series of eight LLRs followed by a second cluster of C-terminal LRRs. Direct interaction of the NgR receptor with Nogo-66 is required to induce growth cone collapse [227]. The most surprising discovery was that NgR is also a receptor for the MAG and OMgp myelin-associated inhibitors of axonal growth [216,217,224]. Although, NgR is essential for Nogo-66, MAG and OMgp to exert their inhibitory effects, it can not transduce the signal across the membrane, because it is a GPI-linked protein and therefore has no transmembrane or cytoplasmatic domains. It is found that the transducing partner interacting with NgR is the p75 neurotrophin receptor (p75^{NTR}). p75^{NTR} (*Figure 1.17*) can be co-precipitated by MAG, Nogo-66 or OMgp, with NgR present in the precipitate of each [229,230]. Neurons from p75^{NTR}^{-/-} mice are not inhibited by any of the three inhibitors or by myelin in general [192].

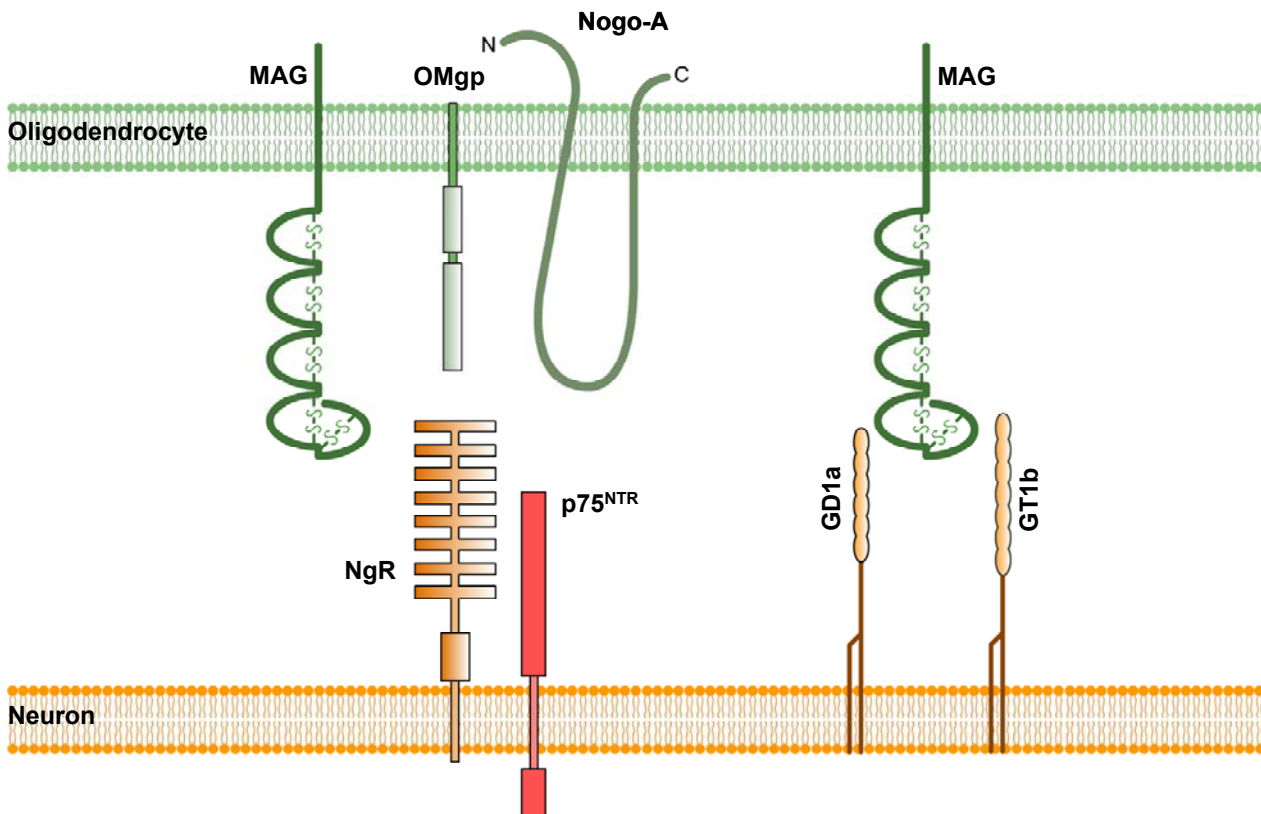


Figure 1.17 The myelin-associated inhibitors of axonal regeneration in the adult mammalian CNS interact with the same receptor complex. The Nogo-66, the Mag and the OMgp interact with the same glycosyl phosphatidylinositol-linked Nogo receptor (NgR) to bring about inhibition of neurite outgrowth. The NgR contains two regions of LRRs – a cluster of eight together, and a series closer to the carboxyl terminus. Interaction of the MAG with the Ngr is independent of sialic acid binding. However, the MAG binding to the gangliosides is sialic acid dependent. The NgR interacts with the p75^{NTR} to transduce the inhibitory signal across the membrane. The receptor for amino-Nogo is not known. The amino-Nogo, the Nogo-66, the MAG and the OMgp activate Rho to trigger the inhibition. The MAG has been shown to inactivate Rac, but it is not known whether this effect is required for inhibition [192].

The three main myelin-associated inhibitors that have been identified to date, MAG, Nogo-66 and OMgp, interact with the same receptor complex, NgR – p75^{NTR} (Figure 1.17) which transduces the inhibitory signal across the axonal membrane to prevent axonal regeneration after injury. This implies that there is functional redundancy between these inhibitors, *i.e.* the presence of any one inhibitor is sufficient to prevent regeneration by activating an inhibitory signal through the single receptor complex. This idea of redundancy can explain many of the previous results of *in vivo* experiments in which either

MAG or Nogo was blocked or absent. In the MAG^{-/-} mouse, only a small amount of spontaneous axonal regeneration was recorded in one study, and none at all in another [231,232]. Likewise an IN-1 antibody application to Nogo allowed only a small percentage (5-10%) of axons to regenerate [195,233,234].

The additional inhibitory activity of amino-Nogo, which does not act through NgR – p75^{NTR}, and perhaps other as yet unidentified myelin inhibitors, might make a relatively minor contribution since the blocking of NgR or p75^{NTR} can substantially block the inhibitory effects of total myelin for the neurons tested so far.

1.5.3 Gangliosides as a MAG functional ligands

Beside the common pathway used by MAG, Nogo and OMgp to transduce the inhibitory signal using the NgR or p75^{NTR} receptor complex, for a certain time it was thought that MAG mediates neurite growth inhibition by the interaction with gangliosides (*Figure 1.17*). This assumption was questioned after the discovery of NgR as a main binding partner of MAG. Although it is more likely that gangliosides potentiate and augment MAG-initiated inhibition by facilitating the clustering of signaling molecules, there is much evidence to support the hypothesis that the gangliosides expressed by nerve cells are specific functional ligands responsible for the MAG-mediated neurite outgrowth inhibition [235,236].

Gangliosides (see chapter 1.2.8.1) are major sialic acid-containing glycoconjugates expressed in the brain, on the surface of the nerve cells [237]. Brain gangliosides are characterized by their structural diversity which is mainly generated by variation in the number and linkage positions of sialic acid on the neutral sugar core. The major brain gangliosides are mainly responsible for maintenance of myelin stability and for the control of neurite regeneration. Both of these functions are assumed to be mediated through specific interaction with a MAG [194].

MAG as a member of the Siglec family (siglec-4a) (see chapter 1.5.1.1) requires α -2,3-linked sialic acid, preferentially, NeuNAc α (2,3)Gal β (1,3)GalNAc terminus as implicated by an initial specificity study [236]. Direct binding studies showed that MAG binds to GD1a and GT1b, which are considered as major brain gangliosides, and related gangliosides with high specificity and affinity *in vitro* [98].

These gangliosides abound on the neuronal cell surface and along the axons, and are placed directly apposed to MAG *in vivo* [194]. The presence of the MAG binding glycan sequence on gangliosides, and their location on the axon surface led to the hypothesis that gangliosides may be endogenous ligands for MAG, and may, therefore, mediate MAG's physiological functions.

2 Aims

The work of our laboratory is focused on the Myelin-Associated Glycoprotein (MAG) and its physiological ligands, *i.e.* brain gangliosides. Among these, GQ1b α is the most potent natural ligand identified so far and was therefore chosen as a lead structure for the development of MAG antagonists. Only the sialic acid containing part of GQ1b α was shown to be important for MAG binding. Therefore, we decided to use a chemo-enzymatic approach for the syntheses of the GQ1b α mimetics. In order to perform preparative chemo-enzymatic synthesis of sialylated structures, it was of great importance to set-up the enzymatic platform concerning distinct sialyltransferases. Hence, this involved expression of different enzymes having the ability to catalyze the formation of α -2,3, α -2,6 and α -2,8 glycosidic-linkages of sialic acid.

Consequently, the first aim was the expression, purification and biochemical characterization of the eukaryotic *r*ST3Gal III, and its application in the preparative chemo-enzymatic synthesis of GQ1b α mimetics. Furthermore, the second aim was the expression and characterization of eukaryotic *h*ST6Gal I in order to have enzyme within the enzymatic library. The main project was cloning, expression and characterization of the prokaryotic, *Campylobacter jejuni* bifunctional α -2,3/2,8 sialyltransferase. This enzyme was initially targeted for the preparative chemo-enzymatic synthesis in order to produce GQ1b α derivatives containing α -2,8 glycosidic-linkages.

3 Materials and Methods

3.1 *r*ST3Gal III expression in baculovirus-infected cells, purification and characterization

3.1.1 Insect cell culture and virus methods

Recombinant virus DNA containing the γ -interferon export sequence fused to the soluble form of the rat liver Gal β (1,3/4)GlcNAc α -2,3-sialyltransferase (*r*ST3Gal III; EC 2.4.99.6) was kindly received from Dr. Markus Streiff [72].

3.1.1.1 Insect cell culture

Complete culture medium SF-900 II with L-glutamine supplemented with 10% FCS and 1% Penicillin/Streptomycin) at 27°C

Several established insect cell lines are highly susceptible to AcNPV virus infection. In this work, the *Sf9* cell line was used for the *r*ST3Gal III production. The *Sf9* cell line was originally established from ovarian tissues of *Spodoptera fugiperda* (*Sf9*) larvae. Healthy insect cells attach well to the bottom of the cell culture plate at 27°C, forming a monolayer and double every 18-24 hours. Infected cells become round, enlarged, develop enlarged nuclei, do not attach and stop dividing.

3.1.1.2 Long-term insect cell storage [238]

The *Sf9* cells were kept for long-term storage at – 80°C or in liquid nitrogen. Aliquots of stock cultures were frozen down periodically to provide a backup in case of contamination.

Table 3.1 Components for long-term insect cell storage.

| | |
|--|---|
| Healthy cells (>98% viable) free from contamination in exponential growth | |
| Complete culture medium SF-900 II with L-glutamine supplemented with 10% FCS and 1% Penicillin/Streptomycin) at 27°C | |
| Trypan blue, hemocytometer, sterile cryovials (1 ml) | |
| Freezing medium | 85% complete culture medium, 15% DMSO, sterile filtrated (0.22 µm filter) |

Freezing:

The cells were examined for health, viability (>98%), exponential growth ($\approx 1 \times 10^6$ cells/ml) and signs of contamination.

Cells were pelleted by gentle centrifugation at 1000 x g, for 5 min at 27°C, the old media was removed, and the pellet was resuspended in fresh media to a density of $1-2 \times 10^7$ cells/ml. An equal volume of the freezing medium was added (1-2 ml/flask) and placed on ice (*Table 3.1*). The cell suspension was aliquoted in cryovials (1 ml) and frozen at – 20°C for 1 h, then kept 2 days at – 80°C and finally stored in liquid nitrogen. After 2 weeks cell-aliquotes were thawed and checked for viability.

Thawing frozen cells:

The cell suspension was thaw at 37°C within 40 – 60 sec. The content of 1 vial (1 ml) was transferred to a 25 cm² tissue-culture flask containing 10 ml of complete culture medium (medium with two-fold of normal FCS concentration). Cells were incubated at 27°C for 3 h, checked for viability and finally the culture medium was replaced with 10 ml of fresh complete medium. The cell culture was further incubated at 27°C for 24 h. Additionally, 7 ml of complete medium was added to the culture flask and incubated at 27°C until the cells showed confluence.

3.1.1.3 Amplification of virus stocks [238]

Table 3.2 Components for virus stock amplification.

| |
|---|
| Sf9 cell (1×10^6 cells/ml) |
| Complete culture medium (SF-900 II with L-glutamine supplemented with 10% FCS and 1% Penicillin/Streptomycin) |
| 35 mm and 100 mm tissue-culture plates or 200 ml spinner culture |
| Purified virus stock to be amplified |

Cells growing in the tissue-culture plates

First amplification of virus stock:

Cells (1×10^6) were seeded in a 35 mm tissue-culture dish in final volume of 2 ml of culture medium. The cell-culture plate was kept for 1 h at 27°C ensuring the attachment of the cells to the bottom of the tissue-culture plate. Culture medium was aspirated and cells were infected with 0.5 ml of purified virus stock inoculum (*Table 3.2*). Cells were incubated at room temperature (RT) for 1 h with gentle rocking. 1.5 ml of complete culture medium was added and incubation was preceded for 3 days.

Second amplification of virus stock:

Four 100 mm tissue-culture dishes were seeded with 5×10^6 cells each in a final volume of 10 ml of complete tissue medium. After the cells attached to the cell-culture plate, the culture medium was aspirated. 1 ml of the first amplification virus stock was diluted with 3 ml complete tissue medium and added to the cell-culture plate. Cells were incubated at room temperature for 1 h with gentle rocking. 9 ml of additional complete culture medium was added and incubated further for 3 days.

A large-scale working stock of virus was prepared repeating this procedure and using many tissue-culture dishes, and infecting the cells with 0.1 of multiplicity of infection (MOI) which is defined as plaque-forming units per number of cell (pfu/cell).

Cells grown in suspension

Cells were grown in 200 ml Erlenmeyer flask until they reached a density of 1×10^6 cells/ml. They were collected by centrifugation at $1000 \times g$ for 5 min at room temperature and resuspended gently in 20 ml of complete culture medium. Second amplification virus

stock was added to give a MOI of 0.1 (1×10^7 pfu of virus) and incubated at room temperature for 1 h with gentle rocking. Cells and virus were returned to an Erlenmeyer flask and fed with 180 ml complete culture medium. The Erlenmeyer flask was stirred at 27°C for 3 days. The tissue-culture fluid was harvested by centrifugation to remove cell debris, and the supernatant was titrated and stored at 4°C.

3.1.1.4 Determining virus titer by end-point dilution

The determination of the virus titer by end-point dilutions (*Table 3.3*) involves the inoculation of multiple cultures with different dilutions of the virus, and estimation of the dilution of virus that would infect 50% of the cultures (the end-point dilution). This quantity of virus is known as the 50% tissue-culture infectious dose, or TCID₅₀. Virus titers determined in this manner may be expressed as TCID₅₀/ml, or converted to pfu/ml.

Table 3.3 Components for end-point dilution analysis.

| |
|---|
| Sf9 cells (1×10^6 cells/ml) |
| Complete culture medium (SF-900 II with L-glutamine supplemented with 10% FCS and 1% Penicillin/Streptomycin) |
| 96-well tissue-culture plates |
| Virus stock to be titrated |

Twelve-fold serial dilutions of the virus stock were prepared (10^{-1} , 10^{-2} , 10^{-3} , 10^{-4} 10^{-12}) in a final volume of 10 ml. Cells were diluted to a concentration of 1×10^5 cells/ml with complete culture medium. 100 µl of Sf9 cell suspension was seeded into a 96-well microtiter plate and mixed gently with 10 µl of each dilution. Four wells were seeded with 100 µl of Sf9 cell suspension as uninfected controls. Cell-culture plates were placed with a damp paper towel into a plastic box to avoid dehydration, and incubated at 27°C for 5 days. On the third day cells were checked in order to monitor their normal growth. Five days later each well was examined for infected cells (virus replication). Wells with signs of infection (one infected cell) were scored as positive. All positive and negative wells were counted for each dilution.

The virus titer was calculated by the following method [239]:

All cultures infected at a given dilution would have been infected at all lower dilutions, and

conversely, all cultures uninfected at that dilution would have been uninfected at all higher dilutions.

$$PD = (A - 50) / (A - B)$$

PD – proportionate distance

A – is the % response above 50%

B – is the % response below 50%

$$\text{Titer of virus} = 1/\text{TCID}_{50}$$

$$\text{pfu} = \text{TCID}_{50} \times 0.69/\text{ml}$$

3.1.1.5 Virus storage [238]

For short-term storage, working stocks of virus were sterile filtrated (0.2 μm) and stored in culture medium supplemented with 5% FCS at 4°C for optimal virus stability. Infected cells and cell debris were removed from the virus stock by centrifugation at 1000 x g for 5 min at 4°C without loss in titer of virus. For long-term storage virus stock aliquots were frozen in a culture medium at -80°C.

3.1.2 rST3Gal III expression in baculovirus infected insect cells

Table 3.4 Components for rST3Gal III expression.

| |
|--|
| Sf9 cell (1 x 10 ⁶ cells/ml) |
| Complete culture medium SF-900 II with L-glutamine supplemented with 10% FCS and 1% Penicillin/Streptomycin) |
| 2 l Erlenmeyer flasks |
| Recently titrated virus stock |

Cells grown in tissue-culture plates.

The soluble rST3Gal III was produced by infecting Sf9 insect cells in monolayer culture (Table 3.4) with the recombinant virus (MOI of 20 pfu/cell). Complete medium was removed from confluent cells, and the fresh medium containing 20 pfu/cell was added. After 1 h at room temperature incubation, inoculum was removed, fresh medium was added, and the culture was returned to the incubator at 27°C. Conditioned medium was

collected 72 h post-infection, spun, filtrated through a 0.2 µm membrane and stored at –20°C.

Cells growing in the suspension

Two liter Erlenmeyer flasks containing 500 ml of *Sf9* cell suspension in serum free medium supplemented with antibiotics were shaken in Erlenmeyer flasks (70 rpm) at 27°C (Table 3.4). At a cell density of 1.8×10^6 cells/ml the culture was infected with 5 ml of virus stock (2.2×10^{10} pfu/ml end point dilution) and incubated at room temperature for 1 h while gently rocking. 72 h post-infection the culture was harvested, and the cells and debris were removed by centrifugation at 9000 rpm for 30 min at 4°C.

The cleared supernatant containing the rST3Gal III from 6 to 8 Erlenmeyer flasks was first pre-filtered through a submicron filter (Gelman preflow DCF-CFG95NG) and then concentrated in an Amicon Ultrafiltration cartridge (YM-30) to 300 ml. This was followed by addition of 300 ml 50 mM sodium-cacodylate (pH 6.5) and reconcentration to 150 ml. Finally, the concentrate was stored at –20°C in 50 ml aliquots.

3.1.3 Analysis of the expressed rST3Gal III

3.1.3.1 Sodium dodecyl sulfate – polyacrylamide gel electrophoresis (SDS-PAGE)

SDS-PAGE is used to separate proteins depending on their molecular weight [240]. The negatively charged detergent, SDS, disrupts non-covalent bonds while mercaptoethanol, reduces disulfide bonds. The molecular mass can be estimated using a molecular marker. Under native conditions, neither SDS nor β-mercaptoethanol is added to the protein sample, which enables migration of proteins according to their native charge and shape (Table 3.5).

Table 3.5 Components for SDS-PAGE analysis.

| | |
|---|---|
| Stacking buffer | 0.5 M Tris, 0.4% SDS (Bio Rad), adjusting pH to 6.7 |
| Separating buffer | 1.5 M Tris, 0.4% SDS, adjusting pH to 8.8 |
| SDS-PAGE sample buffer (3 x reducing) | 65 mM Tris, 20% (v/v) glycerol anhydrous (Fluka BioChemika), 10% (v/v) β -mercaptoethanol (Fluka BioChemika), 4% (w/v) SDS, 1 dip bromphenol blue (Bio Rad), adjusting pH to 6.75 |
| SDS-PAGE sample buffer (2 x non-reducing) | Reducing sample buffer without β -mercaptoethanol |
| SDS-PAGE sample buffer (2 x native) | Reducing sample buffer without β -mercaptoethanol and SDS |
| Electrophoresis buffer (10 x) | 0.25 M Tris, 2 M glycine (Fluka BioChemika), 1% SDS adjusting pH to 8.3 |
| Low molecular weight marker (LMW) (Sigma) | |

Table 3.6 The SDS-PAGE reaction protocol.

| Components | Separating gel | Stacking gel |
|--|----------------|--------------|
| | 12.5% | 4% |
| Deionized water | 3.75 ml | 5.67 ml |
| Acrylamide 4K solution (30%) (AppliChem, BioChemika) | 6.25 ml | 1.33 ml |
| Stacking gel buffer / separating gel buffer | 5 ml | 3 ml |
| <i>N,N,N',N'</i> -tetramethylethylenediamine (TEMED) (Serva) | 30 μ l | 20 μ l |
| Ammonium persulfate (APS) (40%) (Sigma) | 30 μ l | 20 μ l |

The reducing SDS-PAGE:

The components of the separating gel (12.5%) were mixed except for APS, which was added just before pouring the gel (*Table 3.6*). After polymerization of the resolution gel, the stacking gel was prepared, poured in the same way and the comb placed. Before samples were loaded on the gel, they were mixed with reducing SDS-PAGE sample buffer (3 x). The samples prepared with reducing buffer as well as a marker (LMW) were heated for 5

min at 95°C in a heated block. All the samples were centrifuged at 13 200 rpm for 1 min. The samples were run through the stacking gel at 75 V. When the samples entered the separating gel, the voltage was increased to 150 V.

The non-reducing SDS-PAGE gel was prepared in the same way as reducing SDS-PAGE gel with exception of using 2 x non-reducing SDS-PAGE sample buffer.

For the native SDS-PAGE gel, 2 x native SDS-PAGE sample buffer as well as all buffers without SDS and β -mercaptoethanol were used.

3.1.3.2 SDS-PAGE staining [240]

The Coomassie blue dye was used for 45 min to stain the gel followed by destaining solution (*Table 3.7*) until the bands were visible and the background almost decolorized.

Table 3.7 The Coomassie blue staining solutions.

| | |
|------------------------------------|---|
| Coomassie blue staining solution | 1 g Coomassie brilliant blue G250 (Bio Rad), 1 g Coomassie brilliant blue R250 (Bio Rad), 200 ml methanol (Riedel-de Haën), 200 ml deionized water (Millipore), filtrated (Fluted filter, Ø 32 cm, Schleicher & Schuell AG) |
| Coomassie blue destaining solution | 150 ml acetic acid glacial (Hänseler AG), 500 ml methanol, add 2000 ml deionized water (Millipore) |

In order to visualize small amount of protein (as little as 10 ng), gels were treated with silver stain (*Table 3.8*) which is 100 time more sensitive than Coomassie blue.

Table 3.8 The silver staining solutions.

| | | |
|-----------------|--|-----------|
| Fixation | 100 ml ethanol, 25 ml acetic acid glacial, make up to 250 ml with deionized water | 30 min |
| Sensitizing | 75 ml Ethanol, glutardialdehyde (25% w/v), sodium thiosulphate (5% w/v), 17 g sodium acetate. make up to 250 ml with deionized water | 30 min |
| Washing | Deionized water | 3 x 5 min |
| Silver reaction | Silver nitrate solution (2.5% w/v), formaldehyd (37% w/v), make up to 250 ml with deionized water | 20 min |
| Washing | Deionized water | 2 x 1 min |
| Developing | 6.25 g Sodium carbonate, formaldehyd (37% w/v), make up to 250 ml with deionized water, stir | 2-5 min |

| | | |
|----------------------------------|--|-----------|
| | vigorously to dissolve sodium carbonate | |
| Stopping | (3.65 g) EDTA-Na ₂ x 2H ₂ O | 10 min |
| Washing | Deionized water | 3 x 5 min |
| Preserve for plastic backed gels | Glycerol (87% w/w), make up to 250 ml with deionized water | 20 min |

3.1.3.3 Western blot analysis [241]

Table 3.9 The Western blotting solutions.

| | |
|---|---|
| Anode buffer I | 0.3 M Tris, 20% (v/v) methanol |
| Anode buffer II | 0.025 M Tris, 20% (v/v) methanol |
| Cathode buffer | 0.04 M 6-aminocaprone acid, 20% (v/v) methanol |
| Ponceau S solution | 0.1 Ponceau (w/v) in 5% acetic acid (v/v) (Sigma) |
| Trans-Blot [®] Transfer Medium Nitrocellulose membrane (0.45 μm) | |
| Filter paper 3 mm (Whatman [®]) | |

Proteins separated by SDS-PAGE can be transferred to a nitrocellulose membrane by semi-dry-blotting, and particular proteins can be detected by staining with a specific antibody. Two filter papers were soaked in anode buffer I, one filter paper in anode buffer II and three filter papers in cathode buffer (*Table 3.9*). A nitrocellulose membrane was placed in the anode buffer II, and the SDS-PAGE gel into cathode buffer. The assembly was prepared in the following way: filter papers in anode buffer I were placed on top of the anode followed by the filter papers in anode buffer II, the membrane and the gel. The filter papers in cathode buffer were added and the protein transfer was run for 1 h at 15 V. The membrane was stained in Ponceau S solution to verify the efficiency of the protein transfer. The molecular weight standards were marked and the membrane was washed with deionized water.

3.1.3.4 Immunodetection

Table 3.10 The immunodetection buffers.

| | |
|------------------------------------|---|
| Tris-buffered saline (TBS) | 20 mM Tris, 500 mM NaCl (Fluka Chemika) |
| Tween Tris-buffered saline (TTBS) | 0.05% Polyoxyethylene Sorbitan Monolaurate (Tween 20) (Sigma) in TBS |
| Primary antibody | rabbit ST6Gal I purified serum (1:500) [242], 1% BSA, 0.1% NaN ₃ , 10 ml TBS |
| Secondary antibody | Goat anti-rabbit IgG (whole molecule) alkaline phosphatase (AP) conjugated (1:10 000) (Sigma), 1% BSA, 0.1% NaN ₃ , 10 ml TTBS |
| BCIP/NBT | 5-bromo-4-chloro-3-indolylphosphat / Nitroblau-tetrazolium chloride 50 mg/ml in 100% dimethylformamide (Fluka BioChemika) |
| Developing buffer | 100 mM Tris, 100 mM NaCl (Fluka Chemika), 5 mM MgCl ₂ x 6H ₂ O (Fluka BioChemika), adjusting the pH to 8.8 |
| Bovine serum albumin (BSA) (Sigma) | |

The immunodetection is a method based on antigen/antibody interaction. The proteins were transferred to the nitrocellulose membrane and the unoccupied binding sites on the membrane blocked with 2% BSA in TBS buffer (*Table 3.10*). The membrane was incubated for 1 h at room temperature on the shaker. In order to remove BSA, the membrane was washed 3 times for 5 min with TTBS buffer and incubated overnight at room temperature with the primary antibody that specifically binds to the protein. The membrane was washed 3 times for 5 min with TTBS and incubated for 2 h with the secondary antibody coupled to alkaline phosphatase. Finally, the membrane was washed twice for 5 min with TTBS buffer and 5 min with TBS buffer.

For visualization of the reaction, the membrane was incubated with 10 ml developing buffer containing 40 µl NBT/BCIP until a precipitate was visible. Violet precipitation is caused by oxidative dephosphorylation of BCIP and the reduction of NBT under basic conditions (pH 8.8). The developing reaction was stopped by washing the membrane with deionized water.

3.1.4 Purification of the rST3Gal III protein [243]

Table 3.11 Buffers for the protein purification by affinity chromatography.

| | |
|--|--|
| Buffer A | 50 mM Na cacodylate (pH 6.5), 0.1 M NaCl |
| Buffer B | 50 mM Na cacodylate (pH 6.5), 1 M NaCl |
| Buffer C | 50 mM Na cacodylate (pH 6.5), 50 mM NaCl |
| 5 ml CDP-hexanolamine-agarose (10 μ mol CDP/ml gel slurry), Calbiochem | |
| Centrifugal filter devices, Centricon YM-30 (Amicon) | |
| BioLogic Duo-Flow FPLC system | |

The media containing the rST3Gal III (40 ml) was filtrated through 0.45 μ m filter and diluted to 80 ml with 40 ml of buffer C (*Table 3.11*). The column was equilibrated with 1 column volume (CV) of buffer B and 5 CV of buffer A by using the Fast Performance Liquid Chromatography (FPLC) system (Bio-Rad). Samples were then applied to a CDP-hexanolamine-agarose column and after washing the column with buffer A for 10 CV, the column was eluted with 1 CV of buffer B. Fractions containing the rST3Gal III enzyme were pooled and concentrated using centrifugal filter devices (Centricon YM-30).

3.1.4.1 Bradford protein assay [244,245]

Table 3.12 Buffer components for Bradford protein determination.

| | |
|---|--|
| Solution A | 100 mg Coomassie Brilliant Blue G-250 (Bio-Rad), 10 ml phosphoric acid 85% wt. (Aldrich [®]), 5 ml ethanol (Merck), add 100 ml deionized water |
| Solution B | 1 M NaOH (Fluka BioChemika) |
| Protein standard (BSA 400 μ g/ml protein) (Sigma Diagnostics) | |

The Bradford method is used for the protein quantification. Under acidic conditions, the Coomassie color binds to the protein, whereby the maximal absorption of the dye is shifted from 465 nm to 595 nm and can be measured spectrophotometrically, which enables estimation of the protein concentration.

Standard curve: a dilution series from 20 to 200 μ g/ml of the protein-standard BSA was

prepared. 20 μ l of each dilution was mixed with 50 μ l of 1 M NaOH and 1 ml of solution A was added (*Table 3.12*). After incubation for 5 min at room temperature, 300 μ l of the mixture was transferred on a test-plate and the absorbance was measured at 595 nm.

The same reaction mixture was prepared for fractions with unknown protein concentrations. The absorbance was measured at 595 nm and the protein concentration was kept in the linear range corresponding to the standard curve.

3.1.5 *r*ST3Gal III enzyme activity assay [246]

Table 3.13 Components for enzyme activity assay.

| | |
|--|---|
| Column equilibration C18 Sep-Pak Cartridges (Waters) | 5 ml Methanol, 10 ml H ₂ O |
| IRGA-SAFE plus high flash point LSC-cocktail | 10 ml |
| Reaction buffer [247] | 100 mM Na cacodylate (pH 6.0), 0.3% Triton X-100, 10 mM MgCl ₂ |
| Acceptor substrate | Table 3.14 |

The standard assay mixture (20 μ l) contained 600 μ M of Type II (**1**) acceptor substrate (*Table 3.14*), expressed *r*ST3Gal III (0.007 mU), 0.2 mM CMP-NeuNAc (4 nmol), and 60 000 cpm of CMP-[¹⁴C] NeuNAc in a reaction buffer (*Table 3.13*). After incorporation of [¹⁴C] NeuNAc (~10%) by incubation for 1 h at 37°C, the reaction mixture was diluted with 5 ml of water and applied to Sep-Pak C18 cartridges. The column was washed two times with 5 ml of water and eluted with 6 ml of methanol. Incorporation of the [¹⁴C] NeuNAc was determined using liquid scintillation counting twice the same eluate.

This standard assay was also used to calculate the enzyme units. Taking into consideration that one unit of enzyme activity corresponds to transfer of 1 μmol of NeuNAc to Type II (1) per minute, enzyme activity was determined using the following equation:

$$\frac{\frac{\text{count 1+2}}{2} - \text{blank cpm}}{\text{total cpm}} \times 2.1 \text{ pmol}$$

$$\text{mg (protein)} \times \text{incubation time (min)}$$

3.1.5.1 Stability of *r*ST3Gal III during the long-period incubation

In order to determine the enzyme stability over a long period of incubation, as an important parameter for preparative syntheses, the activity of the *r*ST3Gal III over time at 37°C was investigated. Enzyme incubation was performed in a reaction buffer containing 0.1 mM CMP-NeuNAc (2 nmol), CMP-[¹⁴C] NeuNAc (60 000 cpm) and 200 μM of Type I acceptor substrate at 37°C over a long period. Samples were taken after 0, 6, 9, 12, 24, 60 and 84 h of incubation and the activity of the sialyltransferase was determined by standard enzymatic assay (see chapter 3.1.5).

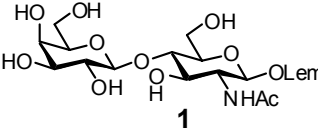
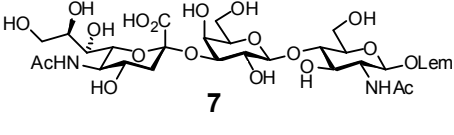
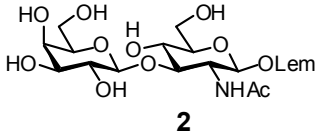
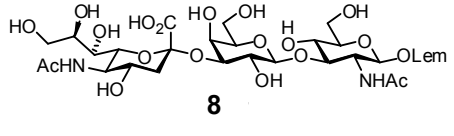
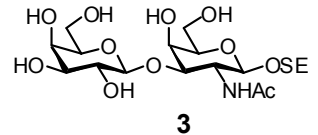
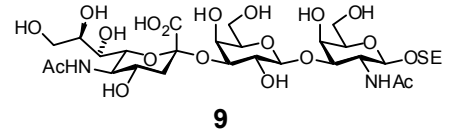
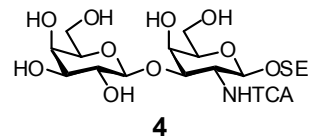
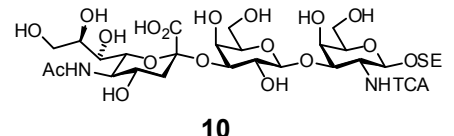
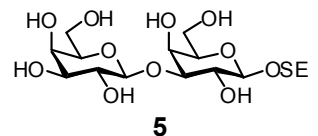
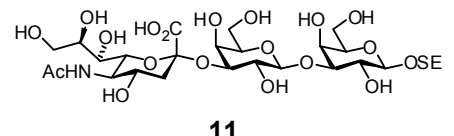
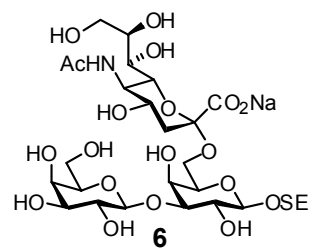
3.1.6 Long-term enzyme storage

Enzyme aliquots were mixed with 20% and 50% of glycerol solution and stored at 4°C and -20°C as well as a control-aliquot which was free of glycerol. Enzyme activity was checked after 2 weeks and 15 months incubating for 1 h at 37°C in the reaction buffer containing 200 μM of Type II acceptor substrate, CMP-[¹⁴C] NeuNAc (60 000 cpm) and 100 μM non-labeled NeuNAc (see chapter 3.1.5).

3.1.7 Determination of the enzyme kinetic parameters [248]

Table 3.14 Molecular structure of acceptor substrates used for kinetic parameters determination.

OSE: O-(trimethylsilyl)ethyl (O-CH₂CH₂-Si(Me)₃), OLem: O-(Methoxycarbonyl)octyl (O-(CH₂)₈CO₂Me), TCA: tri-chloro acetyl (COCCl₃).

| Acceptor | Molecular structure | Product |
|---|---|---|
|  1 | Gal β (1,4)GlcNAc- β -OLem Type II |  7 |
|  2 | Gal β (1,3)GlcNAc- β -OLem Type I |  8 |
|  3 | Gal β (1,3)GalNAc- β -OSE Type III |  9 |
|  4 | Gal β (1,3)GalNHTCA- β -OSE |  10 |
|  5 | Gal β (1,3)Gal- β -OSE |  11 |
|  6 | Gal β (1,3)[NeuNAc α (2,6)]Gal- β -OSE | 12 |

Determination of enzyme kinetic parameters of *r*ST3Gal III was performed as described in the chapter 3.1.5 using different concentrations of each acceptor substrate (Table 3.14) ranging from 25 μ M to 0.6 mM for a native, and 50 μ M to 2 mM for non-native acceptor substrate. All acceptors were linked to either OLem or OSE aglycones to facilitate a product isolation using C18 columns. Relative activity for each di(tri)saccharide acceptor substrate was calculated as a percentage of the incorporation of [¹⁴C] NeuNAc into the *D*-Gal-containing di(tri)saccharide. Under standard incubation conditions (37°C; pH 6.0)

formation of the product was shown to be linear in time. Furthermore, enzyme kinetic parameters were obtained from double-reciprocal plots by linear regression analysis of Lineweaver-Burk plots.

3.1.8 Preparative syntheses [249,250]

After determination of enzyme kinetic parameters and *r*ST3Gal III long-period activity with Type I natural substrate, enzyme was used for chemo-enzymatic preparative synthesis. Substrates and CMP-NeuNAc were incubated with *r*ST3Gal III for 3-5 days at 37°C in a mixture of 50 mM sodium cacodylate buffer (pH 6.5), 60 mM MnCl₂-solution (the same effect as MgCl₂), water containing BSA and the calf intestine alkaline phosphatase (CIAP, Roche; EC 3.1.3.1) used to prevent the enzyme inhibition caused by CMP [251]. After 17-24 hours of incubation, an additional aliquot of transferase was added (except for the natural substrates Type I and Type II). The reactions were monitored by TLC (silica gel, DCM/MeOH/H₂O 10:4:0.8).

3.1.8.1 A synthesis of NeuNAc α (2,3)Gal β (1,4)GlcNAc- β -OLem (7) product

Disaccharide **1** (3.0 mg, 5.4 μ mol) and CMP-NeuNAc (5.3 mg, 8.1 μ mol) were dissolved in a mixture of 50 mM sodium cacodylate-buffer pH 6.5 (0.6 ml), 60 mM aqueous MnCl₂ (0.6 ml) and deionized water (0.4 ml) containing BSA (0.4 mg, Fluka). The mixture was incubated at 37°C with CIAP (2 U) and recombinant *r*ST3Gal III (0.6 mU). After 3 d TLC (silica gel, DCM/MeOH/H₂O 10:4:0.8) indicated complete consumption of **1**. The turbid solution was centrifuged and the supernatant passed over a RP-18 column which was washed with water before the product was eluted with MeOH. After evaporation of methanol, the residue was chromatographed on silica gel (DCM/MeOH/H₂O 10:4:0.4, then 6:4:1) to yield trisaccharide **7** (3.5 mg, 76%) as colorless powder after a final lyophilization from water. The spectroscopic data of **7** were in accordance to those reported [252].

3.1.8.2 A synthesis of NeuNAc α (2,3)Gal β (1,3)GlcNAc- β -OLem (8) product

According to the procedure described for the synthesis of **7**, compound **2** (3.0 mg, 5.4 μ mol) was incubated with CMP-NeuNAc (5.3 mg, 8.1 μ mol) and *r*ST3Gal III (0.45 mU). Reaction control by TLC (silica gel, DCM/MeOH/ H₂O 10:4:0.8) indicated complete consumption of **2** after 3 d. After work-up, the crude product was purified on RP-18

(H₂O/MeOH gradient 1:0 to 1:1) to yield trisaccharide **8** (4.1 mg, 90%) as colorless powder after a final lyophilization from water. The spectroscopic data of **8** were in accordance to those reported [253].

3.1.8.3 A synthesis of NeuNAc α (2,3)Gal β (1,3)GalNAc- β -OSE (9**) product**

Disaccharide **3** (10.0 mg, 20.6 μ mol) and CMP-NeuNAc (20.4 mg, 31.1 μ mol) were dissolved in a mixture of 50 mM sodium cacodylate-buffer pH 6.5 (2 ml), 60 mM aqueous MnCl₂ (2 ml) and deionized water (1.3 ml) containing BSA (2.0 mg). The mixture was incubated at 37°C with CIAP (2 U) and recombinant rST3Gal III (1.5 mU). After 1 d, additional rST3Gal III (0.75 mU) was added and the incubation continued for 4 d. The turbid solution was centrifuged and the supernatant passed over a RP-18 column which was washed with water before the crude product was eluted with MeOH. After evaporation of the solvent, the residue was chromatographed on RP-18 (H₂O/MeOH gradient 1:0 to 1:1) to yield trisaccharide **9** (9.0 mg, 56%) and starting material **3** (4.4 mg, 44%) as colorless powders after a final lyophilization from water.

3.1.8.4 A synthesis of NeuNAc α (2,3)Gal β (1,3)GalNHTCA- β -OSE (10**) product**

According to the procedure described for the synthesis of **9**, compound **4** (12.0 mg, 20.4 μ mol) was incubated with CMP-NeuNAc (20.2 mg, 30.1 μ mol), BSA (2.1 mg), CIAP (2 U) and rST3Gal III (1.5 mU). After 1 d additional rST3Gal III (0.75 mU) was added and the incubation continued for 3 d. After work-up, the residue was chromatographed on silica gel (DCM/MeOH/H₂O 10:4:0.4, then 6:4:1) to yield starting material **4** (7.5 mg, 62%) and trisaccharide **10** (6.4 mg, 36%) as colorless powders after a final lyophilization from water.

3.1.8.5 A synthesis of NeuNAc α (2,3)Gal β (1,3)Gal- β -OSE (11**) product**

According to the procedure described for the synthesis of **9**, compound **5** (10.0 mg, 22.6 μ mol) was incubated with CMP-NeuNAc (22.3 mg, 33.9 μ mol), BSA (2.3 mg), CIAP (2 U) and rST3Gal III (1.5 mU). After 1 d additional rST3Gal III (0.75 mU) was added and the incubation continued for 3 d. After work-up, the residue was chromatographed on silica gel (DCM/MeOH/H₂O 10:4:0.4, then 6:4:1) to yield starting material **5** (4.0 mg, 40%) and trisaccharide **11** (9.7 mg, 59%) as colorless powders after a final lyophilization from water.

3.1.8.6 A synthesis of NeuNAc α (2,3)Gal β (1,3)[NeuNAc α (2,6)]Gal- β -OSE (12**) product**

According to the procedure described for the synthesis of **9**, trisaccharide **6** (10.0 mg, 13.2

μmol) was incubated with CMP-NeuNAc (13.0 mg, 19.8 μmol), CIAP (2 U) and *r*ST3Gal III (1.5 mU). in a mixture of 50 mM sodium cacodylate-buffer pH 6.5 (2 ml), 60 mM aqueous MnCl_2 (2 ml) and deionized water (1.3 ml) containing BSA (2.0 mg). After 1 d, additional *r*ST3Gal III (0.75 mU) was added and the incubation continued for 3 d. After work-up, the crude product was chromatographed on silica gel (DCM/MeOH/ H_2O 10:4:0.8) to yield exclusively starting material **6** (9.5 mg, 95%) as colorless powder after a final lyophilization from water.

3.2 *h*ST6Gal I expression in BHK-21 cells, purification and characterization

3.2.1 BT-*h*ST6Gal I cloning and expression

Using the strategy described by Grabenhorst for the construction of chimeric secretable α -1,3/4-fucosyltransferase [246,254], a chimeric secretable protein (BT-*h*ST6Gal I) was constructed by fusion of the full-length human β -trace protein (β -TP; EC 5.3.99.2) sequence to the *N*-terminus of the catalytic domain of human Gal β (1,4)GlcNAc α -2,6 sialyltransferase (*h*ST6Gal I; EC 2.4.99.1) protein [255].

3.2.1.1 Cell culture

Table 3.15 The cell culture media and buffers.

| | |
|----------------------------|---|
| DME culture medium (Gibco) | Dulbeccos Modified Eagle Medium; supplemented with HEPES, 45 mM NaHCO ₃ , 2 mM Glutamin, 65 mg/l Ampicillin and 100 mg/l Streptomycinsulfate, pH 7.0 |
| Culture medium | DME supplemented with 10% FCS |
| Selective medium | DME supplemented with 10% FCS, different Hygromycin B concentrations (25, 50 and 100 μ g/ml) |
| Production medium | DME without or supplemented with 2% FCS |
| PBS | Phosphate-buffered saline (autoclaved) |
| EP | 1 mM EDTA (pH 8.0; sterile) in PBS |
| TEP | 0.1% Trypsin in 0.6 mM EDTA in PBS |
| Freezing medium | 5% DMSO in FCS |

Adherent baby hamster kidney (BHK-21) cells were grown in 5 ml of culture medium in a 25 cm² tissue-culture flask (Table 3.15). Cells were incubated in a humid 5% CO₂-containing environment at 37°C. After 2-3 days, confluent BHK-21 and CHO cells were washed with 5 ml of PBS buffer and detached from the bottom of the cell-culture plate using 0.5 ml EP or TEP solution, respectively, for several minutes at 37°C. Cells were resuspended in 5 ml of culture medium and 1/25 of the cell suspension was used as

inoculum. For long-term storage, 5×10^7 cells were transferred to 1.5 ml of freezing medium and stored in liquid nitrogen.

3.2.1.2 Long-term storage

Cell freezing:

Cells were growing in 25 cm² culture flask until they reached 80% confluence. Culture medium was aspirated and cells were incubated in 0.5 ml EP solution for few minutes at 37°C. Cells were collected in 5 ml of fresh culture medium, and centrifuged at 1000 rpm for 5 min at 4°C. The cell pellet was resuspended in 1.5 ml of freezing medium (*Table 3.15*), kept at – 80°C for several days and finally, after verifying cell viability, was stored in liquid nitrogen.

Thawing frozen cells:

Cells stored in liquid nitrogen were placed in a water-bath at 37°C and thawed rapidly. Immediately afterwards, they were placed in culture medium (*Table 3.15*), the volume of which depended on the size of the tissue-culture flask, e.g., 5 ml of culture medium for a 25 cm² flask. They were further incubated for several hours, after which the medium was replaced, and culturing was allowed to proceed until cells reached confluence.

3.2.1.3 Determination of cell number and viability [256]

| | |
|---------------------|--|
| Trypanblue solution | 2 V trypanblue (0.2%), 1 V of NaCl (4.25%) |
|---------------------|--|

Cell suspensions (50 µl) were mixed with Trypan blue solution (50 µl), transferred to a hemocytometer and analyzed under a microscope. The viability of the cells (ratio between non-colored and colored cells > 98%) and cell counting was measured using Trypan blue solution. The cells were counted, the average number of cells was multiplied by 10⁴ and the dilution factor, and the final number of cells was given in cell number/ml.

3.2.1.4 Stable transfection and selection [255]

Table 3.16 Components for stable transfection and selection.

| Substances | Solution concentration | Final solution |
|---|------------------------|----------------|
| pCR BT- <i>hST6Gal I</i> (β -Trace Protein – | 0.65 g/l | 10 µg |

| | | |
|----------------------------|---|--------|
| <i>hST6Gal I</i>) | | |
| pCR Hyg (Hygromycin) | 0.5 g/l | 2.5 µg |
| CaCl ₂ solution | 2.5 M | 25 µl |
| HEBS (2 x) | 40 mM Hepes, pH 7.05, 300 mM NaCl, 10 mM KCl, 1.4 mM Na ₂ HPO ₄ | 250 µl |
| Sterile H ₂ O | Autoclaved | 206 µl |
| Solution A | 1/10 CaCl ₂ + pCR BT-ST6Gal I+ pCR Hyg + H ₂ O | 250 µl |
| Solution B | HEBS (2 x) | 250 µl |

Transfection of BHK-21 cells was performed, as described by Sambrook *et al.* [257], using a calcium phosphate precipitation method.

For stable transfection, solution A was prepared by adding 10 µg of pCR BT-*hST6Gal I* and 2.5 µg of pCR Hyg plasmid DNA to the 250 mM CaCl₂ solution (*Table 3.16*). The suspension was vortexed thoroughly and mixed with 250 µl of solution B. The transfection mixture of 500 µl was transferred to a 25 cm² culture flask containing exponentially growing, app.1/4 confluent BHK-21 cells in 5 ml culture medium. Consequently, when 6-well cell-culture plates were used for the transfection, DNA concentration was proportionally scaled down according to the surface of the tissue-culture plate. Cells were incubated for a further 24 h. The following day, DME culture medium was exchanged for the selective medium (*Table 3.15*) in such a way that a 1/6, 2/6 and 3/6 volume of the cells was growing in culture medium in the presence of 25 µg/ml, 50 µg/ml and 100 µg/ml Hygromycin B, respectively. Selective medium was replaced for 2-3 times over the following days. Hygromycin B-resistant BHK-21 cells were finally transferred to a 25 cm² culture flask and grown until they reached confluence. The selective medium was replaced with culture medium (*Table 3.15*) and cells were incubated for a further 2 days. Supernatant was finally analyzed for protein expression by Western blotting and an ST enzyme activity assay.

3.2.1.5 The cell clone selection [258]

Stably-transfected BHK-21 cells expressing sufficiently the gene of interest were highly diluted in order to get single cell clones (see chapter 3.2.2.3), which were each then transferred to a 12-well cell-culture plate. Clones were cultured in 0.5 ml selective medium

(Table 3.15) until they reached confluence. Selective medium was finally replaced with 0.5 ml culture medium. Supernatant was collected 2 days later, analyzed by Western Blotting method and checked for *hST6Gal I* activity. The clones giving the strongest band intensity (Western blotting) and the highest enzymatic activity were chosen for further culturing.

3.2.1.6 Optimization of the protein expression

Positive clones were grown for 3 days in a 25 cm² culture flask containing 5 ml production medium (Table 3.15). Each day a 250 µl sample was collected and centrifuged at 800 x g for 10 min at 4°C. After the three days, the supernatant was collected by centrifugation and stored at – 20°C. Cells were fed with 5 ml fresh production medium, and grown for a further 3 days repeating the same procedure mentioned above. Samples were examined by Western Blotting (see chapter 3.2.2.2) and the ST activity enzyme test.

3.2.2 Analysis of the expressed BT-*hST6Gal I*

BT-*hST6Gal I* chimeric protein was analyzed using the previously mentioned biochemical methods, e.g. SDS-PAGE and Western blotting (see chapter 3.1.3). In some experiments, described standard methods were modified as follows.

3.2.2.1 SDS-PAGE [246]

| | |
|---|--|
| Reducing sample buffer (1 x) | 1 ml SDS-buffer, 150 µl 0.3 M DTE, 200 µl glycerol, 200 µl Bromphenol blue |
| SDS-buffer | 10 ml stacking buffer, 20 ml 10% SDS, add up to 100 ml with deionized H ₂ O |
| Bromphenolblau | 0.05% in glycerol/H ₂ O (1:1) |
| Low molecular weight marker (LMW) (Bio Rad) | |

Preparation of the samples:

Collected protein samples (250 µl) were precipitated with 5 V of absolute ethanol and incubated either for 1 h, if used immediately for the experiment, or overnight (o/n) at – 20°C.

After incubation, samples were centrifuged at 13 000 rpm for 10 min at 4°C, supernatant

was discarded and the pellet was dried at RT until the ethanol evaporated completely. Samples were incubated with 20 μ l of reducing sample buffer (1 x) for 5 min at 37°C and vortexed periodically, and finally heated for 5 min at 95°C in a heating block. The samples were run through the stacking gel at 75 V, and upon entering the separating gel, the voltage was increased to 150 V.

Preparation of the standards:

Different concentrations of the human β -TP (0.7 μ g/ μ l stock solution) were produced and purified from BHK-21 cells, and used in SDS-PAGE and Western blotting as a standard protein.

3.2.2.2 Western blot analysis [246]

Table 3.17 Components for Western blotting.

| | | |
|----------------------------|--|--------------------------|
| BSA blocking buffer | 10 mM Tris, pH 7.4, 3% BSA, 0.9% NaCl, 10% horse serum | |
| Tris-buffered saline (TBS) | 50 mM Tris pH 7.4, 0.8% NaCl, 0.02% KCl | |
| Developing buffer | 0.1 M Tris, pH 9.4, 0.1 M NaCl, 0.05 M MgCl ₂ | |
| Stopping buffer | 1 mM Tris, pH 7.5, 1 mM EDTA | |
| Primary antibody | Rabbit anti-BT polyclonal serum (1:1000) [246] | Incubation o/n at RT |
| Secondary antibody | Goat anti-rabbit immunoglobulin alkaline phosphatase (AP) conjugated (1:500) | Incubation for 2 h at RT |

Western blotting was done as it was described before except the BSA blocking step which was performed for 1 h at 42°C.

3.2.2.3 Overlay assay

This assay is based on Western blot and immunodetection analysis of the particular protein transferred to the nitrocellulose membrane which was placed on cells growing in cell culture.

Different cell dilutions (100, 200 and 400 cells/plate) were seeded into Petri-dishes and grown in a DME medium for 6 days (at 37°C, 5% CO₂). Medium was aspirated and cells

were fed with 1-2 ml of production medium (*Table 3.15*). An autoclaved nitrocellulose membrane was cut to fit the Petri-dish and placed on the cells. An additional 7 ml of production medium was transferred to the Petri-dish covering the membrane, the position of which was marked on the bottom of the Petri-dish. Cells were grown for a further 16 h (at 37°C, 5% CO₂). The nitrocellulose membrane was analyzed by western blotting (see chapter 3.2.2.2) using rabbit anti-ST6Gal I purified serum (1:1000) as a primary antibody and goat anti-rabbit immunoglobulin-coupled alkaline phosphatase (1:500) as a secondary antibody in the reaction (*Table 3.17*).

Clones growing in the Petri-dish were incubated for further several hours more in the culture medium. After the western blotting results were known, 12 clones showing *hST6Gal I* expression were carefully picked and transferred to 12 well cell culture plates containing 1 ml of culture medium. Clones were grown until they reached confluence, at which point they were checked for ST enzyme activity. Positive clones showing enzyme activity were transferred to 25 cm² culture flasks containing culture medium.

Clones which were not picked, they were allowed to continue growing in culture medium (8 ml) until they reached confluence. These cells served as a back-up in the possible case of contamination.

3.2.3 BT-*hST6Gal I* production [246]

For the production of 0.5-1 mg of recombinant BT-*hST6Gal I* protein, BHK-21 cells were cultivated in ten tissue-culture plates (175 cm²), each filled with 50 ml of selective medium (*Table 3.15*). They were grown until they reached confluence. The selective medium was removed and replaced every 2 days or 3 days with 50 ml or 100 ml of production medium (*Table 3.15*), respectively. Cells were grown in the culture for a further 10 production cycles. Supernatant was collected by centrifugation at 800 x g, for 10 min at 4°C, analyzed by Western blotting (see chapter 3.2.2.2) and a ST enzyme activity assay, and stored at –20°C before a purification step.

3.2.4 Purification of recombinant BT-*h*ST6Gal I

Table 3.18 Buffers for protein purification by affinity chromatography.

| | |
|----------|---|
| Buffer A | 20 mM MES, pH 6.5, 0.1 M NaCl, 1 mM DTE, 0.02% Azid, 20% glycerol |
| Buffer B | Buffer A + 1 M NaCl |
| Buffer C | Buffer A + 5 mM CDP |
| Buffer D | Buffer A + 20 mM CDP |

The cell supernatant was centrifuged at 1500 rpm for 5 min at 4°C. A supernatant was mixed with 20% glycerol and 0.02% azid. The recombinant BT-*h*STGal I protein was purified in a single step from the supernatant of BT-*h*ST6Gal I cells growing in production medium by CDP-hexanolamine-agarose affinity chromatography.

Purification strategy 1

CDP-hexanolamine-agarose column (10 ml) was first equilibrated with 10 CV of buffer A or PBS buffer containing 0.02% azid with a flow rate of 1.5 ml/min (*Table 3.18*). Supernatant was loaded onto the column (flow rate of 1.25 ml/min) at room temperature by using the FPLC system (Amersham Pharmacia Biotech). After the loading step, the column was washed with 10 CV of buffer A (1.5 ml/min) until the absorption baseline was stable, and finally the protein was eluted with 4 CV of buffer B (1.25 ml/min).

Purification strategy 2

In this strategy the purification was performed using 2 CV of buffer C (*Table 3.18*), followed by 2 CV of buffer D with the flow rate of 1.25 ml/min, and finally buffer B. During the purification step different fractions were collected: load (L), flow-through (FT), wash (W), and main fractions (Fr). These were stored at 4°C. The column was immediately regenerated for the following purification step using 10 CV of buffer A.

The purity of the eluted fractions was analyzed by SDS-PAGE. The activity of the enzyme-containing fraction was checked by ST activity assay after dilution (1:5) with buffer A.

3.2.4.1 Protein dialysis

Table 3.19 Components for protein dialysis.

| | |
|-----------------------------|--|
| 8/32 dialysis tubes (YM-10) | 30 min in 30% ethanol, 2 h in 30% 1-propanol, 2 h x 2 in deionized water |
| Storage solution | 30% 1-propanol |

Purified protein eluted with buffer B, C and D was dialyzed against 50-fold (V) of buffer A (*Table 3.19*).

Protein samples were dialyzed for 2 days at 4°C changing two times the same volume of buffer A. Dialyzed samples were checked for the activity using ST enzyme activity assay.

3.2.4.2 Enzyme concentration [246]

The eluate containing the enzyme was concentrated 7-fold using Diaflo YM-10 ultrafiltration membranes (Amicon, Witten, Germany), diluted with six volumes of 20 mM MES, pH 6.5, and again concentrated 7-fold by ultrafiltration.

3.2.4.3 Enzyme storage and stability

Purified enzyme was stored at 4°C in 20% glycerol, at – 20°C in 20% and 50% glycerol, and after a defined time enzyme was checked for the activity using a ST enzyme assay.

3.2.5 *h*ST6Gal I enzyme activity assay [246]

Table 3.20 Reaction mixture composition (20 µl).

| | Asialofetuin mixture | Type II mixture |
|----------------------------------|--|-----------------------|
| Acceptor (Asialofetuin; Type II) | 20 µg/µl | 0.4 µg/µl |
| 2 mM CMP-NeuNAc | 4 nmol | 4 nmol |
| CMP-[¹⁴ C] NeuNAc | 0.1 nmol (60 000 cpm) | 0.1 nmol (60 000 cpm) |
| MES reaction buffer (1 x) | 25 mM MES, pH 6.5, 50 mM NaCl, 10 mM MnCl ₂ | |

The master mix (all components except the enzyme) for 100 reactions was prepared as

described in *Table 3.20* and stored at 4°C. The ST activity of extracts and culture supernatants of cells transfected with BT-*hST6Gal I* was tested at 37°C with up to 8 µl of the sample in 20 µl of reaction mixture. After this, samples were incubated for up to 3 h. The reaction mixtures (see *Table 3.20*) containing 0.4 µg/µl Type II acceptor were diluted with water to 0.5 ml and applied to Sep-Pak (Waters) C18 cartridges. The columns were washed twice with 2.5 ml of water and eluted with 1.5 ml of methanol. Transfer of [¹⁴C] NeuNAc was determined by liquid scintillation counting of the eluate.

The reaction mixture (see *Table 3.20*) containing 20 µg/µl asialofetuin as an acceptor in the ST reaction mixture was precipitated with 1 ml of 0.5 M HCl containing 1% phosphotungstic acid (PTA) and transferred under vacuum to glass microfiber filters (Whatman GF/C). The filters were washed once with 4 ml of 0.5 M HCl containing 1% PTA and twice with 4 ml of methanol, and analyzed for radioactivity with a liquid scintillation counter (Beckman, LS 6000 SC).

This standard assay was also used to calculate the enzyme units. Taking into consideration that one unit of enzyme activity corresponds to transfer of 1 µmol of NeuNAc to asialofetuin per minute.

3.2.5.1 *hST6Gal I* turnover

Table 3.21 The reaction mixture for enzyme catalytic activity.

| | |
|-------------------------------|--|
| Acceptor Diantennary | 20 nmol |
| CMP-NeuNAc | 200 nmol |
| CMP-[¹⁴ C] NeuNAc | 0.1 nmol (60 000 cpm) |
| MES reaction buffer (1 x) | 25 mM MES, pH 6.5, 50 mM NaCl, 10 mM MnCl ₂ |
| BSA | 50 µg |
| Purified enzyme | 50 µU (1.64 mU/ml) |
| Total | 200 µl |

Reaction mix described in *Table 3.21* was incubated for 12 hours at 37°C taking the aliquots at different time points (0, 30', 2 h, 3 h, 6 h 12 h). Samples were purified (see chapter 3.2.6.1) and dried by centrifugation under vacuum. Lyophilized substance was

dissolved in 20 μ l or 40 μ l deionized water, and half of the sample was injected onto the CarboPac PA1 column used for high-pH anion-exchange chromatography with pulsed amperometric detection (HPAEC-PAD) analysis. The rest of the sample was stored at -20°C .

3.2.5.2 Cell lysis [246]

Table 3.22 Components for cell lysis method.

| | |
|--------------------|---|
| Cell concentration | 5×10^7 cells/ml |
| Lysis buffer | 20 mM MES, pH 6.5, 1% Triton X-100, 1 mM dithioerythriol (DTE), 0.02% Azide, inhibitors |

In order to verify the *hST6Gal I* solubility, cells were lysed and cell pellets checked for the enzyme activity.

Cell suspensions (1 ml) were centrifuged at 800 x g for 10 min at RT, supernatant was removed and the pellet resuspended in a lysis buffer (*Table 3.22*) to a final cell concentration (5×10^7 cells). The mixture was centrifuged briefly and incubated for 30 min at 4°C . After incubation lysed cells were centrifuged at 800 x g for 10 min at 4°C and the supernatant was used for the enzyme activity assay.

3.2.6 Preparative (*in vitro*) sialylation of glycoconjugates [246]

Table 3.23 Reaction mixture for preparative *in vitro* sialylation.

| | |
|---------------------------|--|
| Acceptor | Diantennary <i>N</i> -acetyllactosamine type acceptor 20 mg/ml; MW= 1800 g/mol |
| Acceptor conc. | 2 nmol (0.1 mM) |
| CMP-NeuNAc | 10 nmol (0.5 mM) |
| MES reaction buffer (1 x) | 25 mM MES, pH 6.5, 50 mM NaCl, 10 mM MnCl_2 |
| Enzyme | 1.83 μ U (0.1 mU/ml), 82 μ U (1.64 mU/ml), supernatant |

centrifugation under vacuum. The dried pellet was diluted in 20 μ l of deionized water and injected onto the CarboPac PA1 column used for HPAEC-PAD analysis.

3.2.8 Neuraminidase (sialidase) specific cleavage

Oligosaccharide products obtained after incubation with purified *hST6Gal I* enzyme were checked for the α -2,6 NeuNAc glycoside linkage using neuraminidase (sialidase) enzyme from New Castle disease virus (NDV) hitchner B1 strain (EC 3.2.1.18). This enzyme specifically cleaves terminal NeuNAc linked only α -2,3 to *N*- or *O*- glycosidically bound oligosaccharide chains of glycoproteins and glycolipids. It also cleaves NeuNAc that is bound in the α -2,8 position to neuraminic acids. It is also able to cleave *N*-glycolyl, 4-*O* acetyl and 9-*O* acetylsialic acids, however it does this with a low turnover rate.



Sialylated oligosaccharides were incubated overnight with 3 mU of NDV enzyme (1 U/ml) at 37°C. The resulting product was purified using HyperSep Hypercarb PGC column and injected onto the CarboPac PA1 column used for HPAEC-PAD analysis.

3.2.9 High pH anion-exchange chromatography – pulse amperometric detection of oligosaccharides (HPAEC-PAD) [255]

| | Asialo method | Oligo method |
|----------|-------------------------|--|
| Buffer A | 0.2 M NaOH | |
| Buffer B | 0.2 M NaOH; 0.6 M NaOAc | |
| Buffer C | | 0.1 M NaOH in deionized H ₂ O |
| Buffer D | | 0.1 M NaOH; 0.6 M NaOAc |

A Dionex Bio LC System (Dionex, Sunnyvale CA, USA), equipped with a 0.4 x 25 cm CarboPac PA1 column was used in combination with a pulsed amperometric detector. Detector potentials (*E*) and pulse durations (*T*) were E_1 +50 mV, T_1 480 ms; E_2 +500 mV,

T_2 120 ms; E_3 – 500 mV, T_3 60 ms; the output range was 500 – 1500 nA. The oligosaccharides were then injected onto the CarboPak PA1 column that was prior to injection equilibrated with 100% of solvent A or solvent C using the asialo or oligo method, respectively. The elution profile included an initial 5 min isocratic run with 100% buffer A or C, a 30 min linear gradient from 0 – 20% of solvent B or D, and finally 2 min linear gradient to 100% buffer B or D, each at the flow rate of 1 ml/min.

The HPAEC-PAD was also used to prepare the total *N*-glycans, which were desalted on the graphitized carbon cartridges, for subsequent mass spectrometry. In some cases *N*-glycans were desialylated prior to HPAEC-PAD analysis by dissolving in sialidase buffer (10 mM sodium acetate, 1 mM CaCl₂, 0.02% sodium azide) and by incubating with 0.2 U/ml NDV neuraminidase.

3.2.10 Mass spectrometry and methylation analysis of *N*-glycans

The *N*-glycans were analyzed by matrix-assisted laser desorption ionization time of flight mass spectrometry (MALDI/TOF-MS). Briefly, the *N*-glycans were analyzed by positive ion MALDI/TOF-MS using Bruker REFLEX TOF instrument. One microliter of samples containing equal volumes of the *N*-glycan solution (~3-10 pmol/l) in defined conditions was spotted onto a stainless steel target and dried at room temperature.

For the methylation analysis samples of the *N*-glycans were permethylated, hydrolyzed, reduced and acetylated. The resulting partially methylated alditol acetates were subsequently analyzed on a ThermoQuest CGQ ion trap GC/MS system.

3.3 α -2,3/2,8 bifunctional *Campylobacter jejuni* sialyltransferase (α -2,3/2,8 ST) expression in *E. coli* cells

3.3.1 Bacterial cell growth and culture

3.3.1.1 Bacterial strains [259,260]

Campylobacter jejuni ATCC 43438

The strain *Campylobacter jejuni* ATCC 43438 (Serotype O:10) was ordered from American Type Culture Collection (ATCC) and cultivated by Dr. Silvia Gautsch at the Cantonal Laboratory in Basel. The cells were incubated in Brucella Broth (Oxoid) supplemented with growth factor and antibiotic (Polymyxin, Trimetoprim and Vancomycin) under microaerophilic conditions (7% CO₂) (Anaerocult ® C, Merck KGaA, Germany) for 2 days at 37°C. Aliquots of 1.5 ml cell culture were centrifuged at 13'000 rpm for 2 min at room temperature (Eppendorf Centrifuge 5415D, Vaudaux-Eppendorf AG). The supernatant was discarded and the pellet stored at –20°C.

Long-term storage:

Using aseptic techniques, cells in the exponential growth phase (18/24 h) growing on agar plates supplemented with sheep blood (Biomérieux), were transferred to vials containing beads in cryopreservation fluid (Technical Service Consulting Ltd.), making a thick cell suspension. Fluid was removed and the vial was stored at – 80°C. Similarly, cells were transferred to 1 ml of sheep blood and several 1 ml aliquots were stored at – 80°C.

Cloning strains:

DH5 α TM *E. coli* cells (Invitrogen)

This is a cell strain usually used for cloning. The transformation efficacy is high and they can take up plasmids up to 30 kbp. In these cells, the plasmid is strongly replicated and can be transiently maintained. Due to the fact that even low levels of basal expression can disturb growth and stability of plasmids, background expression must be minimal. This is possible in DH5 α cells, because they do not have a T7-RNA polymerase.

JM109 *E. coli* cells

Top10 *E. coli* cells

Production strains:

The most widely used host for target gene expression. A sequence called DE3 contains the *lacI* gene, the *lacUV5* promoter and the T7 RNA polymerase gene. These hosts are lysogens of the bacteriophage DE3. For transcription of the host T7 RNA polymerase, the *lacUV5* promoter must be induced by isopropyl- β -D-thiogalactopyranoside (IPTG). The T7 RNA polymerase transcribes the target DNA sequence, the target gene.

| <i>E. coli</i> expression strains | Description/Application | Antibiotic resistance |
|-----------------------------------|---|--|
| AD494(DE3) (Novagen) | <i>trxB</i> ⁻ expression host; allows disulfide bond formation in <i>E. coli</i> cytoplasm | Kanamycin (15 μ g/ml) |
| Rosetta-gami (DE3) (Novagen) | general expression host; two mutations in cytoplasmic disulfide reduction pathway enhance disulfide bond formation in <i>E. coli</i> cytoplasm, provides rare codon tRNAs | Tetracycline (12.5 μ g/ml) Kanamycin (15 μ g/ml) Chloramphenicol (34 μ g/ml) |
| BL21(DE3) (Novagen) | general purpose expression host | none |

3.3.1.2 Growth media [257]

The *Table 3.24* describes the preparation of the culture media [257] used in this work.

Table 3.24 Composition of cell culture growth media.

| Media | Recipes for 1 l |
|--------------------------|--|
| LB | 1% w/v Bacto Tryptone (BD), 0.5% w/v Bacto Yeast Extract (BD), 1% w/v NaCl (Fluka), adjust pH to 7.5 with 2 M NaOH, sterilize by autoclaving and store at RT |
| Selective LB medium | LB medium 100 μ g/ml Ampicillin was added just before use |
| LB agar plates | LB medium, 1.5% w/v Bacto agar (BD), sterilize by autoclaving, store at 4°C |
| Selective LB agar plates | LB medium, 1.5% w/v Bacto agar (BD), sterilize by autoclaving and cool to 50°C, add 150 μ g/ml Ampicillin in precooled medium, store at 4°C |
| SOB | 2% w/v Bacto Tryptonem, 0.5% w/v Bacto Yeast extract, 0.05% w/v NaCl, |

| | |
|-----------------------|---|
| | 2.5 ml 1 M KCl, adjust pH to 7.5 with 2 M NaOH and add H ₂ O to 995 ml; sterilize by autoclaving and store at RT, before use add 5 ml sterile 1 M MgCl ₂ |
| SOC | SOB medium with additional 20 ml of sterile 1 M <i>D</i> -glucose |
| TB [257] | 1.2% w/v Bacto Tryptone, 2.4% w/v Bacto Yeast Extract, 4 ml glycerol, add H ₂ O 900 ml; sterilize by autoclaving and add 100 ml of sterile 10 x TB phosphate and store at RT |
| Selective TYE medium | 3% w/v Bacto Tryptone, 0.5% w/v Bacto Yeast Extract, 70 µg/ml ampicillin |
| Transformation medium | LB medium, 10 mM MgCl ₂ , 20 mM <i>D</i> -Glucose, made before use |

Table 3.25 Stock solutions [257].

| | |
|---|--|
| TB phosphate (10 x) | 2.31 g (0.17 M) KH ₂ PO ₄ , 12.54 g (0.72 M) K ₂ HPO ₄ , dissolve in 90 ml H ₂ O, adjust volume to 100 ml with H ₂ O, sterilize by autoclaving and store at RT |
| <i>D</i> -Glucose stock | 1 M glucose sterilize by filtration and store at 4°C |
| MgCl ₂ | 2 M MgCl ₂ sterilize by autoclaving and store at RT |
| 100 mM IPTG, Roche (isopropyl-β- <i>D</i> -thiogalactopyranoside) | 2.38 g IPTG in 100 ml deionized H ₂ O, sterilize by filtration and store at – 20°C |
| 100 mg/ml Ampicillin (sodium salt), (Fluka) | Aliquots were stored at – 20°C 100 µg/ml (cell suspension) and 150 µg/ml (selective agar plates) was used |

Substances for each media and stock solution were mixed adding deionized water (*Table 3.24*). For media, pH 7.5 was adjusted with 2 M NaOH. The media and stock solution was sterilized by autoclaving for 20 min at 121°C or by filtration (Millex®GP 0.22 µm, Millipore) and all additional substances described in *Table 3.25* were added using aseptic techniques in laminar flow hood.

3.3.2 Cell competence

Normally, *E. coli* cells are not able to take up foreign DNA; instead they need to be treated under special conditions to get competent. Electroporation and heat-shock are two

methods for transformation. Subsequently cells are incubated in growth media and then plated out on Petri-dishes containing the specific antibiotic for selection [261,262].

Competent cells for heat-shock transformation

Table 3.26 Protocol for heat-shock competent *E. coli* cells.

| | |
|--|--|
| Solution A | 50 mM CaCl ₂ , sterilize by autoclaving (Fluka), store at 4°C |
| Solution B | 50 mM CaCl ₂ (Fluka), 20% glycerol, sterilize by autoclaving and store at 4°C |
| <i>E. coli</i> cell strain streaked out on agar plates | |
| LB-medium | |
| Selective LB-agar plates | |

E. coli cells streaked on agar plates were grown overnight. The following day, clones were picked and 3 ml of LB medium was inoculated and incubated at 37°C until the culture entered the logarithmic phase. 1 ml of this culture was transferred to 100 ml LB medium in a 500 ml flask and incubated on a shaker at 37°C until the OD₆₀₀ reached a value of 0.4-0.5. The culture was placed on ice and incubated for a further 20 min. The cell suspension was transferred into sterile 50 ml centrifuge tubes and centrifuged at 5000 rpm for 10 min at 4°C. The supernatant was removed and the pellet was resuspended in 10 ml ice-cold solution A (*Table 3.26*). The cells were kept on ice for 30 min and centrifuged under the same conditions as mentioned before. The pellet was resuspended in 0.5 ml cold solution B, and aliquots of 50/100 µl were frozen rapidly in liquid nitrogen and stored at -80°C.

Competent cells for electroporation

Table 3.27 Protocol for electrocompetent *E. coli* cells.

| |
|---|
| SOB medium |
| 10% Glycerol stock solution (Fluka BioChemika), sterilize by autoclaving and store at 4°C |
| <i>E. coli</i> cell strain streaked out on agar plates |
| Sorvall RC-5B Refrigerated Superspeed Centrifuge, GS 3 Rotor (Sorvall) |
| Selective LB-agar plates |

E. coli cells streaked on agar plates were grown overnight. The following day, *E. coli* colonies were picked and 5 ml of SOB-medium free of magnesium chloride was inoculated for overnight pre-cultures. The pre-culture was transferred into a 1 l flask containing 250 ml of SOB medium (Table 3.27). The culture was grown at 37°C until an OD₆₀₀ of 0.6-0.8 was reached. All the steps during the cell harvesting were performed on ice. Cells were collected by centrifugation at 5000 rpm for 10 min at 4°C. The pellet was resuspended in 250 ml ice-cold 10% glycerol. After centrifugation under the same conditions, the collected cells were washed in 50 ml ice-cold 10% glycerol solution. Cells were harvested by centrifugation and aliquots of 50/100 µl were directly frozen in liquid nitrogen and stored at -80°C.

3.3.3 Cell transformation

Transformation by heat-shock

Table 3.28 Protocol for heat-shock transformation.

| | |
|----------------------------|------------|
| Plasmid DNA construct | 1 – 1.5 µl |
| Heat-shock competent cells | 50 µl |
| Transformation medium | |
| LB-medium | |
| Selective LB-agar plates | |

1 µl of the plasmid DNA construct was added to 50 µl CaCl₂ competent *E. coli* cells (Table 3.28). The cell suspension was kept on ice for 30 min and heat-shocked at 42°C for 90 sec using a heating block (Thermomixer comfort, Eppendorf). After incubation for 5 min on ice, 950 µl of transformation medium was added. The cell suspension was shaken at 500 rpm for 1 h at 37°C and shortly centrifuged at 13 000 rpm. Supernatant was removed and a pellet was resuspended in 100 µl LB medium, plated out on selective LB-agar plates and incubated overnight at 37°C.

Transformation by electroporation

Table 3.29 Protocol for transformation by electroporation.

| | |
|---|----------------|
| Plasmid DNA construct | 2 – 10 μ l |
| Electrocompetent cells | 50 μ l |
| Transformation medium | |
| LB-medium | |
| Filter-paper (VSWP 02500, Type VS, 0.025 μ m) | |
| Selective LB-agar plates | |
| Gene Pulser ® Cuvette (BIO RAD) 0.1 cm electrode | |

Before electroporation, the ligation mixture had to be dialyzed to remove the remaining salts. The ligation solution was applied on a filter that was placed in a Petri-dish containing deionized sterile water and dialyzed for 45 min. As the transformation efficiency decreases 100-fold at room temperature, the following steps were carried out on ice [257]

Electrocompetent cells were transferred into a pre-cold sterile cuvette (4°C), and 10 μ l of the dialyzed ligation solution was added (*Table 3.29*). The cells were electroporated at 400 Ω , 1.75 kV and 25 μ F with time constant in the range of 6 – 8 ms. 950 μ l of transformation medium was added and cells were further incubated in the heating block shaking at 500 rpm for 1 h at 37°C. Furthermore, 300 μ l of the electroporated cell suspension was plated on a selective LB-agar plate and incubated overnight at 37°C.

3.3.3.1 Transformation efficiency test (colony forming units)

Transformation efficiency is defined as the number of colony forming units (cfu) produced by 1 μ g of control DNA (supercoiled plasmid DNA) and is measured by performing a control transformation reaction using a known quantity of DNA, typically 0.1 ng, then calculating the number of cfu formed per microgram DNA.

100 μ l of *E. coli* competent cells were transformed with 1 μ l (4 ng/ μ l) of plasmid DNA. 100 μ l of different cell dilutions (1:10, 1:100, 1:1000) were seeded onto selective agar plates and incubated overnight at 37°C. The following day, cells were counted and transformation efficiency was calculated as follows.

Equation for transformation efficiency (cfu/ μ g):

$$\frac{\text{cfu on control plate}}{\text{ng of control DNA plated}} \times \frac{1 \times 10^3 \text{ ng}}{\mu\text{g}}$$

3.3.4 Long-term storage of *E. coli* strains

Bacteria can be stored as glycerol stocks, which enable long-term storage at -80°C .

Therefore, 0.85 ml logarithmic-phase *E. coli* cell culture was added to the vials containing 0.15 ml sterilized glycerol. The vials were vortexed vigorously to ensure mixing of the bacterial culture and the glycerol, quickly frozen in liquid nitrogen and stored at -80°C .

3.3.5 Cloning, expression and purification of α -2,3/2,8 bifunctional sialyltransferase using pEZZ18 vector

C. jejuni genomic DNA isolation

Genomic DNA isolation from the *C. jejuni* ATCC43438 strain was performed using a Wizard genomic DNA purification kit (Promega Corporation, Madison, WI, USA) as described by the manufacturer.

3.3.5.1 PCR amplification and restriction enzyme digestion of *cst-II* gene [263,264]

Forward primer: $T_m = 67.1$

5' ccg gaattc g aaa aaa gtt att att tct gga aat 3'

Reverse primer: $T_m = 66.5$

5' cgc ggatcc tca tta ttt tcc ttt gaa ata atg 3'

Internal primer:

5' acc tca gga gtc tat atg tgt gca 3'

A specific DNA sequence can be amplified by PCR using cell-free conditions. This method comprises 3 steps: template denaturation, primer annealing and extension of the annealed primers by the DNA polymerase.

A master mix of PCR reaction substances was prepared (*Table 3.30*) with exception of the genomic DNA and the DNA polymerase, which were added just before the beginning of the PCR reaction. The solution was kept on ice to prevent degradation of the DNA.

Taq DNA Polymerase (Sigma) is thermostable enzyme with 5' → 3' DNA polymerase and 5' → 3' exonuclease activity.

Table 3.30 PCR reaction mixture for *Taq* DNA polymerase.

| Reagents | Mixture | Temperature | | Time | Cycles Nr. |
|----------------------------------|----------|------------------|------|------|------------|
| Sterile, deH ₂ O | 39.25 µl | Hold | 94°C | 4' | |
| 10 mM PCR dNTPs | 1 µl | Denaturation | 94°C | 1' | 35 |
| 20 mM 5' primer | 1 µl | Annealing | 52°C | 1' | |
| 20 mM 3' primer | 1 µl | | | | |
| Genomic template DNA | 2.5 µl | | | | |
| PCR buffer (10 x) | 5 µl | Elongation | 72°C | 1' | |
| <i>Taq</i> DNA Polymerase 5 U/µl | 0.25 µl | Final elongation | 72°C | 5' | |
| Total volume | 50 µl | | | | |

Pfu DNA polymerase (Promega) is a thermostable enzyme. It catalyzes the DNA-dependent polymerization of nucleotides into duplex DNA in the 5' → 3' direction in the presence of magnesium ions. The enzyme also exhibit 3' → 5' exonuclease (proofreading activity). A master mix of PCR reaction substances was prepared as described in *Table 3.31*.

Table 3.31 PCR reaction mixture for *Pfu* DNA polymerase.

| Reagents | Mixture | Temperature | | Time | Cycles Nr. |
|-----------------------------|---------|--------------|------|--------|------------|
| Sterile, deH ₂ O | 35.5 µl | Hold | 94°C | 3' | |
| 10 mM PCR dNTPs | 2 µl | Denaturation | 95°C | 1' | 35 |
| 20 mM 5' primer | 2 µl | Annealing | 52°C | 1'30'' | |
| 20 mM 3' primer | 2 µl | | | | |
| Genomic template DNA | 2.5 µl | | | | |

| | | | | | |
|--|------------|------------------|------|-----|--|
| PCR buffer (10 x) | 5 μ l | Elongation | 72°C | 2' | |
| <i>Pfu</i> DNA Polymerase 3 U/ μ l | 1 μ l | Final elongation | 72°C | 10' | |
| Total volume | 50 μ l | | | | |

PCR reaction was performed in Gene Amp PCR System 2400, Perkin Elmer. PCR product was purified using GenElute PCR Clean-up kit (Sigma) following the protocol recommended by the manufacturer and digested for 5 h at 37°C using *EcoR* I and *BamH* I restriction enzymes (Table 3.32). The digested DNA product was loaded onto a 1% agarose gel (see chapter 3.3.5.2), excised from the gel, extracted and eluted in 30 μ l elution buffer using GeneElute gel extraction kit (Sigma).

Table 3.32 Enzyme digestion of the *cst-II* gene.

| Reagent | Volume |
|---|-------------|
| PCR product (<i>cst-II</i> gene) | 80 μ l |
| 10 x New England Biolabs 2 buffer (NEB) | 9.5 μ l |
| <i>EcoR</i> I (20 000 U/ml, NEB) | 2 μ l |
| <i>BamH</i> I (20 000 U/ml, NEB) | 2 μ l |
| H ₂ O (sterile, deionized) | 1.5 μ l |
| Total volume | 95 μ l |

3.3.5.2 Agarose gel analysis [265]

The agarose gel electrophoresis method was used for separation, preparative isolation and purification of DNA fragments. Depending on the size and shape of the DNA fragment, the agar concentration can be varied in order to find an optimal concentration (Table 3.33). An intercalating fluorescent dye, ethidium bromide, was added to the agar gel to visualize DNA fragments under the UV light.

Table 3.33 Components for agarose gel electrophoresis.

| | |
|--|---|
| TBE-buffer (1 x) | 44.6 mM Tris, 44.6 mM Boric acid (Sigma), 1 mM EDTA (Sigma) |
| Loading buffer (6 x) (Sigma) | |
| DNA Molecular Weight Marker X (0.07-12.2 kbp) (Roche Diagnostics GmbH) | |

Table 3.34 The agarose gel preparation.

| | |
|---|-----------|
| 1% agarose gel | |
| Agar (Molecular Biology Grade, Eurogent) | 1 g |
| TBE buffer | 100 ml |
| Ethidium bromide solution 1% (w/v), (AppliChem) | 2 μ l |

Preparation of the gel (*Table 3.34*):

The components were mixed and heated in a microwave until the 1% agar was dissolved. The solution was cooled to 50-60°C and ethidium bromide was added. The agar solution was poured into a gel tray and after polymerization of the gel, a tank was filled with 1 x TBE-buffer.

Preparation of the samples:

The DNA samples were diluted, if necessary, with deionized water and loading buffer (6 x) was added. DNA molecular weight marker X, which is used as standard to compare the size of the DNA fragments, was prepared (*Table 3.33*). The samples were loaded on the gel, run at 80-100 V and fragments were visualized under UV light.

3.3.5.3 pEZZ18 vector preparation [266]

Plasmid DNA, pEZZ18 (Amersham pharmacia biotech) was amplified in the *E. coli* JM109 strain and purified using the GFX Micro Plasmid Prep Kit (Amersham Pharmacia Biotech), according to the protocol recommended by the manufacturer. 50 μ l of pEZZ18 plasmid DNA was digested in a total reaction volume of 60 μ l, using the same protocol used for the digestion of PCR products (*Table 3.32*). After digestion for 5 h at 37°C, plasmid DNA vector was dephosphorylated using calf intestine alkaline phosphatase (CIAP) for 1 hour at 37°C (*Table 3.35*). Enzyme activity was stopped by incubating the reaction mixture for 10

min at 65°C. Digested and dephosphorylated plasmid vector, pEZZ18 was loaded onto 1% agarose gel, excised from the gel using GeneElute gel extraction kit (Sigma), and following the protocol instructions recommended by the manufacturer eluted in 30 µl elution buffer.

Table 3.35 The calf intestine alkaline phosphatase reaction mixture.

| Reagent | Volume |
|---|--------|
| <i>EcoR</i> I/ <i>Bam</i> H I digested pEZZ18 plasmid | 60 µl |
| 10 x CIAP buffer | 7 µl |
| CIAP (1U/µl, Roche) | 1.5 µl |
| H ₂ O (sterile, deionized) | 1.5 µl |
| Total volume | 70 µl |

3.3.5.4 DNA quantification [265]

Plasmid DNA quantification is generally performed by spectrometric measurement of the absorption at 260 nm, or by agarose gel analysis.

DNA quantification by spectrophotometry

Plasmid DNA concentration was determined by measuring the absorbance at 260 nm (A_{260}) in a spectrophotometer using a quartz cuvette. For reliable DNA quantification, A_{260} readings lay between 0.1 and 1.0. An absorbance of 1 unit at 260 nm corresponded to 50 µg plasmid DNA per milliliter.

$$A_{260} = 1 \Rightarrow 50 \left[\frac{\mu\text{g}}{\text{ml}} \right]$$

The DNA sample was diluted in Tris-HCl buffer (pH 7.0) and the absorbance at 260 nm was measured. Calculations were performed using the following equation:

$$c(\text{DNA}) = 50 \left[\frac{\mu\text{g}}{\text{ml}} \right] * A_{260} * \text{dilution factor}$$

DNA quantification by agarose gel analysis

Agarose gel analysis enables quick and easy quantification of DNA, especially for small (0.05 kb) DNA fragments. As little as 20 ng DNA can be detected by agarose gel

electrophoresis with ethidium bromide staining.

The DNA sample was run on an agarose gel alongside known amounts of lambda DNA (25 ng – 100 ng). The amount of sample DNA loaded was estimated visually by densitometric measurement of band intensity and comparison with a standard curve generated using DNA of known concentration.

3.3.5.5 Ligation

Digested DNA fragments and plasmid vector were ligated using the T4 DNA ligase. This enzyme repairs breaks in one strand of a dsDNA molecule. The overhanging single stranded tails were joined resulting in new recombinant DNA plasmids.

Ligation mixture (*Table 3.36*) was incubated overnight, starting the reaction at room temperature and subsequently decreasing to 4°C. Heat-shock DH5α *E. coli* competent cells were transformed with ligation mixture (30 µl) and bacterial clones resistant to ampicillin were picked and checked for *cst-II* gene presence.

Table 3.36 The ligation mixture.

| Reagent | Volume |
|---|--------|
| <i>cst-II</i> gene (<i>EcoR</i> I/ <i>Bam</i> H I digested) | 6 µl |
| pEZZ18 plasmid vector (<i>EcoR</i> I/ <i>Bam</i> H I digested) | 6 µl |
| 2 x T4 rapid ligation buffer (Promega) | 15 µl |
| T4 DNA-Ligase 400 U/l (BioLabs, New England) | 2 µl |
| Water (sterile, distilled) | 1 µl |
| Total volume | 30 µl |

3.3.5.6 Analysis of pEZZ18 recombinants

To prove the presence of the pEZZ18 plasmid-vector recombinant construct, resistant clones growing overnight on selective LB-agar plates were picked and used to inoculate 3 ml selective LB medium. The cultures were grown overnight shaking at 300 rpm (37°C). The following day, plasmid DNA was isolated using the GFX Mikro Plasmid Prep Kit, (Amersham Biosciences) as recommended by the manufacturer, and checked by PCR

(using FW1, RW1 and internal primer) and an enzyme digestion method (*Table 3.37*) for the presence of the *cst-II* gene.

All positive clones were sent for sequence analysis to Microsynth GmbH.

Table 3.37 The restriction digestion mixture.

| Reagent | Volume |
|---|------------|
| Plasmid DNA | 15 μ l |
| 10 x New England Biolabs 2 buffer (NEB) | 2 μ l |
| <i>EcoR</i> I (20 000 U/ml, NEB) | 1 μ l |
| <i>BamH</i> I (20 000 U/ml, NEB) | 1 μ l |
| H ₂ O (sterile, deionized) | 1 μ l |
| Total volume | 20 μ l |

DNA Molecular Weight Marker X (0.07-12.2 kbp) (Roche)

All the components described in *Table 3.37* were mixed adding the restriction enzymes just before starting the incubation. The reaction mixture was incubated in the heating block overnight at 37°C. The samples were analyzed by 1% agarose gel electrophoresis.

Positive clones were stored at – 80°C as glycerol stocks.

3.3.5.7 α -2,3/2,8 bifunctional sialyltransferase expression and determination [266]

| | |
|-----------------|---|
| Reaction buffer | 100 mM Na cacodylate (pH 7.5), 0.3% Triton X-100, 10 mM MgCl ₂ . |
|-----------------|---|

1 ml or 4 ml (for production) of HB101 *E. coli* overnight cell culture was transferred to 50 ml or 200 ml of selective TYE medium, respectively. Cultures were shaken at 300 rpm overnight at 37°C. Cells were collected by centrifugation at 5000 rpm for 15 min at RT, and pellets stored for a short time at – 20°C. This was followed by resuspension in 5 ml of reaction buffer. Pellets were kept on ice and sonicated 6 x 10 sec with 10 sec of pauses at 200-300 W (Vibra cell, Sonics and materials inc, Danbury CT USA). Lysate was ultracentrifuged at 21 000 rpm for 1 h at 4°C. Samples were checked for enzyme expression using SDS-PAGE and Western blotting analysis. Western blotting was

performed using mouse anti protein A IgG (1:1700) as a primary antibody (Sigma) and goat anti-mouse alkaline phosphatase conjugated IgG (1:30 000) as a secondary antibody (Sigma). α -2,3 activity was checked in a reaction with 600 μ M of Type II and acceptor **3**. α -2,8 activity was determined using 600 μ M of **7** acceptor substrate. Incubation was done for 5 hours at 37°C.

3.3.5.8 α -2,3/2,8 bifunctional sialyltransferase purification [266]

Table 3.38 Buffers for protein purification by IgG affinity chromatography.

| | |
|--|---|
| Washing buffer Tris saline tween (TST) | 50 mM Tris (pH 7.6), 150 mM NaCl, 0.05% Tween 20 |
| Binding buffer | 5 mM NH ₄ Ac (pH 5.0), pH adjusted with acetic acid |
| Elution buffer | 0.5 M acetic acid (pH 3.4), pH adjusted with 5 M NH ₄ Ac |

Before usage, IgG sepharose affinity column was equilibrated using 3 CV of elution buffer as the first equilibration step, followed by 3 CV of washing buffer (*Table 3.38*). This procedure was repeated twice. The equilibrated IgG sepharose column was loaded with a cell soluble fraction which was preliminary filtrated (0.22 μ m). The column was washed with 15 CV of washing buffer and 10 CV of binding buffer using a flow rate of 1.5 ml/min, and finally with 7.5 CV of elution buffer with a flow rate of 0.5 ml/min. Eluted fractions were neutralized with 2 M Tris.

Soluble protein fraction was also purified applying to CDP-hexanolamine-agarose column using the protocol described previously in the chapter 3.1.4.

3.3.6 Cloning, expression and purification of α -2,3/2,8 bifunctional sialyltransferase using pET vector expression system

3.3.6.1 PCR amplification of *cst-II* gene [259,264]

The same methods which were used for the pEZZ18 expression system (see chapter 3.3.5) were applied for the pET expression system as well. However, all modifications of the methods will be described.

pET15b primers

Forward primer: T_m = 59.4

5' ggaattc ^{Nde I}catatg atg aaa aaa gtt att att tct 3'

Reverse primer: T_m = 59.5

5' cgc ^{BamH I}ggatcc tca tta ttt tcc ttt gaa ata atg 3'

Reverse primer Δ 32C: T_m = 64.5

5' cgc ^{BamH I}ggatcc tta att aat att ttt tga aaa ttt 3'

pET21b primers

Forward primer: T_m = 59.4

5' ggaattc ^{Nde I}catatg atg aaa aaa gtt att att tct 3'

Reverse primer: T_m = 70.9

5' cgc ^{BamH I}ggatcc cg ttt tcc ttt gaa ata atg ctt 3'

Reverse primer Δ 32C: T_m = 68.3

5' cgc ^{BamH I}ggatcc cg att aat att ttt tga aaa ttt 3'

pET11c primers

Forward primer: T_m = 59.4

5' ggaattc ^{Nde I}catatg atg aaa aaa gtt att att tct 3'

Reverse primer: T_m = 59.5

5' cgc ^{BamH I}ggatcc tca tta ttt tcc ttt gaa ata atg 3'

Primers for gene mutation:

Forward primer (G53S): T_m = 54.3

5' cag tat ttt aca atc cta gtc ttt 3'

Forward primer (R182N): T_m = 64.8

5' ggctc ctg att tta aaa atg ata act cac ac 3'

Forward primer (D177N; R182N): T_m = 64.8

5' ggctc cta att tta aaa atg ata act cac ac 3'

Table 3.39 The PCR reaction mixture for *Pfu* DNA polymerase.

| Reagents | Mixture | Temperature | | Time | Cycles Nr. |
|----------------------------------|---------|------------------|------|--------|------------|
| Sterile, deH ₂ O | 36 µl | Hold | 94°C | 3' | |
| 10 mM PCR dNTPs | 1 µl | Denaturation | 95°C | 1' | 35 |
| 20 mM 5' primer | 1 µl | Annealing | 50°C | 1'30'' | |
| 20 mM 3' primer | 1 µl | | | | |
| Genomic template DNA (1:10) | 5 µl | Elongation | 72°C | 2' | |
| PCR buffer (10 x) | 5 µl | | | | |
| <i>Pfu</i> DNA Polymerase 3 U/µl | 1 µl | Final elongation | 72°C | 10' | |
| Total volume | 50 µl | | | | |

Table 3.40 The PCR reaction mixture for the *PfuTurbo* DNA polymerase.

| Reagents | Mixture | Temperature | | Time | Cycles Nr. |
|--|---------|------------------|------|------|------------|
| Sterile, deH ₂ O | 40 µl | Hold | 98°C | 5' | |
| 10 mM PCR dNTPs | 1 µl | Denaturation | 98°C | 1' | 25 |
| 5' primer (PCR product) | 2 µl | Annealing | 55°C | 30'' | |
| Vector | 0.5 µl | Elongation | 72°C | 13' | |
| PCR buffer (10 x) | 5 µl | | | | |
| <i>PfuTurbo</i> DNA Polymerase 2.5 U/µl | 1 µl | Final elongation | 72°C | 10' | |
| Total volume | 50 µl | | | | |

3.3.6.2 Restriction enzyme digestion of the plasmid DNA and the gene of interest

The *cst-II* gene and a plasmid DNA were digested for 5 h at 37°C with *Nde* I and *Bam*H I restriction enzymes using *Bam*H I reaction buffer (NEB), which was the suggested buffer for double digestion. Additionally, plasmid DNA was dephosphorylated for 1 h at 37°C and finally inactivated incubating for 10 min at 65°C.

3.3.6.3 Ligation

Ligation mixture (*Table 3.41*) was incubated overnight starting the reaction at room temperature and subsequently decreasing to 4°C. Electrocompetent DH5α *E. coli* cells were transformed with ligation mixture (5 µl), and bacterial clones resistant to ampicillin were picked and checked for *cst-II* gene presence.

Table 3.41 The ligation mixture.

| Reagent | 1:2 | 2:2 |
|---|------------|------------|
| pET plasmid vector (<i>Nde</i> I/ <i>Bam</i> H I digested) | 1 μ l | 2 μ l |
| <i>cst-II</i> gene (<i>Nde</i> I/ <i>Bam</i> H I digested) | 2 μ l | 2 μ l |
| 10 mM ATP (Sigma) | 1 μ l | 1 μ l |
| 10 x T4 DNA ligation buffer (NEB) | 1 μ l | 1 μ l |
| T4 DNA-Ligase 400 U/I (BioLabs, New England) | 1 μ l | 1 μ l |
| Water (sterile, distilled) | 4 μ l | 11 μ l |
| Total volume | 10 μ l | 20 μ l |

3.3.6.4 Analysis of pET recombinants

DH5 α *E. coli* transformants were analyzed using the plasmid preparation for the PCR and restriction enzyme analysis described in the chapter 3.3.5.6. All positive clones were sent for sequence analysis to Microsynth GmbH.

3.3.6.5 α -2,3/2,8 bifunctional sialyltransferase expression and determination

After transformation of recombinant pET vector into the expression host, the BL21 *E. coli* cell strain (a λ DE3 lysogen), positive clones were streaked on selective agar plates and grown overnight at 37°C. The following day, single colonies were picked and grown overnight at 37°C in 3 ml of selective LB medium. 1 ml of this culture was used to inoculate 50 ml of selective LB medium. The culture was incubated with shaking at 37°C until the OD₆₀₀ reached 0.6. An uninduced control sample was taken, and the culture was induced with 1 mM IPTG solution (100 mM stock). The cell culture was further incubated for 2-3 h.

Flasks were placed on ice for 5 min, the sample removed and cells were harvested by centrifugation at 5000 x g for 5 min at 4°C. Supernatant was saved for further analysis. The cell pellet was stored at – 20°C and treated according to the protocol.

Determination of the expressed protein was performed using SDS-PAGE method and Western Blotting analysis (see chapter 3.1.3). Western blotting was performed using monoclonal mouse anti His Tag (1:2000) as a primary antibody (Novagen) and goat anti-

mouse (whole molecule) alkaline phosphatase conjugated IgG (1:5 000) as a secondary antibody (Sigma). Enzyme was checked in the MES reaction buffer for the α -2,3/ α -2,8 activity with 600 μ M of Type II substrate. The α -2,8 activity was determined using 600 μ M of 7 acceptor substrate.

3.3.6.6 Determination of target protein solubility [267]

| | |
|-------------------------|---|
| Native lysis buffer | 50 mM NaH ₂ PO ₄ (pH 8.0), 300 mM NaCl, 10 mM imidazole |
| Denaturing lysis buffer | 10 mM Tris-HCl (pH 8.0), 8 M urea, 100 mM NaH ₂ PO ₄ |

1 ml of overnight culture was used to inoculate 50 ml of selective LB medium. Cultures were incubated at 37°C and induced with 1 mM IPTG when the OD₆₀₀ reached 0.6. Further growth occurred for 16 h at 30°C and 37°C. Cells were collected by centrifugation at 10 000 x g for 20 min at 4°C and the pellet was washed five times. This was followed by sonication (6 x 10'') in Tris-HCl buffer (pH 8.0). For isolation of the soluble protein fraction, the pellet was resuspended, twice more sonicated and centrifuged in the native lysis buffer. The insoluble protein fraction was recovered by washing the pellet in denaturing lysis buffer. After each sonication step, a sample (100 μ l) for SDS-PAGE was removed, resuspended in 3 x RB and stored at - 20°C. Collected samples were analyzed using SDS-PAGE method (see chapter 3.1.3).

3.3.6.7 Optimization of the cell growth and enzyme production

Growth curve [265]

E. coli strain BL21(DE3), AD494(DE3) and RG(DE3) grown on LB agar plate

E. coli strain BL21(DE3), AD494(DE3) and RG(DE3) with plasmid-construct grown on selective LB agar plate

E. coli strain BL21(DE3), AD494(DE3) and RG(DE3) with plasmid-vector grown on selective LB agar plate

LB, TB, SOB medium

BL21(DE3): 3 ml LB medium was inoculated with a BL21(DE3) clone picked on a freshly

grown LB agar plate. The culture was incubated with shaking at 300 rpm overnight at 37°C. Flasks containing 4 ml of different media (LB, TB, SOB) were inoculated with 40 µl of overnight culture. Some cultures were incubated at 37°C, and others at 30°C. The optical density was measured at 600 nm (OD₆₀₀) over a period of 24 h.

Cells containing the plasmid-construct: 50 ml cell cultures in selective LB, TB and SOB media were inoculated with 1 ml of overnight culture and incubated with shaking at 300 rpm at 37°C until an OD₆₀₀ of 0.6-0.8 was reached. The protein expression was induced with 1 mM IPTG. After induction, 50 ml cultures were incubated at RT, 37°C and at 30°C with shaking at 300 rpm. The OD₆₀₀ of these cultures was also measured over a period of 24 h. OD₆₀₀ was kept in the linear range by sample dilution.

Cells containing only the plasmid-vector (negative control): Culture-tubes containing 4 ml selective SOB, TB and LB-medium were inoculated with 40 µl overnight culture and incubated at 37°C in the shaker until an OD₆₀₀ of 0.6-0.8 was reached. Further incubation of cultures was done at RT, 37°C, and 30°C shaking at 300 rpm. The OD₆₀₀ was measured over the period of 24 h.

3.3.6.8 Time course analysis [265,267]

E. coli strain BL21(DE3) with plasmid-construct grown on selective LB agar plate

E. coli strain BL21(DE3) with plasmid-vector grown on selective LB agar plate

| | |
|-------------------|---|
| Cell lysis buffer | 20 mM Tris, 0.3 M NaCl, 1% Triton X-100 (Sigma), 5 mM Imidazole (Merck) |
|-------------------|---|

The expression of proteins can be optimized with time course analyses. At different times after 1 mM IPTG induction, the expression of the proteins was analyzed by SDS-PAGE. For this assay, the same 50 ml cultures as for the growth curve were used. Over a period of 24 h, samples of 100 µl were removed from 50 ml cultures grown in different media that were incubated at RT, 30°C and 37°C. They were centrifuged for 5 min at 13 200 rpm. To one of the pellets 50 µl reducing buffer was added to prepare it for SDS-PAGE. The other pellet was resuspended in 100 µl of cell lysis buffer. After sonication over 2 min (rounds of 10 s of sonication followed by a 10 s pause) and following centrifugation, 20 µl of supernatant was mixed with 10 µl of 3 x RB. For the negative control, cultures containing

only the plasmid-vector were induced with 1 mM IPTG. Samples were removed immediately after induction with IPTG and after 27 h from the cultures growing at RT, 30 and 37°C. The samples were treated in the same way as the samples containing the plasmid-construct. Samples were analyzed by SDS-PAGE (see chapter 3.1.3).

3.3.6.9 IPTG induction optimization [259]

E. coli strain BL21(DE3) with plasmid-construct was grown on the selective LB agar plate. Two clones were picked and resuspended in 3 ml selective LB medium. The culture was incubated overnight at 37°C with shaking at 300 rpm. Nine culture tubes containing 4 ml selective LB medium were inoculated with 40 µl overnight culture, and incubated until an OD₆₀₀ of 0.6-0.8 was reached. Eight of these cultures were induced with different IPTG concentrations in the range of 0.2 to 10 mM, except one culture which was not induced and which served as a negative control. After induction, the cultures were incubated for 16 h at 30°C with shaking at 300 rpm. 100 µl of each culture was centrifuged at 13 200 rpm for 5 min. The pellet was resuspended in 3 x RB and analyzed using SDS-PAGE (see chapter 3.1.3).

3.3.6.10 α-2,3/2,8 bifunctional sialyltransferase production

The 250 ml culture was centrifuged at 4000 x g for 20 min at 4°C and stored overnight at –20°C. The cell pellet of 250 ml cell culture was resuspended in 10 ml of native lysis buffer. Cell pellets were kept on ice and sonicated for 6 x 10 s with 10 s of pauses (80-100 W). The cell debris was removed by centrifugation at 21 000 rpm for 1 h at 4°C (Centrifuge 5804 R). The supernatant was filtrated (0.22 µm).

3.3.6.11 α-2,3/2,8 bifunctional sialyltransferase purification

Table 3.42 Buffers for protein purification by Ni-NTA affinity chromatography.

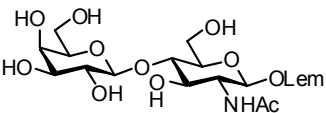
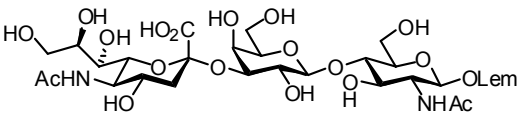
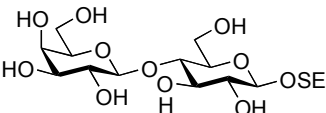
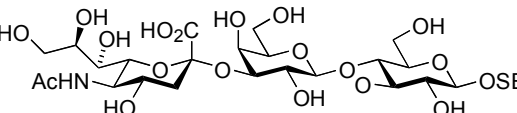
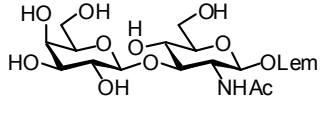
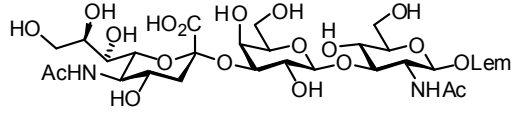
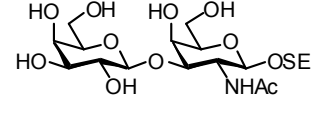
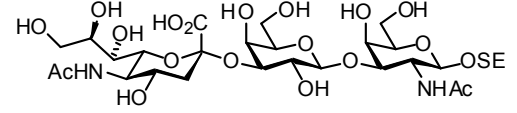
| | Purification under native conditions | Purification under denaturing conditions |
|----------------|---|---|
| Lysis buffer | 50 mM NaH ₂ PO ₄ , pH 8.0, 300 mM NaCl, 10 mM imidazole | 10 mM Tris-HCl, pH 8.0, 8 M urea, 100 mM NaH ₂ PO ₄ |
| Wash buffer | Lysis buffer + 30 mM imidazole | Lysis buffer, pH 6.3 |
| Elution buffer | Lysis buffer + 0.5 M imidazole | Lysis buffer, pH 5.9 |
| | | Lysis buffer, pH 4.5 |

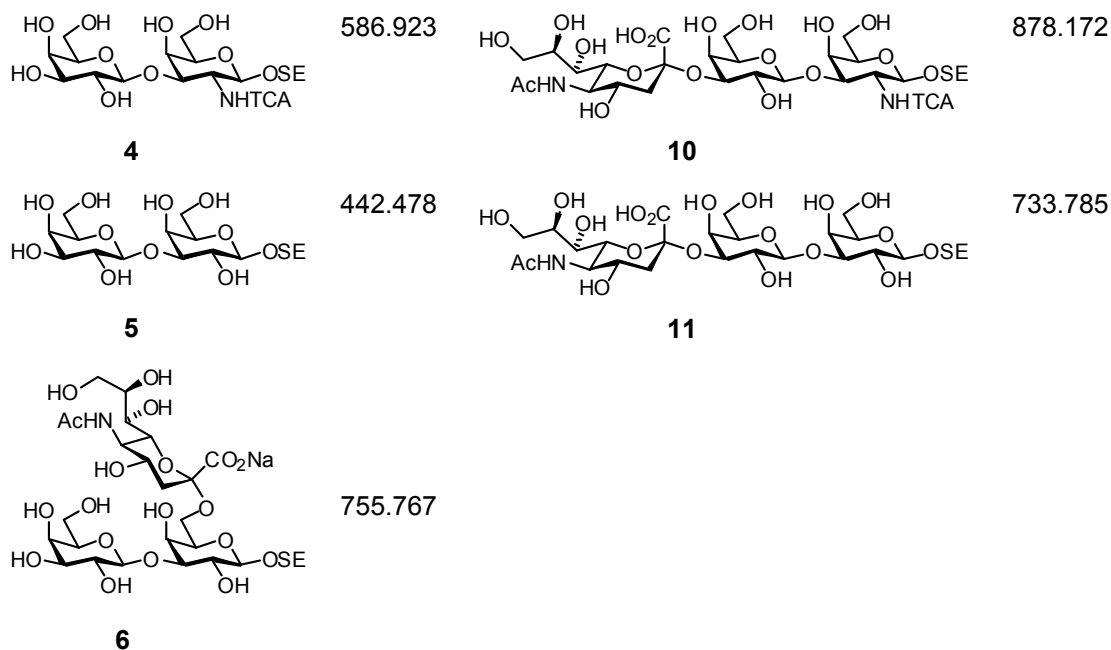
The FPLC purification using Ni-NTA (5/10 ml) superflow under native or denaturing conditions.

The Ni-NTA column was equilibrated with 5 CV of lysis buffer (*Table 3.42*). Appropriate lysate for native or denaturing purification was applied to the column and the column was washed with 5 – 10 CV of lysis buffer until the A_{280} was stable. The column was further washed with 5 – 10 CV of washing buffer to monitor the stability of the baseline at A_{280} . Protein elution under native conditions was performed using 5 CV of elution buffer. Finally, the protein elution under denaturing conditions was performed using 5 CV of elution buffer (pH 5.9) and, if necessary, by application of 5 CV of elution buffer (pH 4.5).

3.3.7 α -2,3/2,8 ST enzyme characterization

Table 3.43 The acceptor substrates used for determination of enzyme kinetic parameters. OSE: O-(trimethylsilyl)ethyl (O-CH₂CH₂-Si(Me)₃), OLem: O-(Methoxycarbonyl)octyl (O-(CH₂)₈CO₂Me), TCA: tri-chloro acetyl (COCCl₃).

| Acceptor | MW | Product / Acceptor | MW |
|--|---------|---|---------|
|  <p>1 or Type II</p> | 553.597 |  <p>7</p> | 844.852 |
|  <p>13</p> | 442.531 |  <p>14</p> | 733.785 |
|  <p>2 or Type I</p> | 553.597 |  <p>8</p> | 844.852 |
|  <p>3</p> | 483.583 |  <p>9</p> | 796.819 |



3.3.7.1 Enzyme activity assay optimization

Reaction buffer optimization

Table 3.44 Reaction buffers used for enzyme activity optimisation.

| | |
|---------------|---|
| NaCaCO buffer | 100 mM Na cacodylate (pH 7.5), 0.3% Triton X-100, 10 mM MgCl ₂ . |
| Hepes buffer | 50 mM Hepes (pH 7.5), 0.3% Triton X-100, 10 mM MgCl ₂ |
| MES buffer | 50 mM MES (pH 7.5), 0.3% Triton X-100, 10 mM MgCl ₂ |

For the enzyme activity assay, a pellet and a supernatant of recombinant *E. coli* cells were checked for α -2,3 and α -2,8 activity using different reaction buffers (*Table 3.44*) in the presence of 600 μ M of Type II and **7** acceptor substrate (*Table 3.43*), respectively. This was done under the same conditions mentioned in the chapter 3.3.7.2.

Calf intestine alkaline phosphatase (CIAP) assay

Additional 1 μ l of CIAP enzyme was added to the reaction mixture containing MES buffer and incubated under the same conditions mentioned previously in the chapter 3.3.7.2.

3.3.7.2 Enzyme activity assay

Table 3.45 Standard protocol for measuring the enzyme activity.

| Reagent | Volume |
|---|------------|
| MES reaction buffer, pH 7.5 | 14 μ l |
| 1 mM CMP-NeuNAc (2 nmol) 10 mM | 2 μ l |
| CMP-[¹⁴ C] NeuNAc 60 000 dpm (0.1 nmol) | 1 μ l |
| 600 μ M acceptor | 2 μ l |
| Purified enzyme fraction | 1 μ l |
| Total Volume | 20 μ l |

A master mix of the different components (*Table 3.45*), not including the enzyme, was prepared. The enzyme (4 mU) was added just before starting the reaction. The mixture was centrifuged and incubated for one hour at 25°C either in the heating block or in the Gene Amp PCR System 2400. Depending on the enzyme concentrations, dilutions were used for different purified fractions. The samples were either immediately checked for activity or stored at -20°C to stop the enzymatic reaction. For separating the product from the reaction mixture, a solid phase extraction using C18 Sep-Pak Cartridges was performed as it was described in the chapter 3.1.5.

3.3.7.3 Catalytic activity

Enzyme was incubated for 72 hours at 25°C in MES reaction buffer containing 600 μ M of Type II acceptor substrate, CMP-[¹⁴C] NeuNAc (60 000 dpm) and non-labeled NeuNAc. Samples were collected on a regular basis and checked for the enzyme activity using C18 Sep-Pak Cartridges (see chapter 3.1.5).

3.3.7.4 Temperature dependent activity

The master mix (*Table 3.45*) was prepared without the acceptor. It was divided into samples of 18 μ l. The mixture was preheated for 5 min at a temperature between 4°C and 72°C either in the heating block or on a Gene Amp PCR System 2400. Then, the acceptor (600 μ M Type I or 600 μ M 7) was added and samples were incubated for 6 h. The enzyme α -2,3/ α -2,8 and α -2,8 activity was measured using the method described in the chapter 3.1.5.

3.3.7.5 pH optimization

The enzyme activity was measured using MES buffers with a wide pH range (5.0-10.0) and 600 μM of Type I acceptor (*Table 3.45*). The samples were incubated for 6 hours at 25°C. The enzyme was added at the start of the reaction.

3.3.7.6 Metal ions optimization

The MES buffer containing 10 mM of different metal cations (MgCl_2 , MnCl_2 , NiCl_2 , KCl , CuCl_2 , ZnCl_2 , FeCl_3 , CaCl_2 and CoCl_2) was prepared and the pH was adjusted after dissolving the cations in the reaction buffer. Buffers containing 600 μM Type I acceptor were used for the sample preparation (*Table 3.45*) in order to measure enzyme activity. The positive control was MES buffer with 10 mM EDTA. After incubation for 6 hours at 25°C, enzyme activity was measured.

3.3.7.7 Cofactor dependent enzyme activity

The enzyme activity was measured with 600 μM Type I acceptor using MES buffers containing 500 μM of different cofactors (NAD, NADH, NADP, NADPH and ATP). All the samples were prepared as described in *Table 3.45*. Positive control was prepared with MES buffer free of metal ions or containing 10 mM of Mg^{2+} ions. The enzyme was added at the start of the reaction and the samples were incubated for 6 hours at 25°C.

3.3.7.8 Dimethyl sulfoxid dependent enzyme activity

The enzyme activity was measured using MES buffers containing different DMSO concentrations (1-80%) and 600 μM acceptor **13** (*Table 3.45*). The enzyme was added at the start of the reaction and the samples were incubated for 6 hours at 25°C. As a positive control, enzyme was incubated in MES buffer free of DMSO solution.

3.3.7.9 Determination of the enzyme kinetic parameters [248]

Enzyme kinetics was performed using the components of reaction mixture described in *Table 3.45*. Relative rates for each free di(tri)saccharide acceptor substrate were calculated as a percentage of the incorporation of [^{14}C] NeuNAc into the *D*-Gal-containing di(tri)saccharide. Under standard incubation conditions, at a temperature of 25°C for α -2,3/ α -2,8 activity, and at 37°C for α -2,8 activity (pH 7.5), formation of the product was shown to be linear in time.

For the K_M value determination, it was used eight to nine different acceptor substrate concentrations were used for each acceptor substrate presented in *Table 3.43*.

Enzyme kinetic parameters were obtained from double-reciprocal plots by linear regression analysis of Lineweaver-Burk plots.

3.3.8 Preparative synthesis

According to the enzyme activity and the kinetic data, first preparative syntheses were performed by Oliver Schwardt using Type I, **4** and *D*-lactose-OSE as acceptor substrates in the reaction.

| Preparative substrate 4 | Preparative substrate 13 | Preparative substrate 2 |
|--|--|---------------------------------------|
| MES buffer, pH 7.5 | MES buffer, pH 7.5 | MES buffer, pH 7.5 |
| 10 mg 4 | 3 mg <i>D</i> -Lactose-OSE | 3.8 mg Type I |
| 1.5 eq CMP-NeuNAc | 1.5 eq CMP-NeuNAc | 2.5 eq CMP-NeuNAc |
| 400 μ l (21.6 U/l) enzyme fraction | 300 μ l (21.6 U/l) enzyme fraction | 350 μ l (3.5 U/l) enzyme fraction |
| Reaction time: 6 days (d) | Reaction time: 3 days (d) | Reaction time: 3 days (d) |

The preparative reaction with **4** and *D*-lactose-OSE was started using 200 μ l of the enzyme fraction. After 24 h, 200 μ l and 100 μ l of the enzyme fraction was added and incubated for 6 d or 3 d, respectively. The product was monitored by TLC and analyzed by MS and NMR.

4 Results and discussions

It is well known that carbohydrates from glycolipids and glycoproteins with terminal sialic acids linked in α -2,3, α -2,6 and α -2,8 manner are involved in a broad variety of biological recognition and adhesion events [268-272]. Gangliosides, a group of sialylated glycosphingolipids widely present in mammalian tissues, have been recognized to play an important role in many biological processes such as cell-cell recognition, cell growth, differentiation, and neural functions [11,272,273]. Thus, the gangliosides GD1a and GT1b have been shown to bind with high affinity to the myelin-associated glycoprotein (MAG), a member of the Siglec family, which is a potent inhibitor of neurite outgrowth of most neurons [205,215,216,235,236].

The most common element recognized by MAG is the terminal NeuNAc α (2,3)Gal β (1,3)GalNAc oligosaccharide moiety of ganglioside, suggesting a special importance of this trisaccharide subunit and its affinity to MAG.

In order to investigate their binding affinity to the MAG, large numbers of natural and modified oligosaccharides have to be applied for broad biological screening. Although numerous glycosylation methods are well known, the chemical synthesis of complex oligosaccharides is still not a routine procedure. Difficulties often occur from time-consuming protecting group manipulations. Finally, chemical sialylations suffer from poor stereoselectivity due to the lack of neighboring group assistance in the sialic acid moiety [274]. A convenient alternative approach is the application of glycosyltransferases [153,275], e.g. with α -2,3 sialyltransferases (STs) a sialic acid moiety can be transferred from CMP-NeuNAc donor substrate α -selectively onto the 3-OH group of a terminal *D*-galactose containing acceptor substrate.

The investigations reported here are concentrated at the expression, purification and characterization of the eukaryotic and prokaryotic sialyltransferases, and their utilization in preparative chemo-enzymatic synthesis of oligosaccharide mimetics.

To achieve this goal, recombinant rat Gal β (1,3/4)GlcNAc α -2,3 sialyltransferase (*r*ST3Gal III, EC 2.4.99.6) [276], recombinant human Gal β (1,4)GlcNAc α -2,6 sialyltransferase

(hST6Gal I; EC 2.4.99.1) [90] and recombinant *Campylobacter jejuni* α -2,3/2,8 bifunctional sialyltransferase (Cst-II) [264] were expressed in different expression systems and applied to enzymatic sialylation for several natural and non-natural acceptor substrates.

4.1 rST3Gal III expression in baculovirus-infected cells, purification and characterization

The Gal β (1,3/4)GlcNAc α -2,3 sialyltransferase was first purified to homogeneity from the rat liver by Weinstein *et al.* [277]. This enzyme forms the NeuNAc α (2,3)Gal β (1,3)GlcNAc and NeuNAc α (2,3)Gal β (1,4)GlcNAc sequence typically found to terminate complex type *N*-linked oligosaccharide chains. These sequences were also found in *O*-linked sugar chains and in glycolipids. This enzyme transferred a sialic acid moiety from CMP-NeuNAc regio- and α -stereoselectively onto the 3-OH group of a terminal galactose. Furthermore, it was demonstrated that the proteolytically sensitive stem region *in vivo* yielded a soluble catalytically active enzyme [32,47].

Since high-level expression and secretion of glycosyltransferases was possible by truncating them to soluble form [47], as mentioned before, recombinant baculovirus DNA containing the γ -interferon export sequence fused to the soluble form of the rat liver Gal β (1,3/4)GlcNAc α -2,3 sialyltransferase (rST3Gal III; EC 2.4.99.6) was kindly received from Dr. Markus Streiff [72].

For the recombinant enzyme expression and preparative production, the powerful baculovirus-based expression system was used. The baculovirus expression vector system (BEVS) is one of the most powerful and versatile eukaryotic expression system available [238,278]. This system has a high integration capacity for large gene inserts. The proteins expressed in BEVS were, in most cases, soluble and functionally active. This system is capable of performing post-translational modifications. This leads to a protein that is similar to its native counterpart, both structurally and functionally. Several post-translational modifications have been reported to occur in baculovirus (BV)-infected insect cells, including *N*- and *O*- linked glycosylation, phosphorylation, acetylation, amidation, carboxymethylation, isoprenylation, signal peptide cleavage and proteolytic cleavage. In addition, tissue- or species-specific post-translational modifications were not performed in the BV, unless the modifying enzyme was co-expressed. Baculovirus-expressed

recombinant proteins were usually localized in the same subcellular compartment as the authentic protein. Insect cell lines were incapable of synthesizing sialylated lactosamine complex-type *N*-glycans or sialylated core 1 *O*-glycans and therefore were not suitable for the production of recombinant pharmaceutical glycoproteins for clinical use [279-281]. Nevertheless, the baculovirus expression system is the preferred system when the production of several 100 mg of protein is required within a short time and a mammalian/human type of glycosylation is not of primary importance.

4.1.1 *r*ST3Gal III expression and purification

4.1.1.1 Amplification of the virus stocks and determination of the virus titer

In order to generate a high titer of recombinant virus stocks for maximal protein production, the recombinant virus was amplified and determined using the end-point dilution method. The basic principle of the method of Reed and Muench [239] is to assume that all cultures infected at a particular dilution would have been infected at all lower dilutions, and conversely, that all cultures uninfected at that dilution would have been uninfected at all higher dilutions. Considering this statement, uninfected and infected cells at certain dilutions (10^{-5} , 10^{-6} , 10^{-7}) were counted 5 days post-infection (pi). Using a given equation and collected cell-infected results, virus titer containing recombinant baculovirus DNA was amplified and estimated at the level of 3×10^7 pfu/ml [238,239]. Enzyme accumulation was monitored over time and a peak of activity was found approximately 72 h post-infection.

4.1.1.2 Purification of the *r*ST3Gal III

After an optimized protein expression of approximately 128.74 mg/l of total protein (*Table* 4.1), and enzyme activity of 1.85 U/l, the 72 h post-infection media of the infected *Sf9* cells was collected.

To purify the *r*ST3Gal III recombinant enzyme from conditioned media produced by cells infected with recombinant baculovirus, the media was applied to a column of CDP-hexanolamine-agarose (10 μ mol CDP/ml agarose, Calbiochem). The FPLC chromatography profile demonstrated only one peak obtained with 1 M Na-cacodylate buffer (*Figure* 4.1).

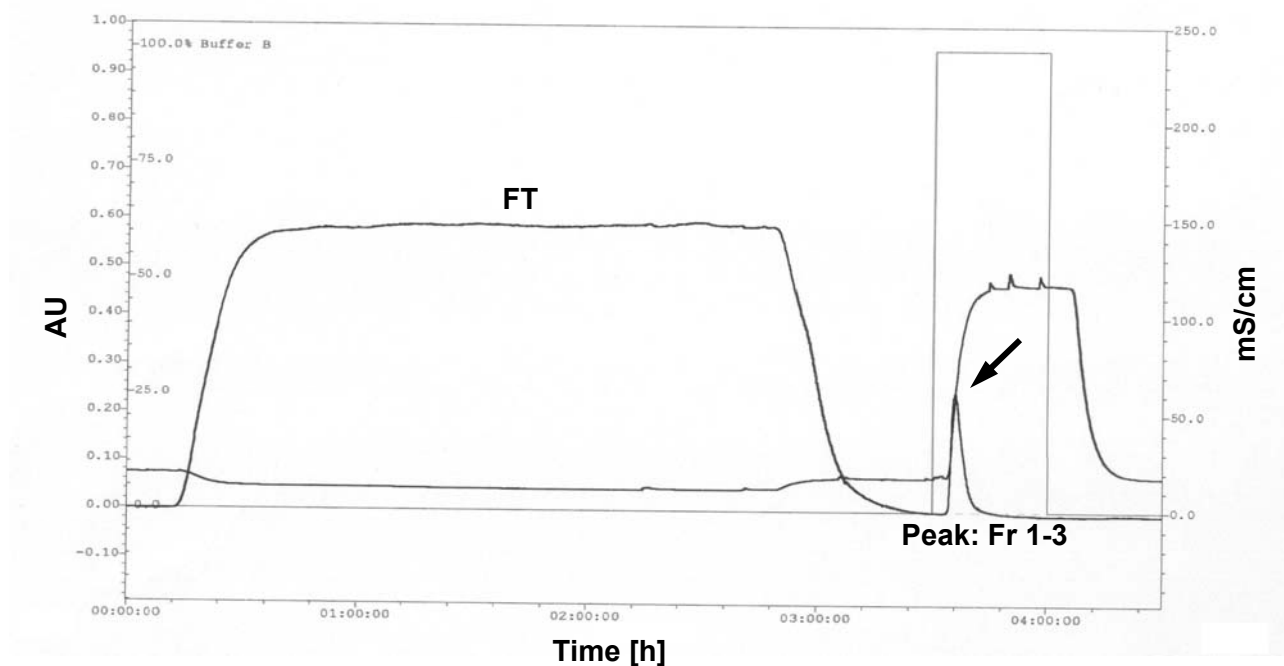


Figure 4.1 The FPLC chromatogram of *rST3Gal III* purification using CDP-hexanolamine-agarose affinity column. The AU determine absorption unit, conductivity is displayed as mS/cm, and the FT describes the flow through. The arrow points the obtained peak collected in the fractions 1-3.

The enzyme has revealed a loss of activity during the purification and concentration procedure (*Table 4.1*). Comparing the total activity of the enzyme measured in milliunits, a nearly nearly 7-fold decreased activity during the purification steps and almost 5-fold during concentration of Fr 2 containing partially purified enzyme was observed. One possible explanation for decreased enzyme activity could be the purification correlated loss of important enzyme cofactors other than metal ions.

Table 4.1 Comparison of the starting material to the final yields of the purified and concentrated enzyme fraction.

| | Total protein [mg/l] | Total [mg] | Total [mU] | U/l | U/g |
|-------------------|----------------------|------------|------------|------|-------|
| Load | 128.74 | 5.15 | 74.00 | 1.85 | 14.37 |
| Fr 2 | 64.84 | 2.59 | 11.70 | 1.30 | 4.51 |
| Fr 2 (16 x conc.) | 24.29 | 0.97 | 2.12 | 4.24 | 2.18 |

SDS-PAGE analysis revealed several additional signals within the eluted peak. Fr 1 showed three weak signals, while two signals were detected in Fr 2 and 3 (*Figure 4.2 a*). Apart from the signal approximately at 66 kDa, which was shown to be recombinant *rST3Gal III* (see below), other signals might have appeared because of unspecific binding to the affinity column.

The fractions were analyzed by Western blot using rabbit anti-human ST6Gal I purified serum as a primary antibody. This antibody was raised against the fusion-protein which contained human ST6Gal I with the β -galactosidase portion [282]. The presence of *rST3Gal III* with a molecular weight of approximately 66 kDa was confirmed in all three fractions. Fr 2 showed the strongest signal and therefore, containing the highest amount of the enzyme (*Figure 4.2 b*). Despite the impurities detected in the obtained fractions, the enzyme activity of 1.3 U/l non-concentrated and 4.2 U/l concentrated Fr 2 was sufficient to perform chemo-enzymatic preparative synthesis (*Table 4.3*).

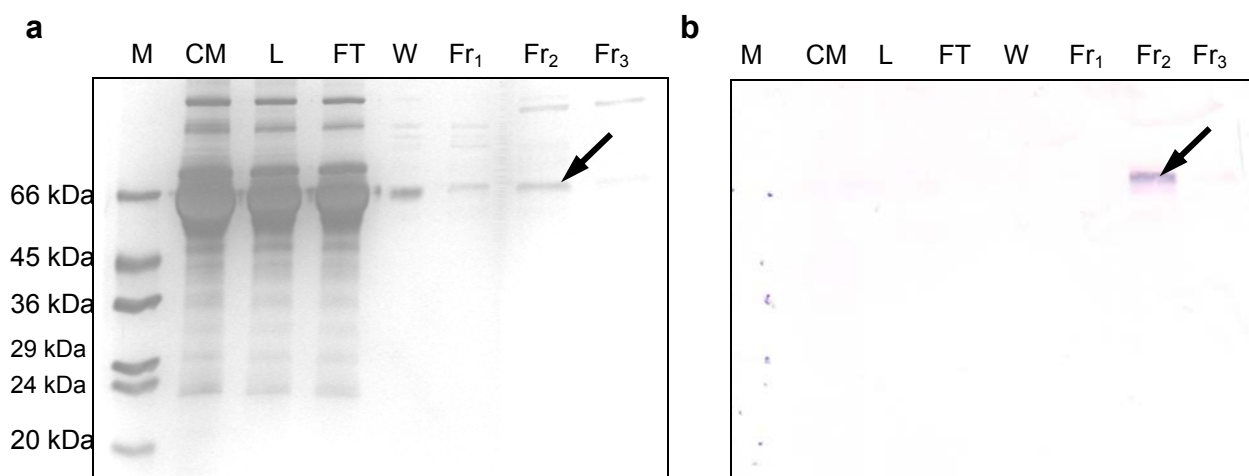


Figure 4.2 (a) SDS-PAGE (12.5%) analysis of the *rST3Gal III* purification by CDP-hexanolamin-agarose affinity chromatography (silver staining) and **(b)** Western blotting. Western blot analysis was performed using rabbit anti-ST6Gal I purified serum as a primary antibody and goat anti-rabbit immunoglobulin G (IgG) alkaline phosphatase (AP) conjugated as a secondary antibody. M: low molecular marker; CM: collected medium; L: load; FT: flow through; W: elution with wash buffer; Fr: fractions collected during the chromatography. The arrow points the *rST3Gal III*.

The ST3Gal III shares three regions of homology with other sialyltransferases [78,101,276]. These two peptide sequences, also called sialyl motifs, were found on all the

sialyltransferases cloned so far and seem to be characteristic for the sialyltransferase family [23]. Hence, the sialyl motifs are potential cross-reactive epitopes. The soluble recombinant rat ST3Gal III and human ST6Gal I share 18.7% homology in a global alignment and 24.9% in a local alignment, particularly in the L sialyl motif domain. Surprisingly, characterization of the expressed and purified rat ST3Gal III revealed an unexpected cross-reactivity of an antibody directed against the human ST6Gal I- β -galactosidase fusion protein with the rat ST3Gal III. A very specific single band was obtained with a molecular weight approximately at 66 kDa (*Figure 4.2 b*). Due to the strong homology at the amino acid level between the same sialyltransferases in different species, interspecies cross-reactivity had already been observed. However, cross-reactivity between different sialyltransferases originating from distinct species has never been reported [72,282]. The unexpected cross-reactivity in this experiment could be explained on the basis of the homology between these different sialyltransferases. Another line of evidence showed the unspecific reaction of this antibody with β -galactosidase [72,282]. This was consistent with my results where the antibody reacted with β -galactosidase, one of the standard proteins with molecular weight of 116 kDa, present in the high molecular weight marker (HMW; Sigma).

Collected fractions obtained during the protein purifications were checked for enzyme activity (*Figure 4.3*) using 200 μ M of natural Type II acceptor substrate (*Table 3.14*). Fr 2 exhibited 45% of the relative enzyme activity, while Fr 3 showed 11%. The relative activity of the enzyme was calculated as a percentage of incorporation of the [14 C] NeuNAc radio-labeled donor in the acceptor substrate.

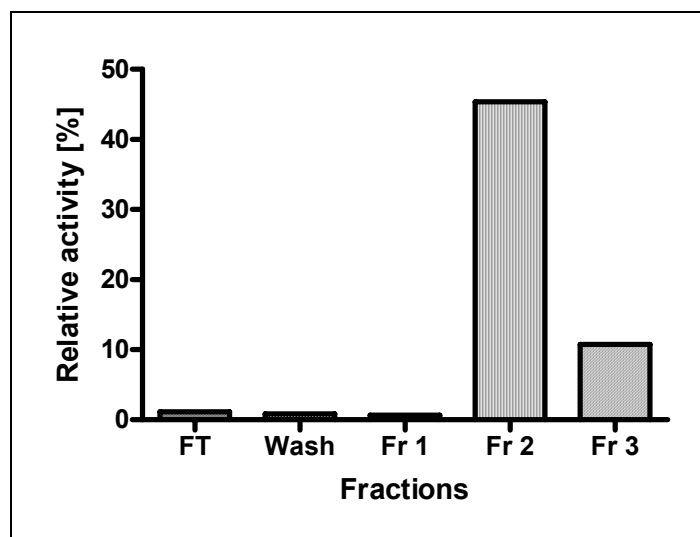


Figure 4.3 Enzyme activity assay of CDP-hexanolamine-agarose affinity chromatography collected fractions. Samples were incubated with 200 μ M of Type II acceptor substrate for 1 h at 37°C (L: load; FT: flow through; W: wash; Fr: fraction). The enzyme activity was calculated as described in chapter 3.1.5.

4.1.2 Characterization of the *rST3Gal III* enzyme

4.1.2.1 *rST3Gal III* catalytic activity

In order to optimize the activity of the enzyme with natural Type II acceptor substrate (*Table 3.14*), an enzyme linearity experiment was performed. The enzyme was incubated for three hours at 37°C. Enzyme activity, as measured by incorporation of radioactive-labeled NeuNAc in the Type II acceptor substrate, was determined during 180 minutes of incubation under standard conditions (see chapter 3.1.5). The enzyme showed highest activity in the first few minutes, exhibiting 18% of sialic acid incorporation, and more than half (57%) of the Type II acceptor substrate was labeled after 15 minutes of incubation (*Figure 4.4*). Near completion of the reaction catalyzed by *rST3Gal III* was already observed after 60 minutes, although the enzyme required as much time again to fully complete product formation.

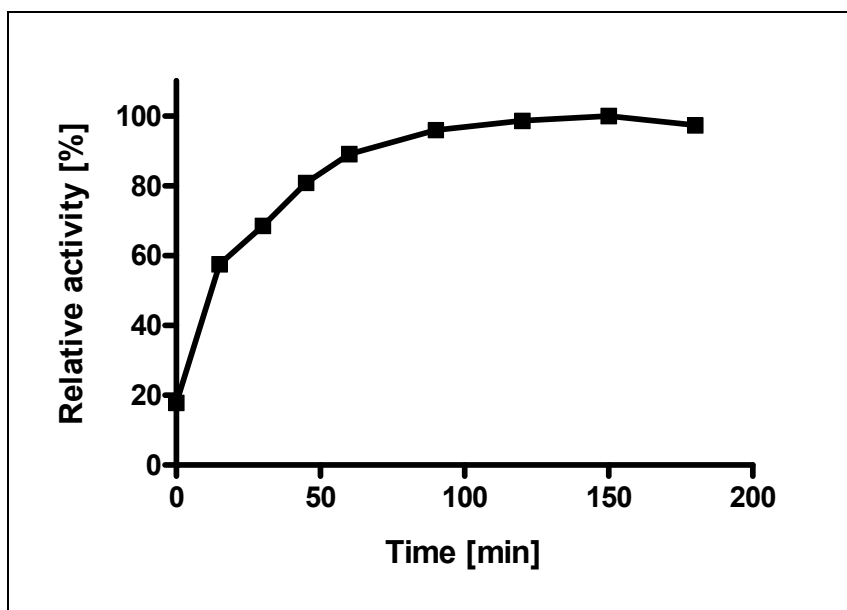


Figure 4.4 Catalytic activity of the *rST3Gal III* enzyme estimated by ST enzyme activity assay. Samples were incubated with 200 μM of Type II acceptor substrate for 3 h at 37°C (see chapter 3.1.5).

4.1.2.2 Determination of the enzyme kinetic parameters

The rat ST3Gal III was further characterized using natural and non-natural disaccharide acceptor substrates. The only difference between some of the published assays and those reported in *Table 4.2* and *Table 4.3* was that all of our acceptor sequences are attached to hydrophobic aliphatic aglycones such as OLem (O-(CH₂)₈CO₂Me) and OSE (O-CH₂CH₂-Si(Me)₃). The acceptors were synthesized with these aglycones so that the reaction product of the enzymatic reaction could be conveniently isolated using a reverse-phase C-18 Sep-Pak assay. All kinetic data as well as structures of the product that have been formed by the action of the rat ST3Gal III are presented in *Table 4.2* and *Table 4.3*. Determination of kinetic parameters in 1982 by Weinstein *et al.* has revealed that asialoagalactoprotease, an acceptor substrate containing the terminal sequence Gal β (1,3)GlcNAc on *N*-linked oligosaccharides is, until now, the best acceptor substrate with a K_M value of 6 μM and V_{max} of 0.34 [277]. Using deoxygenated substrate analogs [283], the enzyme has been previously shown to require an intact D-galacto-3,4,6-triol system on the accepting galactose unit, together with some unidentified additional structural features, for an effective transfer of the NeuNAc residue. The K_M values obtained in our experiment (*Table 4.2*) indicated that rat ST3Gal III preferentially act on

Type I (*Figure 4.5 a*) substrate acceptor exhibiting a K_M of 66 μM and V_{max} of 3.42, but was also able to catalyze the sialylation of Type II (*Figure 4.5 b*), albeit with lower catalytic efficiency (K_M of 87 μM ; V_{max} of 3.19) [249].

A K_M value obtained for the Type I acceptor substrate in our experiments was consistent with the K_M published by Gosselin *et al.* [284]. They reported a K_M value of 60 μM using radiochemical enzyme assay. Weinstein *et al.* [285] published kinetic parameters referred to native rat liver ST3Gal III. The K_M values of Type I and Type II (0.64 mM and 2.66 mM) were 10- and 30-fold increased, and corresponding V_{max} (1.16 and 0.75) almost 3- and 4-fold decreased, respectively, compared to the results gained in this work. Data published by Wlasichuk *et al.* [283] using the same native rat liver enzyme, indicated a K_M of 0.11 mM and relative V_{max} of 1 for Type I, whereas a K_M of 0.90 mM and a relative V_{max} of 0.3 was identified for Type II. The kinetic parameters for Type II acceptor substrate determined in this work (K_M of 87 μM) was only 1.7-fold lower than a K_M value (0.15 mM) obtained for the same acceptor substrate using native rat liver ST3Gal III published by Hindsqual *et al.* [286]. Van Dorst *et al.* [287] reported that recombinant rat liver ST3Gal III exhibited a K_M of 0.49 mM and V_{max} of 1.19 for Gal residue containing trisaccharide (Gal β (1,4)GlcNAc(1,2)Man-octyl aglicon) substrate, whereas the same enzyme was inhibited by all modified trisaccharide derivatives which were shown not to be substrates in the enzyme driven reaction.

It should be emphasized that in order to correctly compare and explain differences and variations between the kinetic parameters (K_M and V_{max}) published so far, various enzyme assays (*e.g.* radioactive, spectrophotometric) and distinct enzyme sources (*e.g.* native or recombinant) should be taken into account.

We considered that the catalytic activity of the enzyme is sufficient for the set up in chemo-enzymatic reaction. Several non-natural substrates, demonstrating a part of the GQ1b α ganglioside mimetic, were used as acceptor substrates. Determination of the kinetic parameters (K_M and V_{max}), indicated that the activity of the rat ST3Gal III with non-natural substrates **3**, **4** and **5** (*Figure 4.5 c; d; e*) was significantly reduced compared to the natural substrates **2** (Type I) and **1** (Type II), but still enough for preparative usage [249,250]. Also, the transfer efficiency V_{max}/K_M was much lower for these unnatural substrates.

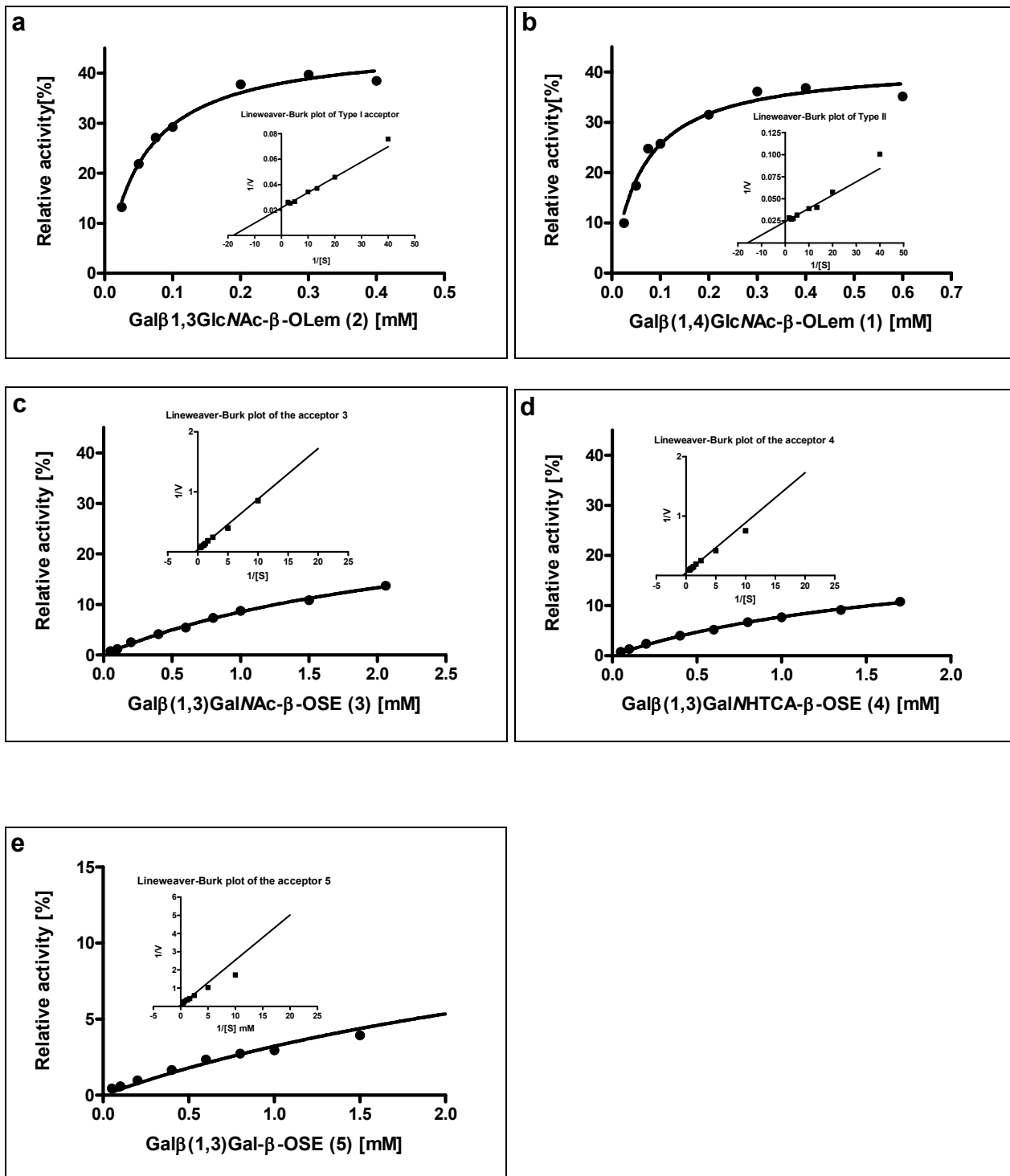


Figure 4.5 Michaelis-Menten kinetics. A plot of the relative reaction activity (V) with the acceptor substrate **(a)** Gal β (1,3)GlcNAc- β -OLem **2** (Type I), **(b)** Gal β (1,4)GlcNAc- β -OLem **1** (Type II), **(c)** Gal β (1,3)GalNAc- β -OSE **(3)**, **(d)** Gal β (1,3)GalNH₂TCA- β -OSE **(4)**, and **(e)** Gal β (1,3)Gal- β -OSE **(5)**. Substrate concentration is designated as [S]. Additional graph shows data represented as a double-reciprocal or Lineweaver-Burk plot.

The enzyme kinetic data (V_{\max} and K_M) for natural and unnatural acceptor substrates are summarized in the *Table 4.2*.

Table 4.2 Determination of the enzyme kinetic parameters. OSE: O-(trimethylsilyl)ethyl (O-CH₂CH₂-Si(Me)₃), OLem: O-(Methoxycarbonyl)octyl (O-(CH₂)₈CO₂Me), TCA: tri-chloroacetyl (COCCl₃).

| Name | Acceptor substrate | K_M [mM] | V_{\max} $\left[\frac{\text{nmol}}{\text{ml} \cdot \text{min}} \right]$ | V_{\max}/K_M [$10^{-3}/\text{min}$] |
|--------------------|---|------------|--|---|
| 2 (Type I) | Gal β (1,3)GlcNAc- β -OLem | 0.066 | 3.42 | 51.8 |
| 1 (Type II) | Gal β (1,4)GlcNAc- β -OLem | 0.087 | 3.19 | 36.7 |
| 3 | Gal β (1,3)GalNAc- β -OSE | 0.995 | 1.11 | 1.1 |
| 4 | Gal β (1,3)GalNHTCA- β -OSE | 0.811 | 0.89 | 1.1 |
| 5 | Gal β (1,3)Gal- β -OSE | 0.990 | 0.43 | 0.43 |

4.1.2.3 Stability of the enzyme during long-period incubation

In order to determine optimal reaction conditions, the activity of the *r*ST3Gal III was investigated over time at 37°C. The *r*ST3Gal III reaction profile (*Figure 4.6*) revealed that the activity of the enzyme remained practically unchanged for the initial 9 h. Incubation for 12 and 24 h, however, led to a significant decrease of activity. It is noteworthy, that even after 84 h of incubation at 37°C about 20% of the original enzyme activity was still preserved. This finding was important since our aim is the application of the produced *r*ST3Gal III for preparative chemo-enzymatic synthesis of oligosaccharide mimetics.

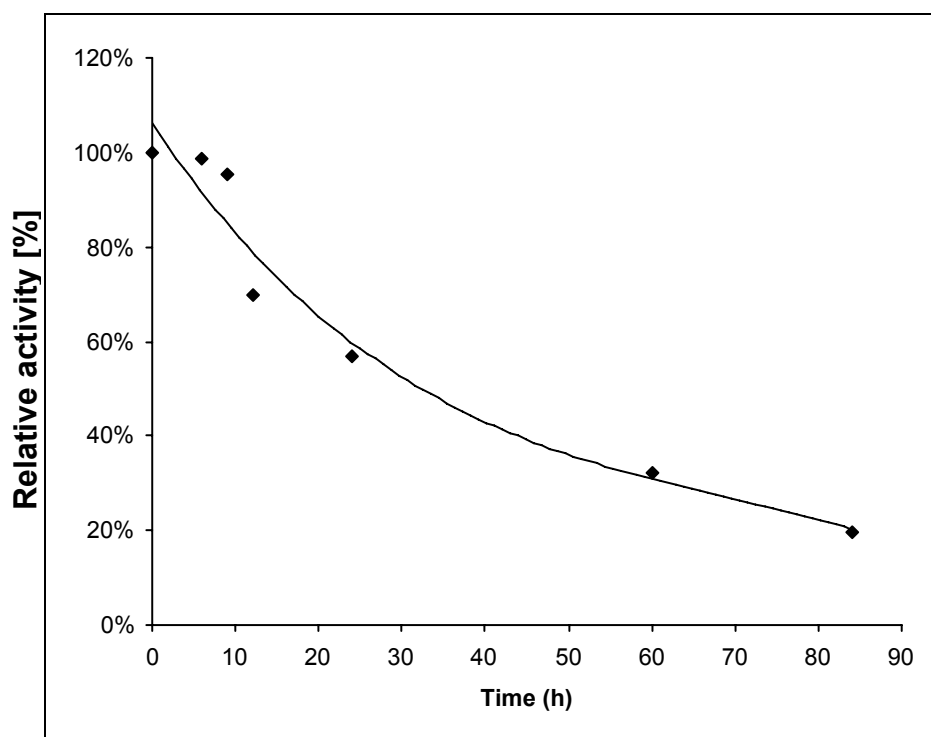


Figure 4.6 Enzyme stability of *rST3Gal III* tested with Gal β (1,3)GlcNAc- β -OLem (Type I) at 37°C.

4.1.2.4 Long-term storage of the *rST3Gal III* enzyme

In order to investigate the long-term stability of purified *rST3Gal III*, the enzyme was stored at 4°C and – 20°C either in the absence or in the presence of 20% and 50% glycerol. The enzyme activity was then measured after 2 weeks and 15 months of storage (*Figure 4.7*). The results show that *rST3Gal III* stored for 15 months in the absence of glycerol was unstable at 4°C. The enzyme aliquots in 20% and 50% glycerol exhibited similar enzyme activity after 2 weeks and 15 months of storage at the aforementioned temperature. The purified *rST3Gal III* stored at –20°C in 20% and 50% glycerol as well as a sample in the absence of the glycerol solution showed a high degree of enzyme stability and preservation of the original enzyme activity. There was no enzyme activity difference between the sample free of glycerol and the *rST3Gal III* stored in 20% of glycerol solution at –20°C. The enzyme stored for 15 months at – 20°C showed a slight loss of activity when stored in 50% glycerol solution. Our findings are consistent with the reported results concerning enzyme stability over a long period [16].

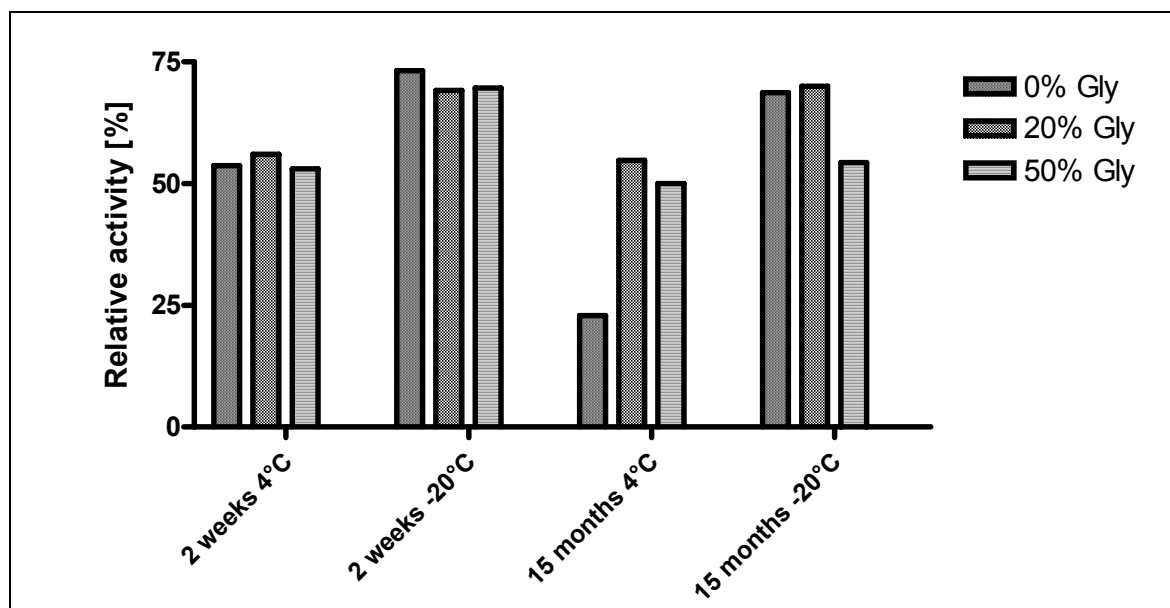


Figure 4.7 Long-term storage and stability of *rST3Gal III* enzyme (Gly: glycerol solution).

4.1.2.5 Preparative chemo-enzymatic synthesis using *rST3Gal III*

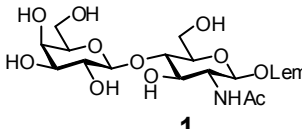
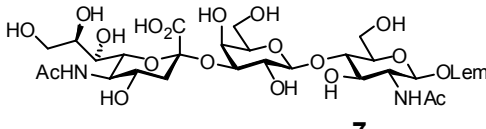
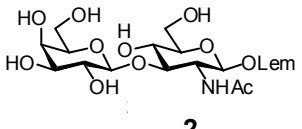
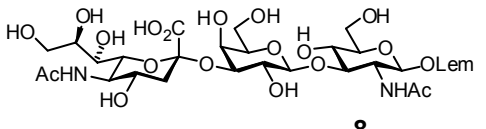
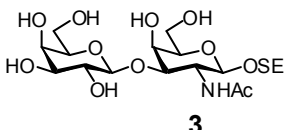
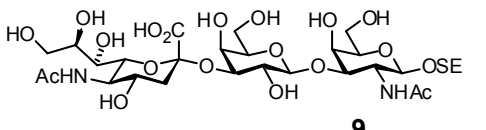
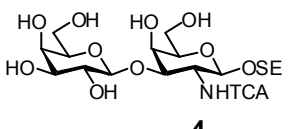
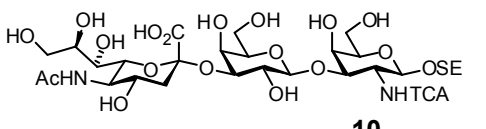
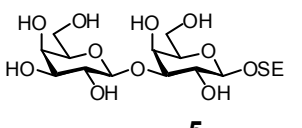
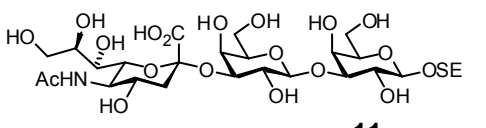
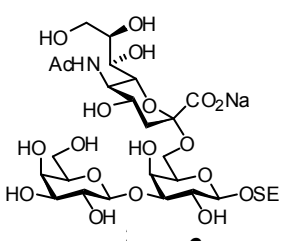
As previously mentioned, non-natural substrates (**3**, **4**, **5**, and **6**), e.g. Type III derivatives are part of the GQ1b α mimetic molecule. This part of GQ1b α was proposed to be involved in the binding of the MAG. The saccharides **3**, **4**, **5** and **6**, and, as control experiments, the natural substrates Type I and Type II were then incubated on a preparative scale with CMP-NeuNAc and recombinant *rST3Gal III*. As shown previously [253,288,289], the natural substrates Type II (**1**) disaccharide and Type I (**2**) were converted quantitatively into the corresponding trisaccharides **7** and **8** (entries 1 and 2 in *Table 4.3*). Although the physiological enzymes for the sialylation of terminal Gal β (1,3)GalNAc disaccharide are ST3Gal I, II and IV (see chapter 1.2.8.5), compounds **3**, **4** and **5** were sialylated by *rST3Gal III* giving the trisaccharides **9-11** in acceptable yields. Although the reaction was supplemented after 17-24 hours with additional aliquot of *rST3Gal III* and CMP-NeuNAc, the yield did not increase. In all cases, unreacted starting materials could be recovered almost completely (*Table 4.3*). Trisaccharide **6** was not tolerated as substrate by the rat ST3Gal III, probably due to the bulky substituent in the 6-hydroxyl position of galactose as we reported [249,250].

Comparative NMR investigations (COSY, HSQC and TOCSY) of the starting sugars and the isolated products confirm the transfer of a sialic acid residue. Additional signals in the ^{13}C NMR spectra at approximately 100 ppm and 40 ppm are characteristic for the C-2 and

C-3 atoms of an α -linked sialic acid. Simultaneous down-field shifts (~ 4 ppm) of the galactose C-3 atom in the ^{13}C NMR spectra and about 0.6 ppm of the galactose H-3 in the ^1H NMR spectra confirm the introduction of sialic acid onto the 3-OH group of the galactose moiety [249,250].

Isolated yields, recovered starting material and kinetic data (V_{max} and K_{M}) are summarized in (Table 4.3).

Table 4.3 Isolated yields and kinetic data of the enzymatic sialidations.

| Entry | Acceptor | Product | Isolated | Recovered | V_{max} | K_{M} |
|-------|---|---|----------------|-----------------|---|-----------------|
| | | | Product [%] | Acceptor [%] | $\left[\frac{\text{nmol}}{\text{ml} \cdot \text{min}} \right]$ | $[\mu\text{M}]$ |
| 1 |  |  | 76 | - | 3.19 | 87.61 |
| 2 |  |  | 90 | - | 3.42 | 66.08 |
| 3 |  |  | 56 | 44 | 1.11 | 995.55 |
| 4 |  |  | 36 | 62 | 0.89 | 811.64 |
| 5 |  |  | 59 | 40 | 0.43 | 990.51 |
| 6 |  | no reaction (12) | - | 95 | - | - |

4.2 *h*ST6Gal I expression in BHK-21 cells, purification and characterization

4.2.1 BT-*h*ST6Gal I cloning and expression

In the present study, as it was described in the chapter 3.2.1, the BHK-21 cells producing β -trace protein (β -TP) were stably transfected with a vector encoding a recombinant soluble form of human ST6Gal I (BT-*h*ST6Gal I). The catalytic domain of ST6Gal I (543 amino acids) was fused to the C terminus of the full-length β -TP (168 amino acids). Moreover, a mammalian host cell line expressing β -TP and recombinant sialyltransferase was used for the *in vitro* ST6Gal I enzyme specificity. *Figure 4.8* shows the four day and one month old BHK-21 cells which stably express the human β -TP and BT-*h*ST6Gal I.

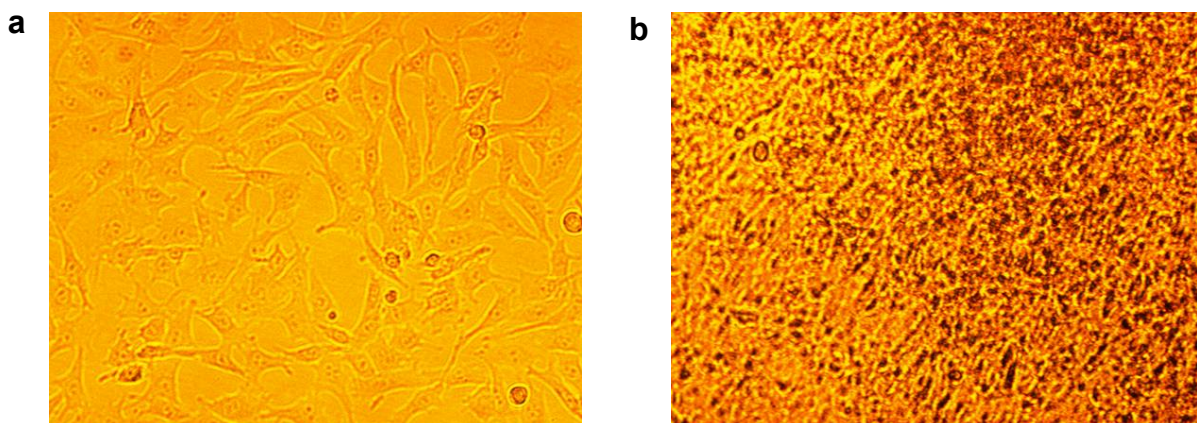


Figure 4.8 Production of BT-*h*ST6Gal I enzyme. BHK-21 cell clone 3 in the culture after (a) 4 days and (b) one month.

Many human *N*-glycosylated serum glycoproteins contain terminal NeuNAc with either α -2,6-linkage to Gal β (1,4)GlcNAc-R, or both an α -2,6- and α -2,3-linkage in different ratios, e.g. AT III, β -TP protein or transferrin. The most frequently used mammalian hosts for the production of recombinant human pharmaceutical glycoproteins are BHK-21 and CHO cells which do not express a Gal β (1,4)GlcNAc-R α -2,6 sialyltransferase [290,291]. Carbohydrate structural analysis of their *N*-linked glycans has revealed that NeuNAc is exclusively attached in α -2,3-linkage to Gal β (1,4)GlcNAc-R [290-293]. Specificity of the

sialyltransferase *in vivo* can only be achieved by structural analysis of the cellular product(s). Alternatively, an *in vitro* assay of sialyltransferases with small acceptor substrates may yield some preliminary information about acceptor substrates properties recognized by the enzyme.

The human Golgi apparatus Gal β (1,4)GlcNAc α -2,6 sialyltransferase (ST6Gal I; EC 2.4.99.1) was cloned in 1990 by Grundmann [90]. This enzyme is involved in the terminal sialylation of complex type asparagine-linked oligosaccharides of glycoproteins. The complete protein consists of 406 amino acids having a molecular weight of 46.6 kDa and two potential *N*-glycosylation sites. The enzyme itself exists in solution as a monomer. Enzymatic properties showed that the enzyme is active between pH 5 and pH 8 with an optimum of pH 6.5 to pH 7.0. No metal requirement has been reported, and the enzyme is equally active in the presence and absence of nonionic detergents (1% Triton X-100) and reducing agents (10 mM 2- β -mercaptoethanol) [16].

4.2.1.1 Overlay assay and Western blotting

With the Western blot based overlay assay it was possible to locate the recombinant cells expressing the BT-*h*ST6Gal I protein. The protein was transferred to the nitrocellulose membrane and immunodetected using rabbit anti-ST6Gal I purified serum as a primary antibody. The BHK-21 clones 1 and 2 were used as a negative control because of the very weak enzyme expression signal. The clones 3-12 were randomly chosen from the clone mixtures and considered as positive clones because of immunodetected BT-*h*ST6Gal I expression (*Figure 4.9*).

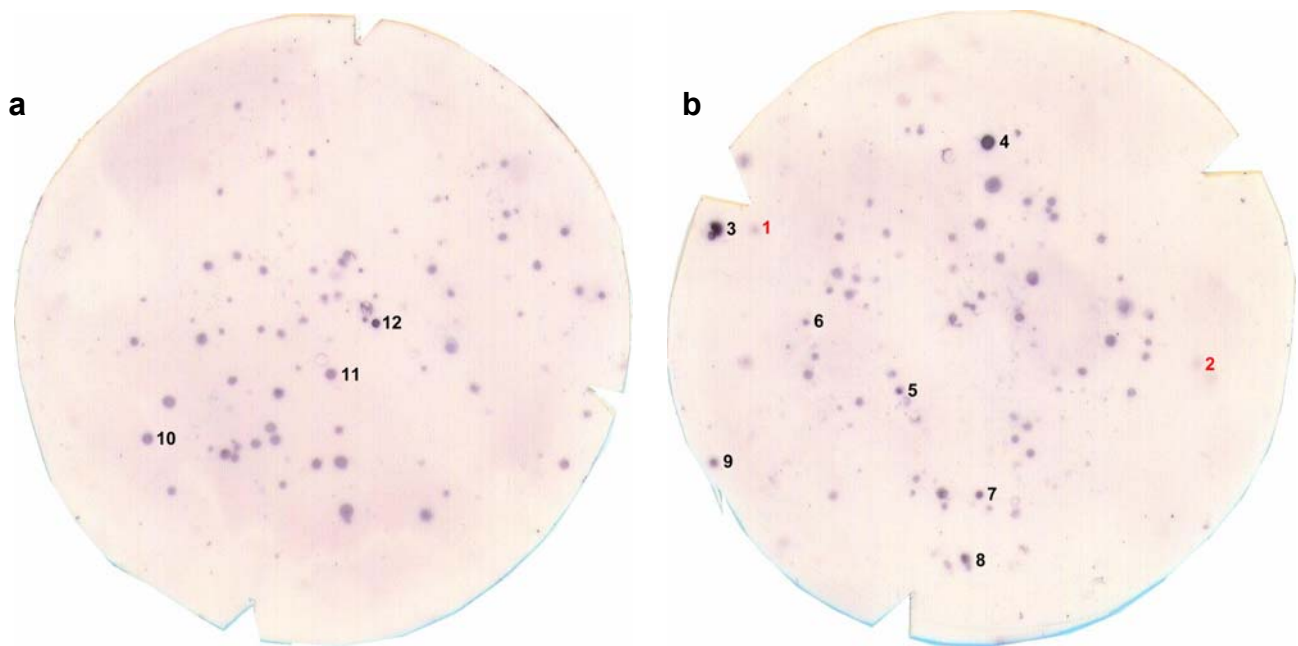


Figure 4.9 Overlay assay: Clones were immunodetected using rabbit anti-ST6Gal I purified serum (1:1000) as a primary antibody and goat anti-rabbit immunoglobulin coupled to alkaline phosphatase (1:500) as a secondary antibody. **(a)** 200 cells and **(b)** 400 cells seeded onto tissue culture dishes (red color refers to the clones considered as a negative-control).

In order to perform Western blot analysis and identify the clones, the supernatant medium of cultivated clones was collected and run on 12.5% SDS-PAGE. Transferred and immunodetected proteins revealed four different major bands (*Figure 4.10*) corresponding to a molecular weight of 43.7 kDa, 52.5 kDa, 66.2 kDa and 98 kDa. The 66.2 kDa polypeptide corresponded to partially glycosylated BT-*hST6Gal I*, which is in agreement with a theoretical molecular weight of 61.6 kDa for the deglycosylated protein as calculated by ExPASy protein engine tool. Because of the four potential *N*-glycosylation sites, the molecular weight of 98 kDa was expected to be a completely mature recombinant BT-*hST6Gal I*. This conclusion was confirmed with data obtained by enzyme purification (see chapter 4.2.2). Two other signals, 43.7 kDa and 52.5 kDa could represent partially degraded BT-*hST6Gal I*, which still maintained potential epitopes for polyclonal antibody recognition. Clone mixtures of transfected BHK-21, grown for 3 and 5 days in culture, showed very weak immunodetection signals (*Figure 4.10*; lane 2 and 3) which corresponded to the extremely low BT-*hST6Gal I* expression. All isolated positive BHK-21 clones (*Figure 4.9*) showed the same expression pattern detected by Western blot and almost the same concentration of the enzyme expression estimated at 0.5 mg/l.

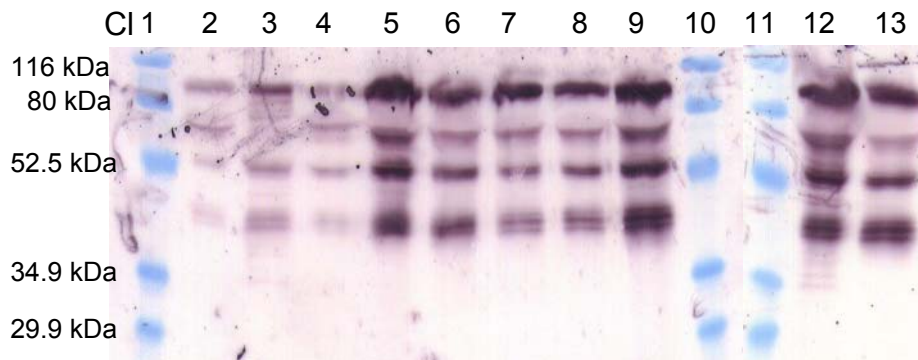


Figure 4.10 Western blot analysis of BT-*hST6Gal I*. Protein was blotted using rabbit anti-ST6Gal I purified serum (1:1000) as a primary antibody and goat anti-rabbit immunoglobulin coupled to alkaline phosphatase (1:500) as a secondary antibody in the reaction (M: low molecular weight marker; d: day; n.c.: negative control). Lane 1: LMW; Lane 2 and 3: clone mix after 3 and 5 d; Lane 4: clone 2 (n.c.); Lane 5-7: Clone 3 batch 1-3; Lane 8 and 9: Clone 4 batch 1 and 2; Lane 10 and 11: LMW; Lane 12 and 13: Clone 12 batch 1 and 2.

4.2.1.2 Enzyme activity of BT-*hST6Gal I* expressed by BHK-21 isolated clones

Although, all positive clones detected by Western blot showed similar expression of BT-*hST6Gal I*, only a cell supernatant of clone 3, 4 and 12 exhibited high and almost identical enzyme activity (*Figure 4.11*). The catalytic activity of the enzyme expressed by those three clones correlated with the incubation time. The negative control, particularly for clone 2, exhibited low enzyme activity. This finding was not surprising since we could confirm by Western blot analysis very low BT-*hST6Gal I* expression of clone 2 (*Figure 4.10*; lane 4).

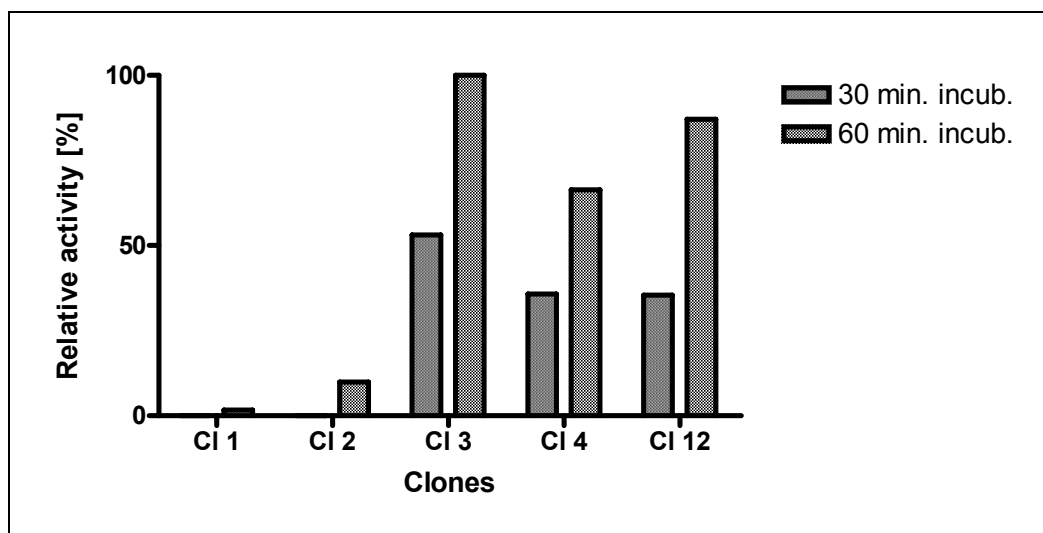


Figure 4.11 The activity measurement of the BT-*hST6Gal I* expressed by different BHK-21 clones. The BT-*hST6Gal I* produced by different BHK-21 clones (72 h) was checked with asialofetuin protein (20 $\mu\text{g}/\mu\text{l}$) used as an acceptor substrate. Enzyme activity was performed under standard conditions (37°C, for 30 and 60 minutes, pH 6.5). CI designates the cell clone.

4.2.2 Purification of recombinant BT-*hST6Gal I* enzyme

The produced BT-*hST6Gal I* was purified by performing CDP-hexanolamine-agarose affinity chromatography [16]. BT-*hST6Gal I* was eluted from the column with elution buffer containing 5 mM and 20 mM CDP. The final purification step, performed with 1 M of NaCl, washed out some additional proteins (*Figure 4.12 a*), which were unspecifically bound to the column. Coomassie stained SDS-PAGE as well as Western blot analysis revealed one major band with a molecular weight of 98 kDa. This signal corresponded to the fully glycosylated BT-*hST6Gal I* (*Figure 4.12 a*). The remaining BT-*hST6Gal I*, as well as one additional, very weak band was detected by Western blot in the fraction eluted with 1 M NaCl (*Figure 4.12 b*). The additional signal corresponded to a molecular weight of approximately 52.5 kDa. The same signal was observed when the supernatant of different clones was analyzed by Western blot (*Figure 4.10*). Since this short protein was not eluted with the more specific-CDP containing buffer, but instead together with other unspecifically bounded proteins, we concluded that this could be the result of partial BT-*hST6Gal I* degradation. Probably, the antibody recognition epitopes of the truncated protein were not affected.

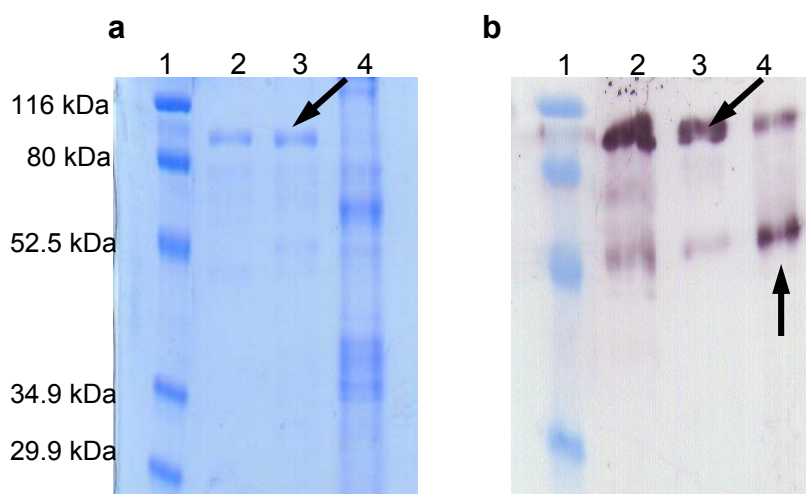


Figure 4.12 SDS-PAGE (12.5%) analysis (Coomassie staining) of the BT-*h*ST6Gal I purified by (a) CDP-hexanolamine-agarose affinity chromatography and (b) Western blotting which was performed using rabbit anti-ST6Gal I purified serum (1:500) as a primary antibody, and goat anti-rabbit immunoglobulin alkaline phosphatase conjugated (1:10 000) as a secondary antibody. Lane 1: LMW marker; Lane 2: 5 mM CDP dialyzed eluate; Lane 3: 10 mM CDP dialyzed eluate; Lane 4: 1 M NaCl dialyzed eluate. Arrows point at proteins at approximately 98 kDa and 52.5 kDa.

Immediately after the purification, measurement of enzyme activity in the CDP and NaCl eluted fractions showed impairment of enzyme activity towards asialofetuin, as measured in U/I. The enzyme fraction eluted with 5 mM CDP revealed 0.6 U/I whereas the elution with 20 mM CDP showed more than 6-fold less active enzyme (0.09 U/I). Specifically, activity of enzyme eluted with 1 M NaCl exhibited 0.19 U/I, which was twice more than the enzyme activity measured with the 20 mM CDP eluate. The same fractions dialyzed against 25 mM MES reaction buffer (pH 6.5) recovered the enzyme activity 3-fold (elution with 5 mM CDP and 1 M NaCl) and 11-fold (elution with 20 mM CDP), and enable the BT-*h*ST6Gal I to produce radioactive-labeled fetuin product (Table 4.4). The inhibition of enzyme activity with CDP and high molarities of salt was not surprising because it was consistent with previously observed and published data [16,294,295]. Furthermore, as early as 1979 Rearick *et al.* [296] reported that the CTP and acceptor, observed by noncompetitive patterns, can bind either to free enzyme, or to enzyme in complex with the first substrate. It was confirmed that CMP, as a side product of the sialyltransferase reaction, inhibits the forward sialyltransferase reaction with a K_i of approximately 50 μ M. CDP was about 10-fold a more potent inhibitor than is CMP. The sialyltransferase is

reversibly inhibited by increasing ionic strength, *i.e.* sialyltransferase was inhibited roughly 50% by 40 mM NaCl, and 80% by 0.2 M NaCl [16].

The purified enzyme exhibits a high degree of specificity for acceptor substrates that contain the terminal disaccharide sequence Gal β (1,4)GlcNAc (*N*-acetylglucosamine), which is commonly found in glycoproteins. Asialoglycoproteins, such as asialofetuin, containing *N*-acetylglucosaminyl linkage at the nonreducing ends of the oligosaccharides prosthetic groups are the best acceptor substrates [297,298]. Thus, one can presume that the *in vivo* role of the ST6Gal I is to form the sequence NeuNAc α (2,6)Gal β (1,4)GlcNAc, which commonly terminates the complex type asparagine-linked oligosaccharides of glycoproteins.

Table 4.4 The BT-*h*ST6Gal I inhibition in CDP and high salt eluted fractions and its recovered activity in MES buffer dialyzed fractions. Enzyme activity was measured with asialofetuin used as an acceptor substrate in the ST activity assay.

| Fractions | Asialofetuin acceptor | 5 mM CDP | 20 mM CDP | 1 M NaCl |
|--------------|---------------------------|----------|-----------|----------|
| Non-dialyzed | U/l | 0.60 | 0.09 | 0.19 |
| | Total mU | 16.82 | 2.54 | 7.22 |
| Dialyzed | Volumen [ml] | 28 | 27 | 37.5 |
| | U/l | 2.25 | 1.07 | 0.63 |
| | Total protein amount [mg] | 0.28 | 0.216 | 0.075 |
| | mg/l | 10 | 8 | 2 |
| | U/mg | 0.225 | 0.133 | 0.315 |
| | Total mU | 62.98 | 28.80 | 23.65 |

The BT-*h*ST6Gal I was checked for the activity using the Type II acceptor substrate. Substrate affinity of BT-*h*ST6Gal I for Type II in different dialyzed fractions was decreased for almost 20-fold (*Table 4.5*) when compared with the activity measured with asialofetuin acceptor substrate (*Table 4.4*). This was not surprising, since it is known that less effective acceptor substrates include lactose (Gal β (1,4)Glc) and other disaccharides with galactose β -linked to the penultimate sugar [298]. The specificity of the ST6Gal I for the Type II

structure was explained by the requirement of a specific substrate rearrangement which involves polar groups on both the β Gal and the GlcNAc residues [283]. However, glycosyltransferases may recognize more extended portions of the natural acceptor, which can explain the higher affinity of the recombinant BT-*h*ST6Gal I for the asialofetuin protein compared to Type II substrate acceptor.

Table 4.5 The enzyme activity with Type II acceptor substrate.

| Type II acceptor | Dialyzed fractions | | |
|------------------|--------------------|-----------|----------|
| | 5 mM CDP | 20 mM CDP | 1 M NaCl |
| U/l | 0.13 | 0.053 | 0.032 |
| Total mU | 3.9 | 1.43 | 1.2 |

In order to increase the enzyme concentration essential for the preparative *in vitro* glycosylation approach, the BT-*h*ST6Gal I expressed and secreted in the BHK-21 cell-medium was 20-fold concentrated, maintaining an extremely high degree of enzyme activity (35.47 U/l).

Table 4.6 Cell-culture medium concentration increases enzyme.

| Asialofetuin acceptor | Culture medium (20 x conc.) | |
|-----------------------|-----------------------------|----------|
| | Non-dialyzed | Dialyzed |
| U/l | 35.47 | 19.27 |
| Total mU | 709.4 | 385 |

4.2.3 Characterization of the BT-*h*ST6Gal I enzyme

4.2.3.1 BT-*h*ST6Gal I catalytic activity

The dialyzed fraction containing enzyme, which was eluted with the 5 mM CDP buffer, was incubated with 20 nmol of diantennary *N*-acetylglucosamine type acceptor substrate over a period of 12 hours (*Figure 4.14*). As expected, the results obtained by HPAEC-PAD analysis demonstrated slow but very clear appearance of one monosialylated peak which was proportional to the incubation time of the enzyme (*Figure 4.14*; filled arrow). Conversely, the peak corresponding to the diantennary *N*-acetylglucosamine acceptor substrate (*Figure 4.13*) proportionally disappeared during the incubation time (*Figure 4.14*;

Mild hydrolysis of NeuNAc was another line of evidence which confirmed the previously mentioned time-dependent peak appearance associated with the formation of the monosialylated glycosidic bond (Figure 4.14). Mild hydrolysis of the monosialylated product formed after 12 h of incubation with BT-*hST6Gal I* (Figure 4.15; black arrow), was correlated with complete loss of the same peak (Figure 4.15; red arrow). As expected, under acetic conditions and temperature of 80°C, the previously formed monosialylated diantennary product (Figure 4.14) was hydrolyzed. Consequently, the peak which corresponds to diantennary *N*-acetylglucosamine type acceptor substrate was recovered (Figure 4.15; dotted arrow). Using HPAEC-PAD and MALDI/TOF-MS analysis, the detected peak was attributed to the formation of the α -2,6-monosialylated glycosidic bond.

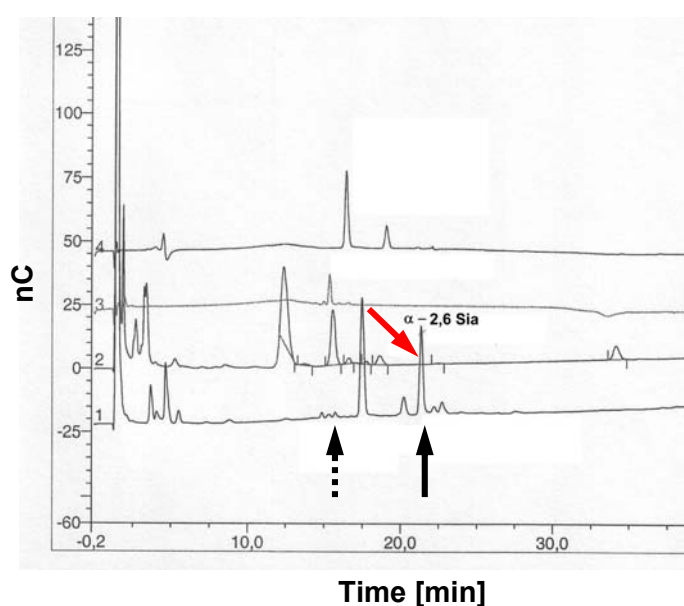


Figure 4.15 Comparison of the sialylated product with its hydrolyzed form. The results were obtained by HPAEC-PAD analysis. 1: monosialylated product obtained after 12 h of incubation with BT-*hST6Gal I*; 2: hydrolyzed BT-*hST6Gal I* monosialylated product; 3: diantennary *N*-acetylglucosamine; 4: CMP-NeuNAc. The black arrow designates the monosialylated product, the red arrow points to the hydrolyzed product (peak disappearance) and the dotted arrow shows peak corresponding to the diantennary *N*-acetylglucosamine acceptor substrate. nC designates nanocoulombs.

4.2.3.2 Neuraminidase specific cleavage

In order to confirm the formation of α -2,6-monosialylated glycoside, the enzymatically synthesized monosialylated diantennary product (Figure 4.14) was incubated with a

Newcastle disease virus (NDV) neuraminidase enzyme. This enzyme specifically cleaves the terminal NeuNAc linked only α -2,3 to *N*- or *O*- glycosidically bound oligosaccharide chains of glycoproteins and glycolipids. It also cleaves NeuNAc that is bound in the α -2,8 position to neuraminic acids. It is able to cleave *N*-glycolyl, 4-*O* acetyl and 9-*O* acetylsialic acids, however with a low turnover rate.

Upon analyzing the HPAEC-PAD chromatogram profile, it can be seen that the NDV neuraminidase remained inactive during the incubation with the monosialylated diantennary *N*-acetyllactosamine type acceptor substrate (*Figure 4.16*; red arrow). This observation suggested the formation of a α -2,6-monosialylated glycosidic bond, which was not, as was predicted, a cleavage sequence and therefore substrate acceptor for the NDV neuraminidase. Thus, the peak-profiles obtained by HPAEC-PAD analysis maintained the original shape before (*Figure 4.16*; black arrow) and after (*Figure 4.16*; red arrow) the incubation of specific NDV neuraminidase with monosialylated diantennary acceptor substrate. In addition, the NDV neuraminidase incubation was performed with only 50% of starting material, therefore the detected peak had half the size as the peak of starting material.

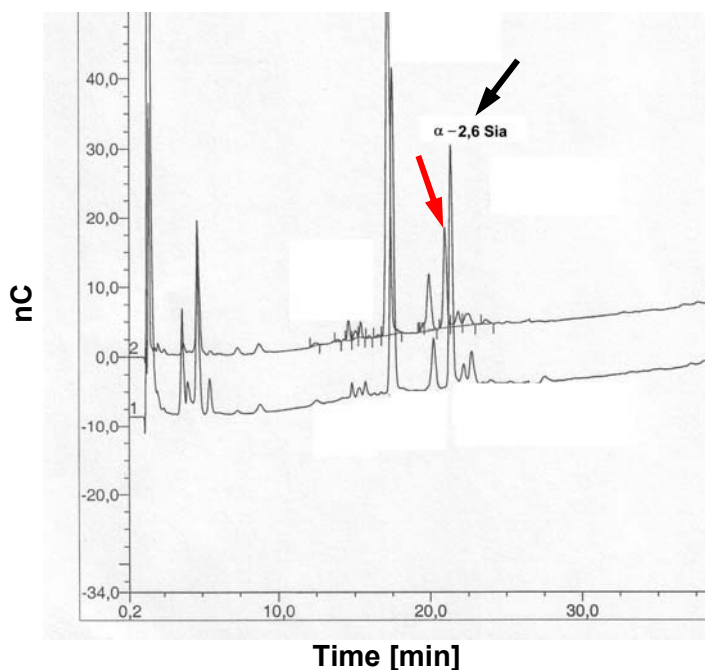


Figure 4.16 The chromatogram of Newcastle disease virus (NDV) neuraminidase activity with α -2,6 sialylated *N*-acetyllactosamine acceptor obtained by HPAEC-PAD analysis. 1: monosialylated product obtained after 12 h of incubation with BT-*h*ST6Gal I; 2: product obtained with NDV neuraminidase incubation. nC designates nanocoulombs.

A control reaction showing NDV neuraminidase activity and specificity was performed using α -2,3 sialylated *N*-acetylglucosamine of *O*-glycosylated acceptor substrate. Initially, the *O*-glycosylation specific α -2,3 ST enzyme was used for the production of α -2,3 sialylated product, which served as a acceptor substrate in the control reaction. The control reaction verified the NDV neuraminidase specific activity with the α -2,3 sialylated acceptor substrate. Monitoring by HPAEC-PAD analysis revealed almost complete loss of the α -2,3 sialylated peak (*Figure 4.17*; red arrow) when compared to the original untreated sample (*Figure 4.17*; black arrow). Since the NDV neuraminidase did not complete the reaction, it was still possible to detect a small signal corresponding to the α -2,3 sialylated substrate (*Figure 4.17*; red arrow). Hence, an efficient NDV neuraminidase activity towards α -2,3 sialylated substrate was confirmed (*Figure 4.17*).

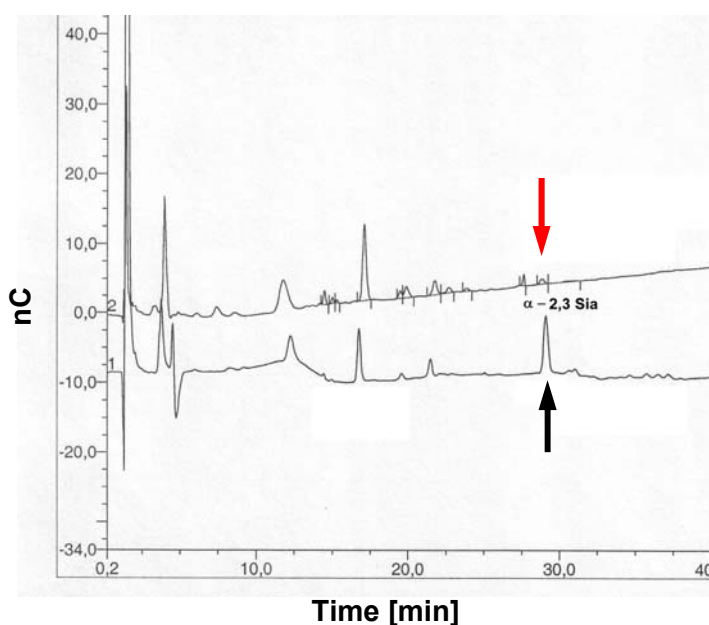


Figure 4.17 The chromatogram of Newcastle disease virus (NDV) neuraminidase activity with α -2,3 sialylated *N*-acetylglucosamine unit of *O*-linked oligosaccharide acceptor. 1: α -2,3 sialylated *N*-acetylglucosamine unit of *O*-linked oligosaccharide acceptor; 2: product obtained with NDV neuraminidase incubation. nC designates nanocoulombs.

4.2.3.3 Preparative *in vitro* sialylation of glycoconjugates

In order to characterize the affinity of the purified soluble BT-*h*ST6Gal I for different branches of a diantennary substrate acceptor, the enzyme was applied for the preparative *in vitro* sialylation of glycoconjugates. The diantennary *N*-acetylglucosamine type acceptor

substrate was sialylated and initially analyzed with HPAEC-PAD to obtain preliminary assignment by comparison of their elution times to those of *N*-glycan standards. Different fractions (17-19) of one peak containing monosialylated diantennary *N*-acetylglucosamine type acceptor substrate (3.7 nmol) were obtained after incubation with purified enzyme (Figure 4.18). Samples were collected and sent for negative ion MALDI/TOF-MS and methylation analysis. Based on the MALDI/TOF-MS signals and methylation analysis one peak, obtained after incubation with purified BT-*h*ST6Gal I, corresponded to the monosialylated derivative of the diantennary *N*-acetylglucosamine type product (Figure 4.18; arrow). The monosialylated product analyzed by MALDI/TOF-MS and methylation showed specific α -2,6-monosialic acid-linkage created with the terminal galactose residue of only one branch.

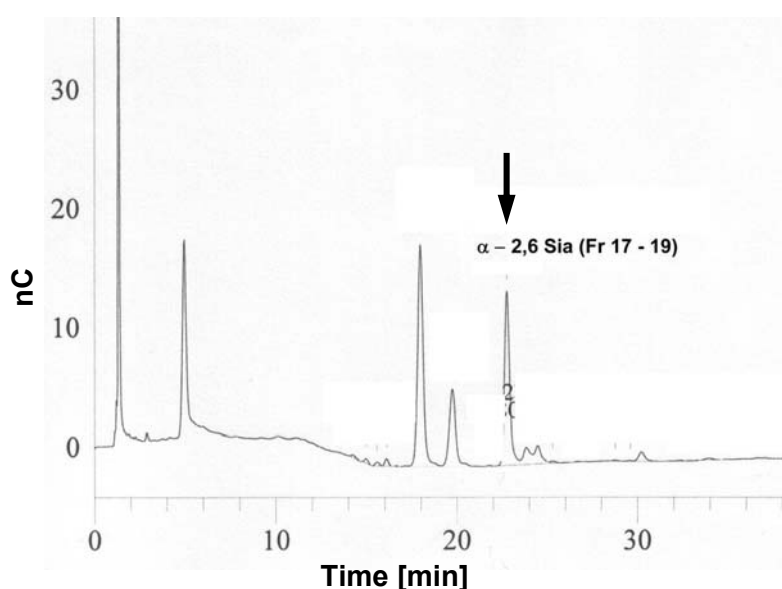


Figure 4.18 The HPAEC-PAD chromatogram of preparative *in vitro* sialylation of diantennary *N*-acetylglucosamine obtained with purified BT-*h*ST6Gal I enzyme. nC designates nanocoulombs.

In addition, the diantennary *N*-acetylglucosamine type acceptor substrate (12 nmol) was incubated with 20-fold concentrated and dialyzed culture medium. The culture medium, used for the preparative sialylation, contained BT-*h*ST6Gal I. Two different peaks (Figure 4.19; black and red arrow) corresponding to mono- and disialylated diantennary *N*-acetylglucosamine type acceptor substrate, were collected in different fractions.

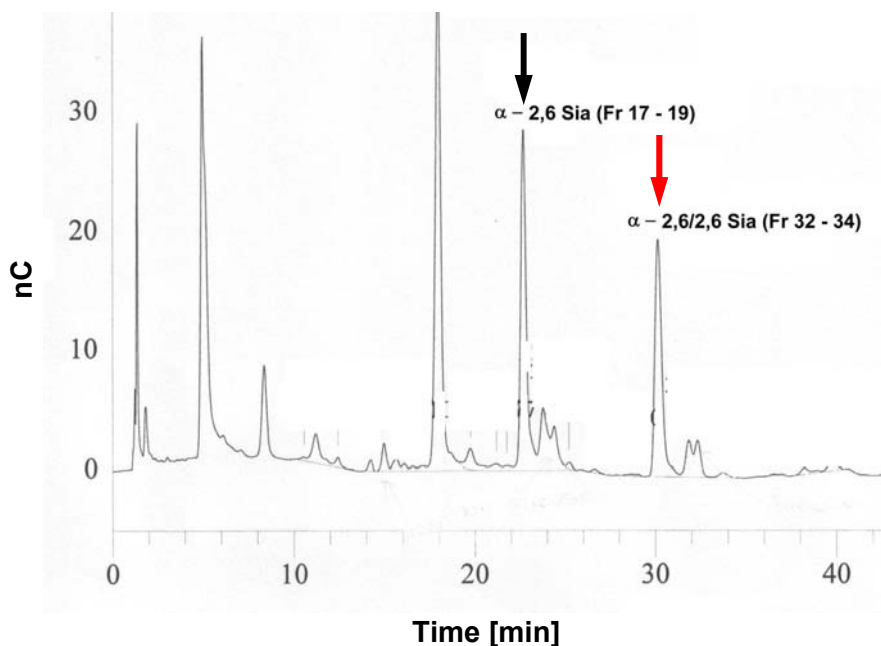


Figure 4.19 The HPAEC-PAD chromatogram of preparative *in vitro* sialylation of diantennary *N*-acetylglucosamine obtained with concentrated and dialyzed culture medium (20 x) containing BT-*h*ST6Gal I enzyme. nC designates nanocoulombs.

Collected fractions containing the same peak were pooled (*Figure 4.20*; black and red arrow) and analyzed further by MALDI/TOF-MS and methylation. Signals based on MALDI/TOF-MS obtained from the reduced and permethylated native diantennary glycan, and methylation data revealed specific α -2,6-mono (*Figure 4.19*; black arrow) and α -2,6-disialylated (*Figure 4.19*; red arrow) derivatives of the diantennary oligosaccharides. The obtained product contained a mono- and disialic acid α -2,6 glycosidically linked to the terminal galactose residue in both Man-3 and Man-6 antennae. *In vivo* investigations of ST6Gal I activity showed the specific enzyme activity with diantennary acceptors, creating asialo, α -2,6-mono and α -2,6 disialylated derivatives of the diantennary oligosaccharides. Taking advantage of BHK-21A cells, which were producing GalNAc β (1,4)GlcNAc-R branches, its efficient recognition as a substrate for the ST6Gal I was confirmed *in vivo* [254].

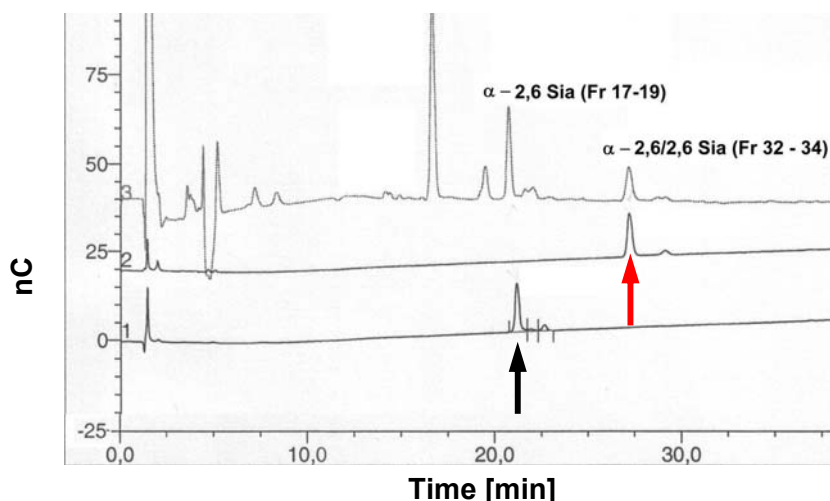


Figure 4.20 The HPAEC-PAD chromatogram presenting isolated fractions of mono- and disialylated diantennary *N*-acetylglucosamine acceptor obtained using concentrated and dialyzed culture medium (20 x) containing BT-*h*ST6Gal I enzyme. 1: fractions 17-19 containing monosialylated diantennary *N*-acetylglucosamine (black arrow); 2: fractions 32-34 containing disialylated diantennary *N*-acetylglucosamine (red arrow); 3: mono- and disialylated diantennary *N*-acetylglucosamine. nC designates nanocoulombs.

The purified enzyme and enzyme concentrated from the supernatant exhibited different affinities towards the same diantennary type acceptor substrate. Although it is well known that a higher degree of branching of the acceptors leads to a decrease in the rate of sialylation, and that the presence of a Man-6 branch strongly inhibits the rate of transfer of both sialic acids [300], the enzyme in the supernatant expressed affinity for the sialylation of both antennae in the α -2,6 sialic acid manner. In contrast, the purified enzyme showed exclusive preference for the α -2,6 NeuNAc attachment to the Man-3 branch *in vitro*. Our finding was in agreement with *in vitro* results reported by Joziassse *et al.* [300] on the branch specificity of the bovine colostrum ST6Gal I, which were obtained with glycopeptides and oligosaccharides as substrates. The same finding was already observed before in *in vivo* experiments, in which the human ST6Gal I had a high preference for the Man-3 branch of oligosaccharides [254]. Due to the competition with endogenous α -2,3 sialyltransferases *in vivo*, the final products contained mixtures of α -2,3/2,6-sialylated oligosaccharides. Almost 60% of the diantennary oligosaccharides *in vivo* were disialylated derivatives, composed of a mixture of α -2,3 and α -2,6 sialic acids in which the α -2,6 was glycosidically linked to the Man-3 branch. In the present work, it was

not clear why the same enzyme behaved differently in preparative *in vitro* sialylation of the *N*-glycoconjugate. One proposed reason could be the original environment, *i.e.* the concentrated supernatant, which can provide some essential factors important for the enzyme specificity.

4.3 α -2,3/2,8 bifunctional *Campylobacter jejuni* sialyltransferase (α -2,3/2,8 ST) expression in *E. coli* cells

This particular project involved the cloning of the *C. jejuni* *cst-II* gene which encodes the Cst-II enzyme responsible for transfer of a sialic acid to the O-3 of galactose and to the O-8 of a sialic acid α -2,3-linked to the galactose residue. The aim of the present work was the isolation of the *cst-II* gene, its functional expression, and final sialyltransferase characterization relative to various factors important for its optimal activity.

The *cst-II* gene encoding the α -2,3/2,8 bifunctional sialyltransferase (Cst-II; α -2,3/2,8-ST) was isolated from genomic DNA of the ATCC43438 strain of *Campylobacter jejuni*. The *C. jejuni* has a circular chromosome of 1 641 481 base pairs (30.6% G-C) which is predicted to encode 1 654 proteins and 54 stable RNA species. The average gene length is 948 bp, and 94.3% of the genome codes for proteins, making it the densest bacterial genome sequenced to date. There are two large regions of lower G-C content that correspond to genes within the LOS and extracellular polysaccharide (EP) biosynthesis clusters, respectively. The genome is unusual in that it contains very few repeated sequences, and no insertion sequences or phage-associated sequences [163].

4.3.1 α -2,3/2,8 ST cloning in pEZZ18 vector and its expression in *E. coli*

4.3.1.1 PCR *cst-II* gene amplification

In order to isolate genomic DNA, the ATCC43438 strain of *C. jejuni* was initially grown under microaerophilic conditions (7% CO₂) at 37°C. Primers for the *cst-II* gene amplification were designed based on the published DNA and protein sequence [151,264], and used in the PCR reaction. Due to the low G-C content of genes within the LOS region [163], the primers had a very high content of A-T nucleotides (~80%). Therefore, the PCR reaction was performed at a very low (52°C) optimal annealing temperature, using 7 ng of genomic DNA as a template (see chapter 3.3.5). The PCR reaction was specific and 1% of the agarose gel analysis revealed a DNA fragment of approximately 900 bp ascertained by comparing to the DNA marker. Based on the construct which included the *cst-II* gene sequence and nucleotides for additional restriction sites, the predicted DNA band size was 895 bp (*Figure 4.21*). DNA sequence was additionally confirmed by Microsynth DNA analysis.

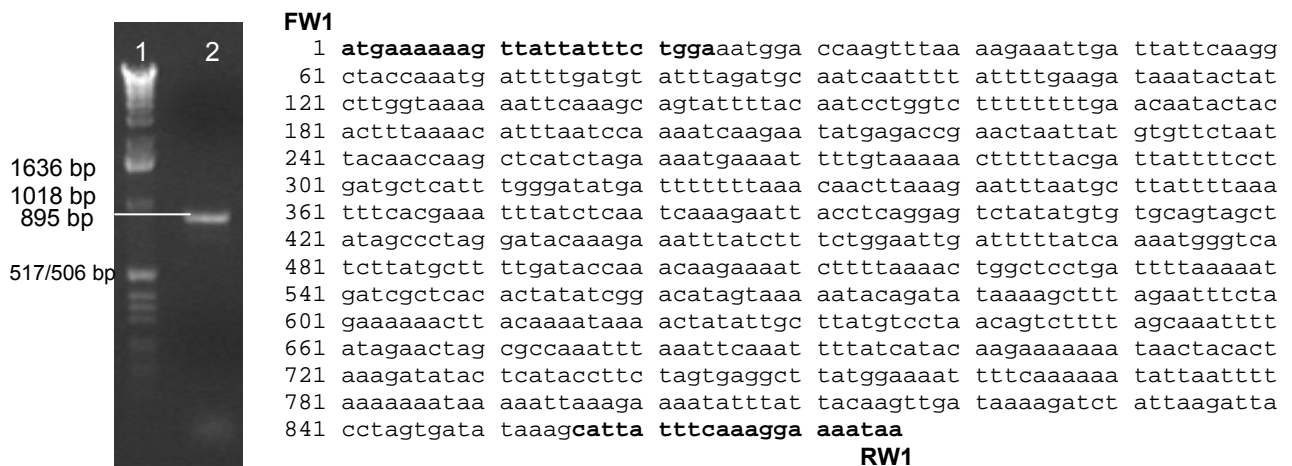


Figure 4.21 Agarose gel analysis (1%) of PCR product of the *cst-II* gene. PCR was performed using FW1 and RW1 primers (see chapter 3.3.5) which are in the sequence presented in bold. Lane 1: DNA molecular weight marker X; Lane 2: PCR product of the *cst-II* gene.

The pEZZ18 vector was used for the expression of the soluble recombinant protein. This vector is based on Protein A signal sequence and two synthetic IgG-binding domains (ZZ) of *Staphylococcus aureus* Protein A [301]. The soluble gene fusion product thus obtained, could be theoretically collected from the culture medium of *Escherichia coli* and rapidly recovered in a one-step procedure by IgG affinity chromatography [266]. Hence, this system was used to express a fusion protein consisting of two Z fragments, *i.e.* IgG binding domains, and the full-length α -2,3/2,8 bifunctional sialyltransferase.

In order to obtain a good insert/vector ratio for subsequent steps in recombinant DNA technology, both the gene of interest and the pEZZ18 vector were digested by *EcoR* I/*Bam*H I. Additionally, the vector was dephosphorylated and finally analyzed on an agarose gel (*Figure 4.22*). The DNA concentration for the *cst-II* gene and the pEZZ18 vector was estimated by agarose gel analysis to be 5 ng/ μ l and 20 ng/ μ l, respectively. The insert/vector DNA ratio was taken into account for the ligation, an essential step in the construction of the recombinant DNA (*Table 4.7*).

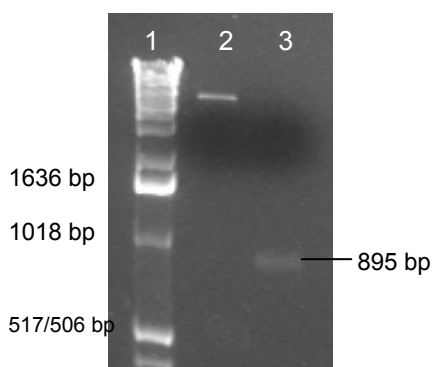


Table 4.7 Estimated DNA concentrations.

| | Concentration |
|------------------------------|----------------|
| <i>C. jejuni</i> genomic DNA | 15 ng/ μ l |
| Insert (895 bp) | 5 ng/ μ l |
| pEZZ18 vector | 20 ng/ μ l |

Figure 4.22 Ratio between vector (pEZZ18) and insert gene using agarose gel analysis (1%). Lane 1: DNA molecular weight marker X; 2: *EcoR* I / *Bam*H I digested and dephosphorylated pEZZ18 vector; Lane 3: *EcoR* I / *Bam*H I digested *cst-II* insert.

4.3.1.2 Analysis of pEZZ18 recombinants

The achieved ligation of pEZZ18 vector with the gene of interest led to the successful heat-shock transformation (see chapter 3.3.3) of the host suitable for cloning, namely the *E. coli* DH5 α strain. After plasmid isolation and restriction digestion, analysis of the six ampicillin resistant DH5 α *E. coli* transformants revealed the incorporation of a recombinant pEZZ18 vector containing the *cst-II* gene. The 1% agarose gel analysis revealed a DNA fragment of approximately ~900 bp (Figure 4.23). This DNA fragment corresponded to the original gene of interest, *i.e.* the *cst-II* gene with a DNA size of 895 bp. In addition, agarose gele analysis of all samples revealed one weak DNA signal with very high molecular size (~5500 bp), which corresponded to the incompletely digested recombinant vector (5486 bp).

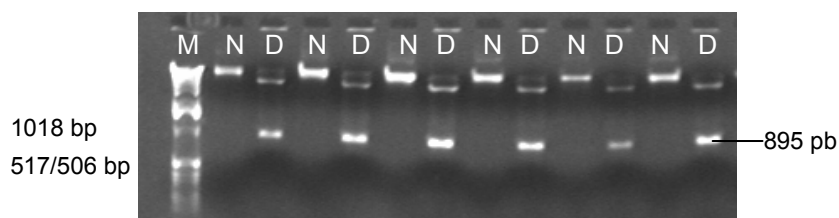


Figure 4.23 Agarose gel analysis (1%) of 6 recombinant DH5 α *E. coli* clones. Lane 1: DNA molecular weight marker X (M); Lane 2 and 3: Non-digested (N) recombinant vector and *EcoR* I / *Bam*H I digested recombinant vector (D) of clone 1; Lane 4 and 5: N and D of clone 2; Lane 6 and 7: N and D of clone 3; Lane 8 and 9: N and D of clone 4; Lane 10 and 11: N and D of clone 5; Lane 12 and 13: N and D of clone 6.

Six clones examined by restriction digestion were further verified by PCR. The amplification of the *cst-II* gene with a forward, internal and reverse primer was the second confirmation of the presence of pEZZ18 containing recombinant *cst-II*. Consequently, the fragments of amplified recombinant DNA containing the *cst-II* gene were approximately 900 bp and 500 bp (Figure 4.24). This result perfectly matches the expected fragment of 895 bp for the forward/reverse and 498 bp DNA fragment for internal/reverse amplification. Finally, the confirmed recombinant DNA was sequenced by Microsynth and, thus, verified on the DNA level. All sequenced positive clones were free of any mutation and contained the original *cst-II* gene amplified initially from the *C. jejuni* bacteria.

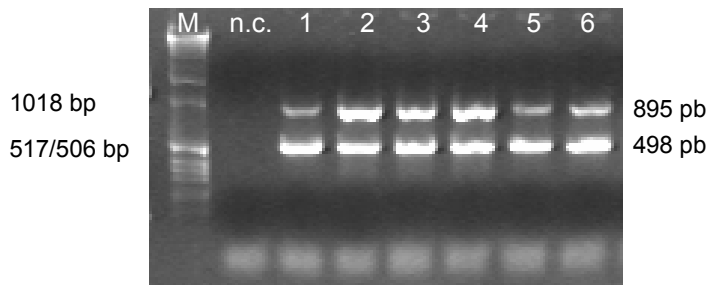


Figure 4.24 Agarose gel analysis (1%) of PCR control. Recombinant vector of 6 positive DH5 α *E. coli* clones. Lane 1: DNA molecular weight marker X (M); Lane 2: negative control (n.c.); Lane 1-6: clone 1-6 coamplified with FW1/RW1 primers (895 bp) and FW1/intern primers (498 bp).

4.3.1.3 α -2,3/2,8 ST enzyme expression

The recombinant pEZZ18 vector containing the *cst-II* gene isolated from DH5 α *E. coli* clone 2 was further used for α -2,3/2,8 bifunctional sialyltransferase expression. In contrast to the expression host strain, DH5 α *E. coli* cloning host strains has an extremely low transcriptional activity of T7 RNA polymerase. The recombinant plasmid was successfully transformed into the HB101 *E. coli* expression strain, and grown in trypton enriched TYE medium. As mentioned before, the selected pEZZ18 vector was suitable for the expression of soluble recombinant proteins [266]. Proteins were expressed as fusions with the ZZ peptide and secreted into the aqueous culture medium under the direction of the Protein A signal sequence [266,302]. Expression of the pEZZ18 vector was controlled by the *lacUV5* (P_{lac}) and protein A promoters (P_{spa}). The fusion proteins, theoretically, should be easily purified using IgG Sepharose 6 Fast Flow to which the ZZ domain can bind tightly [266].

The manufacturer states that due to its unique folding properties, the 14 kDa ZZ peptide has little or no effect on the fusion partners folding into native conformation [301].

Keeping in mind all the characteristics of the chosen vector, it was expected that the recombinant enzyme will be easily obtained using the optimized protocol for pEZZ18 protein expression and purification. The recombinant enzyme expressed in the HB101 *E. coli* production strain was analyzed by silver stained SDS-PAGE. The result showed a very low expression level. None of the cell's fractions revealed the presence of the recombinant protein. Since the enzyme was considered to be soluble, these findings were surprising especially for the samples of culture medium where its overexpression was expected. The overexpressed recombinant enzyme, the molecular weight of which was predicted to lie around 48 kDa, was not detected in the supernatant. The results obtained by silver stained SDS-PAGE analysis revealed overexpression of only one protein in the cell pellet fraction. The signal with a molecular weight of 14 kDa corresponds to the expression of the two synthetic IgG-binding domains (ZZ) (Figure 4.25).

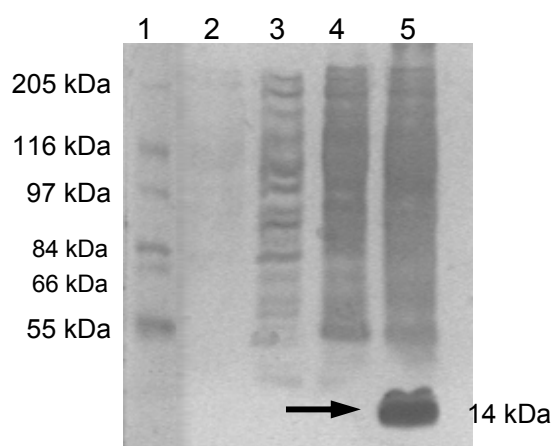


Figure 4.25 SDS-PAGE analysis (12.5%; silver staining) of α -2,3/2,8 ST enzyme expression in recombinant HB101 *E. coli* strain. Lane 1: High molecular weight marker (HMW); Lane 2: supernatant of clone two; Lane 3: 20 x concentrated supernatant of clone two; Lane 4: cell cytoplasm of clone two; Lane 5: cell pellet of clone two.

4.3.1.4 α -2,3/2,8 ST enzyme activity with non-sialylated acceptors

The supernatant and the cell cytoplasm were checked for α -2,3/2,8 sialyltransferase activity. Fractions were incubated with non-sialylated acceptor substrates, 600 μ M Type II (1) and acceptor 3 (Figure 4.26). The results obtained by this enzyme activity assay only

confirmed the data previously obtained by SDS-PAGE. The soluble enzyme expression was missing in the even 20-fold concentrated supernatant fraction, and therefore no detectable enzyme activity was observed. Finally, the enzyme activity was observed only in the cytoplasmic fraction during the incubation with Type II acceptor substrate. Although, the enzyme exhibited some activity when compared to the negative control, this activity was still very low. Our findings revealed that the recombinant enzyme, although expressed as a fusion protein containing the Protein A signal sequence, was captured in the cytoplasmic membrane and therefore not able to leave the cell and enter the culture medium. It could be speculated that the soluble and catalytically active form of the sialyltransferase can be generated by proteolytic cleavage in the membrane binding domain of the enzyme, which is not required for the enzyme activity. This could lead to the formation of a catalytically active α -2,3/2,8 sialyltransferase missing two synthetic IgG-binding domains (ZZ) and the membrane binding domain. SDS-PAGE analysis revealed that those domains were part of the cell pellet fraction. This type of proteolytic cleavage is well known and a common event frequently observed for many different eukaryotic sialyltransferases [32,47].

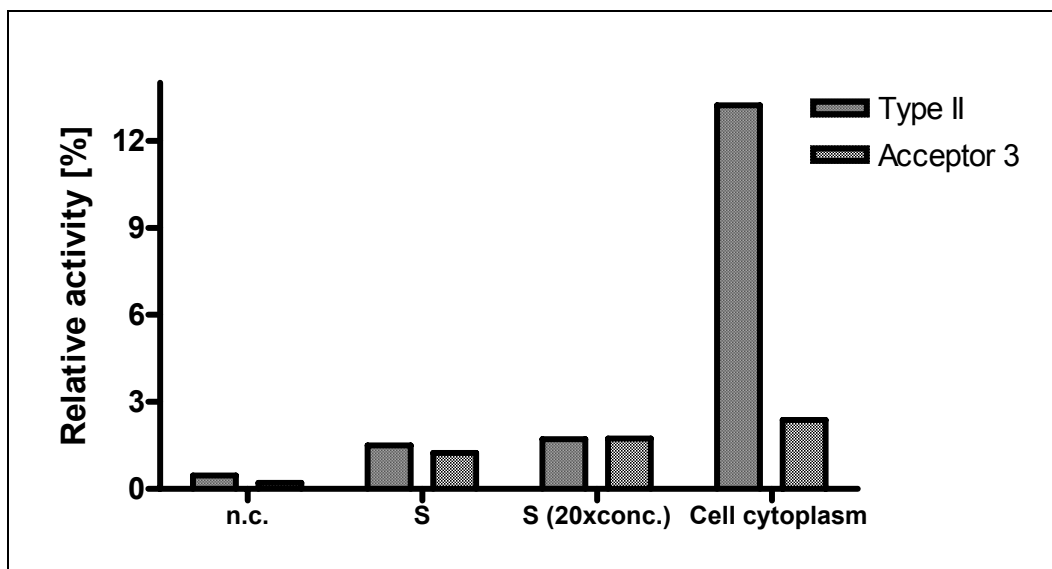


Figure 4.26 The α -2,3/2,8 ST enzyme expression and activity using 600 μ M of Type II (1) and 3 acceptor for 5 h at 37°C (n.c.: negative control; S: supernatant).

4.3.1.5 α -2,3/2,8 ST catalytic activity

The enzyme-containing cell cytoplasm fraction was used to obtain the information about the time-dependent catalytic activity of the α -2,3/2,8 sialyltransferase with 600 μ M of Type II (1) acceptor substrate (Figure 4.27). The enzyme was incubated for 12 hours at 37°C and pH 7.5. The reaction with Type II (1) acceptor substrate was completed after six hours of incubation under standard conditions. Thus, six hours was estimated as the necessary time to complete the consumption of a donor substrate in the presence of acceptor substrate in order to form the final sialylated product.

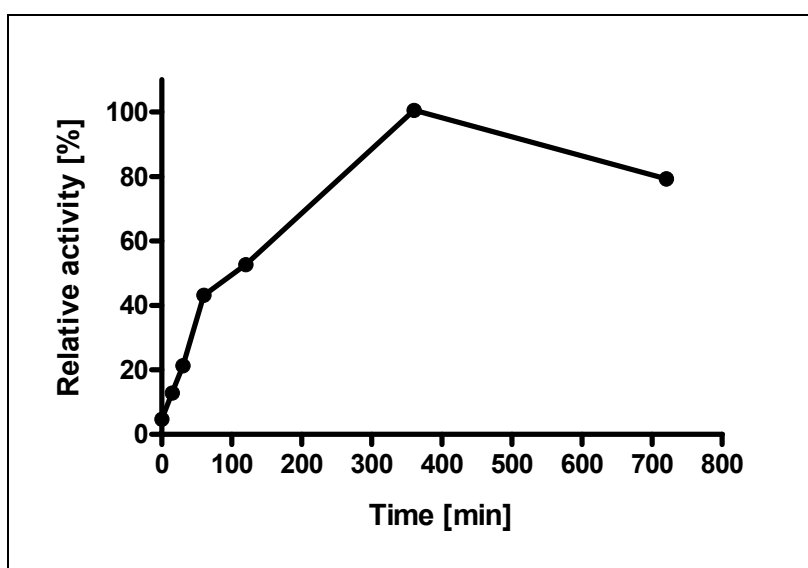


Figure 4.27 Catalytic activity of the α -2,3/2,8 ST enzyme estimated by ST enzyme activity assay. Enzyme was incubated with 600 μ M of 1 (Type II) acceptor at 37°C.

Finally, the cytoplasmic fraction containing the ZZ – α -2,3/2,8 bifunctional sialyltransferase recombinant protein fusion was applied to the IgG Sepharose 6 Fast Flow, according to the recommendations by the vector's supplier. However, with the recommended purification procedure it was not possible to obtain any fraction containing purified recombinant protein. This could be mainly due to the low protein abundance in the *E. coli* cells. As was mentioned before, the pEZZ18 expression vector was considered as not inducible. Since we tried to increase the protein expression by heat shock [303] and by raising the culture temperature to 44°C for two to six hours during the stationary phase of growth, without any results, consequently we decided to change the expression system. Taking into consideration our requirements, our new approach was based on an inducible expression system, which provides overexpressed recombinant protein fused to an

adequate tag-sequence important for facilitating purification.

4.3.2 α -2,3/2,8 ST cloning in pET vector systems and expression in *E.coli*

4.3.2.1 PCR *cst-II* gene amplification

The new system of choice was the pET expression system, as the most powerful yet developed for the cloning and expression of recombinant proteins in *E. coli* [259]. Two very similar vector systems were chosen. The pET15b vector contained an amino-terminal 6xHis tag sequence, whereas the pET21b vector possessed instead a carboxy-terminal 6xHis tag sequence. All other characteristics of the two vectors were identical. The *cst-II* gene was amplified using *C. jejuni* genomic DNA as a template in the PCR reaction (see chapter 3.3.6.1), and using forward and reverse primers with integrated *Nde* I and *Bam*H I restriction enzyme sequences. Different *cst-II* gene forms used for a distinct construct production are shown in *Table 4.8*. The amplified *cst-II* gene revealed a DNA sequence of 901 bp when analyzed on a 1% agarose gel. Next, the amplified *cst-II* gene was digested and agarose gel purified (*Figure 4.28 a*; lane 3). The digested and dephosphorylated pET15b vector containing an amino terminal 6xHis tag sequence exhibited a high level of purity (*Figure 4.28 a*; lane 2). In order to improve the enzyme purification and α -2,8 sialyltransferase catalytic function, we decided to produce a soluble and a mutated version of the *cst-II* gene, respectively.

Recently, the *cst-II* gene isolated from the OH4384 strain of *C. jejuni* was truncated and cloned into the pET21b vector [183]. This construct provided overexpressed recombinant soluble enzyme which was purified with a high yield. Therefore, the same recombinant technology was applied for the amplification of the truncated or truncated/mutated *cst-II* gene, which, compared to the wild type gene sequence, lacks 96 nucleotides (32 amino acids) on the 3' end (*Table 4.8*). In order to increased α -2,8 catalytic activity, the truncated gene was additionally mutated (Gly53→Ser; Asp177→Asn, Arg182→Asn) using site directed mutagenesis (see chapter 4.3.4.8). The truncated as well as mutated gene products with a molecular size of 801 or 802 bp (*Figure 4.28 b*; lane 1) were cloned into either the pET21b or pET15b vector.

Table 4.8 Different *cst-II* gene forms.

| PCR product (<i>Nde</i> I / <i>Bam</i> H I) | Size [bp] |
|---|-----------|
| <i>cst-II</i> gene (wild type) for pET15b vector | 901 |
| <i>cst-II</i> shortened, mutated gene for pET15b/ pET21b vector | 802/801 |

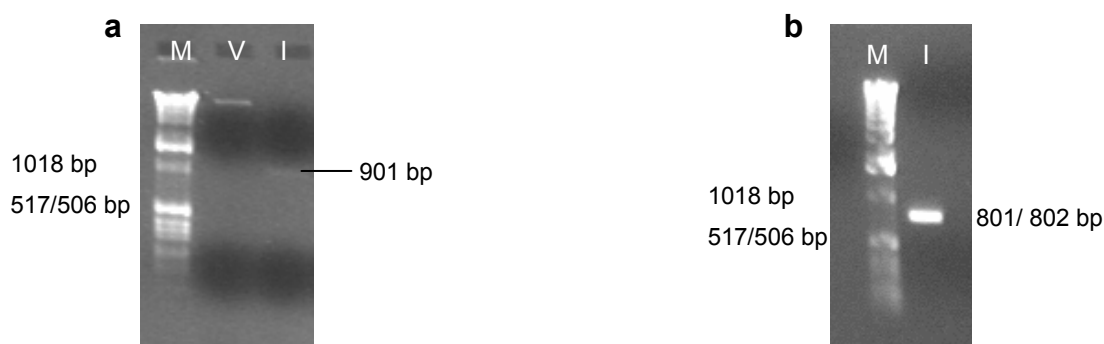


Figure 4.28 Agarose gel analysis (1%) of vector and insert. Lane 1: **(a)** DNA Molecular weight marker X (M); Lane 2: *Nde* I / *Bam*H I digested and dephosphorylated pET15b vector (V); Lane 3: *Nde* I / *Bam*H I digested *cst-II* gene insert (I). **(b)** Truncated *cst-II* gene insert.

4.3.2.2 Analysis of pET recombinants

Randomly picked *E. coli* ampicillin resistant clones were tested for the presence of the *cst-II* gene. Isolation of plasmid DNA and subsequent digestion with restriction enzyme revealed 100% successful incorporation of the target gene, either wild type or truncated, (mutated) into both selected vectors. In *Figure 4.29* it can be seen that the only difference in the two cloning strategies was the length of the gene of interest. The molecular size of the wild type gene was 901 bp whereas the truncated and mutated was 801 or 802 bp long depending on the cloning vector (pET21b or pET15b, respectively). Agarose gel analysis of all digested pET DNA recombinants revealed a small fraction of an incompletely digested vector (~5.5 kbp) when compared to an untreated sample (*Figure 4.29* a and b; lane 2, 4 and 6). In *Figure 4.29* only 3 positive clones are showed for both cloning strategies. Sequencing by the Microsynth confirmed that the wild type sequence was correct and that the truncated and additionally mutated gene sequence was altered by site

directed mutagenesis exactly according to our requirements. As was expected, the sequencing indicated a molecular size of 901 bp for the wild type gene, and 801 bp or 802 bp for either the truncated or truncated/point mutated gene, respectively.

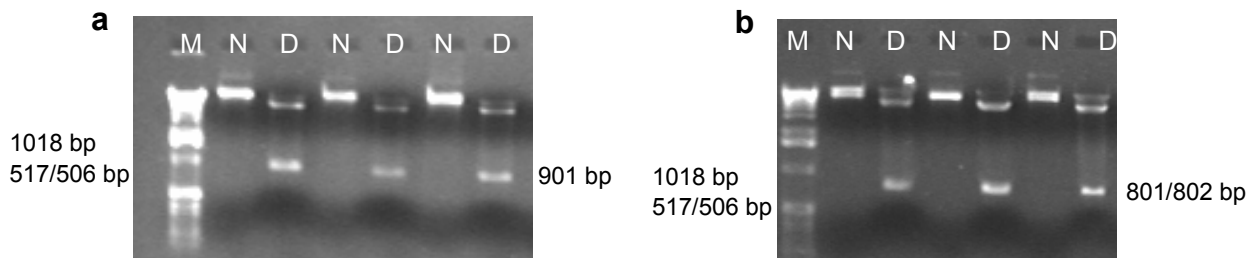


Figure 4.29 Agarose gel analysis (1%) of 3 recombinant DH5 α *E. coli* clones in (a) pET15b and (b) pET21b vector. Lane 1: DNA Molecular weight marker X (M); Lane 2 and 3: Non-digested recombinant vector (N) and *Nde* I / *Bam*H I digested recombinant vector (D) of clone 1; Lane 4 and 5: N and D of clone 2; Lane 6 and 7: N and D of clone 3.

All results obtained by recombinant DNA technology were confirmed by sequencing for their consistency. This conclusion was important for the following experiments concerning the expression and the purification of the recombinant protein.

4.3.2.3 Determination of target protein solubility

For the high level production of the α -2,3/2,8 bifunctional sialyltransferase it was necessary to transform an adequate expression host of *E. coli*. A verified recombinant plasmid of clone 2 was transferred to the BL21 expression *E. coli* strains containing a chromosomal copy of the gene for T7 RNA polymerase. In contrast to the cloning strains, expression hosts are lysogens of bacteriophage DE3, a lambda derivative that has the immunity region of phage 21 and carries a DNA fragment containing the *lacI* gene, the *lacUV5* promoter, and the gene for T7 RNA polymerase [259].

The first, very important step in the protein production was the determination of target protein solubility by SDS-PAGE analysis. For isolation of the soluble protein fraction, the pellet was sonicated and centrifuged in an imidazole-containing buffer. All treatments of the BL21 cell pellet fraction with Tris-HCl- and imidazole-containing buffers revealed the presence of the recombinant protein exclusively in the cell pellet fraction. The insoluble protein fraction was recovered by washing the pellet in the urea-containing buffer. This

buffer liberated the Cst-II15 protein with a molecular weight of ~36 kDa (Table 4.9) dissolving the cell membranes and denaturing the Cst-II15 initially combined with the pellet fraction (Figure 4.30; arrow).

Table 4.9 Full-length and soluble (mutated) α 2,3/2,8 ST enzyme expression forms in pET vector.

| α 2,3/2,8 ST form | Short name | Theoretical protein size [kDa] |
|---|----------------------------------|--------------------------------|
| Wilde type (full-length form) expressed in pET15b | Cst-II15 | 36.867 |
| Truncated (mutated) form expressed in pET15b | Δ 32Cst-II15(S53N177N182) | 32.903 |
| Truncated form expressed in pET21b | Δ 32Cst-II21 | 33.086 |

A very small amount of protein was released with an imidazole-containing buffer during the cell pellet sonication procedure. Because of the very low abundance of the soluble Cst-II15 protein, it was very difficult to perform a purification procedure using a Ni-NTA affinity column (see chapter 4.3.3.4). Hence, additional optimization of the enzyme expression was required in order to obtain an adequate amount of purified enzyme.

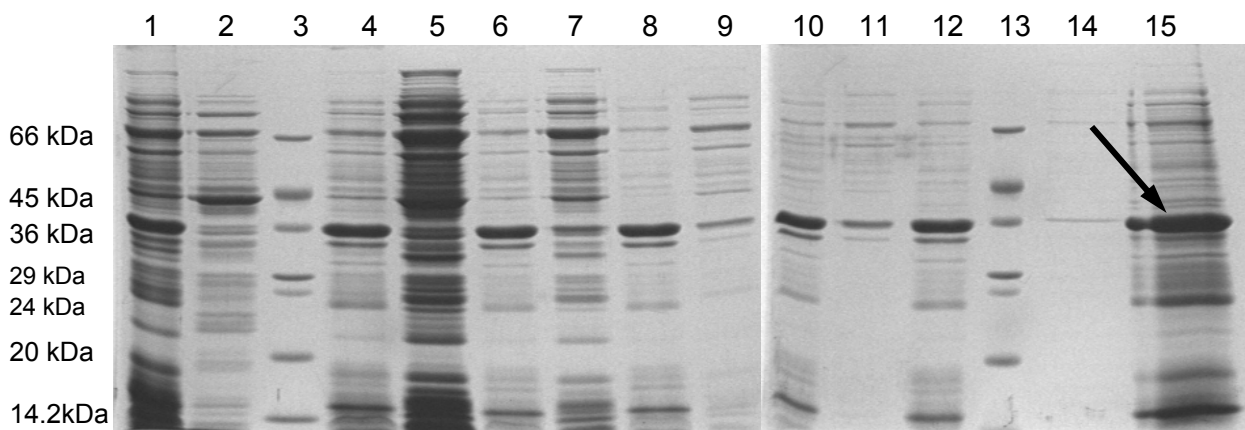


Figure 4.30 Determination of the Cst-II15 protein solubility expressed in BL21(DE3). SDS-PAGE (12.5%; Coomassie staining); Lane 1 and 2: cell pellet (P) and supernatant (S) of Tris-HCl wash 1; Lane 3 and 13: Low molecular weight marker (M); Lane 4 and 5: P and S of Tris-HCl wash 2; Lane 6 and 7: P and S of Tris-HCl wash 3; Lane 8 and 9: P and S of Tris-HCl wash 4; Lane 10 and 11: P and S of Tris-HCl wash 5; Lane 12 and 14: P and S treated with the imidazole-containing buffer

(ICB); Lane 14: P treated with the urea-containing buffer (UCB). P and S were separated by centrifugation 10 000 x g (see chapter 3.3.6.6).

4.3.3 α -2,3/2,8 ST analysis and purification

4.3.3.1 Enzyme expression and activity optimization

As mentioned above, for the high-level production of the α -2,3/2,8 bifunctional sialyltransferase it was necessary to transform an adequate expression host of *E. coli*. A verified recombinant plasmid of clone 2 was transferred to the BL21, AD494 and RG expression *E. coli* strains containing a chromosomal copy of the gene for T7 RNA polymerase. In order to optimize α -2,3/2,8 bifunctional sialyltransferase expression, all mentioned strains were cultured in two different media, LB and TB, and checked for the enzyme expression and activity (*Figure 4.31*). Based on the same total protein amount, preliminary results detected maximal relative activity for the BL21 and the RG strain of *E. coli* when the cells were incubated in LB medium. The same activity was determined for the RG cells incubated in TB medium, whereas the BL21 cells in the same medium showed a 50% decrease in relative activity. The AD494 cells, regardless of culture media, exhibited very low (30%) enzyme activity, which corroborates with the low protein expression in the same cell strain verified by SDS-PAGE analysis. Very low enzyme activity (4%) compared to the induced non-transformed BL21, AD494 and RG cells (*Figure 4.31*), which served in the experiment as a negative control, was detected in the DH5 α *E. coli* cells. This result was not surprising, since DH5 α cells have minimal background expression of recombinant protein. This background expression is due to the host RNA polymerase, which basically does not initiate from the T7 promoter, but instead a cloning site containing the recombinant protein in the pET plasmid can be weakly transcribed by read-through activity of bacterial RNA polymerase [259].

Preliminary results on bacterial growth, protein expression and enzyme activity suggested the utilization of the BL21 *E. coli* expression strain for the optimal scale-up of protein production. Thus, the BL21 cells transformed with the recombinant pET15b vector containing the wild type α -2,3/2,8 bifunctional sialyltransferase (Cst-II15) were cultured in the LB medium for all on-going studies.

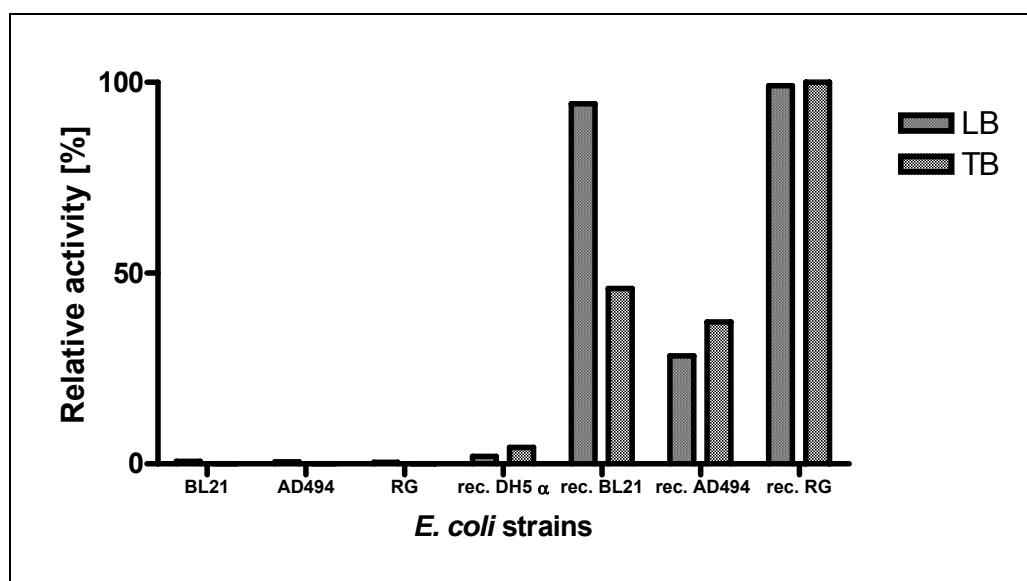


Figure 4.31 The enzyme activity of wild type α -2,3/2,8 ST expressed (Cst-II15) in *E. coli* strains (DH5 α , AD494(DE3), BL21(DE3), RG) and in LB and TB media (see chapter 3.3.6.7). Based on total protein amount, the enzyme was incubated with 600 μ M of **1** (Type II) acceptor for 6 h at 37°C (see chapter 3.3.7.2).

4.3.3.2 Time course analysis of the soluble protein form

A similar strategy for assessment of enzyme solubility was applied for the truncated version of the recombinant enzyme, *i.e.* the enzyme missing the membrane-binding domain (Δ 32Cst-II15 and Δ 32Cst-II21). The majority of the truncated Cst-II protein (Δ 32Cst-II15/21), as shown in the time course analysis, was overexpressed and released in the supernatant (*Figure 4.32*; arrow). The enzyme was released by sonication of the BL21 cell pellet in the imidazole containing buffer. A time course analysis revealed a successful release of the truncated protein with molecular weight of ~33 kDa (Table 4.9) overexpressed from both, the pET15b and pET21b vectors. The same SDS-PAGE analysis gave us the possibility to estimate the optimal incubation time at 16 hours, which is necessary to obtain a high amount of overexpressed recombinant enzyme.

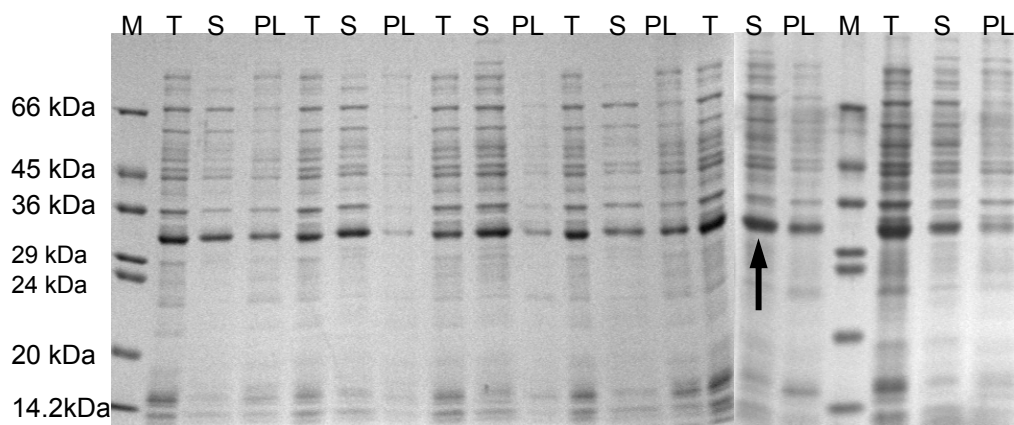


Figure 4.32 Time course analysis of $\Delta 32\text{Cst-II15/21}$ expression. The protein was analyzed by SDS-PAGE (12.5%) and Coomassie stained (see chapter 3.3.6.8). Lane 1 and 17: Low molecular weight marker (M); Lane 2, 3 and 4: total cell protein (T), supernatant (S) and pellet after lysis (PL) after 6 h of growth; Lane 5, 6 and 7: T, S and PL after 8 h of growth; Lane 8, 9 and 10: T, S and PL after 10 h of growth; Lane 11, 12 and 13: T, S and PL after 12 h of growth; Lane 14, 15 and 16: T, S and PL after 16 h of growth; Lane 18, 19 and 20: T, S and PL after 24 h of growth.

4.3.3.3 The enzyme activity related to the culture grown at different temperatures

In order to find the optimal temperature for BL21 cell growth, which would give the best protein production, analysis was carried out with samples collected from cell cultures grown at room temperature (RT), 30°C and 37°C. As it is shown in the *Figure 4.33*, BL21 recombinant cells incubated at RT and 30°C expressed Cst-II15 exhibiting the same activity. In contrast, the Cst-II15 enzyme expressed by BL21 cells, which were grown at 37°C, had 65% activity, 1.5-fold less comparing to expression at RT and 30°C. According to the obtained results, the optimal temperature for the BL21 cell culture growth was at RT and 30°C. The latter temperature revealed the highest expression of the recombinant protein. Therefore, for all on-going studies, BL21 cells containing recombinant enzyme were cultivated for 16 h at 30°C.

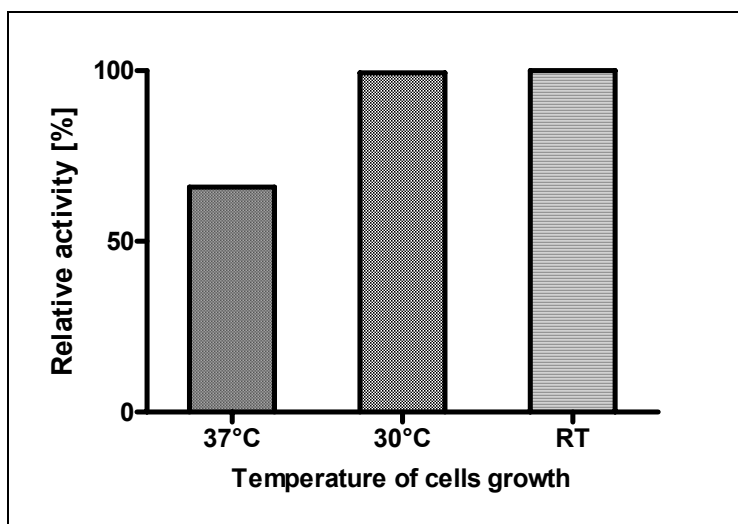


Figure 4.33 The Cst-II15 enzyme activity from BL21 cell cultures grown at different temperatures for 6 hours. Based on the same total protein amount, the enzyme activity was checked with 600 μM of **1** (Type II) acceptor incubating at 37°C (see chapter 3.3.6.8).

4.3.3.4 Purification of the recombinant α -2,3/2,8 ST enzyme

As mentioned before, the pET vector system provides the possibility to express a protein as a N- or C-terminus 6xHis-tagged recombinant protein. The 6xHis affinity tag facilitates binding to Ni^{2+} -nitrilotriacetic acid (Ni-NTA). It is poorly immunogenic, and at pH 8.0 the tag is small, uncharged and therefore does not affect compartmentalization or folding of the fusion protein within the cell. In most cases, the 6xHis tag does not interfere with the structure or function of the purified protein [267].

Purification of the 6xHis-tagged full length Cst-II15, truncated $\Delta 32\text{Cst-II15/21}$ or truncated and mutated protein by Ni-NTA affinity chromatography was performed under native conditions as it was suggested by the Ni-NTA affinity column supplier (Qiagen) [267]. The purification protocol was optimized and adapted to the fusion protein, because of the difficulties observed by the elution of the recombinant Cst-II15 from the column. The chromatography profile, after Ni-NTA affinity purification of the Cst-II15 recombinant protein with optimized purification protocol, showed elution of two peaks with the native lysis buffers containing 50 mM and 500 mM imidazole, respectively (*Figure 4.34 a*; arrows).

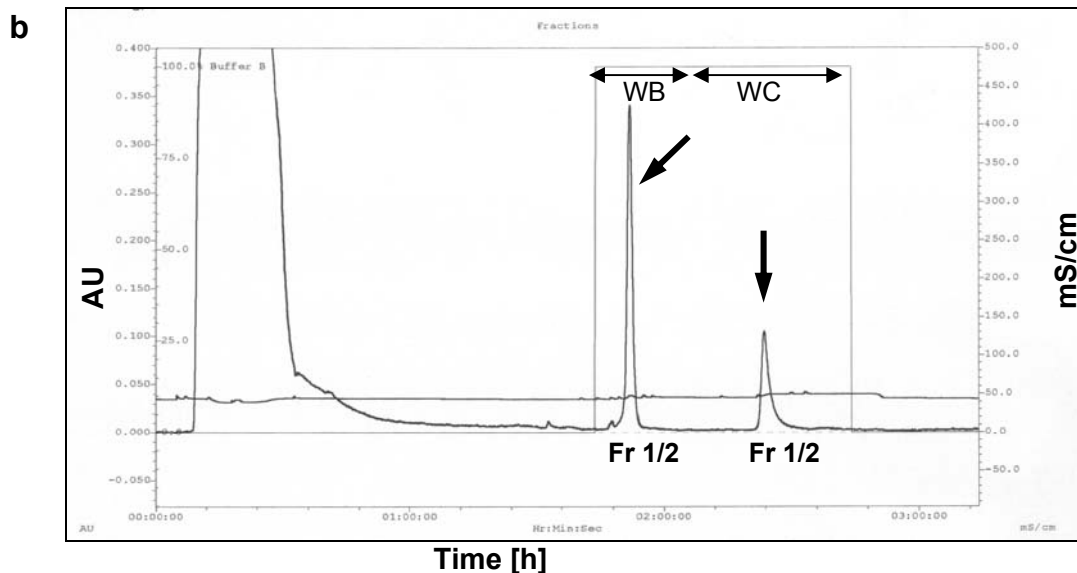
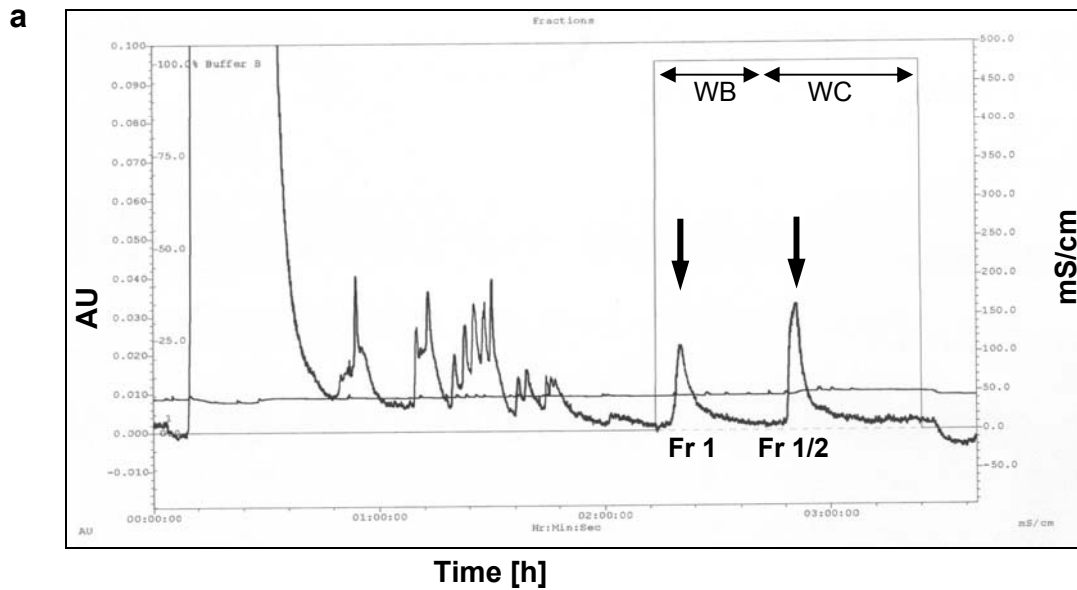


Figure 4.34 The FPLC chromatograms obtained after purification of **(a)** Cst-II15 and **(b)** Δ 32Cst-II15/21 using Ni-NTA affinity column. WB and WC designate native lysis buffer containing 50 mM and 500 mM imidazole, respectively. Arrows point the eluted peak obtained after purification under native conditions.

The single step Ni-NTA affinity purification of the truncated Δ 32Cst-II15/21 and the mutated Δ 32Cst-II15S53N177N182 recombinant protein was performed using the same optimized protocols for the native purification. The purification chromatogram revealed two similar peaks eluted with native lysis buffers containing 50 and 500 mM imidazole.

Comparing the purification profile of the Cst-II15 to the profile obtained with truncated constructs, the later exhibited higher protein absorbance at 280 nm. Although the same quantity of starting material was used, *i.e.* 250 ml of BL21 cell culture grown for 16 h at 30°C (*Figure 4.34 b*; arrows), the peak eluted with 50 mM imidazole containing buffer showed more than 10-fold higher protein absorbance. A similar chromatography purification profile was detected by elution of the mutated $\Delta 32$ Cst-II15S53N177N182 protein.

The SDS-PAGE and Western blot analysis of the Ni-NTA affinity obtained fractions showed a very poor purification profile of the Cst-II15. These fractions contained partially purified Cst-II15 but the quantity of the protein was low. Western bolt analysis using the anti-His tag antibody revealed the presence of Cst-II15 in almost all obtained fractions. The same method detected one specific signal approximately at 36 kDa (*Figure 4.35 b*) in the Fr 1 which was in agreement with the theoretically calculated Cst-II15 molecular weight (*Table 4.9*). Additionally, a signal at about 24 kDa was observed in the 34-fold concentrated Fr 1 (*Figure 4.35 b*; lane 8). This finding can indicate possible unspecific proteolytic cleavage within the membrane-binding domain of the Cst-II15 (see later).

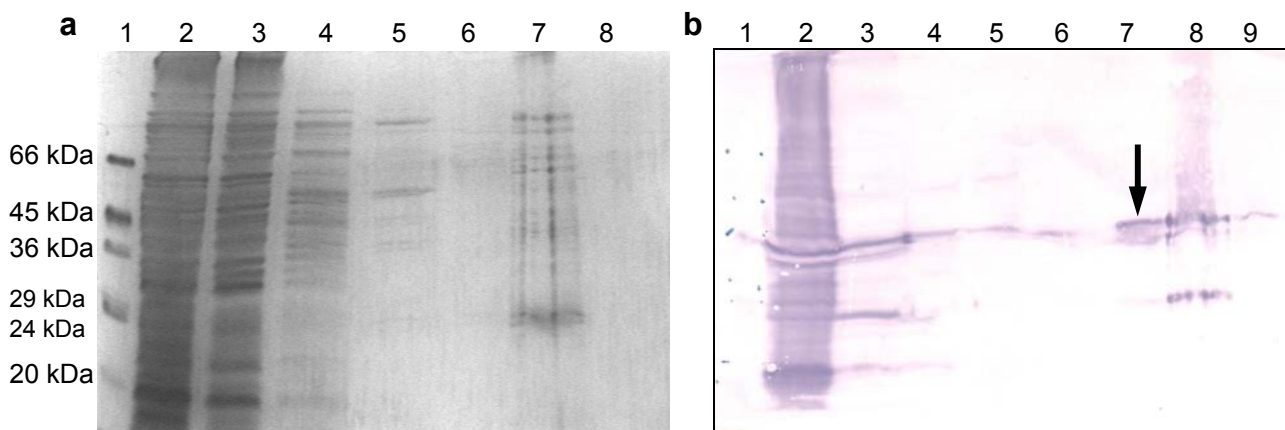


Figure 4.35. SDS-PAGE and Western blot analysis of the Cst-II15 Ni-NTA affinity chromatography purification under native conditions. **(a)** SDS-PAGE (12.5%; silver staining); Lane 1: Low molecular marker (M); Lane 2: load (L); Lane 3: flow through (FT); Lane 4: wash (W); Lane 5: fraction 1 (Fr 1) eluted with WB buffer; Lane 6: 34 x concentrated Fr 1; Lane 7: Fr 1 eluted with WC buffer; Lane 8: Fr 2 eluted with WC buffer. **(b)** Western blot analysis which was performed using monoclonal mouse anti-His tag (1:2 000) as a primary antibody (Novagen) and goat anti-mouse immunoglobulin alkaline phosphatase conjugated (1:5 000) as a secondary antibody (Sigma); Lane

1: Low molecular marker (M); Lane 2: pellet after sonication (Ps); Lane 3: load (L); Lane 4: flow through (FT); Lane 5: wash (W); Lane 6: fraction 1 (Fr 1) eluted with WB buffer; Lane 7: 34 x concentrated Fr 1; Lane 8: Fr 1 eluted with WC buffer; Lane 9: Fr 2 eluted with WC buffer. WB and WC designate native lysis buffer containing 50 mM and 500 mM imidazole, respectively. Arrow points Cst-II15 enzyme.

The partially purified Cst-II15 was expressed at a level of 1.69 mg/l, determined by Brathford protein analysis. While concentrating the main fraction for a factor of 50, enzyme was partially lost probably due to the protein binding to the Centricon membrane, and concentration (1.23 mg/l) decreased for 27% (*Table 4.10*). The Cst-II15 was definitely overexpressed since the SDS-PAGE analysis of enzyme solubility showed its high expression in the cell pellet (*Figure 4.30*; arrow). The Cst-II15 which was released to the supernatant was probably proteolytically cleaved in the membrane binding domain during its preparation. Actually, this membrane bound enzyme was not expected to be secreted, but it could be presumed that because of the spontaneous proteolytic cleavage it was forced to act as a secreted protein. In fact, this can explain the very low protein amount in the fraction, which was applied to the affinity chromatography column. A similar purification problem was observed, when the protein was expressed using pEZZ18 vector (see chapter 4.3.1). However, when comparing expression from pET and pEZZ18, the recombinant protein differed only in the protein expression level. The HB101 *E. coli* cells transformed with the recombinant pEZZ18 expressed the Cst-II15 at an extremely low level. In contrast, the BL21 cells containing the recombinant pET15b showed cell-membrane overexpression. Determination of target protein solubility demonstrated possible inclusion body (IB) formation. With the issue of the protein insolubility in mind, the purification procedure was carried out under denaturing conditions as well. With this method it was also not possible to purify the recombinant fusion protein. Initially, the idea was to compare the kinetic data obtained with N-terminal His tag fusion protein, *i.e.* Cst-II15 to its C-terminal His tag counterpart, the Cst-II21. In order to get the purified Cst-II21, full-length protein expressed using the pET21b vector was applied onto Ni-NTA column. The purification of Cst-II21 under native conditions did not show any positive results and therefore, the Cst-II21 enzyme was not used for the further enzyme characterization. A possible explanation could be the topology of the Cst-II21 recombinant enzyme. Since the LOS is assembled on the cytoplasmic face of the inner membrane and transported onto

the cell surface by means of the ABC transporter, the active site of the protein should be placed inside the cytoplasm [183]. According to that, the catalytically active domain of the proteolytically cleaved C-terminal His tagged protein, the Cst-II21, was released in the cytoplasm, whereas the membrane binding domain fused to the His tag sequence remained in the plasma membrane. The activity of the cytoplasmic fraction which contained small fraction of the proteolytically cleaved, soluble Cst-II21 was verified. The preliminary check of soluble Cst-II exhibited enzyme relative activity of 50%. The soluble, proteolytically cleaved Cst-II21 was not possible to purify comparing to the proteolytically cleaved Cst-II15 fusion protein which still contained N-terminal His tag sequence. The reason for this was that the His tag sequence, together with the membrane binding domain of an enzyme, remained in the plasma membrane as a part of the fusion protein. Taking all this together, these preliminary results partially confirmed our general concept about proteolytical cleavage prediction.

The $\Delta 32$ Cst-II15/21 and mutated protein showed similar Ni-NTA purification profile (*Figure 4.34 b*). The SDS-PAGE and Western blot analysis revealed the single step protein purification. The aforementioned analysis confirmed also overexpression and revealed identical results for both constructs, truncated and additionally mutated. As expected, Western blot demonstrated the molecular weight of approximately 33 kDa which completely correlated with our theoretically calculated data (*Table 4.9*). The main fraction 2, containing pure recombinant truncated enzyme was eluted with the native lysis buffer containing 50 mM imidazole (*Figure 4.36*; lane 8). The following fractions eluted with 500 mM imidazole contained a small fraction of the purified enzyme as well. Therefore, measuring the purified protein concentration, a high variation in protein expression was noticed, which depended on the vector system and recombinant construct. In conclusion, the BL21 cells containing the $\Delta 32$ Cst-II21 construct within the pET21b vector showed higher protein production, roughly 460 mg/l (*Table 4.10*). Interestingly, the same construct within the pET15b vector was produced at the level of 120 mg/l, which is an almost 4-fold difference. The mutated $\Delta 32$ Cst-II15S53N177N182 construct expressed in the BL21 cells using the pET15b vector revealed a concentration of only 65.04 mg/l, which is 2.5-fold less compared to the same vector system expressing the $\Delta 32$ Cst-II under the standard conditions. The reason for the low expression level is not clear, but since the enzyme is mutated, triple mutation could have had a certain influence on its folding and expression behavior.

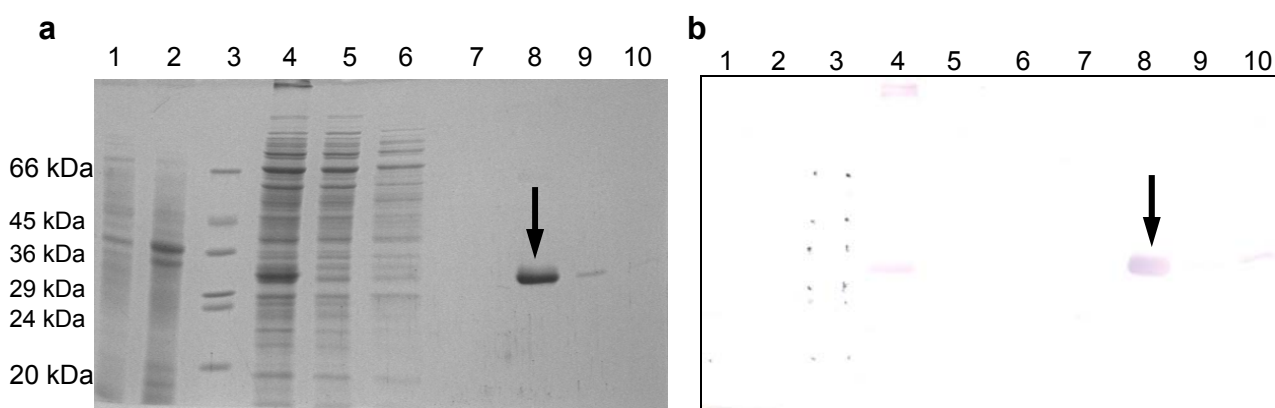


Figure 4.36 (a) SDS-PAGE (12.5%, Coomassie staining) and (b) Western blot analysis of the $\Delta 32$ Cst-II15/21 Ni-NTA affinity chromatography purification under native conditions. Western blot was performed using monoclonal mouse anti-His tag (1:2 000) as a primary antibody (Novagen) and goat anti-mouse immunoglobulin alkaline phosphatase conjugated (1:5 000) as a secondary antibody (Sigma). Lane 1: pellet (P); Lane 2: pellet after sonication (Ps); Lane 3: Low molecular marker (M); Lane 4: load (L); Lane 5: flow through (FT); Lane 6: wash (W); Lane 7 and 8: Fractions 1 and 2 eluted with WB buffer; Lane 9 and 10: Fractions 1 and 2 eluted with WC buffer. WB and WC designate native lysis buffer containing 50 mM and 500 mM imidazole, respectively. Arrow points purified soluble enzyme.

Table 4.10 Concentration of α -2,3/2,8 ST expressed by different pET recombinant constructs on 1 l scale, and enzyme activity measured with 600 μ M of **2** (Type I) acceptor substrate (see chapter 3.3.7.2.).

| Type I acceptor | Cst-II15 | | $\Delta 32$ Cst-II | | $\Delta 32$ Cst-II15S53N177N182 |
|-----------------|-----------|-------|--------------------|--------|---------------------------------|
| | Non-conc. | Conc. | 15 | 21 | |
| U/l | 2.39 | 35.26 | 21.69 | 21.62 | 3.46 |
| U/mg | 1.41 | 28.61 | 0.12 | 0.05 | 0.05 |
| Volumen [ml] | 11.8 | 0.24 | 10.8 | 14.8 | 19.7 |
| mg/l | 1.69 | 1.23 | 177.27 | 463.24 | 65.04 |

4.3.4 α -2,3/2,8 ST enzyme characterization

After the high quantity expression of the soluble enzyme and its qualitative purification, it was very important to optimize all parameters, e.g. temperature, pH, metal cofactors etc., essential for the enzyme maximal performance. In order to use expressed enzyme for the chemo-enzymatic preparative synthesis of GQ1b α mimetics, it was of great interest to obtain reliable kinetic data, K_M and k_{cat}/K_M , related to Type I and Type II as a natural and Type III derivatives as a non-natural acceptor substrates.

4.3.4.1 α -2,3/2,8 ST catalytic activity

The catalytic activity of Cst-II15 with 600 μ M of **1** (Type II) acceptor substrate confirmed the results obtained with the full length enzyme expressed by pEZZ18 vector (*Figure 4.27*). Indeed, the maximal catalytic activity and correlated sialylated Type II production was accomplished after six hours of incubation under standard conditions, at 37°C and pH 7.5 (*Figure 4.37*). This fact proved the enzyme stability and its independence concerning two completely different vector expression systems.

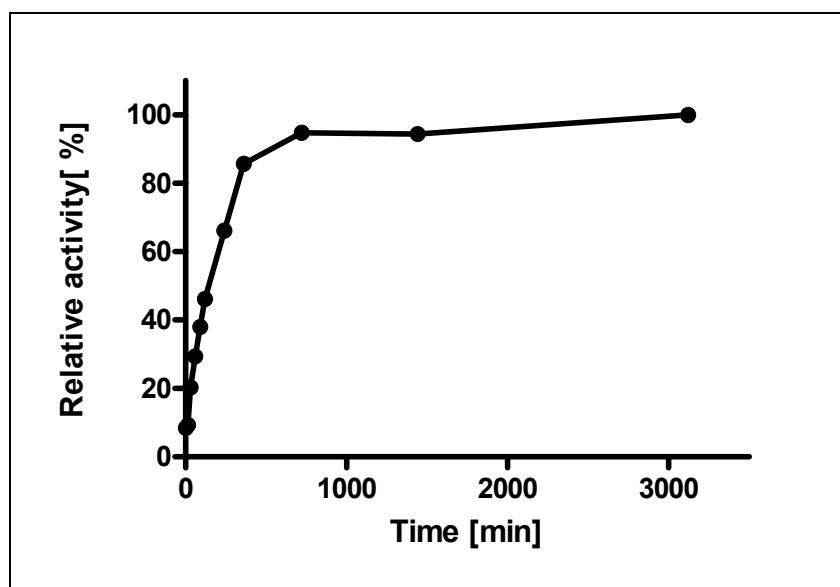


Figure 4.37 Catalytic activity of the Cst-II15 estimated by ST enzyme activity assay as described in the chapter 3.3.7.3. Enzyme was incubated within the incubation buffer consisting of 600 μ M of **1** (Type II) acceptor, 1 mM CMP-NeuNAc and 60 000 dpm radioactive donor substrate at 37°C and pH 7.5.

4.3.4.2 Temperature dependent enzyme activity

Proving the temperature stability of the $\Delta 32Cst-II15$, it was found that the enzyme exhibited different catalytic performance concerning its α -2,3/2,8 and α -2,8 specific sialyltransferase activity (Figure 4.38). The enzyme exhibited slightly distinct specificity with non-sialylated **1** (Type II) and sialylated acceptor substrate (**7**) (Table 3.43), when incubated at different temperatures for the same time period. To isolate the product, either α -2,3- or α -2,3/2,8 sialylated, it was used C18 SepPak cartridges. The radioactive background, obtained by counting the C18 SepPak washing step, was very low (Figure 4.38, n.c.) what eliminate a difference in enzyme activity as a product of possible contamination during the product isolation. The maximal α -2,3/2,8 sialyltransferase relative activity of the $\Delta 32Cst-II15$ was estimated at 25°C, whereas 37°C revealed the optimal temperature for the α -2,8 enzyme activity. Interestingly, the enzyme demonstrated bifunctional behavior when it was incubated within the range of 20°C to 56°C showing a temperature overlapping for the both catalytic activities, α -2,3/2,8 and α -2,8. The most surprising result was the relative α -2,3/2,8 enzyme activity of 12.5% obtained for the $\Delta 32Cst-II15$ incubated with Type II acceptor on ice. At the temperatures of 56°C and 60°C almost 6% and 3% of the α -2,3/2,8 $\Delta 32Cst-II15$ activity was preserved, whereas these values were more than two-fold higher for the α -2,8 activity of the $\Delta 32Cst-II15$, respectively. It could be speculated that two optimal temperatures as well as the temperature overleaping of enzyme activity could be an indication of an important role of the α -2,3/2,8 bifunctional enzyme activity during host infection. These differences in temperature might be one important factor in the *C. jejuni* life cycle. The bifunctionality of the *cst-II* might have an impact on the outcome of the *C. jejuni* infection. It has been suggested that the expression of the terminal disialylated epitope might be involved in the development of neuropathic complications such as the Guillain-Barré syndrome (GBS). In 1996 it was published by Salloway *et al.* [172] that Miller-Fisher Syndrome (MFS) and GBS neuropathies in some patients were preceded by intestinal infections with the specific *C. jejuni* strains such as O:10, O:19. It is known that lipopolysaccharides (LPSs) from some strains of *C. jejuni* mimic the structure of human gangliosides [180], and attention has focused on the possibility that molecular mimicry is a factor in the pathogenesis of human neurological disease. The ganglioside-mimicking has been found to be located in the terminal regions of the core oligosaccharides (OSs) of the LPS [180,304]. Molecular

mimicry of host structures by the saccharide portion of LOS is considered to be a virulence factor of various mucosal pathogens which could use this strategy to evade the immune response [142,173]. The specific saccharide-containing region of LPS can act as an immunoantigen and play an important role in different bacterial-host recognition processes. It is suspected that with changes in temperature, the α -2,3/2,8 bifunctional sialyltransferase can synthesize *in vivo* variable glycosidic bonds and therefore modify the terminal oligosaccharide region of the LOS/LPS molecule. Consequently, this might influence and accelerate some processes in the host infection and in pathogenesis mechanisms.

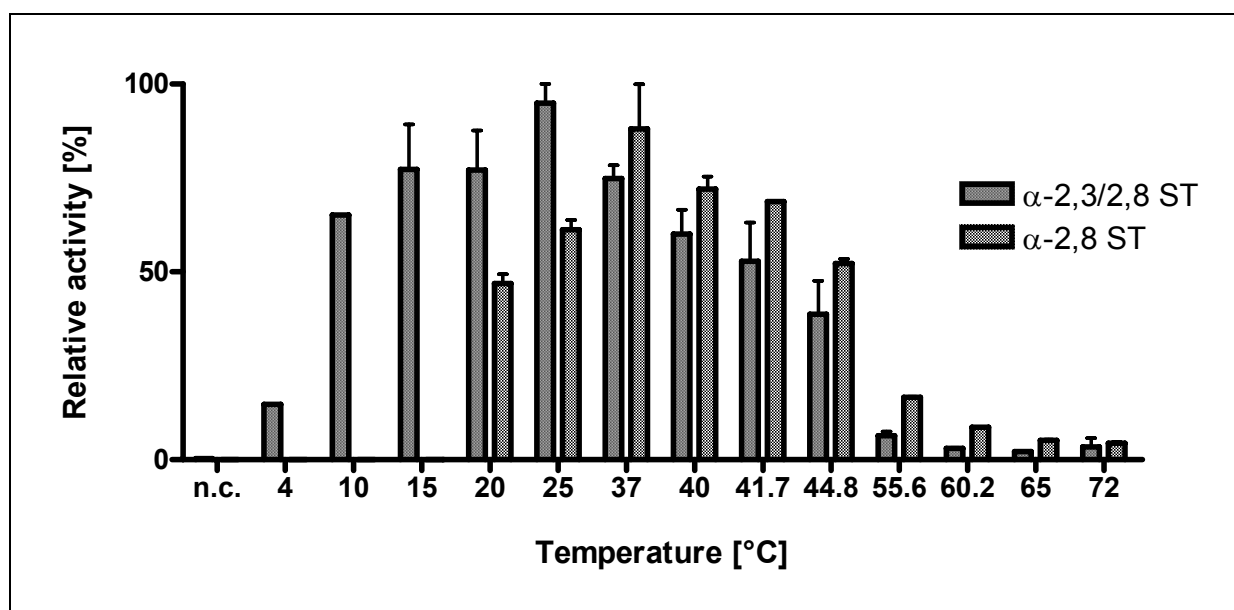


Figure 4.38 Temperature dependent α -2,3/2,8 and α -2,8 sialyltransferase activity. The α -2,3/2,8 ST activity was verified with 600 μ M of **1** (Type II) acceptor substrate, whereas 600 μ M of the acceptor substrate **7** was used to check the α -2,8 ST. Enzyme was incubating at indicated temperatures for 6 h (see chapter 3.3.7.4). Negative control (n.c.) represents the cytoplasmic fraction of non-recombinant BL21 cells.

4.3.4.3 pH dependent enzyme activity

For further biochemical characterizations the enzyme activity was investigated at different pH values. Our kinetic analysis of three different enzyme-constructs, *i.e.* the full length and the soluble forms (Cst-II15 and Δ 32Cst-II15/21) with the Type I (**2**) acceptor substrate revealed that the optimal pH value lies between pH 7.0 – 10.0 (*Figure 4.39*). These results were in agreement with results published by Chiu *et al.* [183] who showed that the optimal

enzyme activity occurs around pH 8.0. It was stated that at this pH, the catalytically important His188 would be expected to be deprotonated as required for a general base catalysis. Upon proton transfer, the positive charge that develops on the histidine side chain could be stabilized through electrostatic interactions with the negatively charged phosphate and carboxylate groups of the donor sugar. Mutation of His188 to alanine results in loss of all detectable transferase activity, indicating its key catalytic role in the transferase mechanism of Cst-II. The most significant difference in enzyme activity between the full length and truncated enzyme occurred at pH 7.0. As described, the flexible lid domain of $\Delta 32$ Cst-II15/21 enzyme is disordered in complex with CMP resulting in the absence of electrostatic interactions and hydrophobic contacts [183]. This might explain lower enzymatic activity of $\Delta 32$ Cst-II15/21 at pH 7.0 comparing to the full length enzyme, where these contacts have been conserved. Testing different buffering reagents such as cacodylate, Hepes and MES buffer, no particular preference was observed. Therefore, we decided to use 50 mM MES buffer in all enzyme activity assays, consistent with the previously described experiments [74].

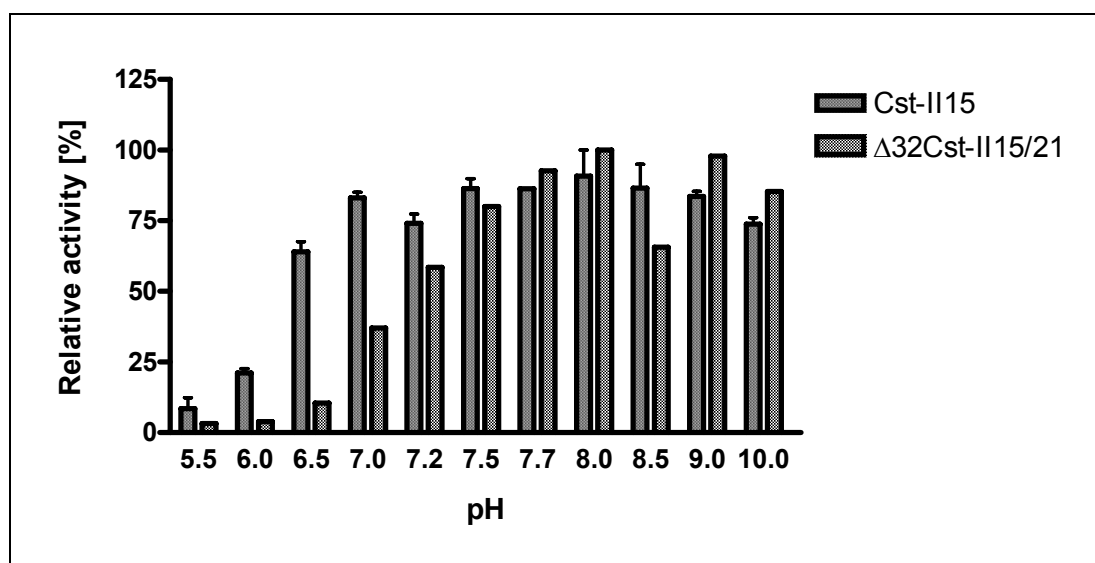


Figure 4.39 pH dependent activity of α -2,3/2,8 ST. As acceptor substrate, 600 μ M of **2** (Type I) was used in the enzymatic reaction performed for 6 h at 25°C (see chapter 3.3.7.5). For 100% of reaction it was converted ~20% of substrate into product.

4.3.4.4 The role of metal ions on enzyme activity

In the present work, we studied the role played by magnesium and other metals in the reactions catalyzed by the soluble recombinant enzyme constructs, $\Delta 32$ Cst-II15 and

$\Delta 32\text{Cst-II21}$. They were incubated in MES buffer containing different metal cofactors and acceptor substrate **2** (Type I). The activity pattern of both enzymes at pH 7.5 was changed with a panel of distinct cations at 10 mM. Both enzymes revealed similar kinetic data with these cations. In fact, it was observed that the cofactors were not essential for enzyme activity, since the enzyme remained active in the presence of EDTA. The enzyme incubated in MES buffer containing divalent magnesium (Mg^{2+}) and calcium (Ca^{2+}) as well as monovalent potassium (K^+) ions exhibited similar kinetic data when compared to the positive control (*Figure 4.40*). The presence of 10 mM EDTA in the Mg^{2+} containing incubation buffer did not disturb enzyme activity. Although the $\Delta 32\text{Cst-II15}$ was in general ~20% less active than $\Delta 32\text{Cst-II21}$, they both showed similar activity, if incubated in the presence of the above mentioned metal cations. Since the only difference in these two recombinant enzymes was the His tag position, we can doubt that its placement might influence enzyme activity. Comparing to the positive control the $\Delta 32\text{Cst-II21}$ activity decreased for 1.5-fold in the presence of trivalent iron ions (Fe^{3+}), whereas the $\Delta 32\text{Cst-II15}$ activity decreased for one-fold. Unlike these cations, incubation with Ni^{2+} , Zn^{2+} and Co^{2+} almost completely abolished enzyme activity (~85%). In the presence of Cu^{2+} no activity was detected (*Figure 4.40*). Surprisingly, Mn^{2+} ions, which are usually utilized instead of Mg^{2+} in many glycosyltransferase activity assays because of similar coordination [305], inhibited enzyme activity. According to that, the activity of the $\Delta 32\text{Cst-II15}$ and the $\Delta 32\text{Cst-II21}$ was impaired 76% and 96%, respectively, compared to the positive control. Although those ions possess the same charge, the inhibition of the enzyme by Mn^{2+} could be explained by the fact that they are, concerning the ionic radius (r), bigger ($r = 0.80 \text{ \AA}$) comparing to Mg^{2+} ($r = 0.66 \text{ \AA}$), which could lead to inhibition due to the possible structural rearrangement.

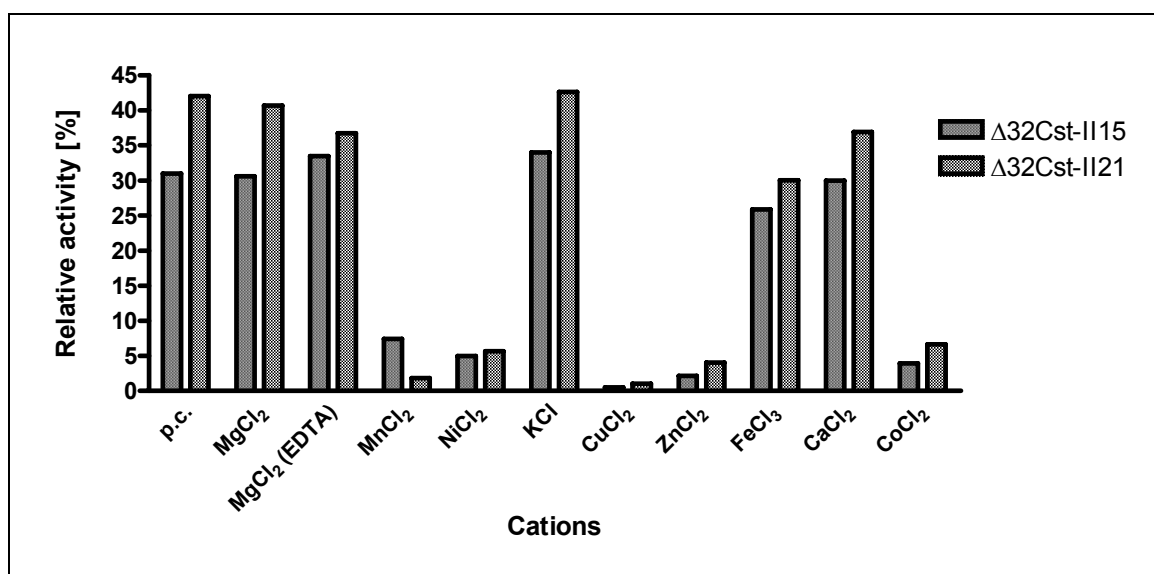


Figure 4.40 Metal ion-dependent activity of the soluble α -2,3/2,8 ST. 600 μ M of **2** (Type I) was used as acceptor substrate in the enzymatic reaction which was performed for 6 h at 25°C in MES buffer containing 10 mM indicated metal cofactors. Positive control (p.c.) represent the enzyme incubated in 10 mM EDTA containing MES buffer (see chapter 3.3.7.6). For 100% of reaction it was converted ~40% of substrate into product.

A very similar experiment was done before, regarding the characterization and acceptor specificity of the recombinant *Neisseria meningitidis* α -2,3 sialyltransferase [306]. Data published by Gilbert *et al.* [74,306] demonstrated the stimulation of enzyme activity due to the metal cofactors. The activity was stimulated three-fold in presence of 20 mM MgCl₂ and four-fold in presence of MnCl₂. We could have assumed that the metals were not required for the activity since the enzyme remains active in the presence of 5 mM EDTA. In that experiment, MnCl₂ provided the best stimulatory effect only in a short-term assay since it caused the α -2,3 sialyltransferase precipitation during long-term incubation. Consequently, it was preferred to perform preparative synthesis with MgCl₂. Results concerning the Cst-II enzyme reported by Chiu *et al.* [183] confirmed the previous finding regarding the activity enhancement due to the manganese and magnesium ions. The results obtained with manganese and magnesium ions showed enhancement of the enzyme activity by ~50%. It was also reported that they were not essential for enzyme catalysis since Cst-II belongs to the GTA group of enzymes. Unlike the other GTs from the same group, a bound metal was not observed in the active site of Cst-II Δ 32. The Cst-II lacks the DXD sequence motif found in a wide range of GTs. This motif is known to

coordinate the divalent cations involved in the binding of the nucleotide sugar through interaction with the diphosphate moiety [62,63]. The metal is generally considered to act as a Lewis acid catalyst, which stabilizes the leaving nucleoside diphosphate. Since the donor substrate in the case of the Cst-II Δ 32 is a nucleoside monophosphate sugar (CMP-NeuNAc), it can be assumed that metal ions are not essential for the stabilization of the departing nucleoside diphosphate [183]. The divalent cations Ni²⁺, Zn²⁺, Co²⁺ and Cu²⁺, which show preferences for other geometries and are coordinated by ligands containing nitrogen and imidazole groups [307], inhibited the enzyme. Inhibition was possibly due to the metal coordination of amino acids essential for catalysis. Such an amino acid could be His-188, for which a key catalytic role in the transferase mechanism of Cst-II was observed [183]. This suggested that the enzyme does not require any metal ion for the catalytic activity. However the enzyme activity could be disturbed or completely abolished in the presence of metal ions preferentially co-ordinated by imidazole containing ligands.

4.3.4.5 Cofactor and dependent enzyme activity

Apart from metal cofactors, the soluble recombinant enzyme was tested for cofactor requirements. Compared to the positive control, the results showed very similar catalytic activity of the enzyme with reduced and non-reduced cofactor forms. Surprisingly, the enzyme incubation with 0.5 mM adenosine triphosphate (ATP) did not change the catalytic activity greatly. In contrast, compared to the positive control, the enzyme retained 90% of its original activity. It is well known that cytosine triphosphate (CTP) is a potent inhibitor of sialyltransferases [296]. In the study of chicken ST3Gal I [295], an inhibition of ST3Gal I by different nucleosides could be demonstrated in the concentration range of 50-300 μ M. CTP together with UTP and GTP strongly inhibited chicken ST3Gal I in a competitive manner with respect to CMP-NeuNAc. In addition, CMP and ATP also acted as inhibitors. In the same study, AMP, UMP and GMP did not show inhibitory effect up to 300 μ M under standard assay conditions. Additionally, considering the nucleosides as inhibitors of prokaryotic sialyltransferases, it was found that CMP as well as CDP were inhibitors. CMP concentration of 1 mM showed 80% inhibition, whereas CDP caused 40% inhibition under standard conditions [306]. Our results displayed highly efficient catalytic activity of the enzyme in the presence of different cofactors, especially ATP. None of them highly disturbed or abolished the enzyme performance; instead the enzyme maintained the

original catalytic efficiency.

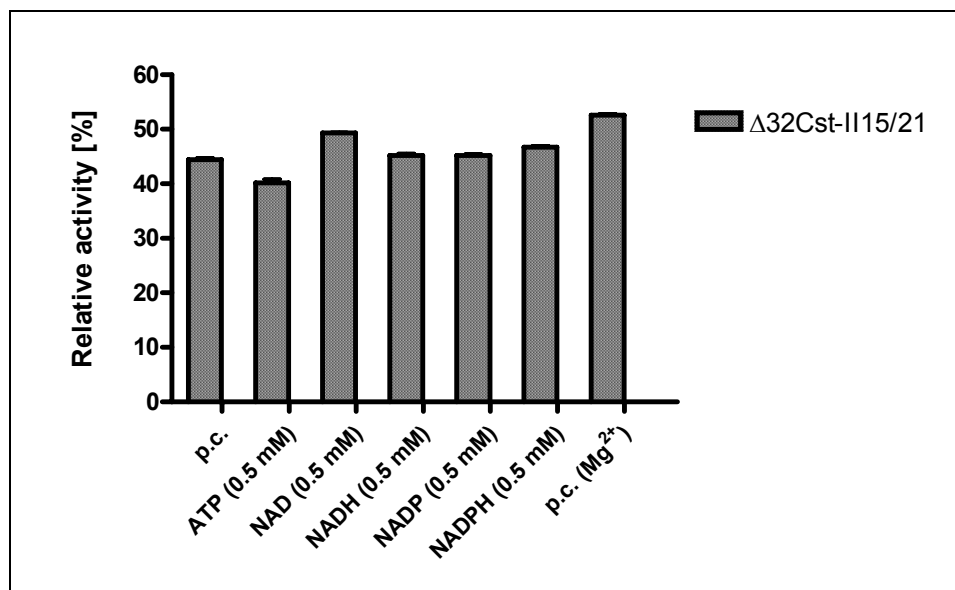


Figure 4.41 Cofactor dependent activity of α -2,3/2,8 ST. Enzyme was incubated with 600 μ M of **2** (Type I) for 6 h at 25°C. Positive control (p.c.) was prepared with the MES buffer free of metal ions and with the MES buffer containing 10 mM Mg²⁺ (see chapter 3.3.7.7).

4.3.4.6 Influence of dimethyl sulfoxide on enzyme activity

Many chemically synthesized substances, especially those containing hydrophobic aliphatic aglycones such as OLeM and OSE are not insoluble in water. In that case, the acceptor substrate needs to be dissolved in organic solvent such as DMSO. Therefore, it was necessary to check the enzyme activity in the presence of variable amounts of DMSO solution. The catalytic activity was checked with acceptor **13** (Table 3.43), since this substrate was not soluble in the water. Enzyme reaction was performed in MES buffer containing different concentrations of DMSO. The enzyme activity, relative to the positive control, revealed the same or slightly better results during the incubation of the enzyme within a wide range of DMSO concentrations (Figure 4.42). 20% of DMSO was estimated as an optimal concentration, associated with a catalytic activity of 47%. With 50% of DMSO, the enzyme exhibited half of the maximal activity whereas 5% of maximal activity was detected at 70% and 80% of DMSO. Interestingly, in pure DMSO solution the enzyme activity was still preserved showing 5% of maximal activity. A low enzyme activity detected at high DMSO concentration could be explained with the hypothesis of Khmel'nitsky *et al.*

[308]. Namely, the presence of water soluble organic solvent could modify the nature of the catalytically active conformation of the enzyme in such a solution. Consequently, the enzyme could be partially inactivated and even precipitated, stopping the active site accessibility to substrates and acceptors [309].

These results clearly showed that the enzyme retained its original activity within the organic solvent catalyzing efficiently the product formation.

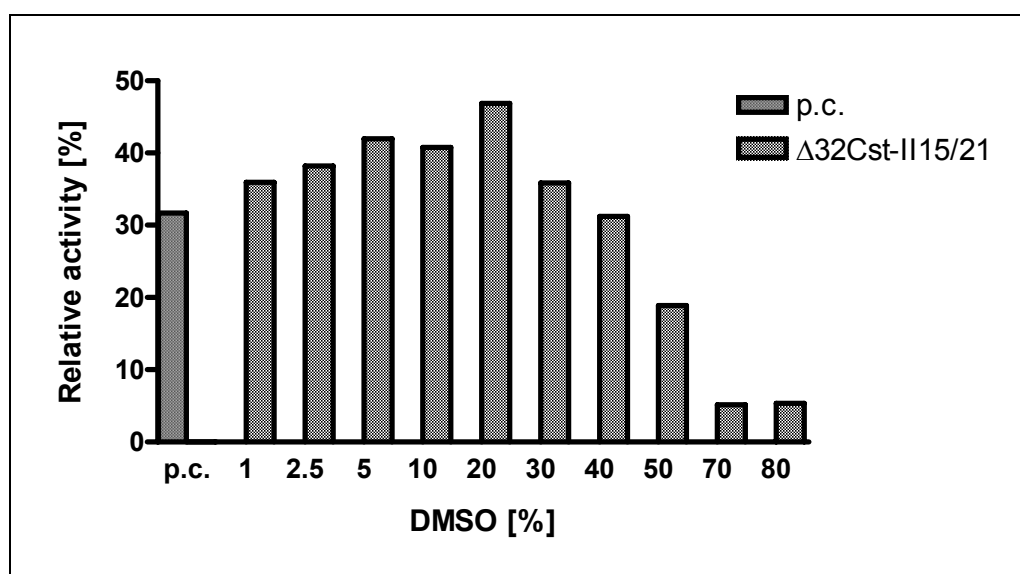


Figure 4.42 Dimethyl sulfoxide dependent activity of the α -2,3/2,8 ST enzyme. Enzyme was incubated with 600 μM acceptor substrate **13** for 6 h at 25°C. Enzyme incubated in the MES reaction buffer free of DMSO was used as a positive control (p.c.) (see chapter 3.3.7.8).

4.3.4.7 Determination of the enzyme kinetic parameters

After we optimized all of the important parameters, such as temperature, pH, enzyme activity in DMSO, metal ions, and importance of cofactor, we were able to determine the kinetic parameters of distinct expressed enzyme constructs relative to different acceptor substrates. The measurement of the kinetic parameters for the Cst-II15 revealed the best α -2,3/2,8 catalytic efficiency of 77.44 min^{-1} and K_M of 0.36 mM for the acceptor **2** (Type I). Very similar catalytic efficiency and K_M , precisely 77.06 min^{-1} and 0.31 mM for the same enzyme construct was obtained for the Type III-derivative acceptor **4** (Table 4.11). The reason for this substrate tolerance and very good enzyme performance with the acceptor **4** could be an indirect influence of the acylgroup on the catalytic efficiency of the enzyme.

Interestingly, catalytic efficiency of the acceptor **5** was almost 1.5-fold decreased (51.83 min^{-1}) compared to the acceptor **4**, whereas the acceptor **3** exhibited catalytic efficiency of 72.31 min^{-1} and the highest Michaelis constant of 2.2 mM. The results obtained for the same construct concerning the α -2,8 sialyltransferase activity generally showed highly decreased catalytic efficiency and increased K_M value, regardless of the incubation temperature. Namely, kinetic parameters for the α -2,8 enzyme activity were obtained at 25°C and 37°C (Table 4.11). The best sialylated Type II enzyme acceptor, acceptor **7**, showed a catalytic efficiency of 59.01 min^{-1} , which was almost the same compared to the acceptor **8** if the enzyme was incubated at 25°C. However, if the enzyme was incubated at 37°C the catalytic efficiency for the acceptor **7** was increased for 1.3-fold, whereas it changed extremely for an acceptor **8** (5.3-fold). Comparing to substrate **7** and **8**, acceptor **10** showed for 1.1-fold decreased catalytic efficiency. Acceptor **7** exhibited K_M of 1.22 mM at 25°C and 2.02 mM at 37°C, whereas acceptor **10** showed K_M of 2.06 mM at 25°C and 2.80 mM at 37°C. A very surprising result was the K_M value obtained for acceptor substrate **8**. Namely, the K_M value of 2.62 mM obtained at 25°C was extremely changed (17.5 mM) when the enzyme was incubated with the same acceptor at the temperature of 37°C. This was surprising, since we were expecting that the α -2,8 catalytic function would indicate different temperature dependent kinetic parameters according to the above mentioned results. The Cst-II15 did not show any activity with the acceptor **9** and **11**, *i.e.* sialylated derivatives of Type III acceptor substrate. This fact can be explained with the probably very high K_M value of the enzyme for the particular acceptor, which was not accessed in the experiments.

Table 4.11 Determination of the enzyme kinetic parameters for the Cst-II15 and $\Delta 32$ Cst-II15 (see chapter 3.3.7.9). OSE: O-(trimethylsilyl)ethyl (O-CH₂CH₂-Si(Me)₃), OLem: O-(Methoxycarbonyl)octyl (O-(CH₂)₈CO₂Me), TCA: tri-chloro acetyl (COCCl₃). It was converted ~20% of substrate.

| | | Cst-II15/ $\Delta 32$ Cst-II15 | | | | | | | | | | | | | | | |
|-------------------------|--|-----------------------------------|-----------|-----------|-----------|---------------|-----------|-----------|-----------|--|-----------|-----------|-----------|---|-----------|-----------|-----------|
| | | k_{cat} (min ⁻¹) | | | | K_M (mM) | | | | k_{cat}/K_M (mM ⁻¹ min ⁻¹) | | | | V_{max} (nmol min ⁻¹ ml ⁻¹) | | | |
| Acceptor | | Full | | Trunc. | | Full | | Trunc. | | Full | | Trunc. | | Full | | Trunc. | |
| α -2,3/2,8 ST | 2 (Type I) (Gal β 1,3GlcNAc- β -OLem) | 77.44 | | 25.07 | | 0.36 | | 0.69 | | 216.08 | | 36.31 | | 26.97 | | 37.70 | |
| | 4 (Gal β 1,3GalNHTCA- β -OSE) | 77.06 | | 21.62 | | 0.31 | | 0.59 | | 247.38 | | 36.55 | | 26.83 | | 32.50 | |
| | 3 (Gal β 1,3GalNAc- β -OSE) | 72.31 | | | | 2.20 | | | | 32.85 | | | | 25.18 | | | |
| | 5 (Gal β 1,3Gal- β -OSE) | 51.83 | | 25.87 | | 0.81 | | 2.09 | | 63.66 | | 12.40 | | 18.05 | | 38.90 | |
| | 13 (D-Lactose- β -OSE) | | | 16.74 | | | | 0.47 | | | | 35.35 | | | | 25.16 | |
| Temperature [°C] | | 25 | 37 | 25 | 37 | 25 | 37 | 25 | 37 | 25 | 37 | 25 | 37 | 25 | 37 | 25 | 37 |
| α -2,8 ST | 8 (Sia α 2,3Gal β 1,3GlcNAc- β -OLem) | 58.23 | 310.65 | 7.14 | 29.43 | 2.62 | 17.49 | 1.77 | 7.68 | 22.27 | 17.76 | 4.02 | 3.83 | 20.28 | 108.17 | 10.74 | 44.25 |
| | 7 (Sia α 2,3Gal β 1,4GlcNAc- β -OLem) | 59.01 | 80.07 | | 35.56 | 1.22 | 2.02 | | 8.09 | 48.25 | 39.56 | | 4.40 | 20.55 | 27.88 | | 53.46 |
| | 10 (Sia α 2,3Gal β 1,3GalNHTCA- β -OSE) | 51.36 | 56.23 | | | 2.06 | 2.80 | | | 24.89 | 20.08 | | | 17.89 | 19.58 | | |
| | 14 (Sia α 2,3-D-Lactose-OSE) | | | | 0.57 | | | | 0.47 | | | | | 1.21 | | | 0.85 |
| | 9 (Sia α 2,3Gal β 1,3GalNAc- β -OSE) | | 0 | | | | 0 | | | | 0 | | | | 0 | | |
| | 11 (Sia α 2,3Gal β 1,3Gal- β -OSE) | | 0 | | | | 0 | | | | 0 | | | | 0 | | |

The same acceptors were used for the kinetic parameter determination of the N- and C-His tag expressed soluble form of the Cst-II enzyme ($\Delta 32\text{Cst-II15}$ and $\Delta 32\text{Cst-II21}$). The soluble $\Delta 32\text{Cst-II15}$ obtained similar results concerning the α -2,3/2,8 catalytic efficiency for two different acceptors. To be more precise, for the acceptors **2** and **5**, catalytic efficiency was $\sim 25 \text{ min}^{-1}$, whereas K_M value for acceptor **5** was ~ 3 -fold higher (2.09 mM) comparing to the acceptor **2**. Acceptor **4** and **13** showed slightly decreased catalytic efficiency, 21.62 min^{-1} and 16.74 min^{-1} but almost similar the Michaelis-Menten parameters 0.59 mM and 0.47 mM, respectively. Comparison of the kinetic parameters obtained for the α -2,3/2,8 catalytic activity of $\Delta 32\text{Cst-II15}$ to those of $\Delta 32\text{Cst-II21}$ revealed similarities and differences. For instance, catalytic efficiency of $\Delta 32\text{Cst-II21}$ was slightly better for the acceptor **2**, **4** and **13**, whereas the K_M value remain almost in the same range. The $\Delta 32\text{Cst-II21}$ with the substrate **5** displayed ~ 3 -fold higher catalytic efficiency and 3-fold higher K_M value (6.18 mM) comparing to the $\Delta 32\text{Cst-II15}$. An additional acceptor **3** was used to obtain kinetic parameters for the $\Delta 32\text{Cst-II21}$. These results demonstrated half of the catalytic efficiency and enzyme affinity obtained for an acceptor **5**. Taking into account the kinetic parameters obtained for α -2,8 catalytic activity of $\Delta 32\text{Cst-II15}$ and $\Delta 32\text{Cst-II21}$ enzymes, similarly a low catalytic efficiency and accordingly very high Michaelis constant was obtained. More precisely, α -2,8 catalytic function of $\Delta 32\text{Cst-II21}$ exhibited catalytic efficiency of 23.03 min^{-1} for acceptor **7**. For the same acceptor, the $\Delta 32\text{Cst-II15}$ showed a catalytic efficiency of 35.56 min^{-1} . Both enzymes exhibited extremely low activity, if any, with acceptor **14**.

Table 4.12 Enzyme kinetic parameters for the $\Delta 32\text{Cst-II21}$ were determined as described in chapter 3.3.7.9. OSE: O-(trimethylsilyl)ethyl (O-CH₂CH₂-Si(Me)₃), OLem: O-(Methoxycarbonyl)octyl (O-(CH₂)₈CO₂Me), TCA: tri-chloro acetyl (COCCl₃). It was converted ~20% of the substrate into product.

| Acceptor | | $\Delta 32\text{Cst-II21}$ | | | | | | | |
|-------------------------|--|--|-----------|---------------|-----------|---|-----------|--|-----------|
| | | k_{cat} (min ⁻¹) | | K_M (mM) | | k_{cat}/K_M (mM ⁻¹ min ⁻¹) | | V_{max} (nmol min ⁻¹ ml ⁻¹) | |
| α -2,3/2,8 | 2 (Type I) (Gal β 1,3GlcNAc- β -OLem) | 28.78 | | 0.54 | | 53.02 | | 101.08 | |
| | 4 (Gal β 1,3GalNHTCA- β -OSE) | 29.70 | | 0.75 | | 39.68 | | 104.33 | |
| | 3 (Gal β 1,3GalNAc- β -OSE) | 31.07 | | 3.998 | | 7.77 | | 109.15 | |
| | 5 (Gal β 1,3Gal- β -OSE) | 70.51 | | 6.18 | | 11.41 | | 247.68 | |
| | 13 (D-Lactose- β -OSE) | 22.64 | | 0.57 | | 39.42 | | 79.52 | |
| Temperature [°C] | | 25 | 37 | 25 | 37 | 25 | 37 | 25 | 37 |
| α -2,8 ST | 8 (Sia α 2,3Gal β 1,3GlcNAc- β -OLem) | 6.14 | | 4.19 | | 1.47 | | 21.55 | |
| | 7 (Sia α 2,3Gal β 1,4GlcNAc- β -OLem) | 7.93 | 23.03 | 1.02 | 3.79 | 7.77 | 6.08 | 27.81 | 80.75 |
| | 14 (Sia α 2,3-D-Lactose- β -OSE) | | 0.24 | | 0.291 | | 0.82 | | 0.42 |

Comparing the results obtained in these experiments with the recently published kinetic data [151,183,264], it was possible to observe some variations in the enzyme's ability to act in the same way with the same acceptor substrate. Thus, the published soluble Cst-II revealed a α -2,3/2,8 catalytic efficiency of 1.1 mM⁻¹ min⁻¹ and K_M of 35 mM with lactose (**13**). In contrast, the α -2,8 function revealed 16-fold higher catalytic efficiency and therefore 10-fold decreased K_M of 3.5 mM with sialylated lactose acceptor (**14**) [183]. In order to evaluate the data, it was very important to make the comparison between the published enzyme sequence and the enzyme sequence used in our experiments. The available data were obtained by the Cst-II enzyme expressed from the OH4384 *C. jejuni* strain. The Cst-II from the mentioned strain differs by eight amino acids from the enzyme expressed in the ATCC43438 strain of *C. jejuni*, which was used in our studies. This similarity on the DNA level and correlated primary protein structure (97.3%) enables both

strains to express the bifunctional activity of the Cst-II enzyme. Nevertheless, comparison of the reported kinetic parameters and those obtained in this study demonstrate very low similarity regarding the same acceptor substrates. It should be mentioned that the observed differences of kinetic parameters might be due to the 6-(5-fluorescein-carboxamido)-hexanoic acid succinimidyl ester (FCHASE)-labeled oligosaccharide acceptors and the enzyme assay used to determine the published OH4384 Cst-II activity. In fact, the reported enzyme exhibited much lower α -2,3 than α -2,8 sialyltransferase activity, while the Cst-II isolated from ATCC43438 showed exactly the opposite behavior. In 2002, Gilbert *et al.* [264] reported cloning and expression of six different Cst-II proteins originating from different *C. jejuni* strains. These *E. coli*-expressed Cst-II recombinant proteins were assayed for the α -2,3 and the α -2,8 sialyltransferase activity using FCHASE-labeled non-sialylated and sialylated lactose oligosaccharides, respectively, as acceptors. It was found that only four out of six Cst-II proteins showed bifunctional sialyltransferase activity, while other two demonstrated exclusively the α -2,3 catalytic activity. An alignment of the amino acid sequences of the various Cst-II versions indicated that only three residues, *i.e.* Asn51, Leu54 and Ile269 were specific for the bifunctional Cst-II versions. Using site directed mutagenesis, it was found that an Asn51→Thr substitution completely abolished the α -2,8 sialyltransferase activity in the OH4384 *C. jejuni* strain. The inversed substitution (Thr51→Asn) in the monofunctional Cst-II from ATCC43446 strain confirmed the importance of Asn51 within the enzyme sequence for the α -2,3 and the α -2,8 activities. The other two residues (Leu54 and Ile269), unique to bifunctional Cst-II variants, as well as the very variable residue 53, were found to affect the relative ratios of α -2,3 and α -2,8 sialyltransferase activities. Only Asn51 was found to be essential for the α -2,8 activity. The amino acid substitution Ile53→Gly increased both activities of the OH4384 version, which suggested that this residue has an important impact on the level of *in vitro* activity. It was noticed as well that the strains with Ser53 have much lower α -2,3 than α -2,8 sialyltransferase activity [264]. A randomly mutated (I53S) and soluble form of the enzyme (Cst-II Δ 32) was generated by deletion of the predicted membrane spanning domain at the C-terminus (32 amino acids), and was co-crystallized with a donor sugar CMP-3-fluoro-*N*-acetylneuraminic acid (CMP-3FNeuNAc) analog (Figure 4.43). The first structure and glycosyl transfer mechanism of sialyltransferase, that of Cst-II from the OH4384 *C. jejuni* strain was reported by Chiu *et al.* [183].

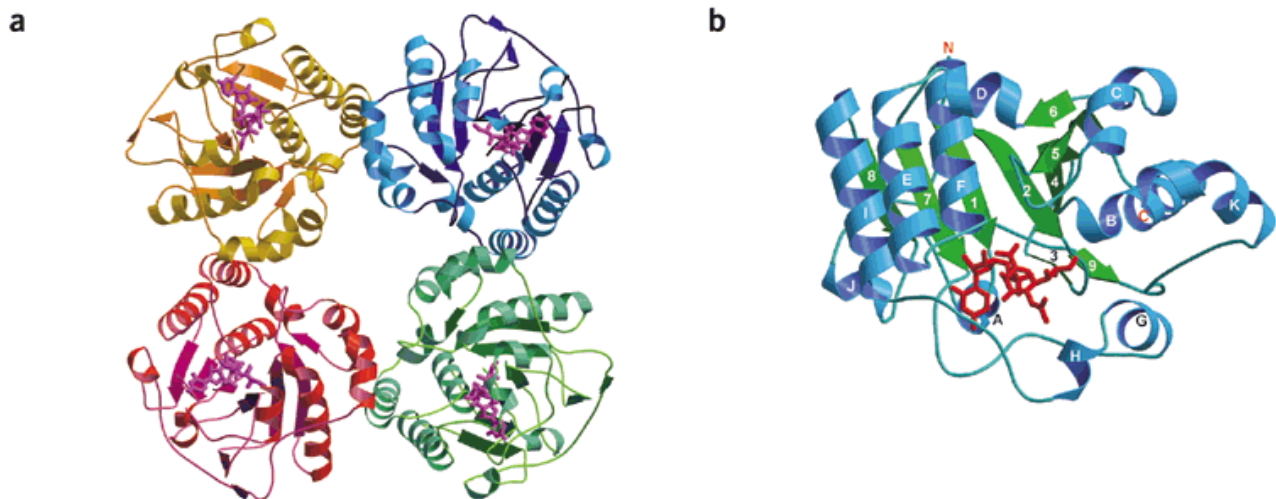


Figure 4.43 (a) The overall architecture of Cst-II Δ 32. Arrangement of the Cst-II Δ 32 tetramer. Each monomer is colored differentially. A donor sugar analog (CMP-3FNeuNAc) is shown as a stick representation in magenta color, indicating the location of the catalytic center. **(b)** View of the Cst-II Δ 32 monomer showing the N-terminal domain and the lid-like domain with bound donor sugar analog. CMP-3FNeuNAc is represented as a red stick. The N-terminus, C-terminus, individual strands and individual helices are labeled [183].

It was shown that the enzyme forms a tetramer in the asymmetric unit of the crystal. Each monomer of Cst-II Δ 32 consists of 259 residues organized in two domains. The first domain (residues 1 – 154, 189 – 259) create the nucleotide-binding domain in the form of the Rossmann fold [56]. The active site is not at the interface between monomers of the tetramer, suggesting that the oligomerization of the enzyme has no direct role in catalysis. The second, smaller domain (155-188) forms a lid-like structure that folds over the active site. This domain is ordered only after binding of the CMP-NeuNAc substrate, suggesting that the lid probably fulfills several functions in catalysis; directly liganding the donor sugar, creating the acceptor sugar binding site and shielding the enzyme active site from bulk solvent thereby minimizing side reactions such as hydrolysis of substrate, as was observed in other GTs [58,59]. Concerning the CMP binding, it was found that CMP binds to a deep cleft in the nucleotide-binding domain at the C-terminal end of the central β -sheet. This suggests that this location of the active site at the protein-membrane interface facilitates transfer of the sugar onto the terminus of the LOS. The LOS is assembled on the cytoplasmic face of the inner membrane, and transported onto the cell surface by ABC transporter. The CMP is relatively buried within the active site cleft with several favorable

interactions formed within the active site (Figure 4.44).

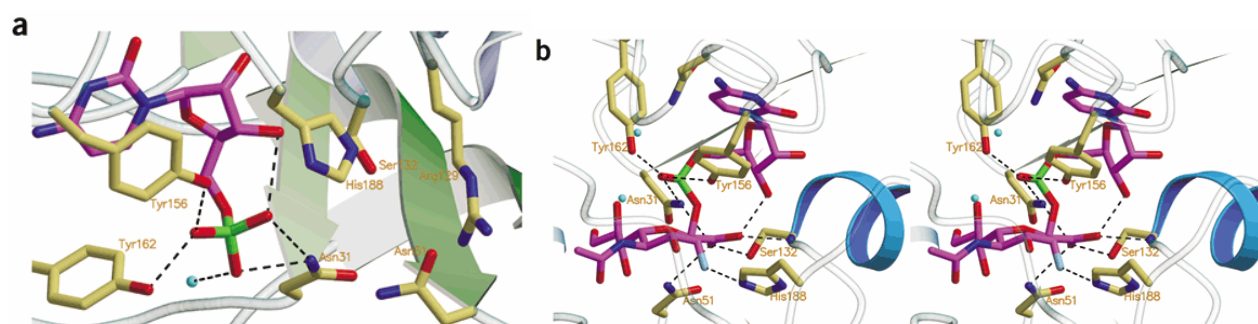


Figure 4.44 The active site of Cst-IIΔ32. **(a)** Interactions of CMP and active site residues. CMP is depicted in CPK coloring with carbon atoms in magenta, nitrogen atoms in blue, oxygen atoms in red and phosphorus atom in green. Active site residues involved in CMP binding and catalysis are labeled and shown with carbon atoms in beige, nitrogen in blue and oxygen in red. H₂O molecules are shown as cyan spheres. Dotted lines indicate hydrogen bonding; **(b)** Interactions of CMP-3FNeuAc and key active site residues. CMP-3FNeuAc is depicted in CPK coloring as in a with the fluorine atom in light blue. The Helix F is highlighted as a blue ribbon [183].

A mutation, I53S, which lies on the periphery of the acceptor sugar binding site, in a cleft adjacent to the NeuNAc, may promote stabilization of the Cst-IIΔ32 construct through interaction with the acceptor substrates.

4.3.4.8 α -2,3/2,8 enzyme activity of the mutated and truncated enzyme

According to these characteristics, regarding the very similar OH4384 Cst-II mentioned above, we decided to improve α -2,8 sialyltransferase activity of the Δ 32Cst-II15 construct using site directed mutagenesis. Increased α -2,8 catalytic activity would be extremely helpful for the preparative chemo-enzymatic synthesis of distinct ganglioside-derivatives. The Cst-II enzyme of both *C. jejuni* strains, the ATCC43438 and the ATCC43432, naturally involved Gly-53. Despite the likely large impact Gly-53 was expected to have on *in vitro* activity [264], this residue was replaced with Ser-53 using site directed mutagenesis. As mentioned before, Ser53 was believed to promote stabilization of Cst-II enzyme, to affect relative ratios of α -2,3 and α -2,8 activities and to enhance α -2,8 sialyltransferase specificity [183,264]. In addition, *in silico* analysis of the X-ray structure of OH4384 Cst-II published by Chiu *et al.* [183], revealed two variable amino acids, *i.e.* Asn177 and Asn182 close to the binding site. These two positions in the case of the ATCC43438 Cst-II enzyme

were occupied by a negatively charged Asp177 and positively charged Arg182. We assumed that this difference in charge might have been the reason for the very low α -2,8 activity of the Cst-II enzyme expressed from ATCC43438 strain. The α -2,3 activity was not disturbed when Gly53 was substituted by Ser. In contrast, one (Asp177→Asn) or two additional mutations (Arg182→Asn) in the truncated Cst-II protein decreased α -2,3 and increased α -2,8 activity. Comparison of the results obtained with soluble wild type (Δ 32Cst-II15) and additionally mutated Cst-II (Δ 32Cst-II15S53N177N182) confirmed previously mentioned differences concerning α -2,3 and α -2,8 activity. Mutated enzyme revealed 50% decreased activity with non-sialylated Type I (**2**) and Type II (**1**) acceptor substrate. In contrast, α -2,8 activity was increased for 50%, when the sialylated acceptor substrates **8** was used for the enzyme activity test (Figure 4.45). Similar results were obtained for the α -2,8 activity of the mutated enzyme incubated with acceptor **7**.

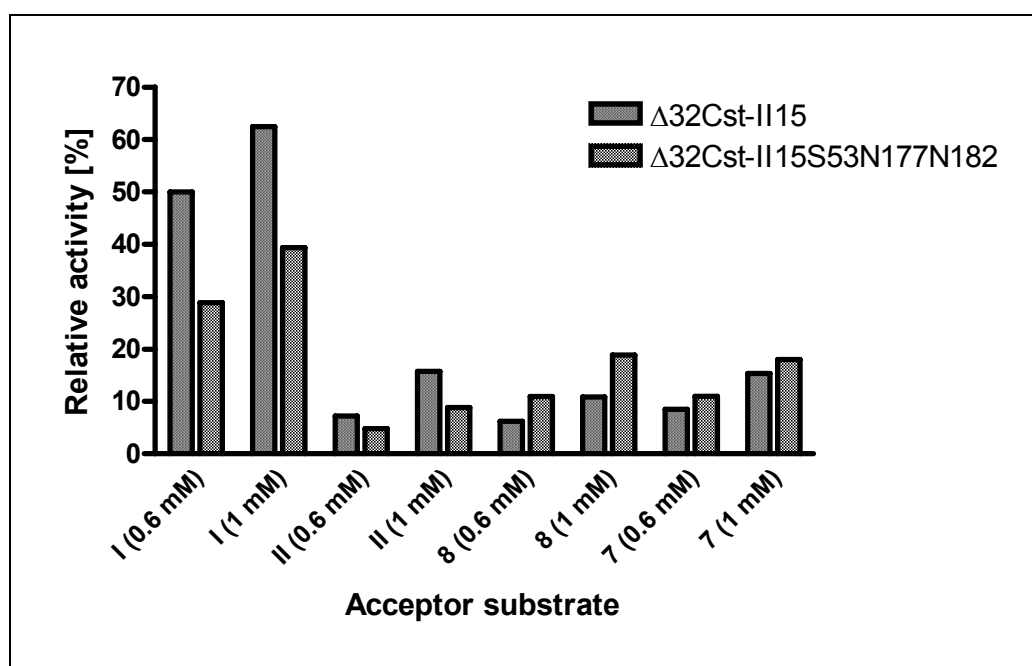


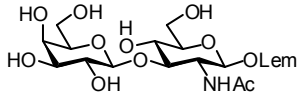
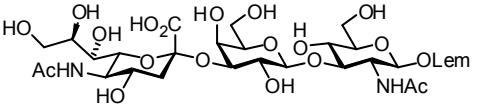
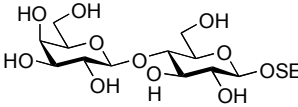
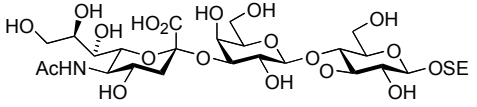
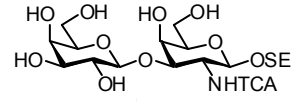
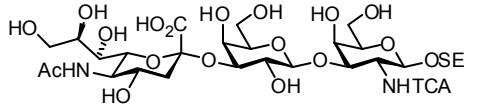
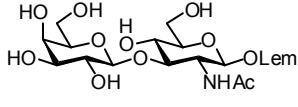
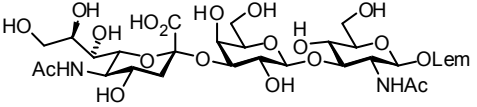
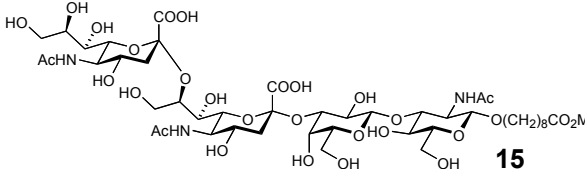
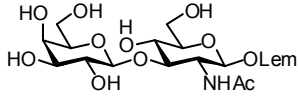
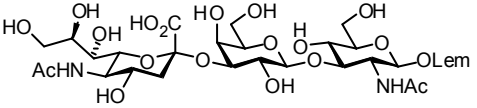
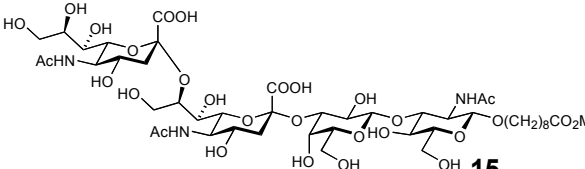
Figure 4.45 The comparison of Δ 32Cst-II15 and Δ 32Cst-II15S53N177N182 activity using 600 μ M and 1 mM of **2** (Type I) and **1** (Type II), and **8** and **7**, for the α -2,3/2,8 and α -2,8 ST activity, respectively.

4.3.4.9 Preparative chemo-enzymatic synthesis using α -2,3/2,8 ST

The successful site directed mutagenesis according to the predicted *in silico* data gave us the possibility to perform preparative chemo-enzymatic synthesis thanks to the improved

α -2,8 activity of Cst-II. The accomplished results, verified by NMR and MS analysis, demonstrated the synthesis of only monosialylated product in the case of acceptor **2** and **13** achieving 76% and 80% of the product **8** and **14**, respectively (*Table 4.13*). However, incubation of Δ 32Cst-II21 with the acceptor **4** did not give any product. Mutated enzyme with improved α -2,8 activity was used for the synthesis of disialylated compounds using **2** (Type I) acceptor as a starting material. Finally, mutated enzyme, which demonstrated 50% improved α -2,8 catalytic activity compared to the wild type enzyme, was able to react and produce tri- and tetrasaccharide. The enzyme exhibited different affinity for the **2** (Type I) and trisaccharide **8**, showing stronger preference for the non-sialylated acceptor substrate. This was expected, since the enzyme should mainly produce trisaccharide product in order to use it as an acceptor substrate in the α -2,8 catalytic activity. Therefore, preparative synthesis followed by TLC indicated formation of 55% of product **8** and 13% of the product **15**. The structure of both products were verified by NMR and MS analysis confirming an occurrence of the α -2,3 and α -2,8 glycosidic-linkages. The preparative synthesis, *i.e.* chemo-enzymatic reaction reproducibly gave approximately 50% of the product **15** using the acceptor substrate **8** as a starting material. It was observed that the reaction slowed down and did not proceed further, although an additional aliquot of the enzyme and donor substrate was added. This could be explained by the hydrolysis of the CMP-NeuNAc. Namely, while crystallizing the Cst-II in the presence of the donor and acceptor substrate, kinetic analysis showed considerable hydrolysis of the CMP-NeuNAc in the absence of an acceptor catalyzed by both truncated and the full-length Cst-II [183]. This finding was very similar to the fact observed almost 25 years ago by Beyer *et al.* [22]. These studies showed that the reactions of the β -galactoside α -2,3 sialyltransferase and the α -*N*-acetylgalactosaminide α -2,6 sialyltransferase were reversible. Thus, it was possible to demonstrate a CMP-dependent “neuraminidase” activity associated with these sialyltransferases. Under conditions used for glycosylation, the equilibrium heavily favored the formation of products.

Table 4.13 Isolated yields and kinetic data of the enzymatic sialidations. OSE: O-(trimethylsilyl)ethyl (O-CH₂CH₂-Si(Me)₃), OLem: O-(Methoxycarbonyl)octyl (O-(CH₂)₈CO₂Me), TCA: tri-chloro acetyl (COCCl₃).

| Entry | Acceptor | Product | Isol. Prod. | Recov. Accept. | Product | Isol. Prod. | Recov. Accept. | Enzyme |
|-------|---|--|-------------|----------------|--|-------------|----------------|----------------------------|
| | | | [%] | [%] | | [%] | [%] | |
| 1 |  2 |  8 | 76 | - | - | - | - | Cst-II15 |
| 2 |  13 |  14 | 80 | 20 | - | - | - | Δ32Cst-II21 |
| 3 |  4 |  10 | - | 93 | - | - | - | Δ32Cst-II21 |
| 4 |  2 |  8 | 55 | 32 |  15 | 13 | - | Δ32Cst-II15S53N 177N182 |
| 5 |  2 |  8 | - | - |  15 | 48/53 | 48/46 | Δ32Cst-II15S53N 177N182 |

5 Conclusions and Outlook

Enzymes responsible for the terminal sialylation are sialyltransferases (STs), a subset of the glycosyltransferase (GT) family that uses CMP-NeuNAc as the activated sugar donor and catalyzes the transfer of sialic acid residues to terminal non-reducing positions of oligosaccharide chains of glycoproteins and glycolipids. Sialylated oligosaccharide sequences have long been predicted to be information – containing molecules and critical determinants, *e.g.* in cell-cell recognition processes, cell-matrix interactions and maintenance of serum glycoproteins in the circulation [79,80]. Our work was focused on the myelin-associated glycoprotein (MAG) and its physiological ligands, *i.e.* brain gangliosides. MAG [199,203,204,213] has been identified as one of the neurite outgrowth-inhibitory proteins, together with Nogo-A and the oligodendrocyte myelin glycoprotein (OMgp) [192,201,310]. Among all physiological ligands of MAG, *i.e.* brain gangliosides, the GQ1b α is the most potent natural ligand identified so far [235,236]. Therefore, this ganglioside was chosen as a lead structure in our MAG project. Moreover, only the sialic acid containing part of the GQ1b α molecule was shown to be important for MAG binding. Thus, we decided to use a chemo-enzymatic approach for the syntheses of the GQ1b α mimetics. In order to perform preparative chemo-enzymatic synthesis of sialylated structures it was necessary to express distinct sialyltransferases able to catalyze the formation of α -2,3, α -2,6 and α -2,8 glycosidic-linkages.

Recombinant eukaryotic rST3Gal III (EC 2.4.99.6) was expressed as a secreted protein in baculovirus infected insect cells and purified by CDP-hexanolamine-agarose. Enzyme activity was confirmed using ST enzyme activity assays. Our investigations [249,250] showed, in addition to previous reports [252,253,275,288,289,311], an unexpectedly high substrate tolerance of recombinant rST3Gal III. The kinetic data for the sialylation reactions indicated that the activity of rST3Gal III with the Type III derivatives was reduced only about 10-fold compared to its Type I and Type II natural substrates. The enzyme, therefore, accepted the replacement of the natural GlcNAc moiety by Gal, GalNAc and GalNHTCA. Thus, the preparative applicability of the sialyltransferase has been substantially extended.

Furthermore, recombinant human ST6Gal I (*hST6 Gal I*; EC 2.4.99.1) was expressed as a soluble protein in a mammalian expression system (BHK cells) and purified to homogeneity by CDP-hexanolamine-agarose affinity chromatography. The activity of the purified protein was confirmed with the ST activity assay. The BT-*hST6Gal I* exhibited 20-fold higher substrate affinity towards asialofetuin than for Type II acceptor substrate. This observation was not surprising, since it is well known, that less effective acceptor substrates include lactose (Gal β (1,4)Glc) and other disaccharides with galactose β -linked to the penultimate sugar [298]. Preparative *in vitro* sialylation of diantennary substrate acceptor using BT-*hST6Gal I* showed mono- and disialylated diantennary *N*-acetylglucosamine type acceptor substrate. Sialylated product analyzed by MALDI/TOF-MS and methylation showed mono- and disialic acid α -2,6 glycosidically linked to the terminal galactose residue in both, Man-3 and Man-6 antennae.

Thirdly, the main project involved recombinant prokaryotic *Campylobacter jejuni* α -2,3/2,8 bifunctional sialyltransferase (Cst-II), and its cloning and expression in *E. coli* as a His-tagged full length (~36 kDa) and truncated, *i.e.* soluble (~33 kDa) enzyme using pET expression systems. The enzyme overexpression and solubility was confirmed with SDS-PAGE and Western blot using monoclonal mouse anti-His tag antibody. Estimated by Bradford, a soluble form of the enzyme was expressed at very high level (~460 mg/l) compared to its full length counterpart (~1.69 mg/l). Therefore, the N- and C-His tagged soluble form of Cst-II, *i.e.* Δ 32Cst-II15 and Δ 32Cst-II21, were successfully purified to homogeneity using Ni-NTA affinity chromatography. Enzyme activity was confirmed using ST activity assay.

The enzyme exhibited slightly distinct specificity with non-sialylated and sialylated acceptor substrates, when incubated at different temperatures. The maximal α -2,3/2,8 sialyltransferase relative activity of the Δ 32Cst-II15 was detected at 25°C, whereas 37°C revealed the optimal temperature for the maximal α -2,8 enzyme activity. The kinetic data revealed the wide optimal pH range, *i.e.* pH 7.0 – 10.0. It was observed that cofactors were not essential for enzyme activity and the enzyme remained active in the presence of EDTA. The activity pattern of the both enzymes at pH 7.5, with a panel of distinct cations, indicated that it could be modulated by these metals, *e.g.* incubation with Ni²⁺, Zn²⁺ and Co²⁺ almost completely abolished the enzyme activity (~85%) or in the presence of Cu²⁺ no activity was detected. The enzyme did not require cofactors, since enzyme activity was not changed in the presence of these substances. Besides, the enzyme also remains

active within the wide range of DMSO concentrations used to dissolve water insoluble acceptors. A full-length and soluble enzyme constructs were used to determine enzyme kinetic parameters with several non-sialylated and sialylated acceptor substrates. In general, all enzyme constructs showed the best α -2,3/2,8 catalytic efficiency with acceptor **2** (Type I), **4** and **13**, whereas very low α -2,8 catalytic efficiency was observed with acceptor substrates **7** and **8**. The Cst-II15 and Δ 32Cst-II21 purified proteins were applied for preparative synthesis using **2** (Type I) and **13** acceptor substrates. The results obtained by synthesis and verified by NMR and MS analysis, demonstrated production of 76% and 80% of monosialylated product **8** and **14**, respectively. In order to improve α -2,8 sialyltransferase activity of Δ 32Cst-II15 construct we have mutated the enzyme using *in silico* obtained data and site directed mutagenesis method. Mutated enzyme, Δ 32Cst-II15S53N177N182 revealed 50% decreased activity with non-sialylated **2** (Type I) and **1** (Type II) acceptor substrate. In contrast, the α -2,8 activity was increased for 50% when sialylated acceptor substrates **8** was used for the enzyme activity test.

The mutated enzyme was used for preparative chemo-enzymatic synthesis of GQ1b α mimetics. Analysis indicated the formation of 55% of monosialylated product **8** and 13% of the disialylated product **15**. The structure and mass of both products were verified by NMR and MS analysis confirming the occurrence of the α -2,3 and α -2,8 glycosidic-linkages.

In outlook, truncated and full length form of the recombinant prokaryotic *Campylobacter jejuni* α -2,3/2,8 bifunctional sialyltransferase (Cst-II) cloned and expressed in *E. coli* should be used for the X-ray crystal structure analysis co-crystallizing with the ligand and acceptor substrate. Prior to these studies, Cst-II should be further purified over a CDP-hexanolamine-agarose affinity column to isolate only a fraction containing the bifunctionally active enzyme. Besides, the enzyme activity towards gangliosides and many other chemically synthesized oligosaccharides should be first verified by determining the enzyme kinetic parameters. It would be important to solve the function and a possible influence of the metal cofactors on the enzyme catalytic efficiency.

More data could further improve the specific activity of the enzyme and contribute to its successful usage for the preparative chemo-enzymatic synthesis of the sialylated GQ1b α mimetics. Hence, the synthesis on a milligram scale of a number of modified sialyloligosaccharides indicates that the sialyltransferases can be exploited as biocatalysts in the synthesis of interesting non-natural compounds, which is particularly valuable in view of the difficulties in chemical sialylation.

6 Abbreviations

| | |
|--------------------|--|
| AcNPV | <i>Autographa californica</i> nuclear polyhedrosis virus |
| Arg | Arginine |
| Asn | Asparagine |
| Asp | Aspartate |
| ATP | Adenosine triphosphate |
| AU | Absorption unit |
| BHK | Baby hamster kidney |
| BmPV | <i>Bombyx mori</i> polyhedrosis virus |
| BSA | Bovine serum albumine |
| β -TP | β -trace protein |
| cAMP | Cyclic adenosine monophosphate |
| cDNA | Complementary deoxyribonucleic acid |
| CDP | Cytidine diphosphate |
| CH ₃ CN | Acetonitrile |
| CIAP | Calf intestine alkaline phosphatase |
| CMP-NeuNAc | cytidine monophosphate- <i>N</i> -acetyl neuraminic acid |
| CRD | Consensus repeat domains |
| Cst-II | <i>Campylobacter jejuni</i> sialyltransferase |
| Cys | Cystein |
| DMSO | dimethyl sulfoxid |
| DTE | 1,4-Dithioerythritol |
| DTT | Dithiothreithol |
| <i>E. coli</i> | <i>Escherichia coli</i> |
| EDTA | Ethylendiaminetetraacetic acid |
| FBS | Fetal bovine serum |
| FCHASE | 6-(5-fluorescein-carboxamido)-hexanoic acid succimidyl ester |
| FCS | Fetal calf serum |

| | |
|---------------|--|
| FPLC | Fast protein liquid chromatography |
| Fuc | Fucose |
| FucT | Fucosyl transferase |
| Gal | Galactose |
| GalNAc | <i>N</i> -acetyl galactosamine |
| Glc | Glucose |
| GlcNAc | <i>N</i> -acetyl glucosamine |
| Glu | Glutamine |
| GuHCl | Guanidium hydrochloride |
| HAB | Hepes assay buffer |
| His | Histidine |
| HMW | high molecular weight marker |
| HPAEC-PAD | high-pH anion-exchange chromatography-pulsed amperometric detection |
| HTS | High throughput screening |
| IFN- γ | Interferon γ |
| IgG | Immunoglobulin G |
| IMAC | Immobilized metal ion affinity chromatography |
| IPTG | Isopropyl- β -D-Thiogalactosid |
| LB | Lauria Bretani |
| LMW | low molecular weight marker |
| LPS | Lipopolysaccharide |
| M.O.I. | Multiplicity of infection |
| mAb | Monoclonal antibody |
| MS | Mass spectrometry |
| NAD | β -nicotinamide adenine dinucleotide (oxidized form) |
| NADH | β -nicotinamide adenine dinucleotide (reduced form) |
| NADP | β -Nicotinamide adenine dinucleotide phosphate (oxidized form) |
| NADPH | β -Nicotinamide adenine dinucleotide phosphate (reduced form) |

| | |
|------------------|--|
| NBT/BCIP | Nitro-blue tetrazolium chloride/5-bromo-4-chloro-3-indolylphosphate |
| N-CAM | Neural cell adhesion molecule |
| NeuNAc | <i>N</i> -acetylneuraminic acid |
| Ni-NTA | Nickel-nitrilotriacetic acid |
| NMR | Nuclear magnetic resonance |
| OD | Optical density |
| OLem | O-(Methoxycarbonyl)octyl (O-(CH ₂) ₈ CO ₂ Me) |
| OSE | O-(trimethylsilyl)ethyl (O-CH ₂ CH ₂ -Si(Me) ₃), |
| PBS | Phosphate buffer saline |
| PCR | Polymerase chain reaction |
| Pi | post-infection |
| pET | expression vector His |
| pEZZ18 | expression vector ssZZ |
| Pfu | Plaque forming units |
| RB | reducing buffer |
| RT | Room temperature |
| SDS-PAGE | Sodium-dodecyl-sulfat polyacrylamide-gel-electrophoresis |
| Sf | <i>Spodoptera frugiperda</i> |
| Sia | Sialic acid |
| sLe ^a | Sialyl Lewis a |
| sLe ^x | Sialyl Lewis X |
| TBS | Tris buffered saline |
| TE | tris-EDTA buffer |
| TEMED | N,N,N',N'-Tetramethylethylenediamine |
| TFA | Trifluoroacetic acid |
| Tris | (Hydroxymethyl)-Aminomethan |
| TTBS | TBS with 0.05% Tween 20 |
| Tyr | Tyrosine |

| | |
|-----|-----------------------------------|
| TYE | trypton enriched medium |
| ZZ | two synthetic IgG-binding domains |

7 References

- [1] J. Montreuil, J.F.G. Vliegthart, H. Schachter, *New Comprehensive Biochemistry, Vol. 30, Glycoproteins and Disease*, Elsevier Science, Amsterdam, **1996**.
- [2] P.H. Wang, W.L. Lee, C.M. Juang, Y.H. Yang, W.H. Lo, C.R. Lai, S.L. Hsieh, C.C. Yuan, *Gynecol Oncol* **2005**,
- [3] E. Dabelsteen, S. Gao, *J Dent Res* **2005**, *84*, 21-28.
- [4] O. Lerouxel, G. Mouille, C. Andeme-Onzighi, M.P. Bruyant, M. Seveno, C. Loutelier-Bourhis, A. Driouich, H. Hofte, P. Lerouge, *Plant J* **2005**, *42*, 455-468.
- [5] F. Dall'Olio, M. Chiricolo, *Glycoconj J* **2001**, *18*, 841-850.
- [6] K. Angata, J. Nakayama, B. Fredette, K. Chong, B. Ranscht, M. Fukuda, *J Biol Chem* **1997**, *272*, 7182-7190.
- [7] F. Dall'Olio, M. Chiricolo, C. Ceccarelli, F. Minni, D. Marrano, D. Santini, *Int J Cancer* **2000**, *88*, 58-65.
- [8] F. Dall'Olio, M. Chiricolo, A. D'Errico, E. Gruppioni, A. Altimari, M. Fiorentino, W.F. Grigioni, *Glycobiology* **2004**, *14*, 39-49.
- [9] M. Leivonen, S. Nordling, J. Lundin, K. von Boguslawski, C. Haglund, *Oncology* **2001**, *61*, 299-305.
- [10] E.V. Chandrasekaran, R.K. Jain, R.D. Larsen, K. Wlasichuk, K.L. Matta, *Biochemistry* **1995**, *34*, 2925-2936.
- [11] A. Varki, *Glycobiology* **1993**, *3*, 97-130.
- [12] E.W. Easton, J.G. Bolscher, D.H. van den Eijnden, *J Biol Chem* **1991**, *266*, 21674-21680.
- [13] J.C. Paulson, K.J. Colley, *J Biol Chem* **1989**, *264*, 17615-17618.
- [14] J.U. Baenziger, *Faseb J* **1994**, *8*, 1019-1025.
- [15] M. Fukuda, M.F. Bierhuizen, J. Nakayama, *Glycobiology* **1996**, *6*, 683-689.
- [16] J.E. Sadler, Beyer T.A., Openheimer C.L., Paulson J.C., Prieels J.P., Rearick J.I. and Hill R.L., *Methods Enzymol* **1982**, *83*, 458-514.
- [17] R. Kleene, E.G. Berger, *Biochim Biophys Acta* **1993**, *1154*, 283-325.
- [18] S. Tsuji, *J Biochem (Tokyo)* **1996**, *120*, 1-13.
- [19] C. Breton, A. Imberty, *Curr Opin Struct Biol* **1999**, *9*, 563-571.
- [20] B.W. Murray, S. Takayama, J. Schultz, C.H. Wong, *Biochemistry* **1996**, *35*, 11183-11195.
- [21] H. Clausen, E.P. Bennett, *Glycobiology* **1996**, *6*, 635-646.
- [22] T.A. Beyer, J.I. Rearick, J.C. Paulson, J.P. Prieels, J.E. Sadler, R.L. Hill, *J Biol Chem* **1979**, *254*, 12531-12534.
- [23] A. Harduin-Lepers, V. Vallejo-Ruiz, M.A. Krzewinski-Recchi, B. Samyn-Petit, S. Julien, P. Delannoy, *Biochimie* **2001**, *83*, 727-737.
- [24] R.L. Hill, K. Brew, *Adv Enzymol Relat Areas Mol Biol* **1975**, *43*, 411-490.
- [25] C. Breton, R. Oriol, A. Imberty, *Glycobiology* **1998**, *8*, 87-94.
- [26] K. Drickamer, *Glycobiology* **1993**, *3*, 2-3.

- [27] A.K. Datta, A. Sinha, J.C. Paulson, *J Biol Chem* **1998**, *273*, 9608-9614.
- [28] R.A. Geremia, E.A. Petroni, L. Ielpi, B. Henrissat, *Biochem J* **1996**, *318 (Pt 1)*, 133-138.
- [29] L. Lemesle-Varloot, B. Henrissat, C. Gaboriaud, V. Bissery, A. Morgat, J.P. Mornon, *Biochimie* **1990**, *72*, 555-574.
- [30] C. Gaboriaud, V. Bissery, T. Benchetrit, J.P. Mornon, *FEBS Lett* **1987**, *224*, 149-155.
- [31] I.M. Saxena, R.M. Brown, Jr., M. Fevre, R.A. Geremia, B. Henrissat, *J Bacteriol* **1995**, *177*, 1419-1424.
- [32] J. Weinstein, E.U. Lee, K. McEntee, P.H. Lai, J.C. Paulson, *J Biol Chem* **1987**, *262*, 17735-17743.
- [33] J.S.a.N. Shaper, *Curr. Opin. Struct. Biol.* **1992**, *2*, 701-709.
- [34] C. Abeijon, E.C. Mandon, C.B. Hirschberg, *Trends Biochem Sci* **1997**, *22*, 203-207.
- [35] G. Lammers, J.C. Jamieson, *Biochem J* **1989**, *261*, 389-393.
- [36] J.C. Paulson, J. Weinstein, E.L. Ujita, K.J. Riggs, P.H. Lai, *Biochem Soc Trans* **1987**, *15*, 618-620.
- [37] M.S. Bretscher, S. Munro, *Science* **1993**, *261*, 1280-1281.
- [38] R.D. Teasdale, F. Matheson, P.A. Gleeson, *Glycobiology* **1994**, *4*, 917-928.
- [39] M.G. Farquhar, *Annu Rev Cell Biol* **1985**, *1*, 447-488.
- [40] G. Griffiths, K. Simons, *Science* **1986**, *234*, 438-443.
- [41] H.P. Hauri, A. Schweizer, *Curr Opin Cell Biol* **1992**, *4*, 600-608.
- [42] I. Mellman, K. Simons, *Cell* **1992**, *68*, 829-840.
- [43] N.K. Pryer, L.J. Wuestehube, R. Schekman, *Annu Rev Biochem* **1992**, *61*, 471-516.
- [44] J.E. Rothman, L. Orci, *Nature* **1992**, *355*, 409-415.
- [45] E.S. Sztul, P. Melancon, K.E. Howell, *Trends Cell Biol* **1992**, *2*, 381-386.
- [46] R.D. Teasdale, G. D'Agostaro, P.A. Gleeson, *J Biol Chem* **1992**, *267*, 13113.
- [47] K.J. Colley, E.U. Lee, B. Adler, J.K. Browne, J.C. Paulson, *J Biol Chem* **1989**, *264*, 17619-17622.
- [48] T. Nilsson, G. Warren, *Curr Opin Cell Biol* **1994**, *6*, 517-521.
- [49] K.J. Colley, *Glycobiology* **1997**, *7*, 1-13.
- [50] P.A. Gleeson, *Histochem Cell Biol* **1998**, *109*, 517-532.
- [51] M. Charron, J.H. Shaper, N.L. Shaper, *Proc Natl Acad Sci U S A* **1998**, *95*, 14805-14810.
- [52] N.W. Lo, J.T. Lau, *Glycobiology* **1996**, *6*, 271-279.
- [53] R.K. Yu, E. Bieberich, *Mol Cell Endocrinol* **2001**, *177*, 19-24.
- [54] C. Breton, J. Mucha, C. Jeanneau, *Biochimie* **2001**, *83*, 713-718.
- [55] A. Vrieling, W. Ruger, H.P. Driessen, P.S. Freemont, *Embo J* **1994**, *13*, 3413-3422.
- [56] M.G. Rossmann, P. Argos, *Mol Cell Biochem* **1978**, *21*, 161-182.
- [57] S.J. Charnock, G.J. Davies, *Biochemistry* **1999**, *38*, 6380-6385.

- [58] K. Persson, H.D. Ly, M. Dieckelmann, W.W. Wakarchuk, S.G. Withers, N.C. Strynadka, *Nat Struct Biol* **2001**, *8*, 166-175.
- [59] U.M. Unligil, S. Zhou, S. Yuwaraj, M. Sarkar, H. Schachter, J.M. Rini, *Embo J* **2000**, *19*, 5269-5280.
- [60] R.P. Gibson, J.P. Turkenburg, S.J. Charnock, R. Lloyd, G.J. Davies, *Chem Biol* **2002**, *9*, 1337-1346.
- [61] S. Ha, D. Walker, Y. Shi, S. Walker, *Protein Sci* **2000**, *9*, 1045-1052.
- [62] F.K. Hagen, B. Hazes, R. Raffo, D. deSa, L.A. Tabak, *J Biol Chem* **1999**, *274*, 6797-6803.
- [63] C.A. Wiggins, S. Munro, *Proc Natl Acad Sci U S A* **1998**, *95*, 7945-7950.
- [64] J.C. Uitdehaag, R. Mosi, K.H. Kalk, B.A. van der Veen, L. Dijkhuizen, S.G. Withers, B.W. Dijkstra, *Nat Struct Biol* **1999**, *6*, 432-436.
- [65] K. Shibayama, S. Ohsuka, T. Tanaka, Y. Arakawa, M. Ohta, *J Bacteriol* **1998**, *180*, 5313-5318.
- [66] C. Busch, F. Hofmann, J. Selzer, S. Munro, D. Jeckel, K. Aktories, *J Biol Chem* **1998**, *273*, 19566-19572.
- [67] G. Zhu, M.L. Allende, E. Jaskiewicz, R. Qian, D.S. Darling, C.A. Worth, K.J. Colley, W.W. Young, Jr., *Glycobiology* **1998**, *8*, 831-840.
- [68] J. Yeh, R.D. Cummings, *Glycobiology* **1997**, *7*, 241-251.
- [69] H. Schachter, *Biochem Cell Biol* **1986**, *64*, 163-181.
- [70] R. Kornfeld, S. Kornfeld, *Annu Rev Biochem* **1985**, *54*, 631-664.
- [71] A. Harduin-Lepers, M.A. Recchi, P. Delannoy, *Glycobiology* **1995**, *5*, 741-758.
- [72] P.C. Burger, M. Lotscher, M. Streiff, R. Kleene, B. Kaissling, E.G. Berger, *Glycobiology* **1998**, *8*, 245-257.
- [73] B.D. Livingston, J.C. Paulson, *J Biol Chem* **1993**, *268*, 11504-11507.
- [74] M. Gilbert, D.C. Watson, A.M. Cunningham, M.P. Jennings, N.M. Young, W.W. Wakarchuk, *J Biol Chem* **1996**, *271*, 28271-28276.
- [75] R.A. Geremia, A. Harduin-Lepers, P. Delannoy, *Glycobiology* **1997**, *7*, v-vii.
- [76] A.K. Datta, J.C. Paulson, *Indian J Biochem Biophys* **1997**, *34*, 157-165.
- [77] T. Yamamoto, M. Nakashizuka, I. Terada, *J Biochem (Tokyo)* **1998**, *123*, 94-100.
- [78] A.K. Datta, J.C. Paulson, *J Biol Chem* **1995**, *270*, 1497-1500.
- [79] T.W. Rademacher, R.B. Parekh, R.A. Dwek, *Annu Rev Biochem* **1988**, *57*, 785-838.
- [80] R. Schauer, *Adv Carbohydr Chem Biochem* **1982**, *40*, 131-234.
- [81] G.N. Rogers, G. Herrler, J.C. Paulson, H.D. Klenk, *J Biol Chem* **1986**, *261*, 5947-5951.
- [82] R. Schauer, A. de Freese, M. Gollub, M. Iwersen, S. Kelm, G. Reuter, W. Schlenzka, V. Vandamme-Feldhaus, L. Shaw, *Indian J Biochem Biophys* **1997**, *34*, 131-141.
- [83] S. Kelm, R. Schauer, *Int Rev Cytol* **1997**, *175*, 137-240.
- [84] M. Muhlenhoff, M. Eckhardt, R. Gerardy-Schahn, *Curr Opin Struct Biol*

1998, 8, 558-564.

- [85] C.L. Stults, C.C. Sweeley, B.A. Macher, *Methods Enzymol* **1989**, 179, 167-214.
- [86] H. Wiegandt, *Behav Brain Res* **1995**, 66, 85-97.
- [87] Y. Nagai, *Behav Brain Res* **1995**, 66, 99-104.
- [88] L. Svennerholm, *Prog Brain Res* **1994**, 101, XI-XIV.
- [89] K.A. Karlsson, *Annu Rev Biochem* **1989**, 58, 309-350.
- [90] U. Grundmann, C. Nerlich, T. Rein, G. Zettlmeissl, *Nucleic Acids Res* **1990**, 18, 667.
- [91] S. Tsuji, A.K. Datta, J.C. Paulson, *Glycobiology* **1996**, 6, v-vii.
- [92] X. Wang, A. Vertino, R.L. Eddy, M.G. Byers, S.N. Jani-Sait, T.B. Shows, J.T. Lau, *J Biol Chem* **1993**, 268, 4355-4361.
- [93] A. Harduin-Lepers, D.C. Stokes, W.F. Steelant, B. Samyn-Petit, M.A. Krzewinski-Recchi, V. Vallejo-Ruiz, J.P. Zanetta, C. Auge, P. Delannoy, *Biochem J* **2000**, 352 Pt 1, 37-48.
- [94] M.L. Chang, R.L. Eddy, T.B. Shows, J.T. Lau, *Glycobiology* **1995**, 5, 319-325.
- [95] H. Kitagawa, M.G. Mattei, J.C. Paulson, *J Biol Chem* **1996**, 271, 931-938.
- [96] H. Kitagawa, J.C. Paulson, *J Biol Chem* **1994**, 269, 1394-1401.
- [97] Y.J. Kim, K.S. Kim, S.H. Kim, C.H. Kim, J.H. Ko, I.S. Choe, S. Tsuji, Y.C. Lee, *Biochem Biophys Res Commun* **1996**, 228, 324-327.
- [98] B.E. Collins, L.J. Yang, G. Mukhopadhyay, M.T. Filbin, M. Kiso, A. Hasegawa, R.L. Schnaar, *J Biol Chem* **1997**, 272, 1248-1255.
- [99] S. Kelm, R. Brossmer, R. Isecke, H.J. Gross, K. Strenge, R. Schauer, *Eur J Biochem* **1998**, 255, 663-672.
- [100] H. Kitagawa, J.C. Paulson, *Biochem Biophys Res Commun* **1993**, 194, 375-382.
- [101] K. Sasaki, E. Watanabe, K. Kawashima, S. Sekine, T. Dohi, M. Oshima, N. Hanai, T. Nishi, M. Hasegawa, *J Biol Chem* **1993**, 268, 22782-22787.
- [102] A. Ishii, M. Ohta, Y. Watanabe, K. Matsuda, K. Ishiyama, K. Sakoe, M. Nakamura, J. Inokuchi, Y. Sanai, M. Saito, *J Biol Chem* **1998**, 273, 31652-31655.
- [103] L.J. Melkerson-Watson, C.C. Sweeley, *J Biol Chem* **1991**, 266, 4448-4457.
- [104] U. Preuss, X. Gu, T. Gu, R.K. Yu, *J Biol Chem* **1993**, 268, 26273-26278.
- [105] T. Okajima, S. Fukumoto, H. Miyazaki, H. Ishida, M. Kiso, K. Furukawa, T. Urano, *J Biol Chem* **1999**, 274, 11479-11486.
- [106] T. Okajima, H.H. Chen, H. Ito, M. Kiso, T. Tai, K. Furukawa, T. Urano, *J Biol Chem* **2000**, 275, 6717-6723.
- [107] Y. Ikehara, N. Kojima, N. Kurosawa, T. Kudo, M. Kono, S. Nishihara, S. Issiki, K. Morozumi, S. Itzkowitz, T. Tsuda, S.I. Nishimura, S. Tsuji, H. Narimatsu, *Glycobiology* **1999**, 9, 1213-1224.
- [108] N. Kurosawa, T. Hamamoto, Y.C. Lee, T. Nakaoka, N. Kojima, S. Tsuji, *J Biol Chem* **1994**, 269, 1402-1409.
- [109] Y.C. Lee, M. Kaufmann, S. Kitazume-Kawaguchi, M. Kono, S. Takashima, N. Kurosawa, H. Liu, H. Pircher, S. Tsuji, *J Biol Chem* **1999**, 274, 11958-11967.

- [110] Y. Ikehara, N. Shimizu, M. Kono, S. Nishihara, H. Nakanishi, T. Kitamura, H. Narimatsu, S. Tsuji, M. Tatematsu, *FEBS Lett* **1999**, *463*, 92-96.
- [111] T. Okajima, S. Fukumoto, H. Ito, M. Kiso, Y. Hirabayashi, T. Urano, K. Furukawa, *J Biol Chem* **1999**, *274*, 30557-30562.
- [112] S. Itzkowitz, T. Kjeldsen, A. Frieria, S. Hakomori, U.S. Yang, Y.S. Kim, *Gastroenterology* **1991**, *100*, 1691-1700.
- [113] J.C. Paulson, J. Weinstein, U. de Souza-e-Silva, *Eur J Biochem* **1984**, *140*, 523-530.
- [114] H.T. de Heij, P.L. Koppen, D.H. van den Eijnden, *Carbohydr Res* **1986**, *149*, 85-99.
- [115] P.M. Lackie, C. Zuber, J. Roth, *Differentiation* **1994**, *57*, 119-131.
- [116] J.B. Rothbard, R. Brackenbury, B.A. Cunningham, G.M. Edelman, *J Biol Chem* **1982**, *257*, 11064-11069.
- [117] H. Hildebrandt, C. Becker, S. Gluer, H. Rosner, R. Gerardy-Schahn, H. Rahmann, *Cancer Res* **1998**, *58*, 779-784.
- [118] K. Sasaki, K. Kurata, N. Kojima, N. Kurosawa, S. Ohta, N. Hanai, S. Tsuji, T. Nishi, *J Biol Chem* **1994**, *269*, 15950-15956.
- [119] Y. Yoshida, N. Kojima, N. Kurosawa, T. Hamamoto, S. Tsuji, *J Biol Chem* **1995**, *270*, 14628-14633.
- [120] N. Kojima, Y. Yoshida, S. Tsuji, *FEBS Lett* **1995**, *373*, 119-122.
- [121] J. Nakayama, M.N. Fukuda, B. Fredette, B. Ranscht, M. Fukuda, *Proc Natl Acad Sci U S A* **1995**, *92*, 7031-7035.
- [122] N. Kojima, Y. Yoshida, N. Kurosawa, Y.C. Lee, S. Tsuji, *FEBS Lett* **1995**, *360*, 1-4.
- [123] M. Muhlenhoff, M. Eckhardt, A. Bethe, M. Frosch, R. Gerardy-Schahn, *Curr Biol* **1996**, *6*, 1188-1191.
- [124] Y.J. Kim, K.S. Kim, S. Do, C.H. Kim, S.K. Kim, Y.C. Lee, *Biochem Biophys Res Commun* **1997**, *235*, 327-330.
- [125] C. Schaffer, M. Graninger, P. Messner, *Proteomics* **2001**, *1*, 248-261.
- [126] M.F. Mescher, J.L. Strominger, S.W. Watson, *J Bacteriol* **1974**, *120*, 945-954.
- [127] U.B. Sleytr, K.J. Thorne, *J Bacteriol* **1976**, *126*, 377-383.
- [128] L.E. Sandercook, A.M. MacLeod, E. Ong, W. R.A.J., *FEMS Microbiol Lett* **1994**, *118*, 1-8.
- [129] H. Lis, N. Sharon, *Eur J Biochem* **1993**, *218*, 1-27.
- [130] T.H. Plummer, Jr., A.L. Tarentino, C.R. Hauer, *J Biol Chem* **1995**, *270*, 13192-13196.
- [131] J. Peters, S. Rudolf, H. Oschkinat, R. Mengele, M. Sumper, J. Kellermann, F. Lottspeich, W. Baumeister, *Biol Chem Hoppe Seyler* **1992**, *373*, 171-176.
- [132] E. Hartmann, H. Konig, *Biol Chem Hoppe Seyler* **1991**, *372*, 971-974.
- [133] E. Hartmann, P. Messner, G. Allmeier, H. Konig, *J Bacteriol* **1993**, *175*, 4515-4519.
- [134] I. Benz, M.A. Schmidt, *Mol Microbiol* **2002**, *45*, 267-276.
- [135] I. Benz, M.A. Schmidt, *Infect Immun* **1989**, *57*, 1506-1511.
- [136] M. Suhr, I. Benz, M.A. Schmidt, *Mol Microbiol* **1996**, *22*, 31-42.

- [137] U. Niewerth, A. Frey, T. Voss, C. Le Bouguenec, G. Baljer, S. Franke, M.A. Schmidt, *Clin Diagn Lab Immunol* **2001**, *8*, 143-149.
- [138] J. Drummelsmith, C. Whitfield, *Embo J* **2000**, *19*, 57-66.
- [139] C. Whitfield, I.S. Roberts, *Mol Microbiol* **1999**, *31*, 1307-1319.
- [140] I. Benz, M.A. Schmidt, *Mol Microbiol* **2001**, *40*, 1403-1413.
- [141] C.M. Szymanski, D.H. Burr, P. Guerry, *Infect Immun* **2002**, *70*, 2242-2244.
- [142] A.P. Moran, M.M. Prendergast, E.L. Hogan, *J Neurol Sci* **2002**, *196*, 1-7.
- [143] S. Kioizumi, *Trends in Glycoscience and Glycotechnology* **2003**, *15*, 65-74.
- [144] M.P. Jennings, D.W. Hood, I.R. Peak, M. Virji, E.R. Moxon, *Mol Microbiol* **1995**, *18*, 729-740.
- [145] E.C. Gotschlich, *J Exp Med* **1994**, *180*, 2181-2190.
- [146] W. Wakarchuk, A. Martin, M.P. Jennings, E.R. Moxon, J.C. Richards, *J Biol Chem* **1996**, *271*, 19166-19173.
- [147] S.M. Logan, J.W. Conlan, M.A. Monteiro, W.W. Wakarchuk, E. Altman, *Mol Microbiol* **2000**, *35*, 1156-1167.
- [148] T. Endo, S. Koizumi, K. Tabata, A. Ozaki, *Glycobiology* **2000**, *10*, 809-813.
- [149] M.A. Kolkman, W. Wakarchuk, P.J. Nuijten, B.A. van der Zeijst, *Mol Microbiol* **1997**, *26*, 197-208.
- [150] S. Yamamoto, K. Miyake, Y. Koike, M. Watanabe, Y. Machida, M. Ohta, S. Iijima, *J. Bacteriol.* **2000**, *181*, 5176-5184.
- [151] M. Gilbert, J.R. Brisson, M.F. Karwaski, J. Michniewicz, A.M. Cunningham, Y. Wu, N.M. Young, W.W. Wakarchuk, *J Biol Chem* **2000**, *275*, 3896-3906.
- [152] M. Watanabe, K. Miyake, K. Yanae, Y. Kataoka, S. Koizumi, T. Endo, A. Ozaki, S. Iijima, *J Biochem (Tokyo)* **2002**, *131*, 183-191.
- [153] H.J. Gijzen, L. Qiao, W. Fitz, C.H. Wong, *Chem Rev* **1996**, *96*, 443-474.
- [154] D.W. Hood, A.D. Cox, M. Gilbert, K. Makepeace, S. Walsh, M.E. Deadman, A. Cody, A. Martin, M. Mansson, E.K. Schweda, J.R. Brisson, J.C. Richards, E.R. Moxon, W.W. Wakarchuk, *Mol Microbiol* **2001**, *39*, 341-350.
- [155] P.A. Jones, N.M. Samuels, N.J. Phillips, R.S. Munson, Jr., J.A. Bozue, J.A. Arseneau, W.A. Nichols, A. Zaleski, B.W. Gibson, M.A. Apicella, *J Biol Chem* **2002**, *277*, 14598-14611.
- [156] J.A. Bozue, M.V. Tullius, J. Wang, B.W. Gibson, R.S. Munson, Jr., *J Biol Chem* **1999**, *274*, 4106-4114.
- [157] D.O. Chaffin, K. McKinnon, C.E. Rubens, *Mol. Microbiol.* **1996**, *45*, 109-122.
- [158] G.J. Shen, A.K. Datta, M. Izumi, K.M. Koeller, C.H. Wong, *J Biol Chem* **1999**, *274*, 35139-35146.
- [159] Z. Ge, N.W. Chan, M.M. Palcic, D.E. Taylor, *J Biol Chem* **1997**, *272*, 21357-21363.
- [160] S.L. Martin, M.R. Edbrooke, T.C. Hodgman, D.H. van den Eijnden, M.I. Bird, *J Biol Chem* **1997**, *272*, 21349-21356.
- [161] G. Wang, P.G. Boulton, N.W. Chan, M.M. Palcic, D.E. Taylor, *Microbiology* **1999**, *145 (Pt 11)*, 3245-3253.

- [162] D.A. Rasko, G. Wang, M.M. Palcic, D.E. Taylor, *J Biol Chem* **2000**, *275*, 4988-4994.
- [163] J. Parkhill, B.W. Wren, K. Mungall, J.M. Ketley, C. Churcher, D. Basham, T. Chillingworth, R.M. Davies, T. Feltwell, S. Holroyd, K. Jagels, A.V. Karlyshev, S. Moule, M.J. Pallen, C.W. Penn, M.A. Quail, M.A. Rajandream, K.M. Rutherford, A.H. van Vliet, S. Whitehead, B.G. Barrell, *Nature* **2000**, *403*, 665-668.
- [164] A. Varki, R.D. Cummings, J. Esko, H. Freeze, G. Hart, J. Marth, *Essentials of Glycobiology*, Cold Spring Harbor Laboratory Press., New York, **1999**.
- [165] B.M. Allos, *Clin Infect Dis* **2001**, *32*, 1201-1206.
- [166] D.J. Bacon, C.M. Szymanski, D.H. Burr, R.P. Silver, R.A. Alm, P. Guerry, *Mol Microbiol* **2001**, *40*, 769-777.
- [167] P. Guerry, C.M. Szymanski, M.M. Prendergast, T.E. Hickey, C.P. Ewing, D.L. Pattarini, A.P. Moran, *Infect Immun* **2002**, *70*, 787-793.
- [168] A.P. Moran, E.T. Rietschel, T.U. Kosunen, U. Zahringer, *J Bacteriol* **1991**, *173*, 618-626.
- [169] G.O. Aspinall, A.G. McDonald, H. Pang, L.A. Kurjanczyk, J.L. Penner, *Biochemistry* **1994**, *33*, 241-249.
- [170] I. Nachamkin, B.M. Allos, T. Ho, *Clin Microbiol Rev* **1998**, *11*, 555-567.
- [171] D. Linton, A.V. Karlyshev, B.W. Wren, *Curr Opin Microbiol* **2001**, *4*, 35-40.
- [172] S. Salloway, L.A. Mermel, M. Seamans, G.O. Aspinall, J.E. Nam Shin, L.A. Kurjanczyk, J.L. Penner, *Infect Immun* **1996**, *64*, 2945-2949.
- [173] A.P. Moran, M.M. Prendergast, B.J. Appelmelk, *FEMS Immunol Med Microbiol* **1996**, *16*, 105-115.
- [174] S.A. Jeong E. Nam Shin, Anupama S. Mainkar, Mario A. Monteiro, Henrianna Pang, John L. Penner and Gerald O. Aspinall, *Carbohydrate research* **1998**, *305*, 223-232.
- [175] B.N. Fry, V. Korolik, J.A. ten Brinke, M.T. Pennings, R. Zalm, B.J. Teunis, P.J. Coloe, B.A. van der Zeijst, *Microbiology* **1998**, *144 (Pt 8)*, 2049-2061.
- [176] C.A. Schnaitman, J.D. Klena, *Microbiol Rev* **1993**, *57*, 655-682.
- [177] J. Hackett, P. Wyk, P. Reeves, V. Mathan, *J Infect Dis* **1987**, *155*, 540-549.
- [178] K.A. Joiner, N. Grossman, M. Schmetz, L. Leive, *J Immunol* **1986**, *136*, 710-715.
- [179] M.A. Preston, J.L. Penner, *Infect Immun* **1987**, *55*, 1806-1812.
- [180] G.O. Aspinall, A.G. McDonald, T.S. Raju, H. Pang, S.D. Mills, L.A. Kurjanczyk, J.L. Penner, *J Bacteriol* **1992**, *174*, 1324-1332.
- [181] G.O. Aspinall, A.G. McDonald, H. Pang, *Biochemistry* **1994**, *33*, 250-255.
- [182] A.P. Moran, J.L. Penner, *J Appl Microbiol* **1999**, *86*, 361-377.
- [183] C.P. Chiu, A.G. Watts, L.L. Lairson, M. Gilbert, D. Lim, W.W. Wakarchuk, S.G. Withers, N.C. Strynadka, *Nat Struct Mol Biol* **2004**, *11*, 163-170.
- [184] M. Fukuda, O. Hindsgaul, Eds., *Molecular Glycobiology*, Oxford University Press., New York, **1994**.
- [185] J.C. McAuliffe, O. Hindsgaul, *In: Molecular and Cellular Glycobiology (Fukuda, M. and Hindsgaul, O. eds.)*, Oxford University Press, New York, **2000**.

- [186] C.H. Wong, S.L. Haynie, G.M. Whitesides, *J. Org. Chem.* **1982**, *47*, 5416-5418.
- [187] H.A. Nunez, R. Barker, *Biochemistry* **1980**, *19*, 489-495.
- [188] P.R. Rosevear, H.A. Nunez, R. Barker, *Biochemistry* **1982**, *21*, 1421-1431.
- [189] C. Auge, S. David, C. Mathieu, C. Gautheron, *Tetrahedron Lett.* **1984**, *25*, 1467.
- [190] J.C. Paulson, *Trends Biochem Sci* **1989**, *14*, 272-276.
- [191] M.E. Schwab, J.P. Kapfhammer, C.E. Bandtlow, *Annu Rev Neurosci* **1993**, *16*, 565-595.
- [192] M.T. Filbin, *Nat Rev Neurosci* **2003**, *4*, 703-713.
- [193] B.J. Alberts, Alexander; Lewis, Julian; Raff, Martin; Roberts, Keith; Walter, Peter, *Molecular biology of the cell.*, 4th ed ed., Garland Science., New York, **2002**.
- [194] A.A. Vyas, R.L. Schnaar, *Biochimie* **2001**, *83*, 677-682.
- [195] L. Schnell, M.E. Schwab, *Nature* **1990**, *343*, 269-272.
- [196] M.E. Schwab, H. Thoenen, *J Neurosci* **1985**, *5*, 2415-2423.
- [197] K.A. Crutcher, *Exp Neurol* **1989**, *104*, 39-54.
- [198] H. Cheng, Y. Cao, L. Olson, *Science* **1996**, *273*, 510-513.
- [199] Y.J. Shen, M.E. DeBellard, J.L. Salzer, J. Roder, M.T. Filbin, *Mol Cell Neurosci* **1998**, *12*, 79-91.
- [200] J. Qiu, D. Cai, M.T. Filbin, *Glia* **2000**, *29*, 166-174.
- [201] T. Spencer, M. Domeniconi, Z. Cao, M.T. Filbin, *Curr Opin Neurobiol* **2003**, *13*, 133-139.
- [202] J.L. Everly, R.O. Brady, R.H. Quarles, *J Neurochem* **1973**, *21*, 329-334.
- [203] L. McKerracher, S. David, D.L. Jackson, V. Kottis, R.J. Dunn, P.E. Braun, *Neuron* **1994**, *13*, 805-811.
- [204] G. Mukhopadhyay, P. Doherty, F.S. Walsh, P.R. Crocker, M.T. Filbin, *Neuron* **1994**, *13*, 757-767.
- [205] P.R. Crocker, E.A. Clark, M. Filbin, S. Gordon, Y. Jones, J.H. Kehrl, S. Kelm, N. Le Douarin, L. Powell, J. Roder, R.L. Schnaar, D.C. Sgroi, K. Stamenkovic, R. Schauer, M. Schachner, T.K. van den Berg, P.A. van der Merwe, S.M. Watt, A. Varki, *Glycobiology* **1998**, *8*, v.
- [206] R.H. Quarles, *J Mol Neurosci* **1997**, *8*, 1-12.
- [207] J.L. Salzer, W.P. Holmes, D.R. Colman, *J Cell Biol* **1987**, *104*, 957-965.
- [208] C. Lai, M.A. Brow, K.A. Nave, A.B. Noronha, R.H. Quarles, F.E. Bloom, R.J. Milner, J.G. Sutcliffe, *Proc Natl Acad Sci U S A* **1987**, *84*, 4337-4341.
- [209] M. Arquint, J. Roder, L.S. Chia, J. Down, D. Wilkinson, H. Bayley, P. Braun, R. Dunn, *Proc Natl Acad Sci U S A* **1987**, *84*, 600-604.
- [210] H.J. Willison, A.I. Ilyas, D.J. O'Shannessy, M. Pulley, B.D. Trapp, R.H. Quarles, *J Neurochem* **1987**, *49*, 1853-1862.
- [211] B.D. Trapp, *Ann N Y Acad Sci* **1990**, *605*, 29-43.
- [212] M. Fruttiger, D. Montag, M. Schachner, R. Martini, *Eur J Neurosci* **1995**, *7*, 511-515.

- [213] M.E. DeBellard, S. Tang, G. Mukhopadhyay, Y.J. Shen, M.T. Filbin, *Mol Cell Neurosci* **1996**, 7, 89-101.
- [214] S. Kelm, A. Pelz, R. Schauer, M.T. Filbin, S. Tang, M.E. de Bellard, R.L. Schnaar, J.A. Mahoney, A. Hartnell, P. Bradfield, et al., *Curr Biol* **1994**, 4, 965-972.
- [215] S. Tang, Y.J. Shen, M.E. DeBellard, G. Mukhopadhyay, J.L. Salzer, P.R. Crocker, M.T. Filbin, *J Cell Biol* **1997**, 138, 1355-1366.
- [216] M. Domeniconi, Z. Cao, T. Spencer, R. Sivasankaran, K. Wang, E. Nikulina, N. Kimura, H. Cai, K. Deng, Y. Gao, Z. He, M. Filbin, *Neuron* **2002**, 35, 283-290.
- [217] B.P. Liu, A. Fournier, T. GrandPre, S.M. Strittmatter, *Science* **2002**, 297, 1190-1193.
- [218] S. Ramon y Cajal, *Cajal's Degeneration & Regeneration of the Nervous System*, Oxford Univer. Press, Oxford, **1928**.
- [219] P. Caroni, M.E. Schwab, *Neuron* **1988**, 1, 85-96.
- [220] P. Caroni, M.E. Schwab, *J Cell Biol* **1988**, 106, 1281-1288.
- [221] M.S. Chen, A.B. Huber, M.E. van der Haar, M. Frank, L. Schnell, A.A. Spillmann, F. Christ, M.E. Schwab, *Nature* **2000**, 403, 434-439.
- [222] T. GrandPre, F. Nakamura, T. Vartanian, S.M. Strittmatter, *Nature* **2000**, 403, 439-444.
- [223] R. Prinjha, S.E. Moore, M. Vinson, S. Blake, R. Morrow, G. Christie, D. Michalovich, D.L. Simmons, F.S. Walsh, *Nature* **2000**, 403, 383-384.
- [224] K.C. Wang, V. Koprivica, J.A. Kim, R. Sivasankaran, Y. Guo, R.L. Neve, Z. He, *Nature* **2002**, 417, 941-944.
- [225] A.A. Habib, L.S. Marton, B. Allwardt, J.R. Gulcher, D.D. Mikol, T. Hognason, N. Chattopadhyay, K. Stefansson, *J Neurochem* **1998**, 70, 1704-1711.
- [226] D.D. Mikol, J.R. Gulcher, K. Stefansson, *J Cell Biol* **1990**, 110, 471-479.
- [227] A.E. Fournier, T. GrandPre, S.M. Strittmatter, *Nature* **2001**, 409, 341-346.
- [228] A. Josephson, A. Trifunovski, H.R. Widmer, J. Widenfalk, L. Olson, C. Spenger, *J Comp Neurol* **2002**, 453, 292-304.
- [229] K.C. Wang, J.A. Kim, R. Sivasankaran, R. Segal, Z. He, *Nature* **2002**, 420, 74-78.
- [230] S.T. Wong, J.R. Henley, K.C. Kanning, K.H. Huang, M. Bothwell, M.M. Poo, *Nat Neurosci* **2002**, 5, 1302-1308.
- [231] U. Bartsch, C.E. Bandtlow, L. Schnell, S. Bartsch, A.A. Spillmann, B.P. Rubin, R. Hillenbrand, D. Montag, M.E. Schwab, M. Schachner, *Neuron* **1995**, 15, 1375-1381.
- [232] M. Li, A. Shibata, C. Li, P.E. Braun, L. McKerracher, J. Roder, S.B. Kater, S. David, *J Neurosci Res* **1996**, 46, 404-414.
- [233] B.S. Bregman, E. Kunkel-Bagden, L. Schnell, H.N. Dai, D. Gao, M.E. Schwab, *Nature* **1995**, 378, 498-501.
- [234] L. Schnell, M.E. Schwab, *Eur J Neurosci* **1993**, 5, 1156-1171.
- [235] A.A. Vyas, H.V. Patel, S.E. Fromholt, M. Heffer-Lauc, K.A. Vyas, J. Dang, M. Schachner, R.L. Schnaar, *Proc Natl Acad Sci U S A* **2002**, 99, 8412-8417.
- [236] L.J. Yang, C.B. Zeller, N.L. Shaper, M. Kiso, A. Hasegawa, R.E. Shapiro, R.L. Schnaar, *Proc Natl Acad Sci U S A* **1996**, 93, 814-818.

- [237] G. Tettamanti, F. Bonali, S. Marchesini, V. Zambotti, *Biochim Biophys Acta* **1973**, 296, 160-170.
- [238] M.L.K. O'reilly David R, Luckow Verne A, *Baculovirus expression vectors. A laboratory manual*, Oxford university press, **1994**.
- [239] L.a.M. Reed, H, *Am J Hyg.* **1938**, 27, 493-497.
- [240] U.K. Laemmli, *Nature* **1970**, 227, 680-685.
- [241] H. Towbin, T. Staehelin, J. Gordon, *Proc Natl Acad Sci U S A* **1979**, 76, 4350-4354.
- [242] H. Bosshart, E.G. Berger, *Eur J Biochem* **1992**, 208, 341-349.
- [243] M.A. Williams, H. Kitagawa, A.K. Datta, J.C. Paulson, J.C. Jamieson, *Glycoconj J* **1995**, 12, 755-761.
- [244] N.J. Kruger, *Methods Mol Biol* **1994**, 32, 9-15.
- [245] M.M. Bradford, *Anal Biochem* **1976**, 72, 248-254.
- [246] E. Grabenhorst, M. Nimtz, J. Costa, H.S. Conradt, *J Biol Chem* **1998**, 273, 30985-30994.
- [247] S. Fukumoto, H. Miyazaki, G. Goto, T. Urano, K. Furukawa, *J Biol Chem* **1999**, 274, 9271-9276.
- [248] S. Lubert, *4th* **1995**,
- [249] O. Schwardt, G. Gao, T. Visekruna, S. Rabbani, E. Gassmann, B. Ernst, *Journal of Carbohydrate Chemistry* **2004**, 23, 1-26.
- [250] G. Gao, O. Schwardt, T. Visekruna, S. Rabbani, B. Ernst, *Chimia* **2004**, 58, 215-218.
- [251] R.I. Duclos, Jr., *Carbohydr Res* **2000**, 328, 489-507.
- [252] G. Baisch, R. Öhrlein, M. Streiff, B. Ernst, *Bioorg. Med. Chem. Lett.* **1996**, 6, 755-758.
- [253] G. Baisch, R. Ohrlein, M. Streiff, *Bioorg Med Chem Lett* **1998**, 8, 157-160.
- [254] E. Grabenhorst, P. Schlenke, S. Pohl, M. Nimtz, H.S. Conradt, *Glycoconj J* **1999**, 16, 81-97.
- [255] E. Grabenhorst, A. Hoffmann, M. Nimtz, G. Zettlmeissl, H.S. Conradt, *Eur J Biochem* **1995**, 232, 718-725.
- [256] W.B. Jacoby, I.H. Pastan, *Methods in enzymology* **1979**, 58,
- [257] J. Sambrook, E.F. Fritsch, T. Maniatis, *Molecular Cloning; A laboratory manual, Vol. 2nd*, Cold Spring Harbor Laboratory Press, **1989**.
- [258] E. Grabenhorst, in *Gesellschaft für Biotechnologische Forschung*, Technischen Universität Carol-Wilhelmina, Braunschweig, **1993**, pp. 1-148.
- [259] Novagen, *pET system manual*, **2002**.
- [260] J.L. Penner, J.N. Hennessy, R.V. Congi, *Eur J Clin Microbiol* **1983**, 2, 378-383.
- [261] M.A.G. Turner P.C., Bates A.D., White M.R.H., *Instant Notes in Molecular Biology*, ed. H. B.D., BIOS Scientific Publishers, **1997**.
- [262] H.F. Lodish, *Molecular cell biology*, 4th ed., W.H. Freeman. 1 v, New York, **2000**.
- [263] *PCR Applications Manual*, Roche Diagnostics GmbH,, Mannheim, **1999**.

- [264] M. Gilbert, M.F. Karwaski, S. Bernatchez, N.M. Young, E. Taboada, J. Michniewicz, A.M. Cunningham, W.W. Wakarchuk, *J Biol Chem* **2002**, 277, 327-337.
- [265] Qiagen, *Bench guide*, **2001**.
- [266] B. Lowenadler, B. Jansson, S. Paleus, E. Holmgren, B. Nilsson, T. Moks, G. Palm, S. Josephson, L. Philipson, M. Uhlen, *Gene* **1987**, 58, 87-97.
- [267] QIAexpressionist, *A handbook for high-level expression and purification of 6xHis-tagged proteins.*, 5th ed., Qiagen, **2002**.
- [268] R.C. Hughes, *Biochimie* **2001**, 83, 667-676.
- [269] U. Rutishauser, L. Landmesser, *Trends Neurosci* **1996**, 19, 422-427.
- [270] T. Feizi, *Immunol Rev* **2000**, 173, 79-88.
- [271] P.R. Crocker, A. Varki, *Trends Immunol* **2001**, 22, 337-342.
- [272] S. Hakomori, *Proc Natl Acad Sci U S A* **2002**, 99, 10231-10233.
- [273] R.L. Schnaar, *Arch Biochem Biophys* **2004**, 426, 163-172.
- [274] S.H. Khan, H. O., in *Molecular Glycobiology*. Fukuda M. Hindsgaul O., Press, Oxford, **1994**.
- [275] B. Ernst, R. Oehrlein, *Glycoconj J* **1999**, 16, 161-170.
- [276] D.X. Wen, B.D. Livingston, K.F. Medzihradzsky, S. Kelm, A.L. Burlingame, J.C. Paulson, *J Biol Chem* **1992**, 267, 21011-21019.
- [277] J. Weinstein, U. de Souza-e-Silva, J.C. Paulson, *J Biol Chem* **1982**, 257, 13835-13844.
- [278] Baculovirus, *Baculovirus Expression Vector System Manual, Instruction Manual*, 6 ed., Pharmingen, A Becton Dickinson Company, San Diego, CA 9212, USA, **1999**.
- [279] E. Grabenhorst, B. Hofer, M. Nimtz, V. Jager, H.S. Conradt, *Eur J Biochem* **1993**, 215, 189-197.
- [280] D.C. James, R.B. Freedman, M. Hoare, O.W. Ogonah, B.C. Rooney, O.A. Larionov, V.N. Dobrovolsky, O.V. Lagutin, N. Jenkins, *Biotechnology (N Y)* **1995**, 13, 592-596.
- [281] T.P. Knepper, B. Arbogast, J. Schreurs, M.L. Deinzer, *Biochemistry* **1992**, 31, 11651-11659.
- [282] E.G. Berger, K. Grimm, T. Bachi, H. Bosshart, R. Kleene, M. Watzele, *J Cell Biochem* **1993**, 52, 275-288.
- [283] K.B. Wlasichuk, M.A. Kashem, P.V. Nikrad, P. Bird, C. Jiang, A.P. Venot, *J Biol Chem* **1993**, 268, 13971-13977.
- [284] S. Gosselin, M. Alhussaini, M.B. Streiff, K. Takabayashi, M.M. Palcic, *Anal Biochem* **1994**, 220, 92-97.
- [285] J. Weinstein, U. de Souza-e-Silva, J.C. Paulson, *J Biol Chem* **1982**, 257, 13845-13853.
- [286] O. Hindsgaul, K.J. Kaur, G. Srivastava, M. Blaszczyk-Thurin, S.C. Crawley, L.D. Heerze, M.M. Palcic, *J Biol Chem* **1991**, 266, 17858-17862.
- [287] J.A. Van Dorst, J.M. Tikkanen, C.H. Krezdorn, M.B. Streiff, E.G. Berger, J.A. Van Kuik, J.P. Kamerling, J.F. Vliegthart, *Eur J Biochem* **1996**, 242, 674-681.

- [288] G. Baisch, R. Ohrlein, *Bioorg Med Chem* **1998**, *6*, 1673-1682.
- [289] G. Baisch, R. Ohrlein, *Carbohydr Res* **1998**, *312*, 61-72.
- [290] M. Nimtz, W. Martin, V. Wray, K.D. Kloppel, J. Augustin, H.S. Conradt, *Eur J Biochem* **1993**, *213*, 39-56.
- [291] E.U. Lee, J. Roth, J.C. Paulson, *J Biol Chem* **1989**, *264*, 13848-13855.
- [292] H. Sasaki, B. Bothner, A. Dell, M. Fukuda, *J Biol Chem* **1987**, *262*, 12059-12076.
- [293] H.S. Conradt, H. Egge, J. Peter-Katalinic, W. Reiser, T. Siklosi, K. Schaper, *J Biol Chem* **1987**, *262*, 14600-14605.
- [294] J.E. Sadler, J.I. Rearick, J.C. Paulson, R.L. Hill, *J Biol Chem* **1979**, *254*, 4434-4442.
- [295] N. Kurosawa, T. Hamamoto, M. Inoue, S. Tsuji, *Biochim Biophys Acta* **1995**, *1244*, 216-222.
- [296] J.I. Rearick, J.E. Sadler, J.C. Paulson, R.L. Hill, *J Biol Chem* **1979**, *254*, 4444-4451.
- [297] J.C. Paulson, J.P. Prieels, L.R. Glasgow, R.L. Hill, *J Biol Chem* **1978**, *253*, 5617-5624.
- [298] J.C. Paulson, J.I. Rearick, R.L. Hill, *J Biol Chem* **1977**, *252*, 2363-2371.
- [299] D.H. van den Eijnden, D.H. Joziassse, L. Dorland, H. van Halbeek, J.F. Vliegthart, K. Schmid, *Biochem Biophys Res Commun* **1980**, *92*, 839-845.
- [300] D.H. Joziassse, W.E. Schiphorst, D.H. Van den Eijnden, J.A. Van Kuik, H. Van Halbeek, J.F. Vliegthart, *J Biol Chem* **1987**, *262*, 2025-2033.
- [301] B. Nilsson, T. Moks, B. Jansson, L. Abrahmsen, A. Elmlblad, E. Holmgren, C. Henrichson, T.A. Jones, M. Uhlen, *Protein Eng* **1987**, *1*, 107-113.
- [302] B. Nilsson, G. Forsberg, M. Hartmanis, *Methods Enzymol* **1991**, *198*, 3-16.
- [303] L. Abrahmsen, T. Moks, B. Nilsson, M. Uhlen, *Nucleic Acids Res* **1986**, *14*, 7487-7500.
- [304] G.O. Aspinall, S. Fujimoto, A.G. McDonald, H. Pang, L.A. Kurjanczyk, J.L. Penner, *Infect Immun* **1994**, *62*, 2122-2125.
- [305] J.S. Lippard, J.M. Berg, *Bioanorganische Chemie*, Spektrum Akademische Verlag GmbH, Heidelberg, **1995**.
- [306] M. Gilbert, A.M. Cunningham, D.C. Watson, A. Martin, J.C. Richards, W.W. Wakarchuk, *Eur J Biochem* **1997**, *249*, 187-194.
- [307] J.J.R. Fraústo da Silva, R.J.P. Williams, *The biological chemistry of elements-the inorganic chemistry of life.*, Oxford University Press Inc, Oxford, **1997**.
- [308] Y.L. Khmel'nitsky, R. Hilhorst, C. Veeger, *Eur J Biochem* **1988**, *176*, 265-271.
- [309] E. Girard, M.D. Legoy, *Enzyme and Microbial Technology* **1999**, *24*, 425-432.
- [310] C.J. Woolf, S. Bloechlinger, *Science* **2002**, *297*, 1132-1134.
- [311] R. Ohrlein, *Mini Rev Med Chem* **2001**, *1*, 349-361.

8 Curriculum vitae

Tamara VISEKRUNA

✉ Spalenring 59, CH-4055 Basel, Switzerland

☎ (Mobile): ++41 (0)76 549 0154 ☎ (Work): ++41 (0)61 267 1561

Email: tamara.visekruna@unibas.ch

Date of birth: 02/07/1976

EDUCATION

- 2001 – present **University of Basel, Institute of Molecular Pharmacy**, Basel, Switzerland
Ph.D. candidate in Pharmaceutical Sciences, graduation planned in April 2005
Research Topic: Investigation of novel recombinant glycosyltransferases with applications to the drug discovery process.
- 1995 – 2000 **University of Zagreb, Faculty of Science, Croatia**
Master degree in Molecular Biology, with honors (full marks with distinction)
Diploma work at the German Institute of Human Nutrition (DifE), Department of Nutritional Toxicology, Potsdam-Rehbrücke, Germany

PROFESSIONAL EXPERIENCE

- Jun 2001 – present **University of Basel, Institute of Molecular Pharmacy**, Basel, Switzerland
- **Project Leader and Coordinator for several graduated thesis**
 1. Bifunctional sialyltransferase enzyme expression and characterization.
 2. Establishment of a bacterial genomic DNA library using different molecular biology methods.
 - **Research Assistant**
Instructing and supervising students' work in "Modern Drug Design" practical course (Bio-Assay). Yearly evaluated by students (full mark 6/6).
- Sep 2001 – Dec 2001 **German Research Center for Biotechnology (GBF)**, Braunschweig, Germany
Research Collaborator, Department of Protein Glycosylation
Achieved human enzyme expression, purification and characterization using recombinant DNA technology and biochemistry methods.
- Oct 1999 – Oct 2000 **Novartis Pharma AG**, Basel, Switzerland
Trainee Position, Department of Biomolecule Production
Successful isolation and purification of recombinant proteins using liquid chromatography methods.
- Sep 1998 – July 1999 **German Institute of Human Nutrition (DifE)**, Potsdam-Rehbrücke, Germany
Diploma Research Position, Department of Nutritional Toxicology
Established genetically engineered cell lines expressing xenobiotic metabolizing enzymes.

PUBLICATIONS

- Gao GP, Schwardt O, **Visekruna T**, Rabbani S and Ernst B. Chemo-enzymatic synthesis of antagonists of the myelin-associated glycoprotein (MAG). *Chimia*, **2004**, *58*, 215–218.
- Schwardt O, Gao GP, **Visekruna T**, Rabbani S, Gassmann E and Ernst B. Substrate specificity and preparative use of recombinant rat ST3Gal III. *J. Carbohydr. Chem.* **2003**, *23*, 1-26.

Attachment

| Expression system | Total protein expression [mg/l] | Scale of expression [ml] |
|--------------------------|--|---------------------------------|
| Baculovirus | 128.74 | 50 |
| Eukaryotic | 0.5 | 40 |
| Prokaryotic | ~300 | 500 |